

Titre: Towards Sustainable Electrochemical Acidification of Kraft Black
Liquor for Lignin Extraction: Proof of Concept, Control of Membrane
Fouling and Yield Enhancement
Title:

Auteur: Maryam Haddad
Author:

Date: 2016

Type: Mémoire ou thèse / Dissertation or Thesis

Référence: Haddad, M. (2016). Towards Sustainable Electrochemical Acidification of Kraft
Black Liquor for Lignin Extraction: Proof of Concept, Control of Membrane Fouling
and Yield Enhancement [Thèse de doctorat, École Polytechnique de Montréal].
Citation: PolyPublie. <https://publications.polymtl.ca/2166/>

 **Document en libre accès dans PolyPublie**
Open Access document in PolyPublie

URL de PolyPublie: <https://publications.polymtl.ca/2166/>
PolyPublie URL:

Directeurs de
recherche: Jean Paris, Oumarou Savadogo, & Laurent Bazinet
Advisors:

Programme: Génie chimique
Program:

UNIVERSITÉ DE MONTRÉAL

TOWARDS SUSTAINABLE ELECTROCHEMICAL ACIDIFICATION OF KRAFT
BLACK LIQUOR FOR LIGNIN EXTRACTION: PROOF OF CONCEPT, CONTROL
OF MEMBRANE FOULING AND YIELD ENHANCEMENT

MARYAM HADDAD
DÉPARTEMENT DE GÉNIE CHIMIQUE
ÉCOLE POLYTECHNIQUE DE MONTRÉAL

THÈSE PRÉSENTÉE EN VUE DE L'OBTENTION
DU DIPLÔME DE PHILOSOPHIÆ DOCTOR
(GÉNIE CHIMIQUE)
JUN 2016

UNIVERSITÉ DE MONTRÉAL

ÉCOLE POLYTECHNIQUE DE MONTRÉAL

Cette thèse intitulée :

TOWARDS SUSTAINABLE ELECTROCHEMICAL ACIDIFICATION OF KRAFT
BLACK LIQUOR FOR LIGNIN EXTRACTION: PROOF OF CONCEPT, CONTROL
OF MEMBRANE FOULING AND YIELD ENHANCEMENT

présentée par : HADDAD Maryam

en vue de l'obtention du diplôme de : Philosophiæ Doctor

a été dûment acceptée par le jury d'examen constitué de :

M. PATIENCE Gregory S., Ph. D., président

M. PARIS Jean, Ph. D., membre et directeur de recherche

M. SAVADOGO Oumarou, D. d'état, membre et codirecteur de recherche

M. BAZINET Laurent, Ph. D., membre et codirecteur de recherche

M. LEGROS Robert, Ph. D., membre

M. MOULIN Philippe, Ph. D., membre externe

DEDICATION

To my beloved family

ACKNOWLEDGEMENTS

This is the end of my PhD study which would not have been rewarding without the people who supported and inspired me. I would like to take this opportunity to express my gratitude to some of them.

First and for most, I would like to thank my supervisor co-supervisors for their encouragement, inspirational ideas, extensive support and patience during my PhD project. It was a great honor to work under your supervisions. Prof. Paris, thank you for believing in me from the beginning on. You are an inspiration of hard work and determination. Prof. Savadogo, I am grateful for your constructive suggestions and advice that helped me to see my project from the fundamental point of view and be a better researcher. Prof. Bazinet, I am immensely grateful for the privilege of working under your supervision and learning from you. Your constant support, motivation and guides were invaluable to me during my PhD study and your motivation and dedication to the scientific work is always an inspiration for me.

I extend my gratitude to Mrs. Beaudry, Mr. Cloutier and Mr. Labreque at Hydro-Québec for their help, productive comments and contribution to this project especially at the beginning of my PhD journey.

A special word of thanks goes to Prof. Perrier and Dr. Marinova for their constructive advice and motivations during my stay at E^2D^2BF group. Also, I take this opportunity to sincerely thank Dr. Mikhaylin for his fruitful contribution to this research and being the co-author of two publications.

Special thanks to the technical staff of the chemical engineering department, especially Mr. Pilon, Mr. Delisle, Mr. Robin, Mrs. Rousseau and Mrs. Mbelu for their help and technical support.

I would like to thank the students and interns who contributed to this research and also all of my colleagues for the fun time over the lunch breaks and potlucks. Francois thank you very much for translating the abstract. Moreover, my heartfelt thanks to my dearest friends. Thanks for your sincere friendship, support, encouragements and for making my life colorful.

Finally, I would like to thank my life, my family. Words are powerless to express my deepest gratitude for your everlasting and unconditional love, your support regardless of distance, your generosity and enormous patience. I would have not made it this far without you. Maman, Baba, Mahmoud and Elmira, thanks for always being there for me, respecting me and inspiring me. Love you all.

RÉSUMÉ

La baisse de la demande en produits traditionnels issus des pâtes et papiers, la concurrence des économies émergentes, les fluctuations du prix du pétrole et les moyens d'incitations envers les produits verts ont poussé l'industrie des pâtes et papiers (P & P) à développer de nouveaux produits issus des composants du bois. La transformation de cette industrie, plus particulièrement des usines Kraft, en bioraffineries forestières intégrées (IFBR) est considérée comme une alternative efficace en vue d'augmenter les revenus des usines et de diversifier de façon durable leur portefeuille de produits.

Le procédé Kraft est la technique de production de pâtes et papier la plus répandue au monde. Dans la plupart de ces usines, environ 50% des composants du bois (pour la plupart les hémicelluloses et la lignine) sont dissouts dans un courant résiduel appelé liqueur noire (LN) et sont brûlés dans la chaudière de l'usine afin de produire de la vapeur, de l'électricité et de régénérer les produits chimiques utilisés dans le procédé. Par convention, lorsqu'une bioraffinerie forestière est intégrée à une usine, les composants du bois sont séparés du courant de pâte et sont transformés en produits biosourcés à valeur ajoutée. Plus précisément, la lignine extraite peut être utilisée comme biocarburant ou comme précurseur à une vaste gamme de dérivés phénoliques. De plus, l'extraction de la lignine peut augmenter la capacité de l'usine Kraft en faisant diminuer la charge de sa chaudière.

Ce doctorat fait partie d'un projet d'étude plus large évaluant le potentiel de l'implémentation d'une bioraffinerie traitant la lignine dans des usines Kraft existante afin d'augmenter leurs revenus, diversifier leur portefeuille, et les rendre durables sur le long terme. Par conséquent, l'objectif principal de cette thèse était d'identifier, de concevoir et de développer une méthode efficace et écologique d'acidification de la liqueur noire pour l'extraction de la lignine (qui peut être une alternative intéressante à la technique d'extraction par acidification) et finalement de l'intégrer dans une usine Kraft existante. L'acidification électrochimique de la LN Kraft par électrodialyse avec membrane bipolaire (EDBM) a été sélectionnée en ce sens comme une voie technologique prometteuse et durable. L'objectif principal de ce projet de recherche a été de valider le concept, d'éliminer les défauts du procédé, et d'en améliorer les performances afin de le rendre réalisable à grande échelle.

La première étape de cette recherche pionnière a été de mener une étude de faisabilité technique afin de déterminer les avantages et les limites de la méthode d'acidification électrochimique. Les résultats en découlant ont indiqué que l'acidification de la LN par la technique d'EDBM requiert une consommation significativement moindre en produits chimiques par-rapport

à l'acidification par voie chimique. Cependant, l'encrassement de la membrane échangeuse d'ions (IEM) en affecte défavorablement les performances. Nous avons trouvé que la protonation des groupes acides de la lignine résulte en une formation de lignine colloïdale déstabilisée puis en amas de lignine sur la surface des IEM.

L'objectif de la seconde phase était d'éliminer l'encrassement de la membrane, d'améliorer la performance du procédé au moyen d'une sélection des IEM les plus fiables disponibles à l'échelle commerciale, et d'améliorer les conditions opératoires du procédé d'EDBM. Les résultats expérimentaux ont mis en évidence que changer le type d'IEM ne permet pas d'atténuer le phénomène d'encrassement et qu'un cycle de nettoyage chimique était nécessaire. De plus, il fut démontré que la composition chimique de la LN ainsi que la température d'opération et les paramètres hydrodynamiques peuvent substantiellement améliorer l'efficacité et la consommation en énergie du système d'EDBM tout en retardant l'encrassement des IEM.

La phase finale mit l'emphasis sur l'amélioration du rendement en intensifiant le procédé d'acidification électrochimique. La mise en place d'une étape de nettoyage en ligne au moyen d'un champ électrique pulsé pourrait supprimer l'encrassement de la membrane, intensifier l'étape d'acidification et augmenter l'efficacité du procédé jusqu'à 80%.

Sur la base des résultats prometteurs présentés dans cette thèse, nous avons conclu que l'application du procédé d'acidification électrochimique par d'EDBM a réduit de manière substantielle la consommation en produits chimiques et la génération d'effluents. De plus, la production in situ de coproduits pouvant être valorisés, tels que la soude caustique, peuvent faire du procédé d'EDBM une opération unitaire écologique et rentable au sein d'une bioraffinerie forestière intégrée à une usine.

ABSTRACT

Decreasing demand of traditional pulp and paper products, competition from emerging economies and oil price volatility as well as incentives for green products encouraged the pulp and paper industry to look for novel products made from wood components. Transformation of the pulp and paper industry and particularly Kraft pulping mills into integrated forest biorefinery (IFBR) is considered as an effective alternative to increase the revenue of the mills and substantially diversify their product portfolio.

Kraft process is the dominant pulp and paper production method worldwide. In most of the conventional Kraft pulping mills around 50% of the wood components (mainly hemicellulose and lignin) are dissolved in a residual stream called black liquor (BL) and combusted in the recovery boiler to produce steam, electricity and re-generate the cooking chemicals. By contrast, in an IFBR plant wood constituents are separated from the pulp stream and transformed into value-added bio-based products. In particular, extracted lignin can be used as biofuels or as a precursor to a vast phenolic platform of chemical pathways. Furthermore, lignin extraction can increase the capacity of the Kraft mill by decreasing the load of its recovery boiler.

This PhD project was part of a broader research study which evaluates the possibility of lignin biorefinery implementation in existing Kraft pulping mills to improve their revenue, diversify their portfolio and make them sustainable in the long term. Therefore, the main objective of this thesis was to identify, design and develop an efficient and eco-friendly BL acidification method for lignin extraction which can be an attractive alternative to the chemical acidification technique and eventually integrated into an existing Kraft pulping mill. To this end, electrochemical acidification of the Kraft BL via electrodialysis with bipolar membrane (EDBM) was selected as a promising and sustainable pathway. The main focus of this research was to validate the concept, eliminate the process drawbacks and enhance the performance of the EDBM process in order to make it practically feasible for a large scale implementation.

As the first step for conducting this pioneering research, a technical feasibility study was carried out to address the advantages and limitations of the electrochemical acidification method. The results of this feasibility study indicated that the acidification of the Kraft BL via the EDBM technique required a significantly less chemicals versus the chemical acidification approach. However, fouling of the ion exchange membranes (IEM) adversely affected its performance. It was found that the protonation of the lignin phenolic groups resulted

in formation of destabilized colloidal lignin and eventually produced lignin clusters on the surface of the IEMs.

The focus of the second phase was to eliminate the membrane fouling and enhance the performance of the process by means of screening the most reliable and commercially available IEMs as well as improving the operational conditions of the EDBM process. The experimental results implied that changing the type of the IEMs could not mitigate the fouling phenomenon and a chemical cleaning cycle was inevitable. In addition, it was demonstrated that BL chemical composition as well as operational temperature and hydrodynamics parameters could substantially improve the current efficiency and energy consumption of the EDBM system and postpone the fouling of the IEMs.

Yield enhancement by intensifying the electrochemical acidification process was the main intention of the final phase. Implementation of an in-line cleaning step by means of pulsed electric field application could successfully suppress the membrane fouling, intensify the acidification step and enhance the process efficiency up to 80%.

On the basis of the promising results presented in this thesis, it was concluded that application of the electrochemical acidification process via the EDBM method substantially reduced the chemical consumption and effluent generation. Furthermore, an in situ production of a valuable side product i.e. caustic soda can make the EDBM process an eco-efficient and profitable operational unit inside the IFBR plant.

TABLE OF CONTENTS

DEDICATION	iii
ACKNOWLEDGEMENTS	iv
RÉSUMÉ	v
ABSTRACT	vii
TABLE OF CONTENTS	ix
LIST OF TABLES	xiii
LIST OF FIGURES	xv
ACRONYMS	xix
CHAPTER 1 INTRODUCTION	1
CHAPTER 2 LITERATURE REVIEW	5
2.1 Ion Exchange Membrane (<i>IEM</i>)	5
2.2 Electro-Membrane Processes Used for Electrochemical Acidification	7
2.2.1 Membrane Electrolysis (<i>EL</i>)	7
2.2.2 Conventional Elctrodialysis (<i>ED</i>)	8
2.2.3 Elctrodialysis with Bipolar Membrane (<i>EDBM</i>)	11
2.3 Critical Literature Review	13
2.3.1 Electrolysis of Black Liquor	13
2.3.2 Electrodialysis of Black Liquor	15
2.3.3 Electrodialysis of Black Liquor using Bipolar Membrane	16
CHAPTER 3 OBJECTIVES AND METHODOLOGY	17
3.1 Main Objective	17
3.2 Methodology	17
3.3 Presentation of Publications	19
CHAPTER 4 ARTICLE 1 : A FEASIBILITY STUDY OF A NOVEL ELECTRO-MEMBRANE BASED PROCESS TO ACIDIFY KRAFT BLACK LIQUOR AND	

EXTRACT LIGNIN	21
4.1 Introduction	21
4.2 Theoretical Background	25
4.2.1 Principle of Electrodialysis by Bipolar Membrane to Acidify Kraft Black Liquor	25
4.2.2 Lignin Precipitation Yield	26
4.3 Experimental	26
4.3.1 Membranes and Materials	26
4.3.2 Methods	27
4.3.3 Protocol	28
4.3.4 Analyses	29
4.4 Results and Discussion	30
4.4.1 Black Liquor Electrical Conductivity	30
4.4.2 Electrochemical Acidification of Kraft Black Liquor	31
4.4.3 Comparison of Electrochemical Acidification and Chemical Acidifica- tion Methods	34
4.5 Conclusion	37
CHAPTER 5 ARTICLE 2 : FOULING IDENTIFICATION OF ION-EXCHANGE MEM- BRANES DURING ACIDIFICATION OF KRAFT BLACK LIQUOR BY ELEC- TRODIALYSIS WITH BIPOLAR MEMBRANE	38
5.1 Introduction	38
5.2 Experimental	40
5.2.1 Membranes and Materials	40
5.2.2 Electrochemical acidification Apparatus and Protocol	41
5.2.3 Analysis Methods	42
5.3 Results and Discussion	44
5.3.1 Global System Resistance	44
5.3.2 Black Liquor Analysis	45
5.3.3 Membrane Thickness and Ash Content	46
5.3.4 Electron Microscopy and Elemental Analysis	46
5.3.5 X-ray Photoelectron Spectrometry (<i>XPS</i>) Analysis	48
5.3.6 Proposed Fouling Mechanisms	50
5.4 Conclusion	53
CHAPTER 6 ARTICLE 3 : ELECTROCHEMICAL ACIDIFICATION OF KRAFT BLACK LIQUOR : EFFECT OF FOULING AND CHEMICAL CLEANING ON	

ION EXCHANGE MEMBRANE INTEGRITY	54
6.1 Introduction	55
6.2 Experimental	57
6.2.1 Membranes and Materials	57
6.2.2 Electrochemical Acidification Set-up	58
6.2.3 Protocol	59
6.2.4 Global System Resistance	60
6.2.5 Membrane Properties	61
6.3 Results and Discussion	63
6.3.1 Global System Resistance	63
6.3.2 Membrane Properties	63
6.3.3 Chemical Cleaning Mechanisms	70
6.4 Conclusion	73
CHAPTER 7 ARTICLE 4 : EFFECT OF PROCESS VARIABLES ON THE PER- FORMANCE OF ELECTROCHEMICAL ACIDIFICATION OF KRAFT BLACK LIQUOR BY ELECTRODIALYSIS WITH BIPOLAR MEMBRANE	74
7.1 Introduction	75
7.2 Experimental	78
7.2.1 Membranes and Materials	78
7.2.2 Electrochemical Acidification Apparatus and Protocol	78
7.2.3 Design of Experiments	81
7.2.4 Analysis and Process Evaluation	81
7.3 Results and Discussion	83
7.3.1 Black Liquor Dynamic Viscosity	83
7.3.2 Black Liquor Electrical Conductivity	84
7.3.3 Influence of Process Variables on Electrodialytic Parameters	85
7.3.4 Influence of Process Variables on System Hydrodynamics (Reynolds Number)	91
7.3.5 Evolution of System Performance	93
7.4 Conclusion	95
CHAPTER 8 ARTICLE 5 : ELECTROCHEMICAL ACIDIFICATION OF KRAFT BLACK LIQUOR : IMPACTS OF PULSED ELECTRIC FIELD APPLICATION ON BIPOLAR MEMBRANE COLLOIDAL FOULING AND PROCESS INTENSI- FICATION	98
8.1 Introduction	99

8.2	Experimental	100
8.2.1	Membranes and Materials	100
8.2.2	Electrochemical Acidification Set-up	101
8.2.3	Protocol	102
8.2.4	Membrane Analyses	104
8.2.5	Process Evaluation	105
8.3	Results and Discussion	106
8.3.1	Membrane Analysis	106
8.3.2	Evolution of Electrodialytic Parameters	109
8.3.3	Evolution of System Performance	116
8.3.4	Proposed Pulsed Electric Field Mechanisms	119
8.4	Conclusion	122
CHAPTER 9 BLACK LIQUOR ACIDIFICATION FOR LIGNIN EXTRACTION : A PRELIMINARY COMPARISON BETWEEN CHEMICAL AND ELECTROCHEMI- CAL ACIDIFICATION PATHWAYS		126
9.1	Introduction	126
9.2	Experimental	126
9.2.1	Membranes and Materials	126
9.2.2	Chemical Acidification Apparatus and Protocol	127
9.2.3	Electrochemical Acidification Apparatus and Protocol	128
9.2.4	Analyses	128
9.3	Results and Discussion	130
9.3.1	Comparison of Electrochemical Acidification and Chemical Acidifica- tion Methods	130
9.3.2	Lignin Impurities	131
9.4	Conclusion and Perspectives	132
CHAPTER 10 GENERAL DISCUSSION		133
CHAPTER 11 CONCLUSIONS, ORIGINAL CONTRIBUTIONS AND RECOMMEN- DATIONS		138
11.1	Conclusions	138
11.2	Original Contributions	139
11.3	Recommendations	139
REFERENCES		141

LIST OF TABLES

Table 1.1 : Three main technologies for lignin extraction from black liquor	3
Table 2.1 : Applied methods for controlling and minimizing the fouling of the <i>IEMs</i> during the electromembrane processes [38]	10
Table 4.1 : Ion exchange membranes specifications provided by their supplier . . .	27
Table 4.2 : Applied operational conditions during electrochemical acidification me- thod	29
Table 4.3 : Characteristics of Kraft Black Liquor	30
Table 5.1 : Ion exchange membranes specifications provided by their supplier . . .	40
Table 5.2 : Applied operational conditions during electrochemical acidification method	41
Table 5.3 : <i>XPS</i> Operational Conditions	44
Table 5.4 : Characteristics of Kraft Black Liquor	45
Table 5.5 : Membrane Thickness and Ash Content	46
Table 5.6 : Identification of main chemical bonding from high resolution <i>XPS</i> scan	49
Table 6.1 : Characteristics of Kraft Black Liquor	58
Table 6.2 : Applied Operational Conditions during Electrochemical Acidification of the Kraft Black Liquor	58
Table 6.3 : Membrane Thickness (<i>mm</i>)	64
Table 6.4 : Contact Angle measurements (°)	68
Table 6.5 : Ion Exchange Capacity of Cation Exchange Membranes (<i>meq. g⁻¹</i>) . .	69
Table 6.6 : Membrane Electrical Resistance ($\Omega\text{ cm}^2$)	70
Table 7.1 : Ion exchange membranes specifications provided by their suppliers . .	78
Table 7.2 : Main specifications of the <i>EDBM</i> stack	79
Table 7.3 : Applied Operational Conditions during Electrochemical Acidification of the Kraft <i>BL</i>	81
Table 7.4 : Characteristics of Kraft <i>BL</i> solutions	86
Table 7.5 : Parameters of the <i>BL</i> electrical conductivity fitting equations	96
Table 7.6 : Parameters of the <i>NaOH</i> electrical conductivity fitting equations . .	97
Table 7.7 : Parameters of the <i>BL</i> pH fitting equations	97
Table 8.1 : Ion exchange membranes specifications provided by their suppliers . .	100
Table 8.2 : Characteristics of Kraft Black Liquor	101
Table 8.3 : Applied Operating Conditions during Electrochemical Acidification of the Kraft Black Liquor	104
Table 8.4 : Membrane Thickness (<i>mm</i>)	107

Table 8.5 : Parameters of the <i>BL</i> electrical conductivity fitting equations	123
Table 8.6 : Parameters of the <i>NaOH</i> electrical conductivity fitting equations . . .	124
Table 8.7 : Parameters of the <i>BL</i> pH fitting equations	124
Table 8.8 : Parameters of the <i>BL</i> sodium concentration fitting equations	125
Table 8.9 : Parameters of the <i>BL</i> lignin content fitting equations	125
Table 9.1 : Ion exchange membranes specifications provided by their suppliers . . .	127
Table 9.2 : Characteristics of Kraft Black Liquor	129
Table 9.3 : Acidification parameters obtained from electrochemical and chemical acidification steps	130
Table 9.4 : Lignin ash content and consumed acid during the washing steps	131

LIST OF FIGURES

Figure 1.1 : Forest industry production trend in Canada [1]	1
Figure 1.2 : A schematic drawing of a conventional Kraft pulping process	2
Figure 2.1 : A cationic exchange membrane (<i>CEM</i>) with fixed carboxylic acid charges	5
Figure 2.2 : The structure of a Bipolar Membrane (<i>BPM</i>)	7
Figure 2.3 : A simple membrane electrolysis (<i>EL</i>) cell	8
Figure 2.4A flow-diagram of a conventional <i>ED</i> stack	9
Figure 2.5 : A schematic representation of the <i>EDBM</i> process	11
Figure 2.6 : Two-compartments <i>EDBM</i> cell arrangement for production of (a) base and (b) acid from their corresponding salts	12
Figure 2.7 : Membrane permselectivity failure that can affect the <i>EDBM</i> perfor- mance [39]	13
Figure 2.8 : Basic operation of the <i>BL</i> electrolysis acidification process	14
Figure 2.9 : Electrodialysis of black liquor in three compartment arrangement . .	15
Figure 2.10 : The <i>BL</i> recaustization steps performed by Koumoundouros <i>et al.</i> [46]	16
Figure 3.1 : A representation of overall methodology phases	18
Figure 4.1 : A simplified illustration of the Kraft pulping process	23
Figure 4.2 : Basic operation of the <i>BL</i> electrolysis (<i>CEM</i> : Cation exchange mem- brane)	24
Figure 4.3 : Principle of electrodialysis with bipolar membrane (<i>EDBM</i>) for the acidification of Kraft <i>BL</i> (<i>BPM</i> : bipolar membrane and <i>CEM</i> : cation ex- change membrane)	26
Figure 4.4 : Schematic diagram of the electrochemical acidification process	28
Figure 4.5 : Evolution of the Kraft <i>BL</i> electrical conductivity as a function of temperature and <i>TDS</i> content of the <i>BL</i>	31
Figure 4.6 : (a) Voltage drop, (b) pH evolution of <i>BL</i> and (c) electrical conductivity profiles of <i>BL</i> and <i>NaOH</i> during electrochemical acidification of Kraft <i>BL</i>	33
Figure 4.7 : Formed deposit layer on the surface and in the space between the ion exchange membranes inside <i>BL</i> compartment during the electrochemical acidification of the Kraft <i>BL</i> (a) : case I (the electrochemical acidification was terminated when the voltage limit of the DC power supply was reached) (b) : case II (the electrochemical acidification was stopped when the voltage drop started to increase rapidly)	34

Figure 4.8 : (a) Filtration rate, (b) lignin precipitation yield and (c) acid consumption of electrochemical and chemical acidification methods	36
Figure 5.1 : A simplified representation of the Kraft pulping process	39
Figure 5.2 : Schematic diagram of the electrochemical acidification apparatus and the <i>EDBM</i> cell	42
Figure 5.3 : Global system resistance during the electrochemical acidification of the Kraft <i>BL</i> via <i>EDBM</i> method	45
Figure 5.4 : Scanning electron microscopy (<i>SEM</i>) images and elemental analysis (<i>EDX</i>) of (a) the fresh and the used <i>CEM</i> in contact with : (b) black liquor and (c) caustic soda solutions	47
Figure 5.5 : Scanning electron microscopy (<i>SEM</i>) and elemental analysis (<i>EDX</i>) of (a) the fresh and (b) the used cation exchange layer as well as (c) the fresh and (d) the used anion exchange layer of the <i>BPM</i>	48
Figure 5.6 : <i>XPS</i> survey spectra of (a) fouled <i>CEM</i> and (b) fouled <i>BPM</i> (KLL peaks represent the auger peaks)	50
Figure 5.7 : Fouling mechanism on the surface of the <i>IEM</i> s during the <i>EDBM</i> process ((a) : Protons production and lignin protonation, (b) : Lignin nucleation phenomenon on the surface of the <i>BPM</i> , (c) : Formation of lignin clusters on the surface of the <i>BPM</i> , (d) : Precipitation of the lignin in the space between the <i>BPM</i> and <i>CEM</i> and interruption of the lignin aggregation on the surface of the <i>CEM</i> due to the hydroxide ions leakage through the <i>CEM</i>)	52
Figure 6.1 : A schematic illustration of Kraft process	55
Figure 6.2 : Electrodialysis with bipolar membrane (<i>EDBM</i>) stack (<i>BPM</i> : bipolar membrane and <i>CEM</i> : cation- exchange membrane)	59
Figure 6.3 : Schematic diagram of the electrochemical acidification set-up	59
Figure 6.4 : Global system resistance during the <i>EDBM</i> process with different cation exchange membranes	63
Figure 6.5 : Scanning electron microscopy (<i>SEM</i>) and elemental analysis (<i>EDX</i>) of the (a) fresh and (b) fouled ion exchange membranes in contact with the <i>BL</i> solution	65
Figure 6.6 : Scanning electron microscopy (<i>SEM</i>) and elemental analysis (<i>EDX</i>) of the cleaned ion exchange membranes with (a) caustic soda solution and (b) fresh diluted black liquor solution (<i>FBM</i> : bipolar membrane, FuMA-Tech, <i>FKB</i> : cation exchange membrane, FuMA-Tech, <i>CMB</i> : cation exchange membrane, Neosepta, <i>CM(H) – PES</i> : cation exchange membrane, Mega a.s., Nafion 324 : cation exchange membrane, DuPont)	66

Figure 6.7 : <i>SEM</i> images of the deposit lignin on the surface of the fouled <i>BPM</i> at (a) 2000 <i>X</i> and (b) 5000 <i>X</i>	71
Figure 6.8 : Chemical cleaning mechanisms : (a) the alkaline cleaning solution interacts with the attractive and repulsive forces, (b) cleavage of the lignin layer into smaller fragments with a larger surface area, (c) ionization of the lignin phenolic groups inside the alkaline medium, (d) repulsion of the charged phenolic groups and lignin solubility	72
Figure 7.1 : A simplified illustration of Kraft process	75
Figure 7.2 : A simplified diagram of the electrochemical acidification set-up	80
Figure 7.3 : A schematic illustration of <i>EDBM</i> stack (<i>CEM</i> : cation exchange membrane and <i>BPM</i> : bipolar membrane)	80
Figure 7.4 : Evolution of the Kraft <i>BL</i> dynamic viscosity as a function of temperature and <i>TDS</i> content of the <i>BL</i> ($BL_{Dynamic\ Viscosity} = \exp(0.078 * BL_{TDS})$)	84
Figure 7.5 : Evolution of the Kraft <i>BL</i> electrical conductivity as a function of temperature and <i>TDS</i> content of the <i>BL</i> ($BL_{Electrical\ Conductivity} = -a * (BL_{TDS})^2 + b * (BL_{TDS}) + c$ & $0.055 \leq a \leq 0.055$, $3.19 \leq b \leq 3.21$ and $49.0 \leq c \leq 56.4$) .	85
Figure 7.6 : Electrical conductivity trends of the <i>BL</i> and <i>NaOH</i> solutions during the electrochemical acidification of Kraft <i>BL</i> via <i>EDBM</i> process (fitting equations can be found in Appendix A)	87
Figure 7.7 : Global system resistance progress during the electrochemical acidification of Kraft <i>BL</i> via <i>EDBM</i> process (fitting equations can be found in Appendix A)	89
Figure 7.8 : Evolution of the pH of the <i>BL</i> during the electrochemical acidification of Kraft <i>BL</i> via <i>EDBM</i> process (fitting equations can be found in Appendix A)	90
Figure 7.9 : Evolution of the Reynolds number as a function of the operational temperature of the <i>EDBM</i> process and <i>TDS</i> content of the <i>BL</i>	93
Figure 7.10 : Influence of the operational temperature and <i>TDS</i> content of the <i>BL</i> on the current efficiency of the <i>EDBM</i> acidification process	94
Figure 7.11 : Effect of the operational temperature and <i>TDS</i> content of the <i>BL</i> on the energy consumption of the <i>EDBM</i> acidification process	95
Figure 8.1 : Electrodialysis with bipolar membrane (<i>EDBM</i>) stack (<i>BPM</i> : bipolar membrane and <i>CEM</i> : cation- exchange membrane)	102
Figure 8.2 : Schematic diagram of the electrochemical acidification set-up	103
Figure 8.3 : Scanning electron microscopy (<i>SEM</i>) and elemental analysis (<i>EDX</i>) of the <i>BL</i> sides of (a) <i>BPM</i> and (b) the <i>CEM</i> used at <i>DC</i> and <i>PEF</i> regimes	109

Figure 8.4 : Conductivity trends of the <i>BL</i> and <i>NaOH</i> solutions during electrochemical acidification of Kraft <i>BL</i> via <i>EDBM</i> process under <i>DC</i> and <i>PEF</i> regimes (fitting equations can be found in Appendix A)	110
Figure 8.5 : Global system resistance progress during electrochemical acidification of Kraft <i>BL</i> via <i>EDBM</i> process under <i>DC</i> and <i>PEF</i> regimes (fitting equations can be found in Appendix A)	112
Figure 8.6 : Evolution of the pH of the <i>BL</i> during the electrochemical acidification of Kraft <i>BL</i> via <i>EDBM</i> process under <i>DC</i> and <i>PEF</i> regimes (fitting equations can be found in Appendix A)	113
Figure 8.7 : Evolution of sodium concentration in the <i>BL</i> solution during electrochemical acidification of Kraft <i>BL</i> via <i>EDBM</i> process under <i>DC</i> and <i>PEF</i> regimes (fitting equations can be found in Appendix A)	115
Figure 8.8 : Evolution of <i>BL</i> lignin content during electrochemical acidification of Kraft <i>BL</i> via <i>EDBM</i> process under <i>DC</i> and <i>PEF</i> regimes (fitting equations can be found in Appendix A)	116
Figure 8.9 : (a) Current efficiency of the <i>EDBM</i> acidification process under <i>DC</i> and <i>PEF</i> regimes with different pulse/pause ratios (b) current efficiency trend as a function of the pause lapse at <i>PEF</i> regime	117
Figure 8.10 : (a) Relative energy consumption of the <i>EDBM</i> acidification process under <i>DC</i> and <i>PEF</i> regimes with different pulse/pause ratios (b) relative energy consumption trend as a function of the pause lapse at <i>PEF</i> regime	119
Figure 8.11 : Schematic illustration of the <i>BL</i> medium under the <i>PEF</i> regime when a (a) short and (b) long pause lapse was applied (steps 1 and 2 illustrate the pulse lapse, steps 3 and 4 show the pause period and step 5 represents the <i>BL</i> medium after several pulse-pause lapses)	121
Figure 9.1 : A schematic drawing of the chemical acidification apparatus	128

ACRONYMS

AEL	Anion Exchange Layer
AEM	Anion Exchange Membrane
BL	Black Liquor
BPM	Bipolar Membrane
CEL	Cation Exchange Layer
CEM	Cation Exchange Membrane
CIP	Cleaning in Place
DLVO	Derjaguin-Landau-Verwey-Overbeek theory
ED	Conventional Electrodialysis
EDBM	Electrodialysis with Bipolar Membrane
EDX	Energy-dispersive X-ray Spectroscopy
EL	Electrolysis
HDPE	High Density Polyethylene
IEL	Ion Exchange Layer
IEM	Ion Exchange Membrane
IFBR	Integrated Forest Bio-Refinery
PE	Polyethylene
PP	Polypropylene
PEF	Pulsed Electric Field
SEM	Scanning Electron Microscope
TDS	Total Dissolved Solids
UF	Ultrafiltration
XPS	X-Ray Photoelectron Spectroscopy

CHAPTER 1 INTRODUCTION

For the past decade, the pulp and paper (*P&P*) industry in Canada has faced a period of decline (Figure 1.1) due to the decreasing demands for the traditional paper commodities and international competition [1]. In order to improve the revenue of the (*P&P*) industry and sustainably comprehensive investigations have been undertaken to identify and develop novel non-paper products which can be manufactured from wood components [1]. In this regard, transformation of the existing pulp mills into integrated forest biorefinery (*IFBR*) plant was proposed as a promising alternative to convert lignocellulosic biomass into new value-added products along with manufacturing the traditional paper commodities [2].

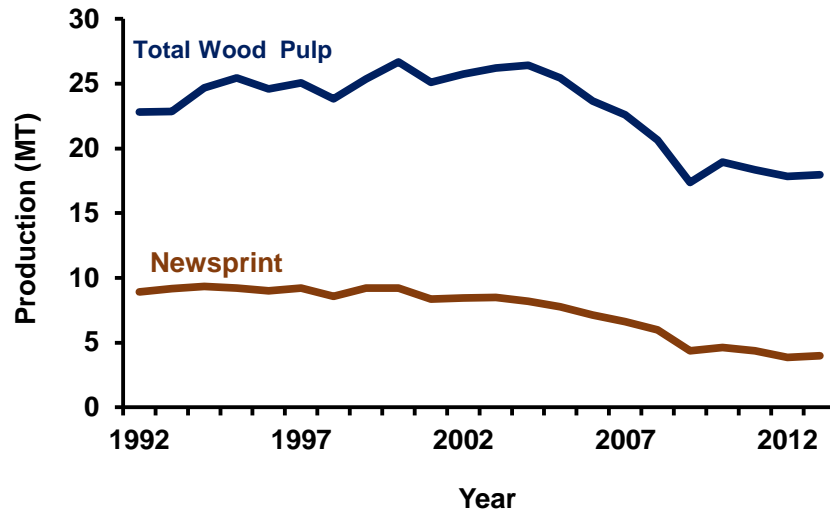


Figure 1.1 Forest industry production trend in Canada [1]

Kraft process, which is the dominant technique for the pulp and paper production world-wide, can be perfectly incorporated into the *IFBR* plant [3]. In a conventional Kraft mill, wood chips are cooked in a digester under strong alkaline and high temperature conditions resulting in delignification of wood. The cooked liquor goes to a washing step where pulp and residual liquors are separated. The pulp stream undergoes a bleaching process to increase its brightness and finally enters the drying step; while, the residual stream, called black liquor (*BL*) is concentrated in a multi-stage evaporators and combusted in the recovery boiler to produce heat and steam and regenerate cooking chemicals (Figure 1.2). The average yield of a Kraft pulping mill is reported to be around 50% since half of the wood components (mainly hemicellulose and lignin) are dissolved in the *BL* and combusted in the recovery boi-

ler [4, 5]. Within the Kraft *IFBR* context, the hemicellulose and lignin can be extracted and converted to a board spectrum of bio-products and bio-chemicals [3]. In particular, a fraction of the lignin can be separated from the *BL* before the combustion stage and converted to value-added products such as biofuels and carbon fibers [6]. Furthermore, lignin extraction increases the capacity of the Kraft mill by decreasing the load of its recovery boiler [5].

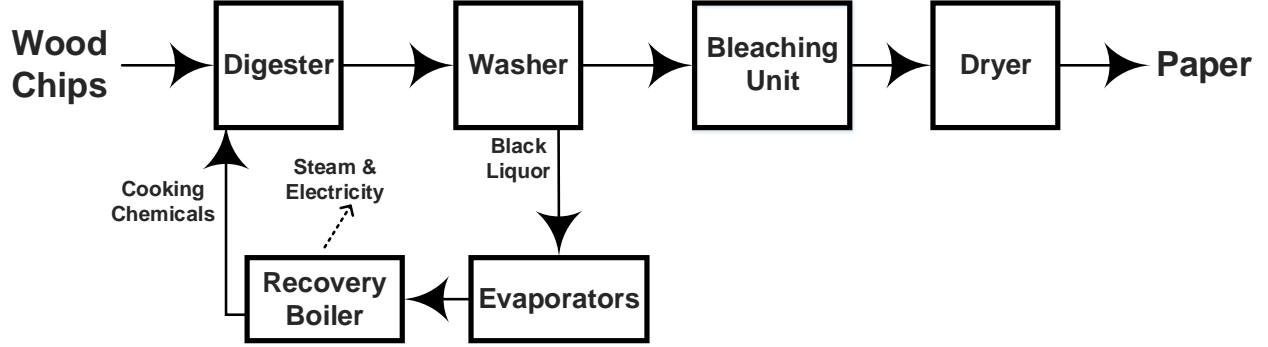


Figure 1.2 A schematic drawing of a conventional Kraft pulping process

Different processes have been proposed for lignin extraction [7, 8, 9, 10, 11]. Among all of the suggested methods chemical acidification, ultrafiltration (*UF*) and electrochemical acidification pathways have attracted more attentions [4, 9, 12, 13]. A summary of these three common techniques and their remarks is given in Table 1.1.

Chemical acidification is the most common lignin extraction technique in which lowering the pH of the *BL* causes lignin precipitation and separation. Utilization of CO_2 and H_2SO_4 as the acidifying agents remarkably enhanced the process yield [4, 5, 10]. However, there are some serious issues regarding the practical implementation of this acidification approach. For instance, the added chemical (acid) can disturb sodium-sulfur balance of the receptor mill. Furthermore, when CO_2 is utilized, the price and the cost-intensive installation of the CO_2 recapturing equipment would challenge the process productivity [4, 12].

UF and nanofiltration method, on the other hand, is still under investigation [9, 14]. A comparison between the chemical acidification and *UF* separation techniques has been done by Uloth *et al.* [15]; they concluded that the chemical acidification process has a higher efficiency as well as a lower cost. Moreover, application of the *UF* process resulting in separation of lignin with a specific molecular weight and to enhance the lignin extraction yield, another acidification step such as *BL* carbonation was required [5].

Table 1.1 Three main technologies for lignin extraction from black liquor

Method	State of Development	Remarks
Chemical Acidification	Industry	<ul style="list-style-type: none"> - High Lignin Yield - Additional amount of solids go to the recovery system - At low pH , washing and filtration are difficult
Ultrafiltration-Nanofiltration	Laboratory	<ul style="list-style-type: none"> - No pH and temperature adjustment needed - Separation based on particle size
Electrochemical Acidification Electrolysis & Electrodialysis	Laboratory	<ul style="list-style-type: none"> - Caustic Soda Production - Moderate Lignin Yield

Since the alkaline BL is an electrolyte solution containing inorganic salts ($NaOH$, Na_2SO_4 , Na_2CO_3 and Na_2S) and organic compounds (lignin and hemicellulose) application of the electrochemical acidification approach is another green alternative to overcome the disadvantages of the chemical acidification method, acidify the *BL* and produce caustic soda as a valuable side-product [13, 16]. The electrochemical acidification of the BL can be performed in different forms : electrolysis (*EL*), conventional electrodialysis (*ED*) and electrodialysis with bipolar membrane (*EDBM*). In all of the aforementioned processes, ion exchange membranes (*IEM*) (membranes having fixed positive or negative charges) are utilized to separate electrolyte solutions under an electric field as the driving force of an electric field. A specific type of the *IEMs* is bipolar membrane (*BPM*), which is made of two ion exchange layers (*IEL*) of opposite charges. A *BPM* enables the electro-dissociation of water into protons and hydroxide ions and can be applied for the acid and base production from their salt solutions [17, 18, 19].

This PhD project is part of a broader research study which evaluates the possibility of lignin biorefinery implementation in existing Kraft pulping mills to improve their revenue, diversify their portfolio and make them sustainable in the long term. Therefore, the main objective of this thesis is to identify, design and develop an efficient and eco-friendly *BL* acidification method for lignin extraction which can be an attractive alternative to the chemical acidification technique and eventually integrated into an existing Kraft pulping mill. To this end, electrochemical acidification of the *BL* via *EDBM* process was selected as a promising and

sustainable pathway. The main focus of this research was to validate the concept, eliminate the process drawbacks and enhance the performance of the *EDBM* method in order to make it practically feasible for a large scale implementation. This PhD thesis is organized as follows : chapter 2 presents the relevant literature review. It introduces the concepts and theories which have been presented in the literature and were useful in this research work. Chapter 3 first presents the objectives and methodology and then describes the organization of the articles. The main results of this project are presented in chapters 4 – 8. Chapter 9 presents an additional study on a preliminary comparison between the chemical and modified electrochemical acidification approaches in order to provide a valuable knowledge about the advantages of *EDBM* method and allow us to reflect on the potential and operating window of this method as a sustainable option for the *BL* acidification and lignin extraction. Chapter 10 provides a general discussion and synthesizes the results obtained in the course of this study. Finally, chapter 11 summarize the most important conclusions of this study followed by recommendations for future work.

CHAPTER 2 LITERATURE REVIEW

2.1 Ion Exchange Membrane (*IEM*)

Membranes are called the heart of any membrane separation technologies and can be considered as «a permselective barrier or interface between two phases» [20]. Ion exchange membranes (*IEM*) are the key elements in electro-membrane processes. These membranes are permeable to either negatively or positively charged ions in an aqueous solution. The *IEM*s are similar to the ion exchange resin in a sheet form. A membrane with fixed positive charges is called an anion exchange membrane (*AEM*). Similarly, a membrane containing fixed negative charges is a cation exchange membrane (*CEM*) [18, 19].

The following charged groups are mainly used as fixed charges in *AEM*s :

$-NH_3^+$, $-NRH_2^+$, $-NR_3^+$, $-PR_3^+$ and $-SR_2^+$ [18, 19].

And, in *CEM*s the fixed charged groups can be :

$-SO_3^-$, $-COO^-$, $-PO_3^{2-}$, $-PO_3H^-$ and $-C_6H_4O^-$ [18, 19].

Figure 2.1 represents a *CEM* containing fixed negative charged groups as well as the mobile cations which can be replaced by other cations existing in the solution close to the membrane. The counter-ion concentration within the membrane is high; hence, most of the electric current is carried by counter-ions [21]. Based on Donnan exclusion phenomenon an ideal *IEM* must be impermeable to the co-ions [22].

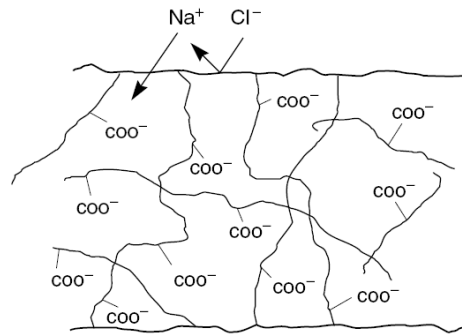


Figure 2.1 A cationic exchange membrane (*CEM*) with fixed carboxylic acid charges

In order to select a suitable *IEM* for an electro-membrane process, the membrane must have some desired properties such as [23] :

- *High Permselectivity* : an *IEM* should be highly permeable to counter-ions and impermeable to co-ions.
- *Low electrical resistance* : the permeability of *IEM* for the counter-ions under the electric field driving force should be as high as possible.
- *High chemical and thermal stability* : the membrane should tolerate a pH range of 0 – 14, be mechanically strong and finally should possess a low degree of swelling.

The properties of the *IEMs* are determined by two parameters : the basic polymer matrix and the type and concentration of the fixed ionic moieties. The basic polymer matrix determines the mechanical, chemical and thermal stability of the membrane. Usually, the matrix of an *IEM* consists of hydrophobic polymers such as polystyrene, polyethylene, or polysulfone. While these basic polymers are insoluble in water and show a low degree of swelling, they may become water soluble by the introduction of the ionic groups. Therefore, the polymer matrix of the *IEMs* is very often cross-linked. The degree of the cross-linking determines the degree of the swelling as well as the chemical and thermal stability, but it also has a significant influence on the electrical resistance and the permselectivity of the membrane [24].

Another type of *IEMs* is called bipolar membrane (*BPM*) which contains the negatively fixed charged groups on one side and the positively fixed charged groups on the other side. As illustrated in Figure 2.2, water diffuses from both sides of the *BPM* to its transition layer and once an electric field is applied, water dissociation reaction takes place inside this layer and generates proton and hydroxide ions. These ions migrate to the aqueous solutions through the cation and anion exchange layers of the *BPM* [17, 18, 19].



Normally, the cation and anion exchange layers of the *BPM* are made of the same materials as *CEMs* and *AEMs*, which can resist in a wide range of pH [25]. The two ion exchange layers (*IEL*) should facilitate the selective transport of the proton and the hydroxide ions generated from the water dissociation reaction. The presence of a catalyst in the transition layer decreases the activation energy of the water splitting since the catalyst generates reactive, activated complexes and provides a different reaction path. Usually, heavy metals ion complexes, such as zirconium, chromium and iron are used as the catalysts [17, 18]. In addition to the catalyst selection, the transition layer should also enjoy a certain surface roughness in order to improve the contact area of the *BPM*. Therefore, beside the aforementioned fundamental properties for an acceptable *IEMs*, the *BPMs* should also have a high capacity for water splitting reaction [17].

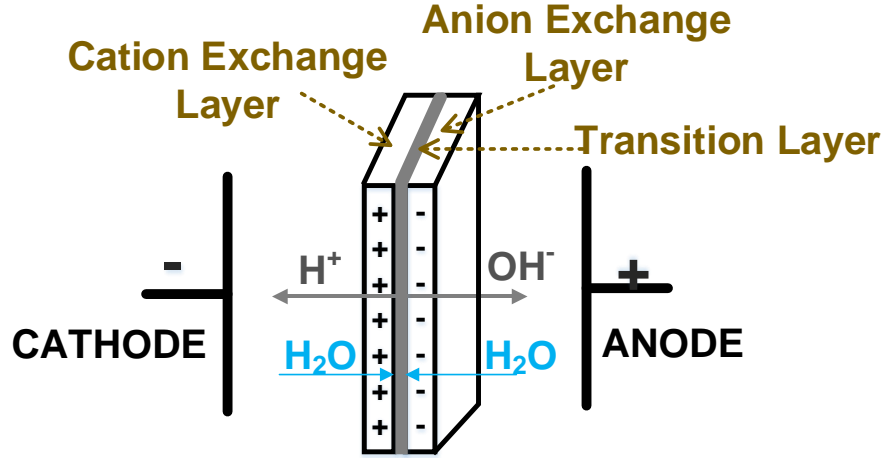


Figure 2.2 The structure of a Bipolar Membrane (*BPM*)

Different methods have been examined for the *BPMs* preparation such as loosely laminating [26], pressing [27], gluing the two *IEMs* [28], or casting one of the *IEM* on top of the other one [29].

Additionally, the *IEMs* can be also classified based on their structure as homogeneous and heterogeneous. The homogeneous membranes, are prepared by means of a direct introduction of the ion exchange components into the polymeric structure of the membranes. Thus, the ion exchange groups are evenly distributed on the surface of the membrane. On the other hand, the heterogeneous membranes are produced, firstly, by preparing a mixture of a fine powder of an ion exchange resin and a binder polymer and then, pressing and sintering the mixture at a high temperature. This preparation procedure resulting in a non-uniform distribution of the ion exchange groups on the surface of the membrane [18, 30].

2.2 Electro-Membrane Processes Used for Electrochemical Acidification

2.2.1 Membrane Electrolysis (*EL*)

Figure 2.3 shows a simple illustration of an *EL* cell. It is made of an anode compartment containing the anode and an anolyte solution, a *CEM* and a cathode compartment consisting of the cathode and a catholyte solution. In the *EL* process, both anodic and cathodic redox reactions are involved in the transfer of the charged ions. Therefore, these electrode reactions play an important role in the process. The *CEM* separates the cathodic and anodic compartments in order to avoid unwanted reactions. The electrolysis of the *NaCl* for production of caustic soda and Cl^- is known as the main industrial application of this method [31].

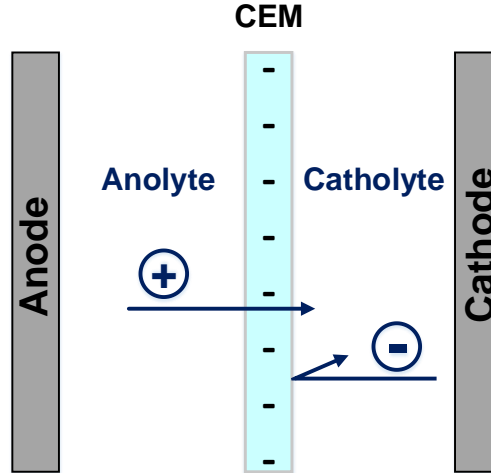


Figure 2.3 A simple membrane electrolysis (*EL*) cell

Generation of oxygen and hydrogen as side-product gases during the *EL* process consumes around 50 % of the electrical energy of the system. Therefore, in a large scale application, the collocation and storage of these gases as well as the high level of energy consumption would make the *EL* process energy and cost intensive. In addition, the requirement of an electrode pair for each repeating cell unit can increase the total cost of the process [32].

2.2.2 Conventional Electrodialysis (*ED*)

The principle of the conventional *ED* is illustrated in Figure 2.4, which shows an *ED* cell consisting of the *CEMs* and *AEMs* positioned in an alternating pattern between an electrode pair. When an ionic solution is pumped through the *ED* stack and the electric field is applied between the electrodes, the cations migrate towards the cathode and the anions go towards the anode. The cations pass easily through the *CEMs* but are rejected by the *AEMs*. Likewise, the anions migrate through the *AEMs* and are retained by the *CEMs*. Therefore, the ion concentration in alternate compartments increases, while the other compartments simultaneously become depleted. The exhausted solution is called dilute and the concentrated solution is called brine or concentrate. Any *ED* cell has five key elements [18, 19] :

- *Electric Field*, which causes the effective ion migration
- *Electrodes*, where the oxidation/reduction reactions occur to establish the driving force for the ion migrations inside the *ED* stack
- *Ion exchange membranes (IEM)*, the key components which allow the transfer of the counter-ions and reject the co-ions
- *Solvents*, which make a continuous ion transport by filling the space between the

electrodes and the *IEMs*

— *Electrolytes*, the current carriers between the electrodes

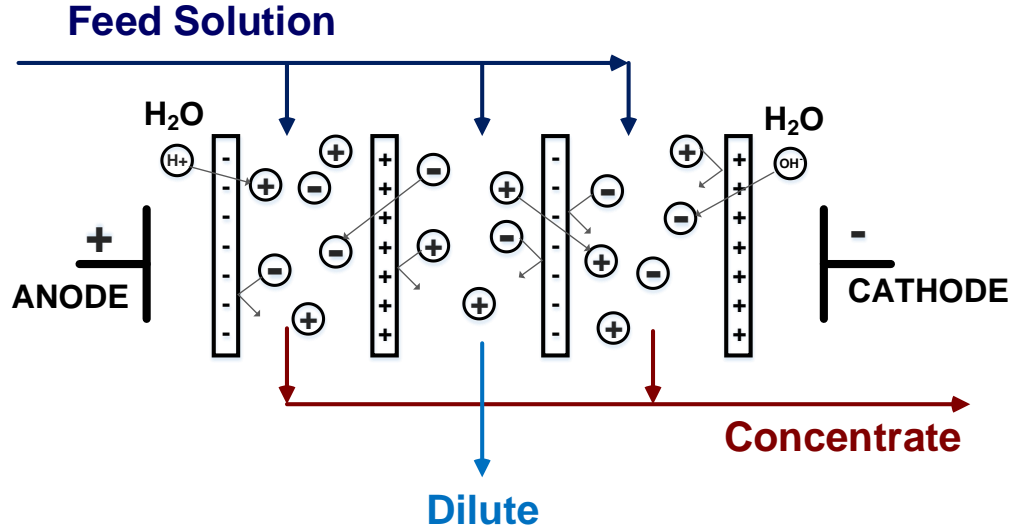


Figure 2.4 A flow-diagram of a conventional *ED* stack

Membrane fouling is considered as the main process drawback for most of the membrane separation techniques; it adversely influence the efficiency of the process [30]. Fouling is caused by the formation of unwanted particles on the surface of the membrane. Generally, these foulants can be categorized into four different groups : colloids, organic matter, inorganic species and biofouling [33]. In an *ED* system suspended charged particles such as humic acids, surfactants, biological matters and polyelectrolytes can attach to the surface of the *CEMs* and *AEMs* and increase their resistance significantly [18, 34, 35, 36, 37]. However, several techniques have been suggested and applied to eliminate the membrane fouling in the *ED* stack. A summary of these methods is given in Table 2.1 [37].

Table 2.1 Applied methods for controlling and minimizing the fouling of the *IEMs* during the electromembrane processes [38]

Method	State of Development	Remarks
Electrodialysis Reversal (<i>EDR</i>)	Industry	<ul style="list-style-type: none"> - Cleaning in place (<i>CIP</i>) - A special system design is required to discharge the dilute and the brine streams - Not applicable for the <i>EDBM</i> system due to the potential <i>BPM</i> damage
Pretreatment	Industry	<ul style="list-style-type: none"> - Removal of multivalent ions, high molecular weight particles and suspended solids - Additional cost and energy due to the installation of the pretreatment unit
Chemical Cleaning	Industry	<ul style="list-style-type: none"> - Cleaning in place (<i>CIP</i>) - Generation of an additional effluent - Additional cost and energy - Some chemicals may affect the <i>IEM</i> integrity
Modification of <i>IEMs</i>	Laboratory	<ul style="list-style-type: none"> - Less power consumption - Less operation cost as no pretreatment step is required - Expensive membranes
Mechanical Action (ultrasound, vibration, and air sparging)	Laboratory	<ul style="list-style-type: none"> - Cleaning in place (<i>CIP</i>) - Additional cost for the special equipment - May affect the <i>IEM</i> integrity
Pulsed Electric Field (<i>PEF</i>)	Laboratory	<ul style="list-style-type: none"> - Cleaning in place (<i>CIP</i>) - Diminishes concentration polarization effect - Simplicity installation
Over Limiting Current Regime	Laboratory	<ul style="list-style-type: none"> - Cleaning in place (<i>CIP</i>) - Eliminates concentration polarization effect - Requires less membrane area - May affect the <i>IEM</i> integrity

2.2.3 Elctrodialysis with Bipolar Membrane (*EDBM*)

The conventional *ED* can be coupled with the *BPMs* and used to produce acids and bases from their corresponding salts. In this process the *CEMs* and the *AEMs* along with the *BPMs* are placed in an alternating pattern inside an *ED* stack as shown in Figure 2.5. As mentioned earlier, when an electric field is applied across the stack, water splitting reaction takes place in the transition layer of the *BPM*. The generated protons and hydroxide ions enter acidic and basic compartments, react with anions and cations migrated from the salt solution (*MX*) and produce an acid (*HX*) and a base (*MOH*), respectively [17, 18, 19] :



The type of application strongly influences the configuration of the *EDBM* cell. For example, if it is intended to produce an acid and a base simultaneously, a three-compartments *EDBM* cell is recommended. On the other hand, when it is not possible to produce acid and base with a high purity, a two-compartment *EDBM* cell is preferred . The three-compartment *EDBM* cell arrangement illustrated in Figure 2.5 is utilized for the simultaneous production of acid and base from their corresponding salt solution. The two-compartment cells which are applied for the base and acid generation are depicted in Figures 2.6 (a) and (b), respectively [18, 38].

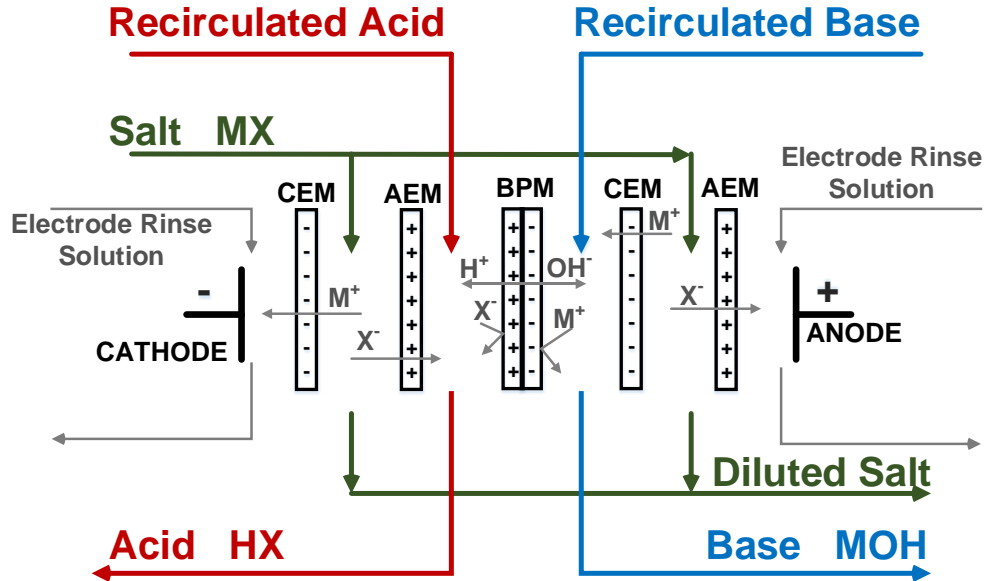


Figure 2.5 A schematic representation of the *EDBM* process

Similar to the conventional *ED*, membrane fouling can impair the productivity of the *EDBM* processes [37]. Most of the techniques listed in Table 2.1 ac also be applied to diminish the fouling phenomenon and sustain the *IEM* integrity throughout *EDBM* process.

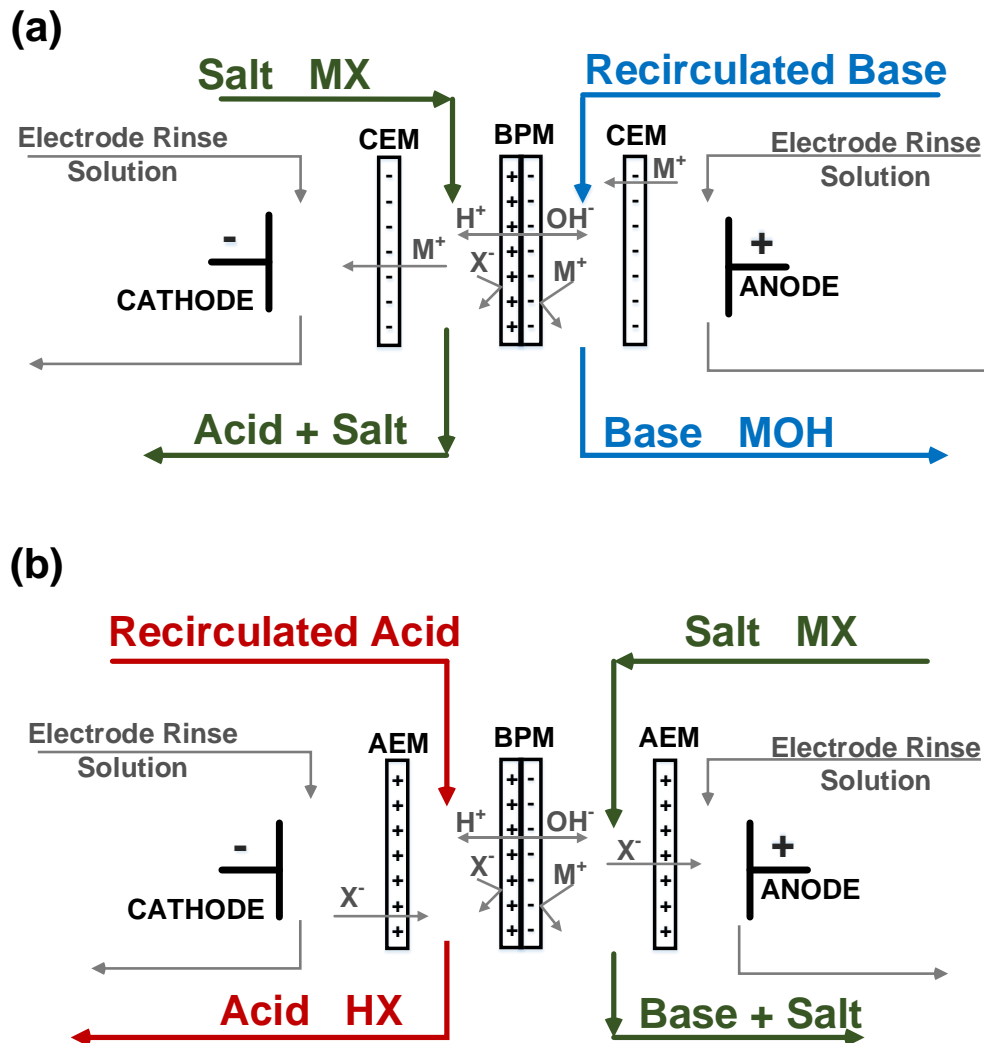


Figure 2.6 Two-compartment *EDBM* cell arrangement for production of (a) base and (b) acid from their corresponding salts

Besides the membrane fouling, poor permselectivity of the *IEMs* can also adversely affect the performance of the *EDBM* system. Figure 2.7, exhibits four different zones : in zone 1, the desirable process takes place ; while, in the rest of the zones, unwanted phenomena affect the current efficiency and hamper the *EDBM* performance. The loss of the permselectivity of the *IELs* of the *BPM* is shown in zone 2. This loss might diminish the purity of the end products. Zone 3 represents the permselectivity failure of the coupled *CEM* and *AEM* which can influence the overall process performance. The diffusional loss is depicted in zone

4, depending on the size of the molecules and structure of the *IEMs*. Weakly ionized small molecules such as HF , NH_3 and SO_2 may cause a concentration gradient and accordingly diffusional failure [38].

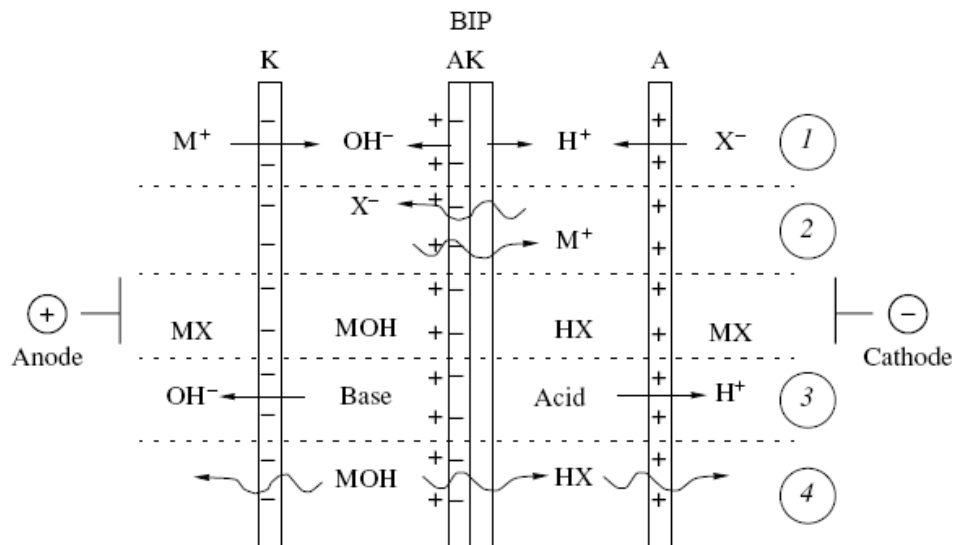


Figure 2.7 Membrane permselectivity failure that can affect the *EDBM* performance [39]

2.3 Critical Literature Review

To the best of our knowledge, there are few scientific papers that report the electrochemical acidification of the Kraft *BL*. Most of the former studies in this area are quite old and do not provide a comprehensive information regarding the best process configuration, effect of the membrane properties, *BL* chemical composition and process conditions on the efficiency of the whole process. Moreover, due to an increasing attention to implementation of the membrane processes in recent years, there are more commercially available *IEMs* with improved specifications which can potentially fulfil the demands as suitable *IEMs* for the electrochemical acidification of the Kraft *BL*. In the following sections, the electrochemical acidification methods are divided into three groups : electrolysis (*EL*), conventional electrodialysis (*ED*) and electrodialysis with bipolar membrane (*EDBM*) techniques.

2.3.1 Electrolysis of Black Liquor

In an electrolytic acidification process, the *BL* is sent to the anode compartment and a diluted $NaOH$ is fed into the cathode compartment of the *EL* cell and a *CEM* separates these two compartments. When the driving force, i.e., the electric field is applied, the sodium

ions go toward the cathode and combine with the hydroxide ions produced from cathodic reduction of water and form the sodium hydroxide. In the other compartment, the hydrogen ions, generated from the anodic oxidation of water, replace the sodium ions. The final main products of the *EL* system are the acidified *BL* and the concentrated caustic soda [16]. An overview of the *EL* acidification of the Kraft *BL* is shown in Figure 2.8.

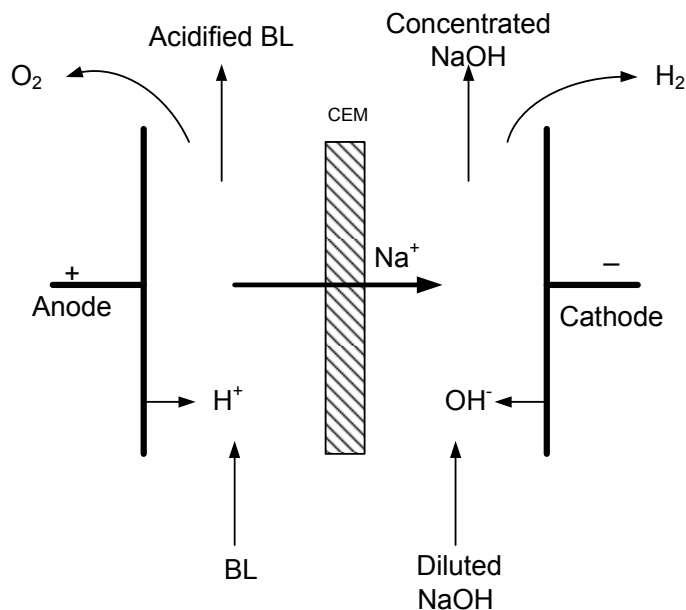


Figure 2.8 Basic operation of the *BL* electrolysis acidification process

Cloutier *et al.* [13, 39, 40] performed a laboratory research on the *EL* acidification of the Kraft *BL* in batch and continuous operational modes. Their studies also covered the effect of the process parameters such as the anode material, current efficiency, operational temperature and the type of the Kraft *BL* on the energy efficiency of the *EL* process. They concluded that the *EL* of the Kraft *BL* process is technically possible but further investigations are required in order to optimize the current density and increase the process efficiency. Furthermore, precipitation of organic materials on the surface of the anode is mentioned in former studies on the *EL* of the Kraft *BL* [16, 39, 40, 41]. This precipitation caused anode's fouling which led to a rapid increase in the voltage drop across the *EL* cell.

In 2005, Nergo *et al.* [16] conducted a study on the electrolytic treatment of straw weak *BL* in a batch mode. They claimed that the anode fouling can be prevented by working under a high current density and a high velocity as well as employing two *Pt* wire electrodes parallel to the flows inside the *EL* cell. They also reported that performing the *EL* process at a higher operational temperature may increase the current efficiency [16].

2.3.2 Electrodialysis of Black Liquor

In a three-compartments *ED* cell that is illustrated in Figure 2.9, the *BL* is fed into the central compartment and the distilled water is sent to the electrode compartments of the cell. Under the electric field, the positively charged ions cross the *CEM* and proceed towards the cathode; conversely, the negatively charged ions pass the *AEM* and go towards the anode. The outlet streams of this process are the treated *BL* and soda [42].

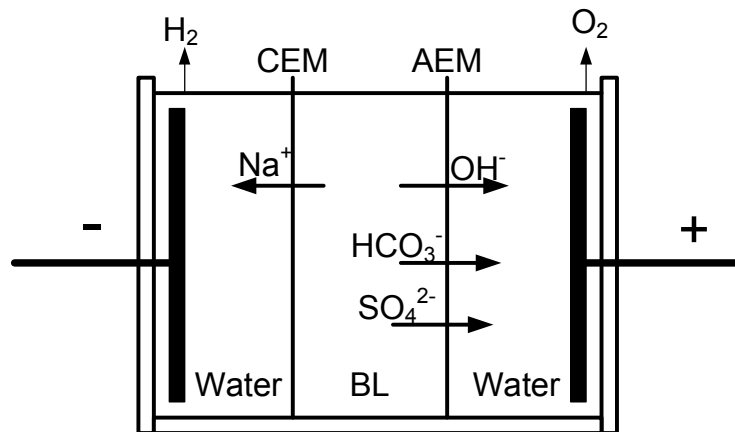


Figure 2.9 Electrodialysis of black liquor in three compartment arrangement

Mishra *et al.* [42, 43] were one of the pioneer research groups who explored the technical feasibility of *ED* treatment of an alkaline *BL* in batch and continuous modes. They examined the effects of the current density, pH, residence time (in batch operation) and amount of recovered soda with the three-compartments *ED* stack. They proposed to use the amount of the energy consumption as a criterion for choosing the best operating conditions. In term of the flow velocity, they reported that at a low flow velocity a higher amount of the soda was recovered and less energy was consumed; however, performing the *ED* process at a low velocity resulted in more pronounced anode fouling.

In 2013, Cloutier *et al.* [44] performed the conventional *ED* treatment of the Kraft *BL* employing an *ED* stack made of four pairs of the *AEMs* and *CEMs* placed in an alternating pattern between the electrode pair. They indicated that the *ED* treatment process cannot completely neutralize the alkalinity content of the Kraft *BL* solution and as a result this technique can only demineralize the Kraft *BL*, to some extent. Therefore, another acidification step is required to complete the acidification process and drop the pH of the Kraft *BL* to a point that lignin can be extracted from it, efficiently [44].

2.3.3 Electrodialysis of Black Liquor using Bipolar Membrane

The *EDBM* acidification of the *BL* attracted less attention in previous studies due to the lack of suitable and available *BPMs* for this process. In 1990, Koumoundouros *et al.* [45] carried out a laboratory feasibility study on the recaustization of the oxidized Kraft *BL* using *EDBM* technique. They built their experimental set-up to obtain information about the current efficiency, energy consumption per gram of produced caustic soda and an estimation of membrane fouling and life time. Prior to the *EDBM* process, they conducted the CO_2 acidification to drop the pH of the Kraft *BL* to 9; afterwards, two filtration steps were done followed by another acidification with sulfuric acid to lower the pH to 2 in order to extract the lignin (Figure 2.10). The outcome of their investigation can be summarized as follow :

- With regards to the type of the Kraft *BL* (softwood vs. hardwood), they observed that working with softwood Kraft *BL* yielded a better current efficiency than with hardwood.
- Further investigation is required to optimize the energy consumption and the stack configuration to make this process ready for the pilot scale.

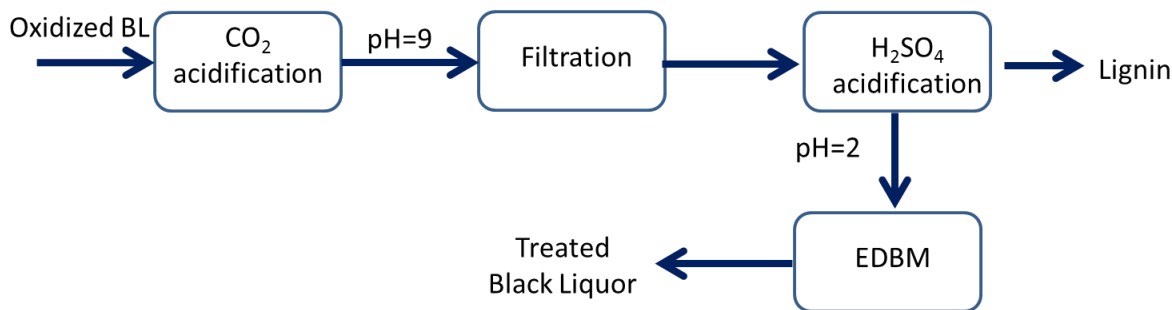


Figure 2.10 The *BL* recaustization steps performed by Koumoundouros *et al.* [46]

CHAPTER 3 OBJECTIVES AND METHODOLOGY

As mentioned in the critical literature review, there are limited scientific studies that have addressed the electrochemical acidification of Kraft *BL*, particularly by means of the *EDBM* process. Most of the former studies are quite old and do not provide comprehensive information regarding the best process configuration, effect of *IEMs*, *BL* chemical composition and operational conditions on the efficiency of the whole process. On the other hand, due to an increasing attention to the membrane processes, nowadays, there are more commercially available *IEMs* and *BPMs* with improved properties which may answer the demands for electrochemical acidification of the Kraft *BL*. Therefore, the main objective of this research project was defined as follow :

3.1 Main Objective

To identify, design and develop an eco-efficient and efficient process to acidify Kraft black liquor and effectively extract lignin.

In order to accomplish the main objective three specific objectives are formulated :

- ***Specific Objective 1*** : To propose and validate a new green technology for Kraft black liquor acidification and efficient lignin extraction
- ***Specific Objective 2*** : To evaluate the performance of the proposed process as a function of membrane properties, black liquor chemical composition and operational conditions
- ***Specific Objective 3*** : To enhance the process performance in terms of high efficiency and low chemical and energy consumption and diminish membrane fouling

3.2 Methodology

In order to achieve the specific objectives and eventually the main objective, this research project was divided into three main phases as illustrated in Figure 3.1.

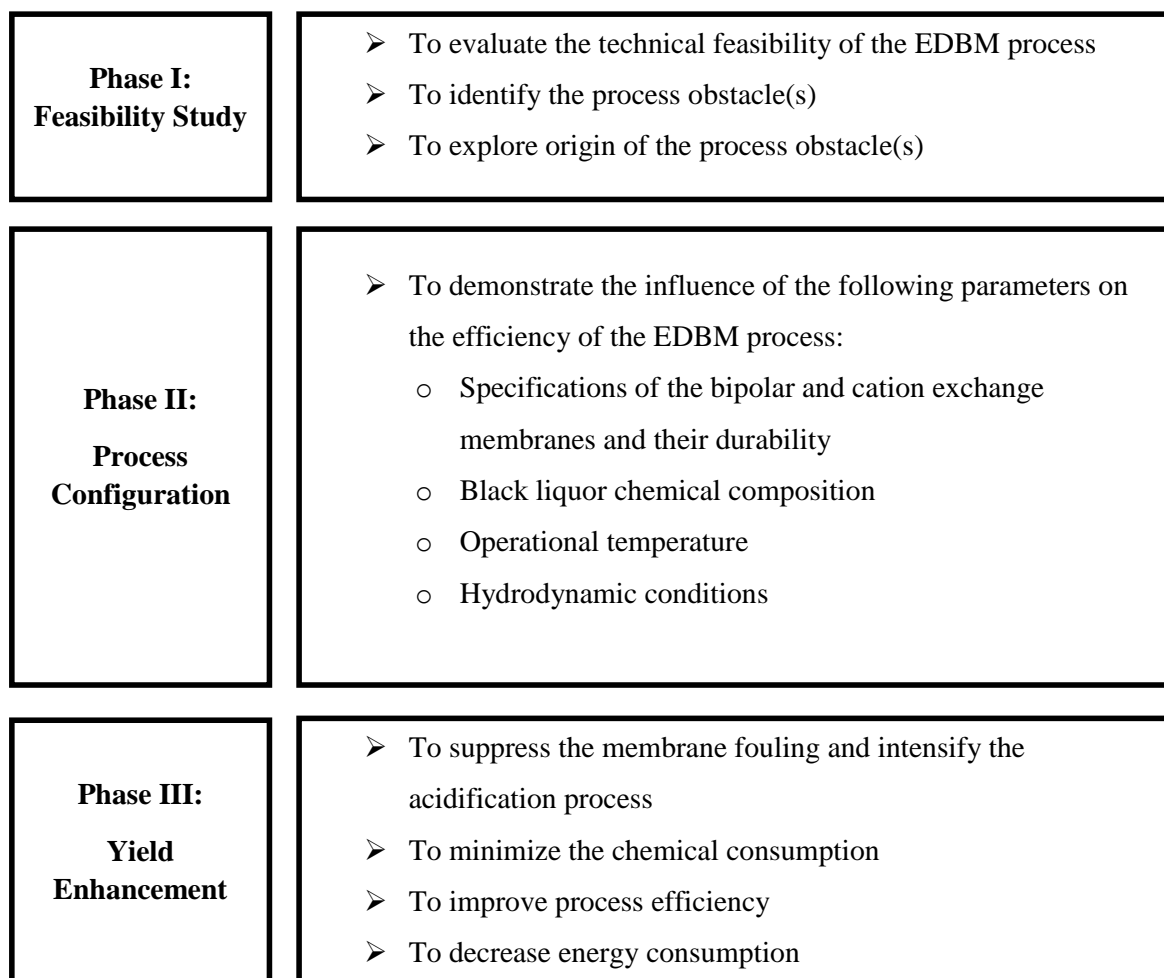


Figure 3.1 A representation of overall methodology phases

Phase I - Feasibility Study : As stated in chapter 1, a portion of lignin can be extracted from the black liquor (*BL*) prior to the combustion step and converted to a wide spectrum of value-added products. In addition, lignin extraction from the *BL* also enhances the capacity of the mill by lowering the load of its recovery boiler. In order to perform this extraction, identification, design and development of a suitable *BL* acidification process is mandatory. The proposed method must accomplish the requirements in terms of a high efficiency, a low chemical and energy consumption along with environmental constrains. To this end, applying electrochemical acidification of Kraft *BL* via electrodialysis with bipolar membrane (*EDBM*) seems to be a promising eco-efficient approach due to its low level of chemical and energy consumption. Furthermore, acidifying the *BL* in the *EDBM* system produces caustic soda which can be used in the Kraft process or other industries. However, to evaluate this preposition and validate the proposed method a technical feasibility study is imperative.

This study must demonstrate the advantages of the *EDBM* method and detect its main drawbacks. Based on the results of this study we can look for appropriate efforts to minimize the obstacles and enhance the process efficiency.

Phase II - Process Configuration : As explained in the literature review, *IEMs* are one of the key elements of the *EDBM* system. Therefore, the first step of this phase involves in screening the most reliable and commercially available *IEMs* and evaluating their performances during the electrochemical acidification process. In addition, in the presence of the membrane fouling, identification and selection of the most appropriate cleaning procedure is prime important.

The final step of this phase determines the influence of the operational process variables on performance of the *EDBM*. In principle, process conditions play an important role in controlling the fouling of the membranes and performance of the membrane-based technologies. The productivity of an *EDBM* process is governed by various parameters. The nature of the feed solutions and desired quality of the products determine a number of these parameters, while some process variables such as applied current density, electrical conductivity, viscosity and operational temperature of the feed solutions can be varied in specific ranges based on the stack and *IEMs* properties and limitations. The obtained results of this phase enables us to enhance the process efficiency and minimize the membrane fouling.

Phase II - Yield Enhancement : Based on the findings of the previous phases adequate efforts need to be taken in order to eliminate any kind of membrane fouling during the *EDBM* process and minimize the chemical consumption, co-ion leakages and improve the current efficiency of the process.

3.3 Presentation of Publications

The five following chapters present the main results of this thesis. The first article is presented in chapter 4. It describes the technical feasibility of the electrochemical acidification of the Kraft *BL* and is entitled «A Feasibility Study of a Novel Electro-Membrane Based Process to Acidify Kraft Black Liquor and Extract Lignin». This article have been submitted to Process Safety and Environmental Protection Journal.

Article 2 presents a comprehensive microscopic study on the fouling identification of the *IEMS* during the electrochemical acidification process. The mechanisms of the lignin colloidal fouling has been elucidated in this article. This article has been submitted to Journal of Colloid and Interface Science.

Article 3 is entitled «Electrochemical Acidification of Kraft Black Liquor : Effect of Fouling

and Chemical Cleaning on Ion Exchange Membrane Integrity» and has been submitted to *ACS Sustainable Chemistry & Engineering Journal*. In this article, the effects of fouling and chemical cleaning cycle on the *IEMs*' integrity were investigated. The one of the main goals of this work was to fundamentally understand the cleaning mechanisms and evaluate the impact of the cleaning solutions on foulants removal for different types of commercially available *IEMs*, in order to select the most reliable *IEMs* as well as the proper cleaning conditions for the chemical cleaning step of the *EDBM* process.

The «Effect of Process Variables on the Performance of Electrochemical Acidification of Kraft Black Liquor by Electrodialysis with Bipolar Membrane» is presented in Article 4. This article has been submitted to *Chemical Engineering Journal*.

Article 5 describes the results of the successful application of an in-line cleaning step on suppression of the lignin colloidal fouling and intensification of the electrochemical acidification process. This article is entitled «Electrochemical Acidification of Kraft Black Liquor : Impacts of Pulsed Electric Field Application on Bipolar Membrane Colloidal Fouling and Process Intensification» and has been submitted to *Journal of Membrane Science*.

«Black Liquor Acidification for Lignin Extraction : A Preliminary Comparison between Chemical and Electrochemical Acidification Pathways» is presented in chapter 9. This chapter is considered as an additional study reporting the assets of the green and sustainable electrochemical acidification pathway. It gives suggestions for further improvements of the lignin aging and filtration steps. The results of this chapter may be extended into an article and will be submitted for a publication.

CHAPTER 4 ARTICLE 1 : A FEASIBILITY STUDY OF A NOVEL ELECTRO-MEMBRANE BASED PROCESS TO ACIDIFY KRAFT BLACK LIQUOR AND EXTRACT LIGNIN

Maryam Haddad ^a, Laurent Bazinet ^b, Oumarou Savadogo ^a, Jean Paris ^a

a : Research Unit on Energy Efficiency and Sustainable Implementation of the Forest Biorefinery (*E²D²BF*), Department of Chemical Engineering, Polytechnique de Montréal, Canada

b : Institute of Nutrition and Functional Foods (*INAF*), Laboratory of food processing and electromembrane processes (*LTAPEM*), Department of Food Sciences, Université Laval, Canada

Abstract

Lignin extraction from black liquor is of utmost importance for decreasing the load of the recovery boiler and consequently increasing the production capacity of Kraft process. A feasibility study of a novel acidification technique (acidification with electrodialysis using bipolar membrane (*EDBM*)) was carried out to drop the pH of Kraft black liquor and extract lignin. In order to evaluate the technical feasibility of the proposed method, the acidification of the Kraft black liquor was performed in two different pathways i.e. electrochemical acidification by means of *EDBM* process and chemical acidification using sulfuric acid. The results have indicated that the implementation of the proposed method yields in use of less chemicals than the chemical acidification method and simultaneously production of caustic soda. The experiments performed in the course of this study addressed the advantages and challenges of this electro-membrane based process in the Kraft black liquor acidification application.

Keywords : Bipolar membrane, electrodialysis, Kraft black liquor, lignin extraction, electrochemical acidification, chemical acidification

4.1 Introduction

Decreasing demand of traditional pulp and paper products, competition from emerging economies and oil price volatility as well as incentives for green products encouraged the pulp and paper industry to look for novel non-paper products made from wood components. Kraft process is a predominant pulping process that could be perfectly incorporated to integrated forest biorefinery (*IFBR*) [3]. An *IFBR* plant is able to produce new value-added products

and chemicals along with traditional pulp and paper products. Lignin extraction is a promising option for the Kraft *IFBR*. In a conventional Kraft mill, wood chips are cooked in a digester under strong alkaline and high temperature conditions resulting in delignification of wood. The cooked liquor goes to a washing step where pulp is separated from the residual liquor i.e. black liquor (*BL*). *BL* contains lignin, organic acids and spent cooking chemicals [46]. In most existing Kraft mills, the *BL* is concentrated in a multistage evaporators and burnt in the recovery boiler to recover pulping chemicals and produce steam and electricity. In a lignin biorefinery context, a portion of the lignin could be extracted from the *BL* before combustion step (Figure 4.1). In addition to enhancing the capacity of the mill by debottlenecking the recovery boiler, the extracted lignin can be utilized as biofuels or as a precursor to a vast phenolic platform of chemical pathways [6].

Various techniques have been examined for lignin extraction such as the application of fungi and bacteria as well as the implementation of a supercritical fluid extraction process. The complex and toxic nature of the *BL* strongly influences the yield of these methods and the high operating cost have limited their applications [7, 8]. An extensive study on lignin separation by means of ultrafiltration (*UF*) membranes has been performed in Sweden. The extraction was based on lignin molecular weight which resulted in a narrow potential market for the lignin separated by *UF* [9, 47, 48, 49]. Chemical acidification is the most practical method in which lignin precipitation and, consequently, lignin separation occurs by reducing the pH of the *BL*. Even though the yield of the acid precipitation pathway is high, utilization of chemicals i.e. CO_2 and H_2SO_4 acid can interact with sodium-sulfur balance in the mill. Loutfi *et al.* and Alen *et al.* [10, 11] recommended CO_2 acidification due to its less impact on the sodium-sulfur balance and easier filterability of the lignin. However, high CO_2 cost is one of the main concerns for a mill to practice this process. Some researchers [11, 50] suggested an internal source of CO_2 in a Kraft mill, mainly utilization of lime kiln flue gas. Most recently, Kannangara [4] conducted a feasibility and economic analysis study on possibility of replacement of the clean CO_2 with existing CO_2 in the lime kiln flue gas. He concluded that the application of the flue gas is less motivating as a consequence of high filtration resistance for non-oxidized *BL* as well as installation of high-priced gas cleaning apparatus.

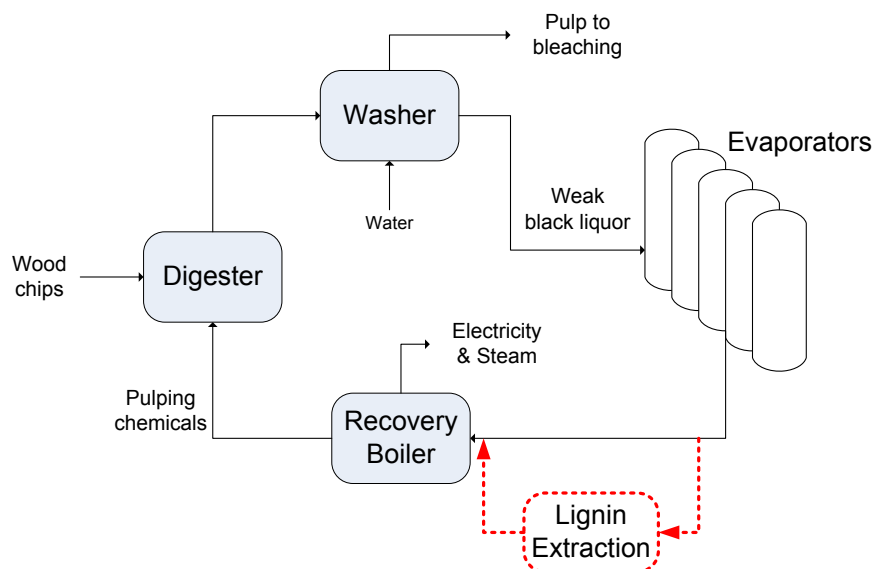


Figure 4.1 A simplified illustration of the Kraft pulping process

The unique nature of the *BL*, which consists of inorganic salts such as Na_2CO_3 , Na_2SO_4 and Na_2S salts as well as organic components such as lignin and hemicelluloses components, motivated researchers to examine electrochemical acidification processes to acidify the *BL* and extract the lignin. Among all electrochemical processes, membrane electrolysis attracted more attentions [13, 16, 39, 40, 41, 51]. In the membrane electrolysis (*EL*) process, the *BL* is sent to an anode compartment and a diluted $NaOH$ is fed into a cathode compartment of an *EL* cell (Figure 4.2). A cation exchange membrane (*CEM*) separates these two compartments. When the driving force (electric field) is applied, in the cathode compartment, the sodium ions presented in the *BL*, migrate toward the cathode and combine with hydroxide ions produced from cathodic reduction of water and form sodium hydroxide. In the other compartment, the hydrogen ions, generated from the anodic oxidation of water, replace the sodium ions presented inside the *BL* solution. The outlet stream of the anodic compartment is the acidified *BL*. The performance of this process is strongly dependent on the anode specifications. Only a few specific types of anode have been reported to possess a reasonable durability for the *BL* acidification process. Moreover, deposit of the lignin on the surface of the anode has been observed [13, 16, 41]. On top of the above constraints, in large scale application, high energy is required for the redox reactions which take place at each electrode pair. In addition, a considerable amount of produced side gases, as well as a high price of electrodes for a multiple *EL* cell configuration have to be taken into account.

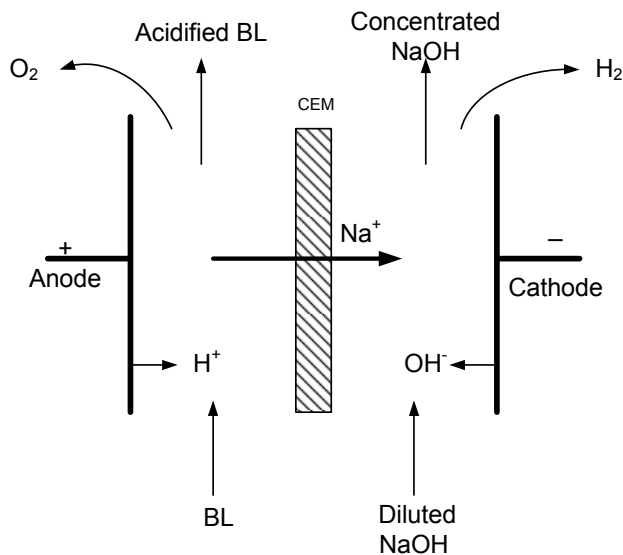


Figure 4.2 Basic operation of the *BL* electrolysis (*CEM* : Cation exchange membrane)

Electrodialysis with bipolar membrane (*EDBM*) can be proposed as a novel and more sustainable electrochemical pathway to acidify the *BL* and extract the lignin. This technique requires a significantly reduced chemical consumption in comparison to acid precipitation methods and simultaneously recaptures caustic soda. In this process, only charged membranes (cation exchange and bipolar) are involved in ion transport phenomena while the electrodes redox reactions do not interplay with the acidification process. Therefore, the applied electrodes in the *EDBM* stack are only electrical terminals, soaked in electrolyte solution, transferring the current [52]. Despite the fact that several successful applications of the *EDBM* are stated in the literature [17, 18, 22, 52, 53, 54], no attention has been paid to this process for the *BL* acidification purpose. One of the reasons is due to a low chemical and mechanical stability of ion exchange membranes at high alkaline conditions. To date, there are commercially available ion exchange membranes with improved specifications which may fulfill the demands for the electrochemical acidification of the *BL*. Thus, the aim of this study is to evaluate the technical feasibility of the *EDBM* process to acidify the Kraft *BL* and address its challenges. This analysis opens a new window to investigate the advantages of a green and sustainable electrochemical acidification method over the chemical acidification process.

4.2 Theoretical Background

4.2.1 Principle of Electrodialysis by Bipolar Membrane to Acidify Kraft Black Liquor

The type of application strongly influences the configuration of the *EDBM* cell. For example, if it is desirable to produce acid and base simultaneously, a three compartment *EDBM* is recommended. On the other hand, wherever it is not possible to produce acid and base with high purity, a two compartment *EDBM* cell is preferred [17, 18, 22]. In this study, a two compartment *EDBM* was utilized in which an alternating series of bipolar membranes (*BPM*) and cation exchange membranes (*CEM*) were placed inside the stack.

Once the electric field is applied, water dissociation reaction takes place inside the *BPM* :



In the *BL* compartment, the sodium ions pass through the *CEM* and enter the caustic soda compartment (Figure 4.3). In this compartment sodium ions can react with hydroxide ions (produced from the water splitting reaction) and form caustic soda.

The presence of proton ions (from the *BPM* water dissociation reaction) inside the *BL* compartment results in pH drop of the *BL*. Therefore, the final products of the *EDBM* process are the acidified *BL* and concentrated caustic soda (Figure 4.3)

It should be noted that during the *EDBM* process, the water oxidation and reduction reactions take place at the electrode compartments ; but they do not interfere with the global process, since both electrode compartments are mixed together and recirculated :

Cathode : Water reduction :



Anode : water oxidation :



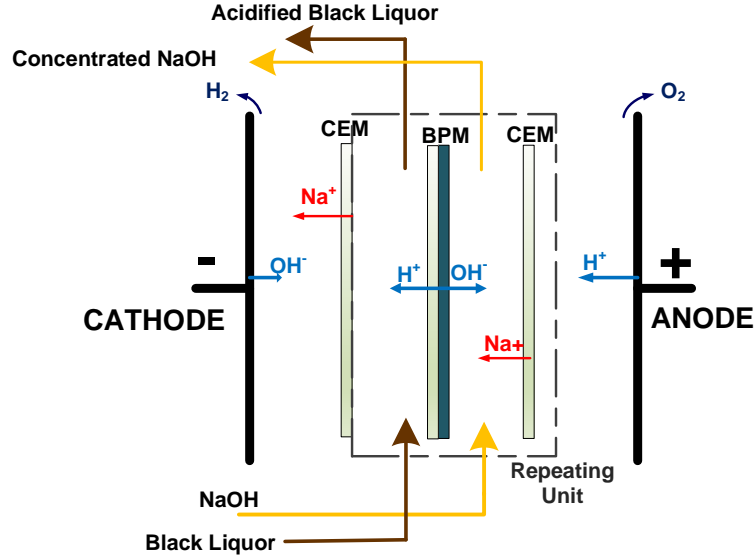


Figure 4.3 Principle of electrodialysis with bipolar membrane (*EDBM*) for the acidification of Kraft *BL* (*BPM* : bipolar membrane and *CEM* : cation exchange membrane)

4.2.2 Lignin Precipitation Yield

Yield of lignin precipitation is determined as follow :

$$Lignin\ Precipitation\ Yield = \frac{L_{BL} - L_f}{L_{BL}} \times 100 \quad (4.4)$$

Where L_{BL} and L_f are the lignin content of the fresh and filtrated *BL* ($g\ Kg^{-1}\ TDS$), respectively [5].

4.3 Experimental

4.3.1 Membranes and Materials

Membranes used in this study were Fumasep *FBM* bipolar membrane and Fumasep *FKB* cation exchange membrane (Fumatech Co., Germany). Their main characteristics are listed in Table 4.1.

Table 4.1 Ion exchange membranes specifications provided by their supplier

Membrane	Type	Thickness (mm)	IEC (meq. g^{-1})	Specific Area Resistance ($\Omega.\text{cm}^2$)	Stability (pH)	Temperature °C
<i>FKB</i>	Cation	0.10 - 0.13	1.2 – 1.3	4 – 6	1 – 14	≤ 60
<i>FBM</i>	Bipolar	0.18 - 0.20	-	-	1 – 14	≤ 60

Softwood black liquor was supplied by a Canadian Kraft mill with a total dissolved solids (*TDS*) content of 50 ± 2 % (wt.). It was diluted to 30 % (wt) and pre-filtered to remove any suspended solid particles larger than $0.010 \mu\text{m}$ utilizing a simple vacuum filtration apparatus and a filter paper (Whatman Grade 111105, UK). Analytical grade sodium hydroxide and sodium sulfate were purchased from Sigma-Aldrich, Canada. Sulfuric acid (10.00 *N* Standard Volumetric Solution) and hydrochloric acid (1.00 *N* Standard Volumetric Solution) were supplied by Fisher Scientific, Canada. Demineralized water was used to prepare all the solutions .

4.3.2 Methods

In this study, two acidification pathways were followed : chemical acidification and electrochemical acidification via *EDBM* method. The amount of acidifying agent (10.00 *N* sulfuric acid) along with the filtration rate and the lignin precipitation yield were considered as the criteria to compare these methods.

Chemical Acidification

The chemical acidification process was performed in a laboratory scale set-up consisting of a 2 *L* open jacket reactor connected to a hot water bath (to maintain the operational temperature), a burette and a pitched blade turbine (*PBT*) impeller attached to a mixer (Model : Caframo *BDC* 2002, Caframo Limited, Canada) with 1 *RPM* accuracy. Three replicates of the chemical acidification experiment were performed for the *BL* at 30 % (wt.) concentration.

Electrochemical Acidification

The electrochemical acidification experiments via *EDBM* were carried out using an *EDBM* cell consisting of two electrode compartments separated by two 0.75 *mm*-thick spacers. The anode was made of platinum plated titanium and the cathode was stainless steel. Three pumps (Model : IWAKI Magnetic Drive Pump *MD. 30 R*, Iwaki America Inc., USA) were

used to pump the solution into the stack. A schematic diagram of the experimental set-up is presented in Figure 4.4. The cell was operated in galvanostatic mode, i.e., the applied current density, supplied by DC power supply (Model : Xantrex XKW 40-25, USA), was constant while the voltage was allowed to vary across the stack. In each reservoir a jacket coil heat exchanger was installed in order to maintain a constant operational temperature.

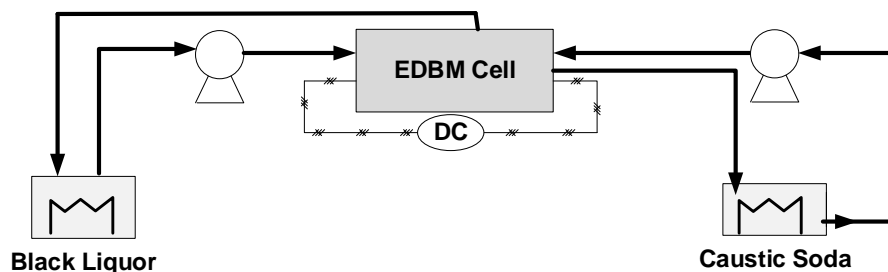


Figure 4.4 Schematic diagram of the electrochemical acidification process

4.3.3 Protocol

Chemical Acidification

The pH of 2 L of BL at a TDS content of 30% (wt.) was brought to 9.7 by manually adding 10.00 N sulfuric acid. A pH range of 8 - 10 was reported to be an optimal range which would result in a high yield and an easy filterability of lignin [10, 11]. The operational temperature was adjusted to 75 ° C [4]. The solution was very well mixed. When the desired pH was obtained, the mixing was carried on for one hour at the same speed (150 RPM) and operational temperature. This phase is referred to as the aging step [4]. The slurry of the aging phase was cooled down to room temperature and then filtered using a simple vacuum filtration set-up (a buchner funnel connected to a 2 l filtration flux) at 75 kPa. A lignin cake was formed on top of the filter paper (Whatman Grade 113, UK). In the washing step, 300 ml of 0.80 N sulfuric acid and 200 ml of demineralized water were poured on top of the lignin cake, respectively. The wet lignin was weighted, then it was dried (24 hours air dried and an overnight oven drying at 105 ° C). Finally, the weight of the dried lignin was recorded.

Electrochemical Acidification

All the experiments were performed in batch mode using 2 L of BL 30% (wt), 2 L of NaOH (0.5 M) and 2 L of Na₂SO₄ (0.5 M) in the BL, caustic soda and electrode reservoirs, respectively. Prior to the acidification process, preliminary measurement of limiting current density was performed based on the Cowan and Brown method [55]. For each experiment, the pH

and the electrical conductivity of the *BL*, *NaOH* and electrode rinse solution (Na_2SO_4) were monitored independently using Metrohm Unitrode glass pH electrodes and Metrohm conductivity meters (Model : 716 conductometer, Switzerland). The operational temperature was kept constant at 35 °C. The applied process conditions are given in Table 4.2

Table 4.2 Applied operational conditions during electrochemical acidification method

Operational Conditions	Data
Number of Operating Units	4
Re-circulation Flow Rate	1.0 l min^{-1}
Pressure Drop	34.5 kPa
Applied Current Density	330 A. m^{-2}
Effective Membrane Surface Area	0.0180 m^2
Operational Temperature	35 °C

After the electrochemical acidification stage, the acidified *BL* was transferred into the chemical acidification apparatus which is described above. The pH of the acidified *BL* was checked at 75 °C; if it was higher than 9.7, 10.00 *N* sulfuric acid was added to the *BL* to adjust its final pH to 9.7. Then, the aging, filtration and washing steps were conducted based on the procedure explained in the earlier part. Three replicate experiments were performed for each set of the electrochemical acidification of the Kraft *BL*.

4.3.4 Analyses

Feed Analyses

The *TDS* of the *BL* was measured by an overnight drying (105 ° C) of weighed samples and then measuring the weight of the residue. *BL* ash content was determined by heating the residual from the *TDS* measurement to 950 ° C for 16 hours and then measuring their weights. The ratio of the residue weight before and after combustion at 950 ° C gives the ash content. Lignin content was measured by a *UV* spectrophotometer at wavelength of 280 *nm*. Prior to the *UV* measurement, 2 *g* of the *BL* was diluted in 100 *ml* of 0.1 *M NaOH* and again diluted with demineralized water to absorbance of 0.3 - 0.8 with an absorption coefficient of $23.7 \text{ dm}^3 \text{ g}^{-1} \text{ cm}^{-1}$. Sodium concentration of the *BL* was analyzed based on *SCAN-N-37* : 98 test method [56]. Residual effective alkali was measured applying the Radiotis *et al.* procedure [57]. The caustic soda concentration was calculated by titration of 20 *ml* of the *NaOH* sample with 1.00 *N HCL* acid using Metrohm (Model : 916 – *TiTouch*, Switzerland) potentiometric titrator. The *BL* specifications are listed in Table 4.3.

Table 4.3 Characteristics of Kraft Black Liquor

Characteristics	Data
Total Dissolved Solid (TDS)(%)	30.2
UV Lignin (% TDS)	40.4
Ash Content (% TDS)	28.1
Sodium Concentration (% TDS)	18.1
Residual Alkali (g/L)	7.2

4.4 Results and Discussion

4.4.1 Black Liquor Electrical Conductivity

It is essential for energy performance purposes to utilize the maximum concentration of the BL at which its electrical conductivity is highest. Generally, the electrical conductivity of an electrolyte solution is based on the ability of the solution to carry an electric field by motion of its charged ions [58]. The electric field is provided by a pair of electrode connected to a DC power supply. The electrical conductivity is the opposite of the electrical resistance [58]. Therefore, for the electrochemical acidification of the Kraft BL , a higher BL electrical conductivity would result in a lower voltage evolution inside the $EDBM$ stack.

Figure 4.5 shows the electrical conductivity profiles of a wide range of BL concentration (5 to 50 % (wt)) measured at two arbitrary temperatures (23 ° C and 35 ° C). Indeed, for all the examined TDS contents, increasing the temperature of the BL solution considerably improved its electrical conductivity. This can be related to the fact that the mobility of the ions in the BL solution increased with the temperature. Thus, at all the examined TDS contents, the electrical conductivity of the BL solution was higher at 35 ° C .

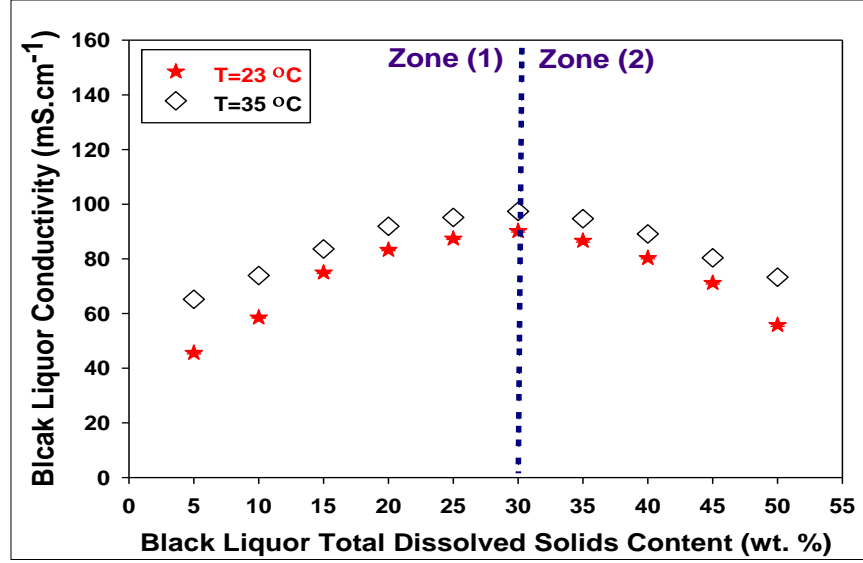


Figure 4.5 Evolution of the Kraft *BL* electrical conductivity as a function of temperature and *TDS* content of the *BL*

The electrical conductivity profiles can be divided into two zone. In zone (1), the *BL* electrical conductivity increases monotonously with the concentration to reach a peak at about 30 % (*wt*) concentration. However, increasing the *BL* concentration further caused its electrical conductivity profiles to decrease (zone (2)). The first increment in the *BL* electrical conductivity profile is explained by the fact that at a higher concentration, more charged ions are present inside the electrolyte solution (*BL*) to carry the electrical field [58]. By contrast, the high viscosity of the concentrated *BL* can adversely affect the ion mobility and decrease its electrical conductivity. In addition, when the concentration of the electrolyte solution (*BL*) rises, the ion-ion interactions become more pronounced and, consequently, the electrical conductivity of the solution declines [58].

4.4.2 Electrochemical Acidification of Kraft Black Liquor

As the pH of the *BL* decreases, the voltage drop across the *EDBM* stack increases slightly, due to the decrease of the electrical conductivity of the *BL* (Figure 4.6 (a) and (b)). However, the trend of the voltage drop profile does not follow a constant pattern throughout the *EDBM* acidification process. In order to identify the cause of this trend, two scenarios were considered :

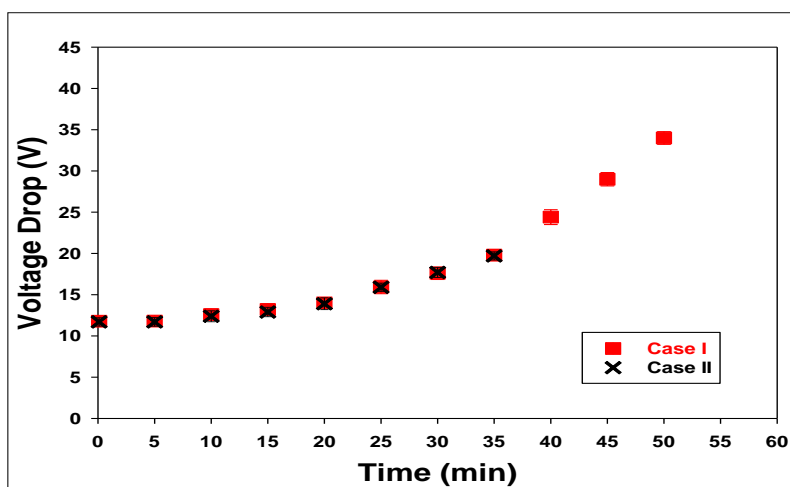
- First scenario (Case I) : the electrochemical acidification process was carried out until the limiting voltage of the DC power supply was reached.

- Second scenario (Case II) : the electrochemical acidification process was stopped when a quick rise in the voltage drop profile occurred.

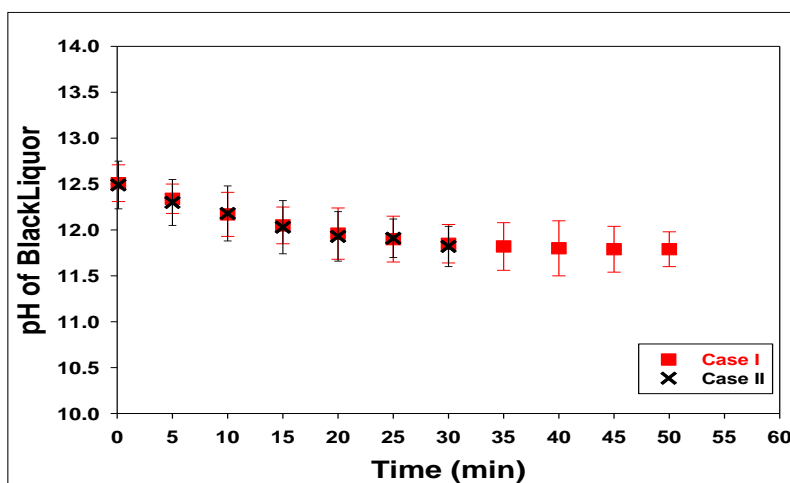
In both cases, at the end of the electrochemical acidification phase, the *EDBM* stack was disassembled for examination and the acidification process was continued in the open jacket reactor using 10.00 *N* sulfuric acid as the acidifying agent.

As illustrated in Figure 4.7 ((a) and (b)), a brownish deposit was observed on the surface of the ion exchange membranes which were in contact with the *BL* solution during the *EDBM* process. It should be noted that the intensity of the deposit was remarkably higher in case I. Since the *BL* is a complex mixture of alkali lignin, inorganic acids and polysaccharides, together with inorganic salts [5, 46, 59], the deposited layer could consist of either colloidal or organic fouling, scaling or a combination of both [54, 60].

(a)



(b)



(c)

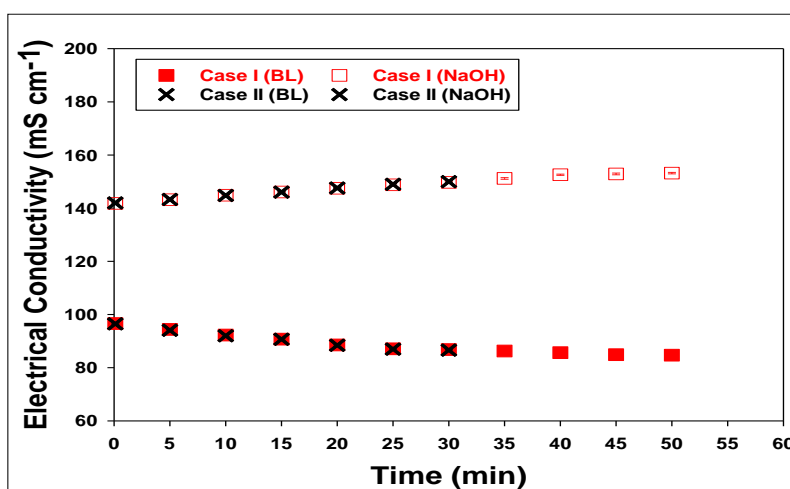


Figure 4.6 (a) Voltage drop, (b) pH evolution of *BL* and (c) electrical conductivity profiles of *BL* and *NaOH* during electrochemical acidification of Kraft *BL*

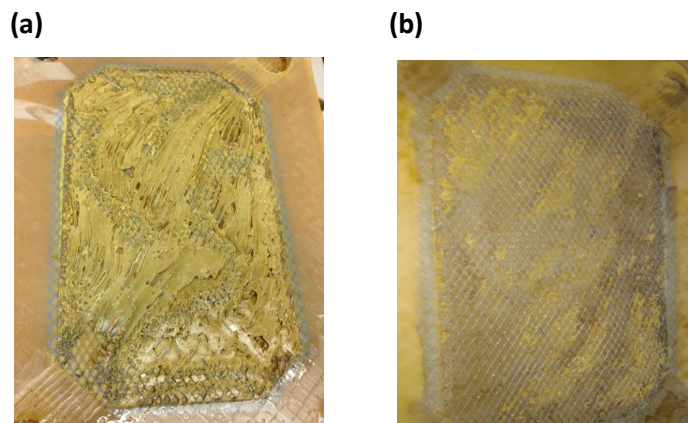


Figure 4.7 Formed deposit layer on the surface and in the space between the ion exchange membranes inside *BL* compartment during the electrochemical acidification of the Kraft *BL* (a) : case I (the electrochemical acidification was terminated when the voltage limit of the DC power supply was reached) (b) : case II (the electrochemical acidification was stopped when the voltage drop started to increase rapidly)

Figure 4.6 ((a) and (b)) shows that when the pH of the *BL* reached 11.7, the voltage drop started to rise rapidly. Thus, it can be presumed that a fraction of this deposited layer is lignin. Frederick [61] stated that at high pH (>12.5) lignin is completely dissolved in the *BL*. By lowering the pH of the *BL* and entering the « intermediate zone » ($12.5 < pH < 11.5$), partial dissolution of lignin takes place [59]. The dissolution phenomenon can induce lignin self-aggregation and subsequently lignin precipitation [4, 5, 62, 63, 64].

In case I, rapid evolution of the voltage drop occurred and, consequently, the system resistance drastically affected the *BL* pH drop pattern and hindered its progress (Figure 4.7 (b), case I). In addition, no significant change was observed in the *BL* and *NaOH* electrical conductivity profiles (Figure 4.7 (c)). Accordingly, it can be presumed that the quick fouling inside the *EDBM* cell could disturb the ions transfer during the electrochemical acidification process.

4.4.3 Comparison of Electrochemical Acidification and Chemical Acidification Methods

To perform the electrochemical acidification process, an electrical field was used as the driving force in the *EDBM* system. Two products were obtained by the electrochemical approach i.e. acidified *BL* and concentrated caustic soda, while by the chemical acidification, acidified *BL* was the only product. The chemical acidification of the Kraft *BL* produced a higher filtration rate and lignin precipitation yield (Figure 4.8 (a) and (b)) which are in agreement with the

data reported by Kouisni *et al.* [12]. Lower filtration rates and lignin precipitation yields in cases I and II indicate that lignin was present in the deposit formed inside the *EDBM* stack. The lignin lost is less pronounced for case II, which suggests that lignin precipitation may cause the significant increase in the system resistance. Clearly, it would be preferable to terminate the electrochemical acidification step just before the fast elevation in the voltage drop would occur and continue the acidification process via a chemical acidification method. In addition, analysis of the fouled layer is crucial in identifying its composition and preventing its occurrence [60, 65].

The amount of consumed acid for all the cases is illustrated in Figure 4.8 (c). From this figure, it is clear that the reference chemical acidification process required about 40% more acid than the combination of electrochemical and chemical acidification techniques (case II); although, in this case, its lignin precipitation yield was ranked only 20% higher than case II. Based on these results, it can be concluded that when the electrochemical acidification process is followed by a chemical acidification step, the amount of consumed chemicals can be reduced. Furthermore, caustic soda is produced during the *EDBM* process which can be used in the Kraft or other chemical industries [39].

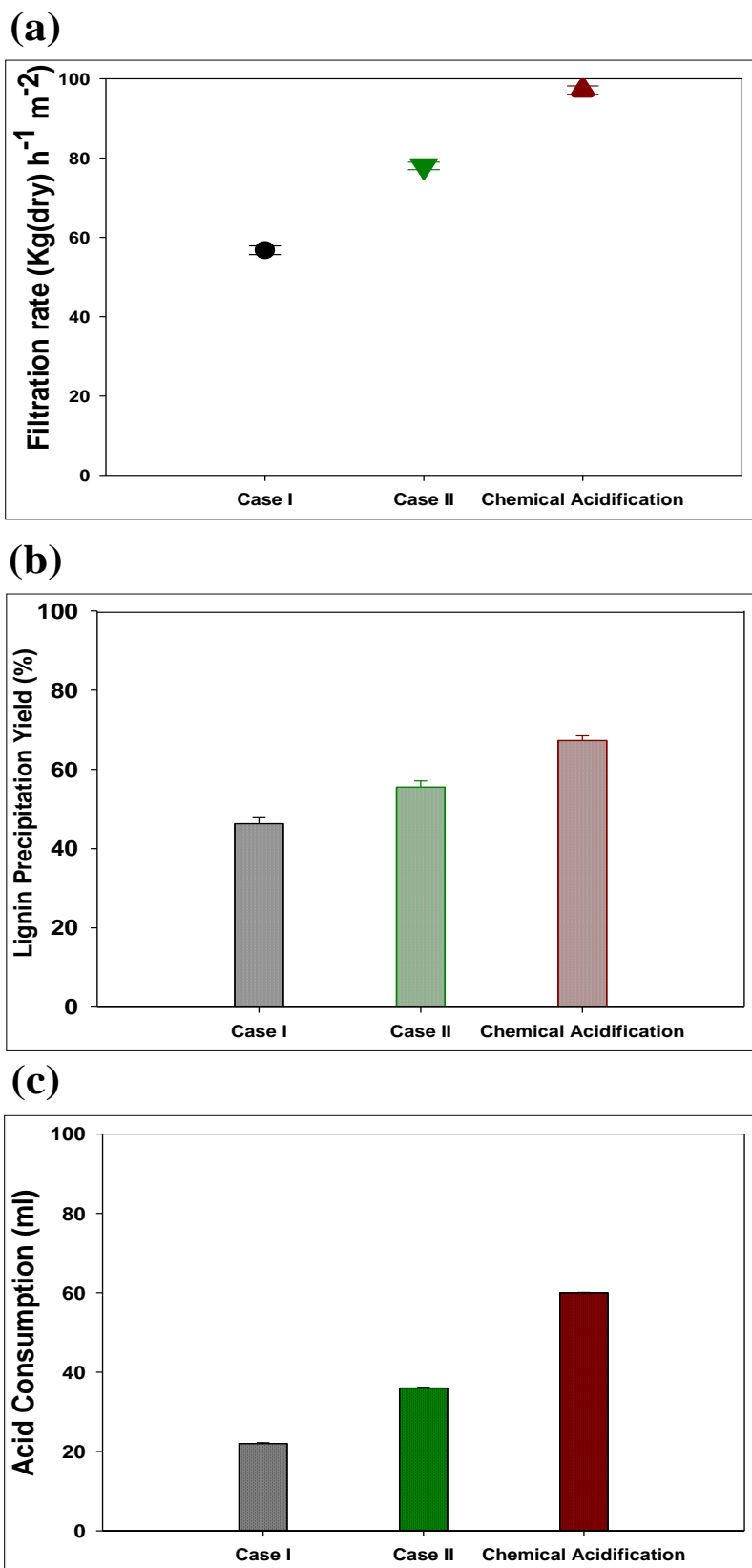


Figure 4.8 (a) Filtration rate, (b) lignin precipitation yield and (c) acid consumption of electrochemical and chemical acidification methods

4.5 Conclusion

In this study, the acidification of Kraft *BL* and lignin separation was carried out via two different techniques : electrochemical and chemical acidification methods. The obtained results illustrated the technical feasibility of the proposed electro-membrane based acidification process. Throughout the *EDBM* process, membrane fouling occurred. The fouling phenomenon forced the termination of electrochemical acidification in order to prevent consuming a high amount of energy to overcome a severe resistance inside the *EDBM* stack. The acidification process was continued using 10.00 N standard sulfuric acid. The extent of the membrane fouling can be minimized by improving the operational conditions of the *EDBM* process and implementing ion exchange membranes with a low fouling tendency. Clearly, further investigation is required to improve operational conditions as well as identification of better ion exchange membranes to prevent membrane fouling and enhance the productivity of the *EDBM* process.

Acknowledgments

The authors acknowledge the financial support of NSERC, BioFuelNet and industrial partners. In addition, the authors wish to thank Hydro Quebec Energy Technology Laboratory (*LTE*) for providing the experimental setup.

CHAPTER 5 ARTICLE 2 : FOULING IDENTIFICATION OF ION-EXCHANGE MEMBRANES DURING ACIDIFICATION OF KRAFT BLACK LIQUOR BY ELECTRODIALYSIS WITH BIPOLAR MEMBRANE

Maryam Haddad^a, Sergey Mikhaylin^b, Laurent Bazinet^b, Oumarou Savadogo^a, Jean Paris^a

a : Research Unit on Energy Efficiency and Sustainable Implementation of the Forest Biorefinery (*E²D²BF*), Department of Chemical Engineering, Polytechnique de Montréal, Canada

b : Institute of Nutrition and Functional Foods (*INAF*), Laboratory of food processing and electromembrane processes (*LTAPEM*), Department of Food Sciences, Université Laval, Canada

Abstract

Integrated forest biorefinery offers promising pathways to sustainably diversify the revenue of pulp and paper industry. In this context, lignin can be extracted from a residual stream, black liquor, of Kraft pulping process and subsequently, converted into a wide spectrum of bio-based products. Electrochemical acidification of Kraft black liquor by electrodialysis with bipolar membrane results in lignin extraction and caustic soda production. Even though the implementation of this method requires less chemicals than the chemical acidification method, fouling of the ion exchange membranes impairs its productivity. Membrane thickness and ash content measurements, along with scanning electron microscopy (*SEM*), elemental analysis (*EDX*) and X-ray photoelectron spectrometry (*XPS*) analysis were performed to identify the nature and mechanism of the membrane fouling. The results revealed that the fouling layer mostly consisted of organic components and particularly lignin. Throughout the electrodialysis process, protonation of lignin phenolic groups led to the production of colloidal lignin. This colloidal lignin became destabilized and consequently formed clusters on the surface of the ion exchange membranes.

Keywords : Bipolar membrane, ion exchange membranes, electrodialysis, Kraft black liquor, colloidal lignin, fouling analyses

5.1 Introduction

Kraft process is the most common pulping process which can be converted into integrated forest biorefinery (*IFBR*) [3]. An IFBR plant could produce various value-added products

along with traditional paper commodities. One of the promising *IFBR* alternatives is the lignin-based biorefinery where a portion of lignin is extracted from the black liquor (*BL*) stream before the combustion step (Figure 5.1) [4]. The extracted lignin could be used as a biofuels or as bio-products such as carbon fibers [6].

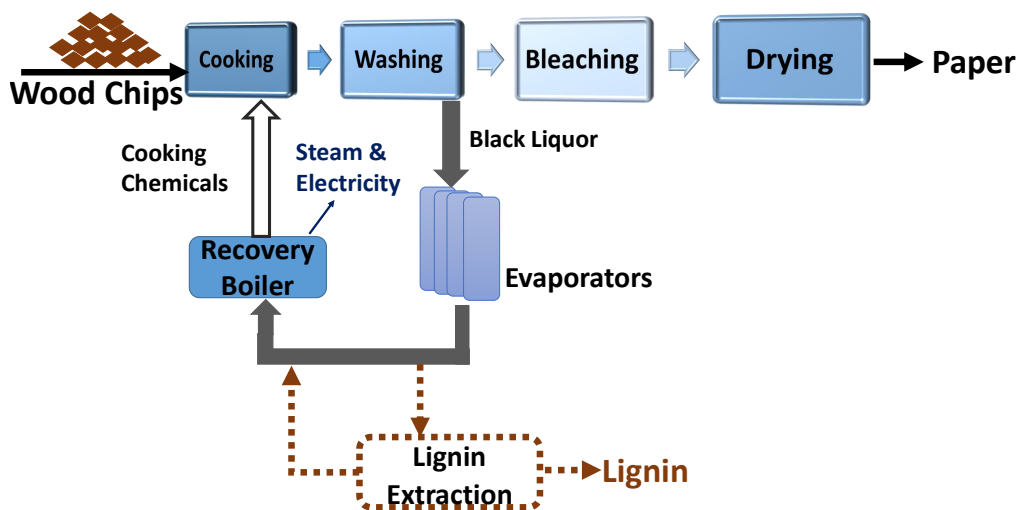


Figure 5.1 A simplified representation of the Kraft pulping process

Chemical composition of the *BL* is strongly affected by the type of wood chips (softwood vs. hardwood) and the operational conditions of the mill. Roughly, *BL* is considered as a complex electrolyte aqueous solution containing organic components (lignin and polysaccharides) and inorganic soluble salts (Na_2S , Na_2CO_3 and Na_2SO_4) [5, 59].

Different processes have been proposed for lignin extraction. The common lignin extraction methods can be classified as chemical acidification, electrochemical acidification (electrolysis and electrodialysis) and ultrafiltration [8, 9, 11, 16, 39]. Among all of the suggested techniques, membrane separation processes are the most sustainable approaches. In particular, the acidification by electrodialysis with bipolar membrane (*EDBM*) process leads to lignin extraction and production of caustic soda [66]. In spite the fact that successful implementations of the *EDBM* process were reported in different fields [17, 18, 22, 52, 53, 54], no attention has been paid to this process for the *BL* acidification purpose. In our earlier work [66], we performed a feasibility study on the electrochemical acidification of the Kraft *BL* via the *EDBM* method. Our findings illustrated that the application of the *EDBM* technique to acidify the Kraft *BL* requires significantly less chemicals versus the conventional chemical acidification method, but fouling of the ion exchange membranes (both cation and bipolar membranes) adversely affects its performance [66].

Generally, fouling referred to any non-dissolved materials that form a deposit on the surface of the membrane. Foulants can be categorized into four different groups : colloids, organic matter, inorganic species and biofouling [33, 67, 68, 69, 70]. Even though an extensive research has been devoted to the fouling identification of cation and anion exchange membranes [67, 69, 71, 72, 73, 74, 75], no study stated the fouling of bipolar membrane (*BPM*). For the first time, we observed the formation of a deposit layer on the surface of cation exchange layers (*CEL*) of the *BPMs* and cation exchange membranes (*CEM*) which were in direct contact with the *BL* solution during the electrochemical acidification process via *EDBM* method [66]. Therefore, the aim of this work is to (1) identify the nature of the ion exchange membranes (*IEM*) fouling layer and (2) investigate the mechanisms of particle deposit on the surface of the membrane during the electrochemical acidification of the Kraft *BL* in order to control and eventually minimize this process drawback. Based on the information obtained from this investigation, one can propose a proper configuration and cleaning methods to prevent and/or minimize this process obstacle.

5.2 Experimental

5.2.1 Membranes and Materials

The membranes used in this study were Fumasep FBM bipolar membrane and Fumasep FKB cation exchange membrane (FuMA-Tech Co., Germany). Their main properties are given in Table 5.1.

Table 5.1 Ion exchange membranes specifications provided by their supplier

Membrane	Type	Thickness (<i>mm</i>)	IEC (<i>meq.g</i> ⁻¹)	Specific Area Resistance ($\Omega.cm^2$)	Stability (<i>pH</i>)	Temperature °C
<i>FKB</i>	Cation	0.10- 0.13	1.2 – 1.3	4 – 6	1 – 14	≤ 60
<i>FBM</i>	Bipolar	0.18- 0.20	-	-	1 – 14	≤ 60

Softwood black liquor was supplied by a Canadian Kraft mill with a total dissolved solids (*TDS*) content of $50 \pm 2\%$ (wt.). It was diluted to 30% (wt) and was pre-filtered to remove suspended solids larger than $0.010 \mu m$ utilizing a simple vacuum filtration apparatus and a filter paper (Whatman Grade 111105, UK). Analytical grade sodium hydroxide and sodium sulfate were purchased from Sigma-Aldrich, Canada. All the aqueous solution were prepared using demineralized water,

5.2.2 Electrochemical acidification Apparatus and Protocol

A two-compartment *EDBM* stack was used. Cation exchange membranes (*CEM*) and bipolar membranes (*BPM*) were placed alternately inside the *EDBM* cell (Figure 5.2). Three pumps (Model : IWAKI Magnetic Drive Pump *MD.30 R*, Iwaki America Inc., USA) recirculated the solutions (*BL*, *NaOH* and electrode rinse solution (*Na₂SO₄*)) from their reservoir to the stack. The constant current between two electrodes was provided by a *DC* power supply (Model : Xantrex *XKW 40 – 25*, USA). The applied current, voltage variation, electrical conductivity and temperature of each reservoir were monitored and recorded using a data acquisition system (Model : Agilent 34970 A, USA) connected to a data logger software. The electrochemical acidification process was performed in batch mode. The process was stopped when the voltage started to rise rapidly and reached the DC power supply limit. The main process conditions are summarized in Table 5.2

Table 5.2 Applied operational conditions during electrochemical acidification method

Operational Conditions	Data
Number of Operating Units	4
Re-circulation Flow Rate	1.0 l min^{-1}
Pressure Drop	34.5 kPa
Applied Current Density	330 A.m^{-2}
Effective Membrane Surface Area	0.0180 m^2
Initial Volume of each Solution	2 L
Operational Temperature	$35 \text{ }^{\circ}\text{C}$

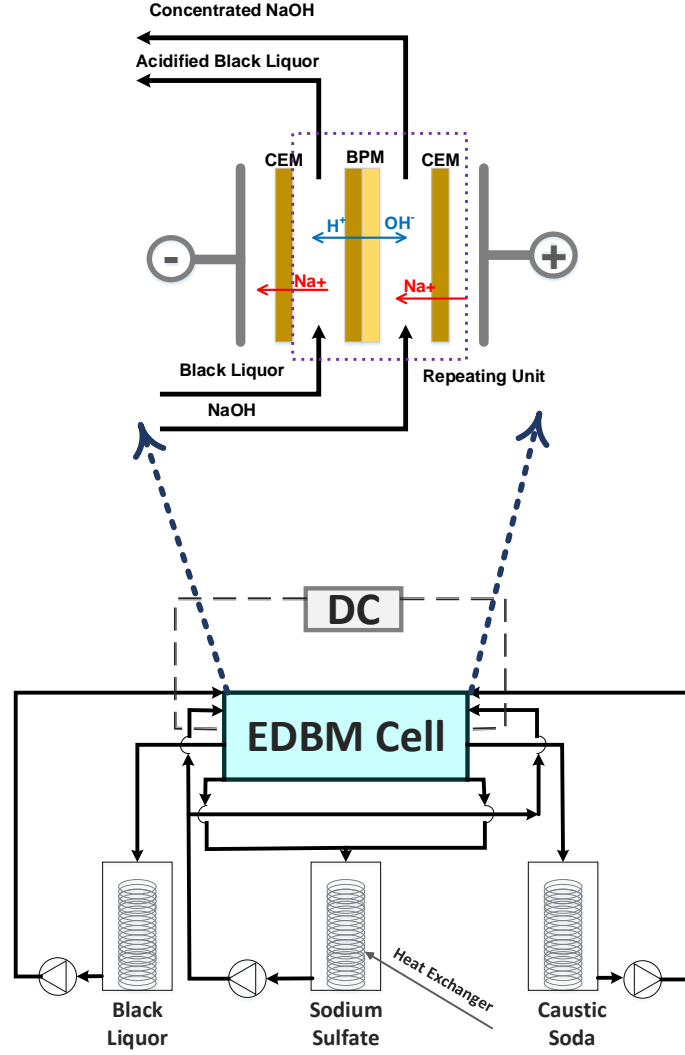


Figure 5.2 Schematic diagram of the electrochemical acidification apparatus and the *EDBM* cell

5.2.3 Analysis Methods

Global System Resistance

The global system resistance was obtained by recording the applied current and voltage variation along the *EDBM* run employing the Ohm's law :

$$R = \frac{U}{I} \quad (5.1)$$

Where R is the global system resistance (Ω), I is the applied current (A) and U represents the voltage drop across the *EDBM* stack (V) [71].

Black Liquor Analysis

The *BL* analyses were performed based on the procedures described earlier [66].

Membrane Ash Content

Ash content measurements were performed on 15 cm^2 samples of fresh and fouled *CEM* and *BPM*. Crucibles were rinsed with concentrated nitric acid and demineralized water in advance and were placed in a muffle furnace (Model : 9493826, Neytech, USA) at 600 °C for 6 hours. The membrane samples were put inside the cooled crucibles and left overnight to dry under vacuum at 100 °C. The dried and weighted samples were placed inside the muffle furnace for 16 hours at 550 °C. The combusted samples were weighed after reaching room temperature [76].

Membrane Thickness

Membrane thickness was measured using a plastic film thickness measurement device (Model : Mitutoyo ID : C112 *EB*, Japan) with 1 μm accuracy and a range of 12.7 mm . The thickness at ten different locations was recorded and the average value was reported as the result.

Electron Microscopy and Elemental Analysis

Images were taken at three different magnifications (50 \times , 100 \times and 250 \times) by means of a field emission gun scanning electron microscope (Model : *JMS – 7600 FEG – SEM*, Jelo, USA). The microscope was equipped with an energy dispersive spectrometer (*EDX*) (Model : Oxford X-Max silicon drift detector, Oxford Instrument, UK). The *EDX* conditions were 5 kV accelerating voltage with a 15 mm working distance and 250 \times magnification. The *EDX* analysis provides relative percentage of the surface elemental compositions. Prior to the *SEM* and *EDX* analyses, vacuum dried samples were coated with a thin layer of gold to improve the image quality [77].

X-ray Photoelectron Spectrometry (*XPS*) Analysis

X-ray Photoelectron Spectrometry (*XPS*) analysis was done on the surface of the fouled *CEM* and *BPM*. The Operational conditions of the *XPS* analysis are given in Table 5.3.

Table 5.3 *XPS* Operational Conditions

Operational Conditions	Data
Apparatus	VG ESCALAB 3 MKII
Source	Mg $K\alpha$
Power	300 W (15 kV, 20 mA)
Analyzed Surface	2 mm \times 3 mm
Analyzed Depth	50 – 100 Å
Survey Scans Energy : Step Size	1 eV
Survey Scans Energy : Pass Energy	100 eV
High Resolution Scans : Energy Step Size	0.05 eV
High Resolution Scans : Pass Energy	20 eV
Background Subtraction	Shirley Method
Sensitivity Factor Table	Wagner
Charge Correction with Respect to C1s at	285 eV

Statistical Analysis

SAS software (SAS version 9.3, 2011) was used to analyze variance of the ash content and the thickness measurement results. LDC, WalLCD and Waller-Duncan post-hoc tests were used at a probability level of 5 %.

5.3 Results and Discussion

5.3.1 Global System Resistance

Figure 5.3 exhibits the evolution of the global system resistance profiles during the *EDBM* process. As can be seen, after almost 25 minutes of the *EDBM* run, the overall system resistance started to increase drastically.

The initial value of the global system resistance corresponds to the intrinsic resistance of the *IEMs* and solution as well as the other compartments of the *EDBM* stack such as spacers [18]; whereas, the acidification and demineralization rates as well as the fouling of the *IEMs* highly control the final value of the global system resistance [78, 79]. Therefore, it can be perceived that the membrane fouling caused the rapid elevation of the global system resistance. Such a rapid increment in the global system resistance due to the occurrence of membrane fouling was also reported by other researchers [71, 72, 75].

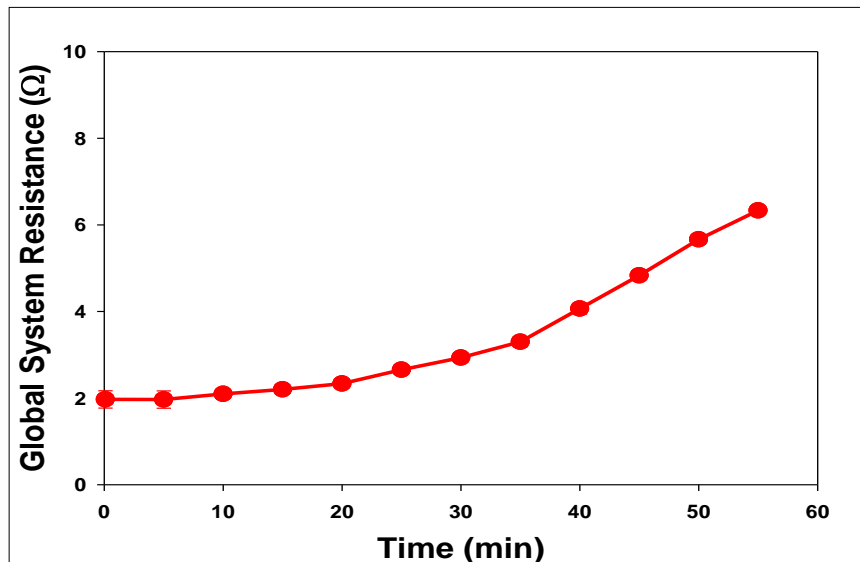


Figure 5.3 Global system resistance during the electrochemical acidification of the Kraft *BL* via *EDBM* method

5.3.2 Black Liquor Analysis

The *BL* specifications before and after the *EDBM* process are listed in Table 5.4. As can be seen, *EDBM* process impacted the *BL* properties. Throughout the *EDBM* process, sodium ions migrated from the *BL* compartment to the *NaOH* compartment and as a result, the concentration of the sodium in the *BL* solution decreased. This decrement could directly affect the *TDS* and ash content values. In contrary, lignin contains negatively charged ions [5, 64] and cannot pass through the *CEMs*. Therefore, it can be assumed that the formed deposit layer inside the *EDBM* stack comprises of lignin and the difference between the initial and final *BL* lignin content is due to the lignin precipitation inside the *EDBM* stack. It should be mentioned that reduction of the *BL* lignin content after the *EDBM* process also accounted for the *BL TDS* content variation.

Table 5.4 Characteristics of Kraft Black Liquor

Characteristics	Before <i>EDBM</i>	After <i>EDBM</i>
Total Dissolved Solids (<i>TDS</i>)(%)	30.1	28.3
UV Lignin (% <i>TDS</i>)	40.4	28.6
Ash Content (% <i>TDS</i>)	28.1	27.6
Sodium Concentration (% <i>TDS</i>)	18.1	15.7
Residual Alkali (<i>g/L</i>)	7.2	-

5.3.3 Membrane Thickness and Ash Content

The results of thickness and ash content of the fresh and the fouled *CEM* and *BPM* are given in Table 5.5. The thickness of the fouled *BPM* was more than 4 times higher than the fresh *BPM*. While for the *CEM*, the thickness of the fouled membrane increased by 0.026 mm. Membrane thickness increment as a result of foulants accumulation on the surface of the *IEM* was also observed in previous studies [65, 80]. Note that based on membrane water content measurements (data not shown), swelling phenomenon had a negligible effect on the thickness measurements.

The ash content of the fouled layers was less pronounced than its organic fraction. This illustrates that there was a small amount of inorganic components on the surface of the *IEMs* during the electrochemical acidification of the Kraft *BL*.

Table 5.5 Membrane Thickness and Ash Content

	<i>CEM</i>		<i>BPM</i>	
	Fresh	Fouled	Fresh	Fouled
Thickness (mm)	$0.112 \pm 0.003^{b*}$	0.138 ± 0.005^a	0.181 ± 0.001^b	0.801 ± 0.032^a
Ash (<i>mg/g dry membrane</i>)	0.190 ± 0.002^b	0.196 ± 0.002^a	0.183 ± 0.002^b	0.220 ± 0.002^a

Table 5.5 * The mean values for fresh and fouled membranes followed by different letters (a and b), are significantly different ($p < 0.05$)

5.3.4 Electron Microscopy and Elemental Analysis

The fresh *CEM* presented a clean surface at all levels of the magnifications (Figure 5.4 (a)). Based on the elemental analysis outcomes, the main detected elements of the membrane structure were C (95 %) and O (5 %).

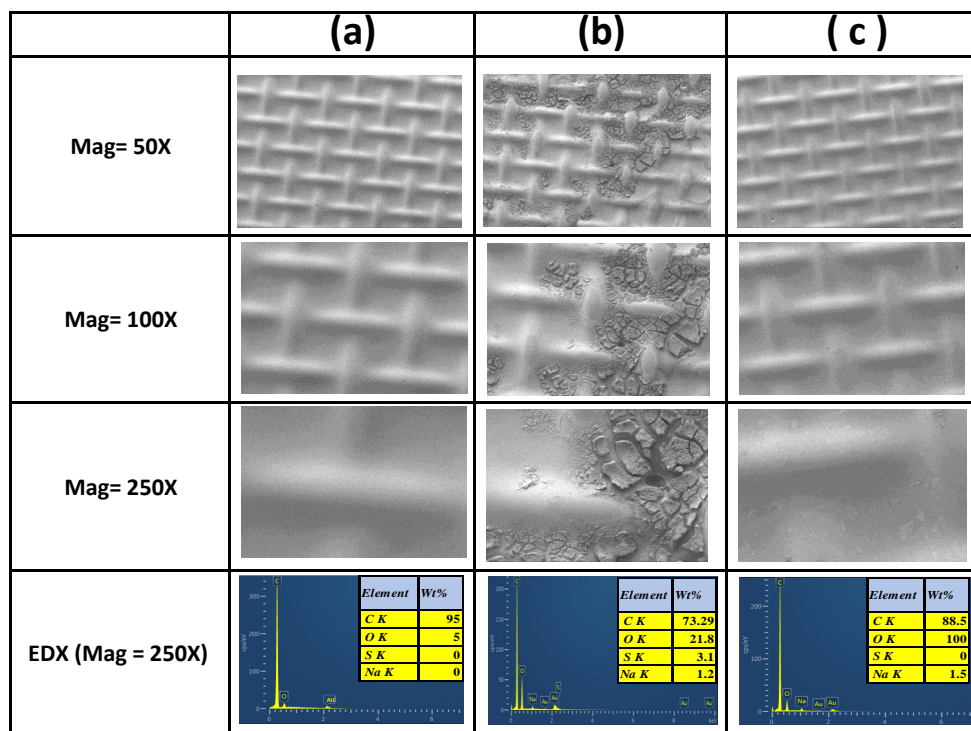


Figure 5.4 Scanning electron microscopy (*SEM*) images and elemental analysis (*EDX*) of (a) the fresh and the used *CEM* in contact with : (b) black liquor and (c) caustic soda solutions

After the electrochemical acidification process, the *BL* side of the *CEM* was loaded with foulants. The elemental analysis results showed that the fouled layer mainly consisted of carbon (73.29 %) and oxygen (21.8 %) with a small quantity of sodium and sulfur (1.2 % and 3.1 %, respectively)(Figure 5.4 (b)). Unlike the *BL* side, the side of the *CEM* in contact with the caustic soda solution was uncontaminated and had the same appearance as the fresh *CEM*. A small fraction of *Na* (counter-ion of *CEM*) was detected during the elemental analysis (1.5 %)(Figure 5.4 (c)). It should be noted that using a pointed tweezer to attach the fouled *CEM* on a brass plate (before placing it under the microscope) caused a hole on the surface of the membrane.

Microscopic images were taken from both sides of the fresh *BPM* (anion exchange layer and cation exchange layer)(Figure 5.5 (a) and (c)). Both sides of the *BPM* were clean as in the case of the fresh *CEM*. After the *EDBM* process, the cation exchange layer (facing the *BL* solution) was covered with a thick layer of foulants. The elemental analysis results indicated that the composition of this layer was mostly carbon (71.3 %) and oxygen (22.8 %) with a small amount of sodium and sulfur (1.1 % and 4.8 %, respectively)(Figure 5.5 (b)). On the

other hand, no noticeable fouling was observed on the anion exchange layer of the *BPM* which was in direct contact with the caustic soda solution.

In accordance with the obtained data from the ash content measurements, the *EDX* results indicated that the organic components, with *O/C* ratio around 0.3, mainly formed the fouling layer.

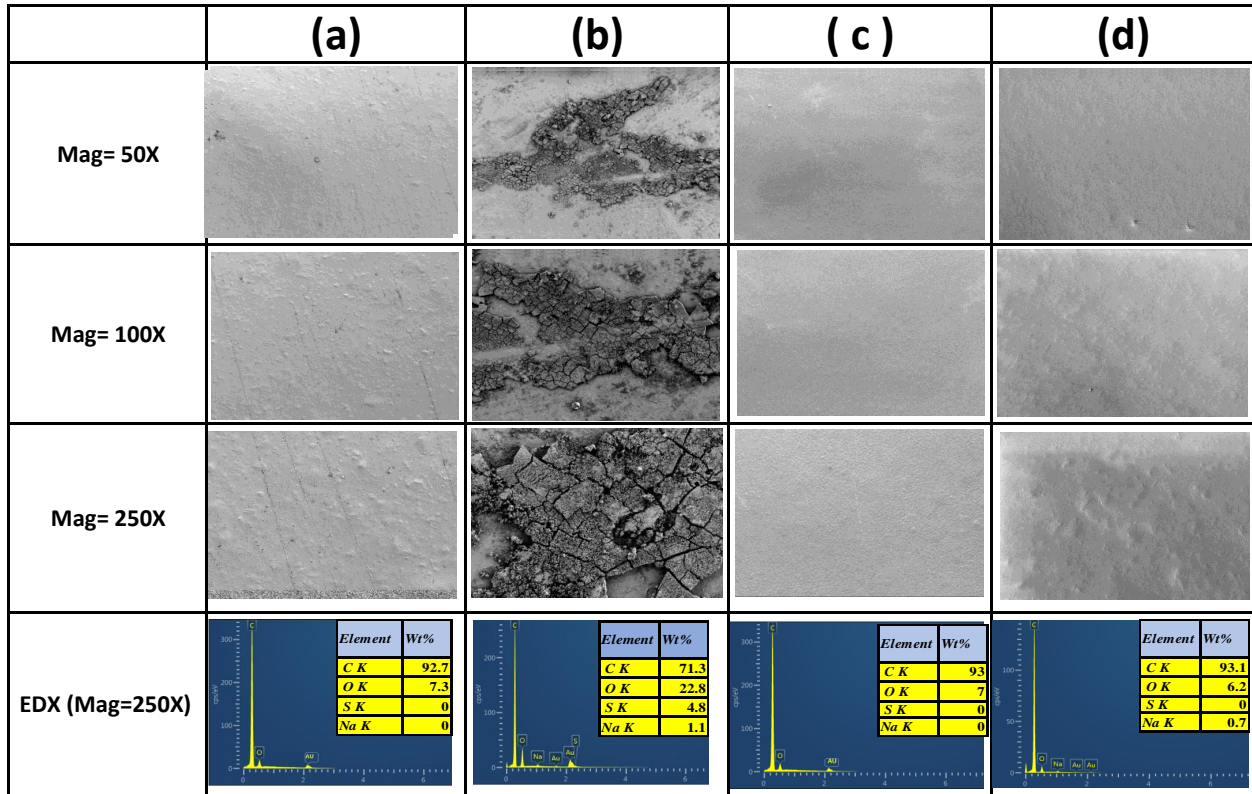


Figure 5.5 Scanning electron microscopy (*SEM*) and elemental analysis (*EDX*) of (a) the fresh and (b) the used cation exchange layer as well as (c) the fresh and (d) the used anion exchange layer of the *BPM*

5.3.5 X-ray Photoelectron Spectrometry (*XPS*) Analysis

X-ray Photoelectron Spectrometry (*XPS*) with a very high sensitivity was used to identify the elemental compositions and chemical bonds at the surface. It can detect all the elements except hydrogen and helium [81]. As can be seen in Figure 5.6 (a) and (b), for both fouled *CEM* and *BPM* surfaces (facing the *BL* solution) the main detected peaks were C1 (at 285 eV) and O1 (at 532 eV). Table 5.6 presents the *O/C* atomic ratio together with the relative percentage of the chemical bonds of the fouled *CEM* and *BPM*. Here, C1 indicates carbon bond to hydrogen or to carbon atoms, C2 shows carbon with one bond to oxygen

atom, C3 represents carbon with a double bond to oxygen atom or with two single bonds to two oxygen atoms and C4 illustrates carbon in carboxyl groups [82]. The *XPS* results support the elemental analysis findings. It has been reported that the O/C atomic ratio of the Kraft lignin varies from 0.25 to 0.44 [82, 83, 84, 85, 86, 87]. The O/C atomic ratios of the fouled membranes fit this range and the data obtained for the chemical bonding from high resolution *XPS* scans are vigorously consistent with the previous studies [82, 84].

Table 5.6 Identification of main chemical bonding from high resolution *XPS* scan

Membrane Type	<i>O/C</i>	<i>C1</i> %	<i>C2</i> %	<i>C3</i> %	<i>C4</i> %
<i>CEM</i>	0.33	56	34	8	2
<i>BPM</i>	0.37	50	41	6	3

Taking into account the membrane thickness and ash content measurements, *SEM*, *EDX* and *XPS* results as well as the *BL* specification before and after the *EDBM* process, one can conclude that the nature of the fouled layer is organic matter consisting of primarily lignin. Previous studies reported that precipitated Kraft lignin possesses a considerably high impurities or ash content (mainly sodium and sulfur) [11, 88, 89]. Therefore, the small fraction of the detected inorganic components was the ash content of the precipitated lignin on the surface of the *IEMs*. In addition, no detectable scaling was observed on the surface of the *IEMs* throughout the fouling analyses.

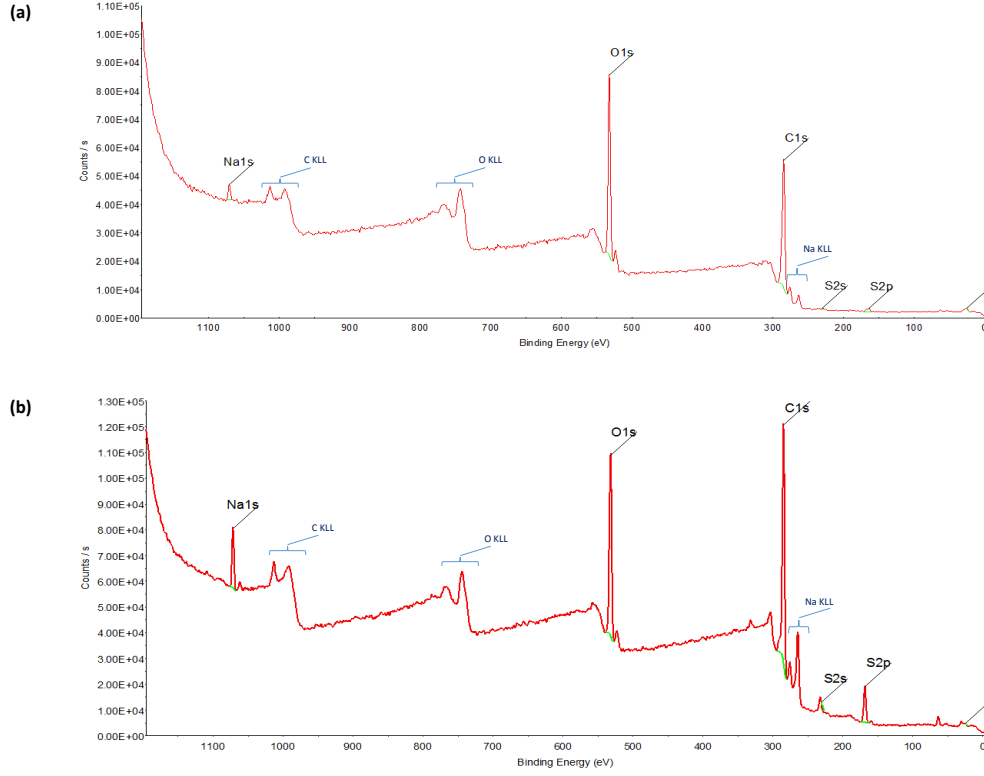
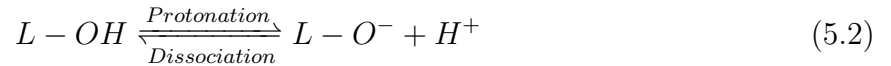


Figure 5.6 XPS survey spectra of (a) fouled *CEM* and (b) fouled *BPM* (KLL peaks represent the auger peaks)

5.3.6 Proposed Fouling Mechanisms

Kraft lignin is a macro-molecule consisting of weakly ionic groups (mainly phenolics). The phenolic groups dissociate at a high pH and become soluble in the *BL* aqueous solution (Equation 5.2) [5, 64]. Various factors can influence the alkali lignin solubility such as pH, temperature, molecular weight, ionic strength and valence of cations [5, 64, 90]. Throughout the *EDBM* acidification process and as the pH of the *BL* drops, phenolic groups of the Kraft lignin become protonated :

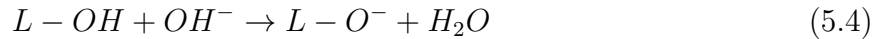


Here, *L* represents the lignin macro-molecule and $-OH$ stands for the lignin phenolic group. The dissociation constant can be defined as the ratio of the activities of $a_{(L-OH)}$, $a_{(L-O^-)}$ and $a_{(H^+)}$:

$$K_a = \frac{a_{(L-O^-)} a_{(H^+)}}{a_{(L-OH)}} \quad (5.3)$$

The logarithmic constant, pK_a , is mainly used to describe the lignin dissociation and protonation reaction. It varies from 6.2 to 11.3 depending on the substantial pattern of the phenolic groups [5, 91].

Norgren *et al.* [63] showed that Kraft lignin behaves like a polyelectrolyte inside a solution and its colloidal stability can be described by means of the well-known *DLVO* theory. Based on this theory an interplay between the attractive and repulsive forces dictates the colloidal stability in a solution [92]. During the *EDBM* process, when the electrical driving force is applied, the proton ions produced from the water dissociation reaction inside the *BPM* induce the protonation of the phenolic groups (Figure 5.7 (a)). Once the phenolic groups become protonated, the repulsive forces between the lignin macro-molecules reduce and attractive forces (van der Waals forces) become dominant. As a result, lignin starts to self-aggregate and forms nuclei (Figure 5.7 (b)) [5, 63, 64, 93]. These nuclei can attach to the *CEL* of the *BPM* via hydrogen bonds, grow in size and number and ultimately form lignin clusters on the membrane surface (Figure 5.7 (c)) [64, 94]. Even though the lignin deposit was profoundly thicker on the surface of the *BPM*, a large surface of the *CEM* was also covered with lignin. This is due to the precipitation of the lignin in the space between the *BPM* and the *CEM*. However, it should be taken into account that most of the commercially available *CEMs* are prone to co-ion leakage, particularly hydroxide ion leakage, during electro dialysis processes [18, 23, 77, 95, 96]. During the electrochemical acidification of the Kraft *BL*, the OH^- leakage through the *CEM* can slightly disturb the lignin accumulation on the surface of the *CEM* (Figure 5.7 (d)) :



Therefore, less lignin was precipitated on the surface of the *CEM*. The results of the fouling analyses and particularly the thickness measurements substantiate this hypothesis, as the thickness of the fouled *CEM* increased considerably less than the thickness of the fouled *BPM*.

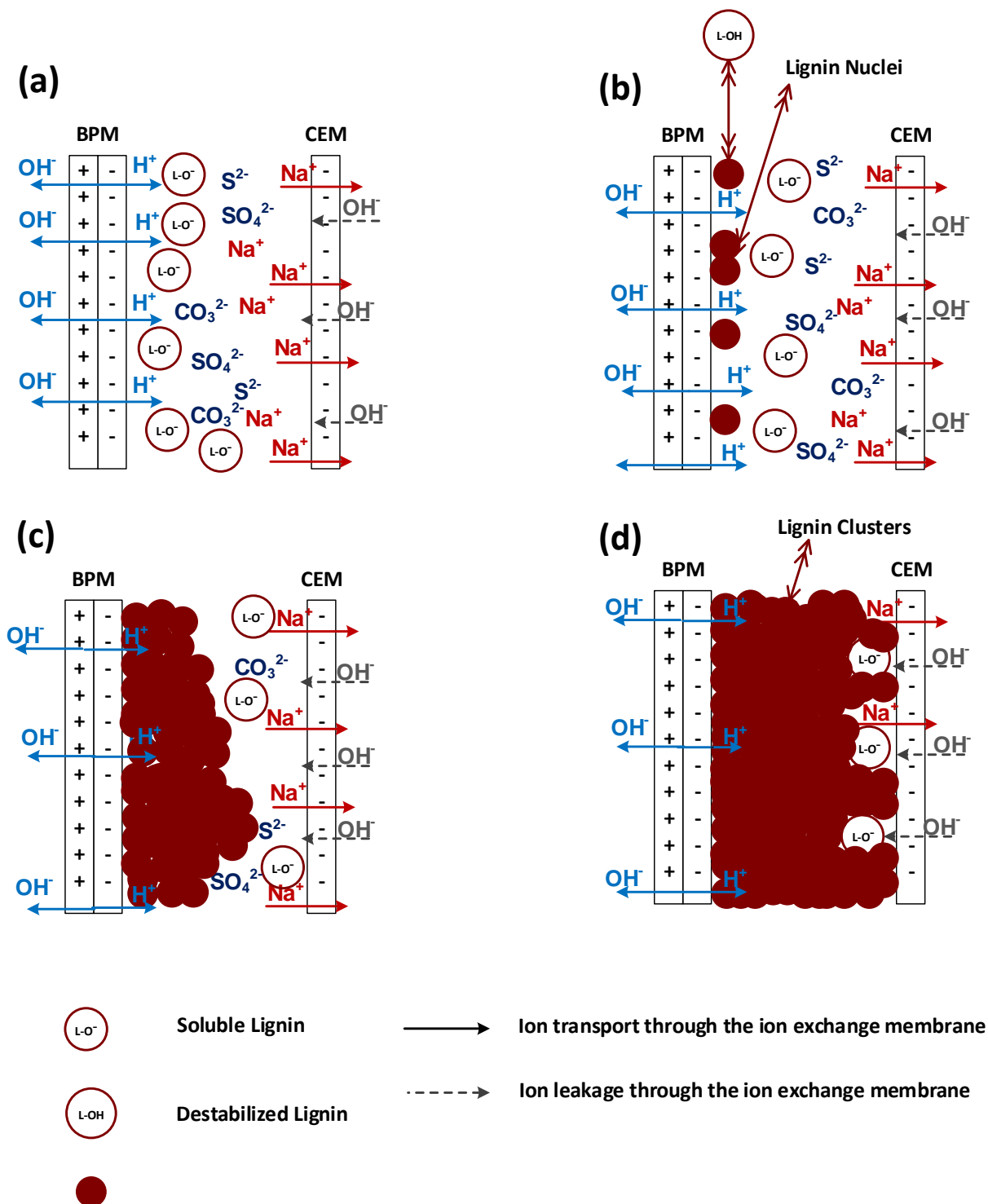


Figure 5.7 Fouling mechanism on the surface of the *IEMs* during the *EDBM* process ((a) : Protons production and lignin protonation, (b) : Lignin nucleation phenomenon on the surface of the *BPM*, (c) : Formation of lignin clusters on the surface of the *BPM*, (d) : Precipitation of the lignin in the space between the *BPM* and *CEM* and interruption of the lignin aggregation on the surface of the *CEM* due to the hydroxide ions leakage through the *CEM*)

5.4 Conclusion

Fundamental analyses were performed to identify the composition of the fouling of the *IEM* during the electrochemical acidification of Kraft *BL*. The results indicated that the major amount of the *IEMs*' fouling was lignin. Protonation of phenolic groups existing on the surface of the Kraft lignin caused lignin self-aggregation and deposit on the surface of the *CEL* of the *BPM*. Throughout the *EDBM* process, the formed lignin layer on the surface of the *BPM* grew and led to lignin precipitation in the space between the *BPM* and the *CEM*. As a result, the surface of the *CEM* was contaminated with lignin particles. However, hydroxide ion leakage through the *CEM* disturbed, to some degree, the lignin aggregation on the surface of the *CEM*. The fouled layer increased the thickness of the *IEMs*. Ash content measurements revealed that a small fraction of the deposited layers was consisted of inorganic components. The *IEMs*' fouling decreases the efficiency of the *EDBM* process and can affect the membrane integrity in a long term operation. Therefore, it is essential to screen the most reliable and commercially available *IEMs* which are less prone to the membrane fouling and also implement appropriate cleaning procedures. In addition, the effect of the *IEMs*' specifications on the fouling phenomenon and, consequently, on the performance of the process is critically important. Work on those issues is ongoing and will be presented in future papers.

Acknowledgments

This work was financially supported by the NSERC and BioFuelNet Canada. The authors are grateful to Hydro-Québec Energy Technology Laboratory (*LTE*) for providing the experimental set-up and the Kraft pulping mill for supplying the black liquor samples.

CHAPTER 6 ARTICLE 3 : ELECTROCHEMICAL ACIDIFICATION OF KRAFT BLACK LIQUOR : EFFECT OF FOULING AND CHEMICAL CLEANING ON ION EXCHANGE MEMBRANE INTEGRITY

Maryam Haddad^a, Sergey Mikhaylin^b, Laurent Bazinet^b, Oumarou Savadogo^a, Jean Paris^a

a : Research Unit on Energy Efficiency and Sustainable Implementation of the Forest Biorefinery (*E²D²BF*), Department of Chemical Engineering, Polytechnique de Montréal, Canada

b : Institute of Nutrition and Functional Foods (*INAF*), Laboratory of food processing and electromembrane processes (*LTAPEM*), Department of Food Sciences, Université Laval, Canada

Abstract

In the essence of the green biorefinery concept an interest in further implementations of wood compounds has gained a lot of attention. Therefore, it is crucial to identify and develop efficient and eco-friendly extraction processes. In particular in a lignin biorefinery plant, electrochemical acidification of Kraft black liquor via electrodialysis with bipolar membrane is considered as a sustainable avenue to acidify the Kraft black liquor and subsequently extract lignin. Even though the application of this acidification technique results in less chemical consumption than the chemical acidification method the colloidal fouling of the ion exchange (bipolar and cation exchange) membranes adversely affects its performance. This study was performed to determine the influence of the colloidal fouling and chemical cleaning process on the integrity of the ion exchange membranes. Four commercially available cation exchange membranes and one bipolar membrane were examined. Membrane analyses such as thickness, contact angle, ion exchange capacity and electrical resistance measurements as well as scanning electron microscopy with energy dispersive X-ray analysis were carried out. It was found that changing the type of the cation-exchange membrane cannot eliminate the fouling phenomenon and a chemical cleaning cycle is required. Caustic soda and fresh diluted black liquor were tested as the cleaning solutions. The initial properties of the bipolar membrane and two cation-exchange membranes (*CMB* and Nafion 324) were reestablished after the chemical cleaning step. Furthermore, in terms of sustainability concept, the utilization of in situ and free of charge fresh diluted black liquor, as the cleaning agent, can be an interesting eco-efficient approach.

Keywords : Bipolar membrane, cation-exchange membrane, electrodialysis, membrane fouling

ling, chemical cleaning, lignin extraction, biorefinery

6.1 Introduction

Kraft pulping process is the most dominant technique for the pulp and paper production. Van Heiningen [3] proposed the conversion of the Kraft process into an integrated forest biorefinery (IFBR) in order to sustainably increase its revenue. Lignin biorefinery is a promising receptor for the IFBR in which a fraction of the lignin is extracted from a residual stream, black liquor (BL), before the combustion step (Figure 6.1) [4]. The extracted lignin can be subsequently transformed into a broad spectrum of value-added products such as biofuels and carbon fibers [6].

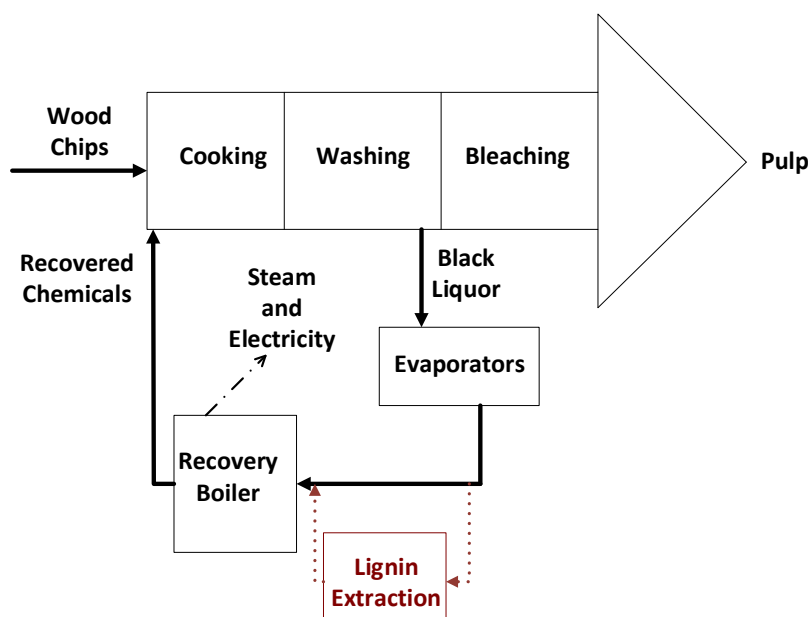


Figure 6.1 A schematic illustration of Kraft process

For several years, a great effort has been devoted to investigate a suitable lignin extraction method [10, 11, 39, 47]. Among all the examined processes, chemical acidification is found to be the most common technique where lowering the pH of the *BL* causes the lignin precipitation and separation [4, 5]. Utilization of CO_2 and H_2SO_4 as the acidifying agents remarkably enhanced the process yield [4, 5, 10, 11, 12]. However, there are some serious issues regarding the practical implementation of the chemical acidification method. For instance, the chemical (acid) addition can disturb the sodium-sulfur balance of the receptor Kraft mill. Furthermore, when the CO_2 is used, the price and the cost-intensive installation of CO_2 recapturing equipment would challenge the process productivity [4, 5, 10, 11, 12].

Since the alkaline *BL* is an electrolyte solution containing inorganic salts ($NaOH$, Na_2SO_4 , Na_2CO_3 and Na_2S) and organic compounds (lignin and hemicellulose), utilization of the electrochemical acidification approach seems to be an attractive proposition to overcome the disadvantages of the chemical acidification method, acidify the *BL* and produce caustic soda as well [16, 39, 43]. The electrochemical acidification of the *BL* can be performed in an electrolysis (*EL*) or electrodialysis (*ED*) systems. In the *EL* cell, a cation-exchange membrane (*CEM*) separates the two electrode compartments. The *BL* is sent to the anode compartment and diluted caustic soda solution is pumped to the cathode compartment. When the driving force (the electric field) is applied to the system, the sodium ions present in the *BL* solution migrate to the cathode compartment, through the *CEM*, react with the hydroxide ions produced from the water reduction reaction at the cathode and form caustic soda. The water oxidation reaction takes place at the anode and generates proton ions. The presence of these ions, gradually, drop the pH of the *BL*. As a result, the acidified *BL* and the concentrated caustic soda are the main outlet streams of the *EL* system [16, 39]. The efficiency of the *EL* technique is strongly dependent on the anode specifications. Only a few specific types of anode have been reported to tolerate the severe alkaline conditions [13, 16]. Furthermore, a deposit of lignin on the surface of the anode has been observed [13]. On top of the above constraints, in a large scale application a high energy level is required for the redox reactions which take place at each electrode pair. In addition, a considerable amount of side gases, as well as a high price of the electrodes for a multiple *EL* cell configuration have to be taken into account.

On the other hand, electrodialysis with bipolar membrane (*EDBM*) was recently suggested as a novel and more sustainable pathway to acidify the *BL* and extract the lignin [66]. This technique requires a significantly reduced chemical consumption in comparison to the chemical acidification method and simultaneously recaptures caustic soda [66]. In this technique, only charged membranes (cation-exchange and bipolar membranes) are involved in the ion transport phenomena while the electrodes reactions do not interfere with the acidification process. Thereby, the applied electrodes in the *EDBM* stack are only electrical terminals, soaked in the electrolyte solution, transferring the current [52]. Similar to most of the membrane separation technologies, a major drawback to the practical application of the *EDBM* acidification process is the fouling of its ion exchange membranes (*IEMs*). Generally, membrane fouling results from the formation of a deposit layer on the surface of the membrane which decreases membrane performance and eventually causes shortness of the membrane life time [33, 68, 69, 70]. Despite the wealth of the information that can be found in the literature regarding the fouling and practical cleaning techniques for the anion and cation-exchange membranes [67, 69, 71, 72, 73, 74, 75], no publication has reported the fouling of

the bipolar membrane (*BPM*). In our recent investigation [66, 97], we observed a deposit layer on the surface of the *BPMs* and *CEMs* during the *EDBM* process. It was found that the protonation of the lignin phenolic groups resulted in formation of destabilized colloidal lignin and eventually produced lignin clusters on the surface of the *IEMs*.

Normally, in practical membrane process plants, an adequate cleaning in place (*CIP*) step is applied to clean up the fouled membranes and maintain the process performance and integrity of the membranes [32]. The nature of the foulants along with the chemical compatibility of the *IEMs* and the other components of the stack dictate the cleaning conditions [98, 99, 100]. Thus, the focus of the present work is to determine the effect of fouling and chemical cleaning cycle on the *IEMs*' integrity. With a better understanding of the cleaning mechanisms and the impact of the cleaning solutions on foulants removal for different types of *IEMs*, one can choose the most appropriate and commercially available *IEM* as well as the proper cleaning conditions for the chemical cleaning step of the electrochemical acidification of the Kraft *BL* via *EDBM* approach.

6.2 Experimental

6.2.1 Membranes and Materials

Four commercially available *CEMs* were tested, namely *FKB* (FuMA-Tech, Germany), *CMB* (Neosepta, Japan), *CM(H) – PES* (Mega a.s., Czech Republic) and Nafion 324 (DuPont, USA). According to the membrane suppliers, these membranes can tolerate severe alkaline conditions. Bipolar membrane was purchased from FuMA-Tech, Germany (*FBM*). It is worth mentioning that due to the limited number of commercially available *BPMs* and restrictions against the *BPM* analysis from some of the membrane suppliers, only one type of *BPM* was examined. A Canadian pulp mill supplied the softwood Kraft *BL*. The main characteristics of this *BL* are listed in Table 6.1. Analytical grade chemicals were purchased from Sigma-Aldrich, Canada and standard volumetric solutions were supplied by Fisher Scientific, Canada. Aqueous solutions were prepared with demineralized water.

Table 6.1 Characteristics of Kraft Black Liquor

Characteristics	Data
Total Dissolved Solids (TDS) (%)	30.1
UV Lignin (% TDS)	40.4
Ash Content (% TDS)	28.1
Sodium Concentration (% TDS)	18.1
Residual Alkali ($g. L^{-1}$)	7.2
pH at room Temperature	12.9

6.2.2 Electrochemical Acidification Set-up

A two-compartment *EDBM* cell (consisting of the *BL* and *NaOH* compartments) was used. Inside the cell, the *CEMs* and *BPMs* were encapsulated on one end by an anode compartment and on the other end by a cathode compartment (Figure 6.2). The electrodes were connected to a DC power supply (Model : Xantrex *XKW* 40 – 25, USA). Three pumps (Model : IWAKI Magnetic Drive Pump *MD.30 R*) re-circulated the *BL*, *NaOH* and the electrode rinse solution (Na_2SO_4) from their tanks to the stack. A jacket coil heat exchanger was installed in each reservoir to maintain a constant operating temperature. Table 6.2 gives the *EDBM* process conditions. The *EDBM* process was terminated once the maximum voltage of the DC power supply was reached. A simplified diagram of the experimental set-up is shown in Figure 6.3.

Table 6.2 Applied Operational Conditions during Electrochemical Acidification of the Kraft Black Liquor

Operational Conditions	Data
Number of Operating Units	4
Re-circulation Flow Rate	1.0 l. min^{-1}
Pressure Drop	34.5 kPa
Applied Current Density	330 A. m^{-2}
Effective Membrane Surface Area	0.0180 m^2
Initial volume of each Solution	2 L
Operating Temperature	$35 \text{ }^{\circ}\text{C}$

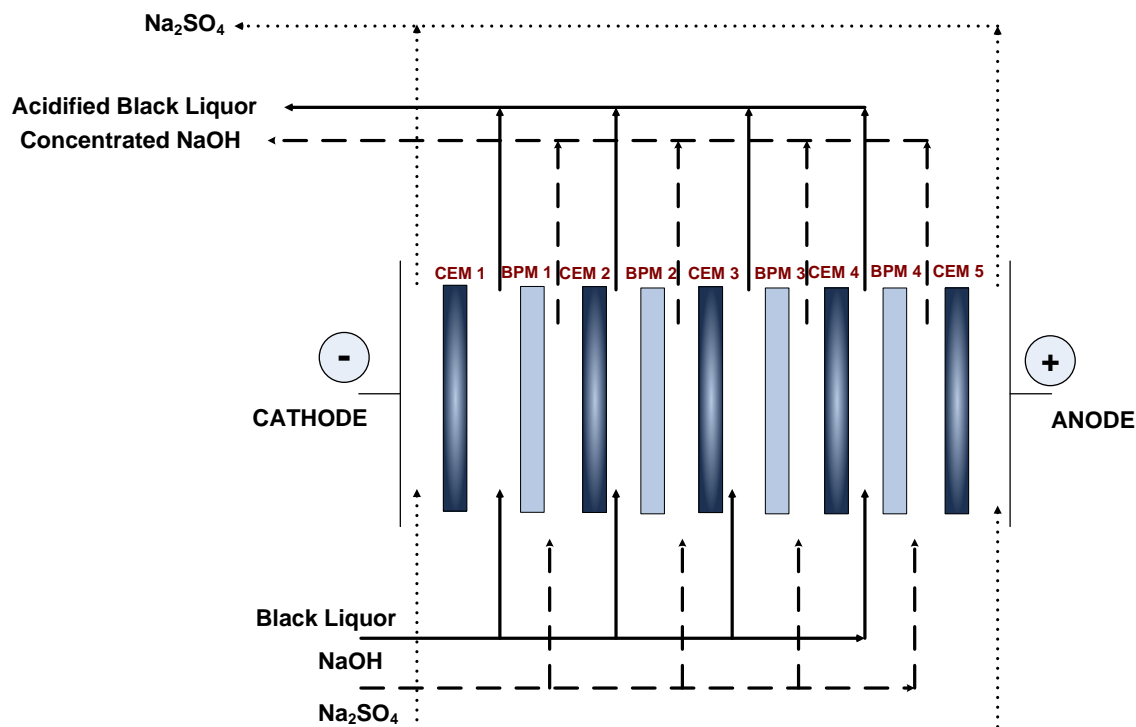


Figure 6.2 Electrodialysis with bipolar membrane (*EDBM*) stack (*BPM* : bipolar membrane and *CEM* : cation- exchange membrane)

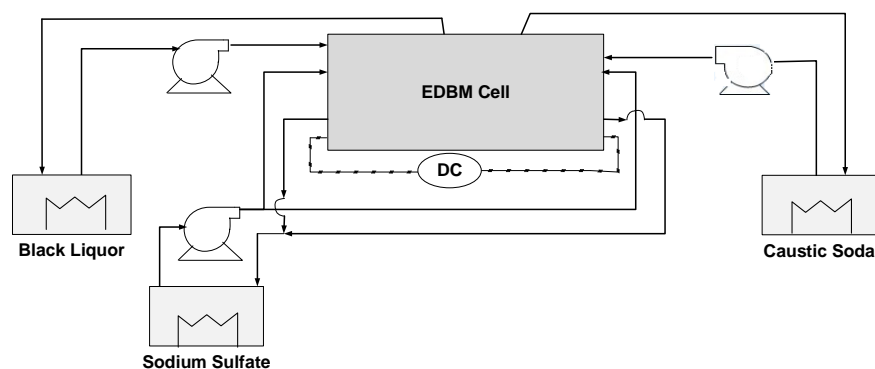


Figure 6.3 Schematic diagram of the electrochemical acidification set-up

6.2.3 Protocol

Electrochemical Acidification

The *EDBM* acidification process was performed in batch mode applying a constant current density. For each set of the experiments, identical *IEMs* (five *CEMs* and four *BPMs*) were

cut and placed at the same side and position inside the stack. *BPMs* 1, 2, 3, 4 and *CEMs* 2, 3, 4 were in direct contact with the *BL* (which became acidified) on one side and caustic soda that became concentrated on the other side (Figure 6.2). All the experiments were performed three times and prior to each series of experiments, the limiting current density was measured based on Cowan and Brown procedure [55].

Chemical Cleaning

From mass transfer perspective, dynamic cleaning i.e. circulation of the cleaning chemical through the set-up is more efficient than soaking the *IEMs* inside the cleaning solution [99]. Hence to carry out the dynamic cleaning step at the end of each *EDBM* run the acidified *BL* and the concentrated *NaOH* solutions were discharged from their reservoirs and these reservoirs were filled with the cleaning chemical and demineralized water, respectively. The power supply was disconnected and the solutions were circulated through the *EDBM* stack for 30 minutes. At the end of the cleaning cycle, the cell was dismantled and the *IEMs* were taken for further investigations. As stated in the literature and according to the compositions of the fouled layer [97], alkaline chemicals can be utilized to remove the lignin deposit from the surface of the *IEMs* [33, 98, 99, 101]. In this study, caustic soda with concentration of about 2.5 (*wt. %*) and fresh diluted *BL* (total dissolved solids (*TDS*) \simeq 10%) were chosen as cleaning solutions.

The original membrane properties were measured on fresh membranes cut from the sheet. Membranes 2 (control membranes) were not cleaned. Thus, prior to the cleaning cycle, the *EDBM* cell was disassembled, the control membranes were replaced by the fresh membranes and the cell was re-assembled and connected to the set-up. At the end of each *EDBM* set, the control and the cleaned membranes characteristics were performed.

6.2.4 Global System Resistance

Ohm's law was applied to calculate the global system resistance :

$$R = \frac{U}{I} \quad (6.1)$$

Where, R represents the global system resistance (Ω), I stands for the applied current (A) and U is the voltage across the *EDBM* stack (V) [71]. The applied current and voltage drop were recorded continuously using a data acquisition system (Model : Agilent 34970 A, USA) connected to a data logger software.

6.2.5 Membrane Properties

In order to improve the membrane life time and eventually enhance the feasibility of the electrochemical acidification process, the initial properties of the membranes have to be restored after each experiment. Therefore some fundamental membrane analyses were performed to examine how the feed, *EDBM* process and nature of the foulants affected the *IEMs*' integrity. Membrane thickness and contact angle measurements along with scanning electron microscopy with energy dispersive X-ray analysis were carried out for all the fresh, fouled and cleaned *IEMs*. It should be noted that all the *SEM* and *EDX* analyses as well as *CA* measurements were done on both sides (*BL* side and *NaOH* side) of the *IEMs*. As indicated in our earlier investigation [97], the *NaOH* solution sides of the *IEMs* were cleaned with no fouling or change in the membrane properties. Thus, to avoid confusion, only the analysis results of the *BL* sides of the *IEMs* were presented here.

In addition, to the best of the authors' knowledge, no systematic protocol was found in the literature to measure the electrical resistance and ion exchange capacity (*IEC*) of the *BPMs*. Hence, the *IEC* and the membrane electrical resistance measurements were only done for the *CEMs*. Moreover, due to the possibility of detachment of the fouled layer from the membrane surface during the long preparation procedure of these measurements and data inconsistency, only the electrical resistance and the *IEC* findings of the fresh and cleaned *CEMs* were reported in this paper.

Membrane Thickness

The thickness of each membrane was measured on ten different spots using a plastic film measurement device (Model : Mitutoyo ID : *C112 EB*, Japan), with $1\ \mu\text{m}$ accuracy and a range of $12.7\ \text{mm}$. The average value was presented as the result.

Scanning Electron Microscopy with Elemental Analysis

Scanning electron microscopy (*SEM*) images were taken at $250\ X$ magnification using a field emission gun electron microscope (Model : *JMS - 7600 FEG - SEM*, Jelo, USA). Then, an energy dispersive spectrometer (Model : Oxford X-Max silicon drift detector, Oxford Instrument, UK) was connected to the microscope to perform the elemental analysis of the membrane surface (*EDX*). The *EDX* analysis was carried out at the same magnification as the *SEM* analysis ($250\ X$), at $5\ \text{kV}$ accelerating voltage and a $15\ \text{mm}$ working distance. All the samples were vacuum dried and coated with a thin layer of gold to improve the image quality [77].

Contact Angle

The membrane surface hydrophobicity was characterized by measuring the water contact angle (CA) using an optical tensiometer (Model : $T - 200$ Theta, Biolins, USA) with a measurement range of $0 - 180^\circ$. The tensiometer was connected to One Attension Software and Sessile drop method was applied to record the CA . Prior to the CA measurements, a filter paper was used to mop the excessive water from the membrane surface [102].

Ion Exchange Capacity

Ion exchange capacity (IEC) is defined as the number of IEM fixed groups per unit weight of dried membrane. The functional groups of the $CEMs$ were brought into the H^+ ion form by soaking membrane samples in 1 M hydrochloric acid for 24 hours. To complete the ion exchange transfer, the HCl solution was renewed three times. Then, the membrane samples were rinsed with demineralized water to remove any residual acid. As the next step, the functional groups were brought to sodium ion form by soaking the $CEMs$ inside a 2 M sodium chloride solution for 24 hours. Similar to the previous step, the solution was refreshed three times and each time the $NaCl$ solution was titrated with 1 M caustic soda to determine its proton concentration which is related to the total charge of the membrane samples [103]. Then the IEC was calculated as :

$$IEC = \frac{100 - 4v}{10m} \quad (6.2)$$

Here, IEC shows the ion exchange capacity of the CEM ($meq.g^{-1}$), 100 is the volume of the 1 M HCl (ml), v represents the total volume of 1 M NaOH (ml) and m is the weight of the dried membrane sample (g) [104].

Membrane Electrical Resistance

Electrical resistance of the fresh and cleaned $CEMs$ was determined by measuring electrical conductivity of the membrane based on the procedure described by Ltei *et al.* [105].

Statistical Analysis

Variance analysis of the membrane thickness, contact angle, membrane electrical resistance and IEC data was performed by *SAS* software (*SAS* version 9.3, 2011). LSD and Waller-Duncan post-hoc tests were applied at a 5% probability level.

6.3 Results and Discussion

6.3.1 Global System Resistance

Figure 6.4 depicts the evolution of the global system resistance profiles during the *EDBM* process, utilizing four different *CEMs*. In all cases after almost 30 minutes of the *EDBM* process, the overall system resistance started to rise rapidly. This quick increase is due to the fouling of the *IEMs* [66]. Even though all the global system resistance profiles followed the same pattern, a slight delay was observed when the *CMB* and Nafion 324 were used. Clearly, changing the *CEM* type had insignificant affect on the evolution of overall system resistance.

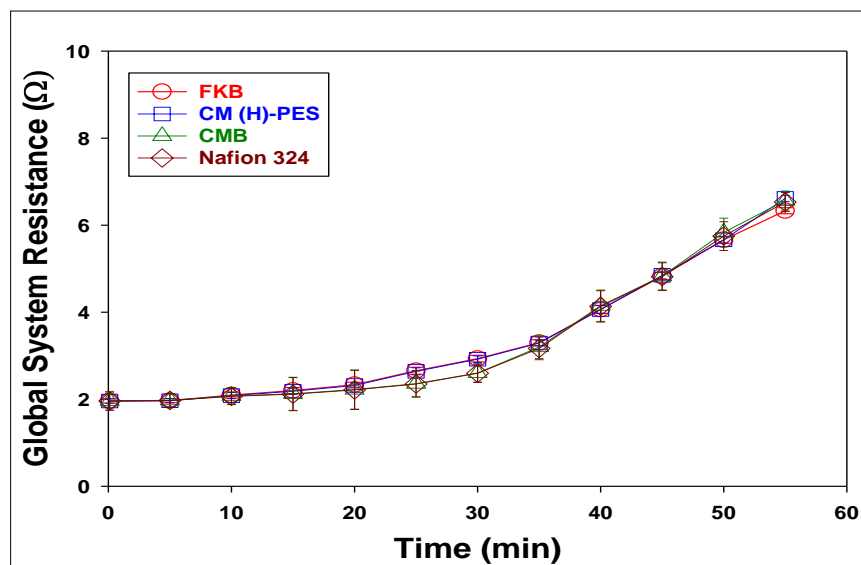


Figure 6.4 Global system resistance during the *EDBM* process with different cation exchange membranes

6.3.2 Membrane Properties

Membrane Thickness

The thickness data of the fresh, fouled and cleaned membranes are given in Table 6.3. The thickness of the fouled *BPM* was more than 4 times higher than the fresh *BPM*. Among the utilized *CEMs*, the thickness of the fouled heterogeneous *CM(H) – PES* increased by 33%, the fouled *FKB* had a thickness increase of about 24%, while the fouled Nafion 324 and *CMB* had the lowest increments (9% and 8%, respectively). Based on the thickness values of the cleaned membranes, it can be presumed that both of the cleaning solutions were able to

clean , effectively the surface of the fouled *IEMs* and restore their initial values. It is worth mentioning that based on membrane water content measurements (data are not shown here), swelling phenomenon had a negligible effect on the thickness measurements.

Table 6.3 Membrane Thickness (*mm*)

Membranes	Fresh	Fouled	Cleaned with <i>NaOH</i>	Cleaned with <i>BL</i>
<i>FBM</i>	$0.181 \pm 0.001^{b*}$	0.801 ± 0.032^a	0.184 ± 0.001^b	0.184 ± 0.001^b
<i>FKB</i>	0.112 ± 0.003^c	0.138 ± 0.005^a	0.115 ± 0.002^{cb}	0.116 ± 0.001^b
<i>CMB</i>	0.180 ± 0.001^b	0.194 ± 0.003^a	0.182 ± 0.001^b	0.182 ± 0.001^b
<i>CM(H) – PES</i>	0.402 ± 0.004^b	0.537 ± 0.020^a	0.406 ± 0.003^b	0.407 ± 0.003^b
Nafion 324	0.248 ± 0.008^b	0.270 ± 0.010^a	0.251 ± 0.002^b	0.252 ± 0.002^b

Table 6.3 * The mean values (presented at each row) for fresh, fouled and cleaned membranes followed by different letters (a, b and c), are significantly different ($p < 0.05$)

Scanning Electron Microscopy with Elemental Analysis

All the fresh *IEM* samples exhibited a clean surface (Figure 6.5 (a)). The fresh *FBM*, *FKB* and *CMB* presented a smoother surface than the fresh *CM(H) – PES* and Nafion 324. The difference in the surface roughness can be caused by the membrane preparation methods[106, 107]. Homogeneous membranes, such as *FBM*, *FKB* and *CMB*, are prepared by means of a direct introduction of the ion exchange components into the polymeric structure of the membranes. Therefore, the ion exchange groups are evenly distributed on the surface of the membrane. *CM(H) – PES* is a heterogeneous *CEM* and these membranes are produced, firstly, by preparing a mixture of a fine powder of an ion exchange resin and a binder polymer and then, pressing and sintering the mixture at a high temperature. This preparation procedure resulted in a non-uniform distribution of the ion exchange groups on the surface of the heterogeneous membranes [19, 30]. Nafion 324 is a chemically and mechanically stable *CEM* made of a perfluorosulfonate ionmer membrane and contains a hydrophobic backbone and hydrophobic cation exchange sites which can interpret its rough surface [108, 109, 110].

After the *EDBM* process, the *BL* sides of the *IEMs* were contaminated with the foulants. From the *EDX* results, one can realize that the deposit layer, mainly, consisted of carbon and oxygen with a small fraction of sodium and sulfur. (Figure 6.5 (b)). The *O/C* ratios of the fouled *IEMs* deviates between 0.25 - 0.4 which are in good agreement with the *O/C* ratio

of the Kraft lignin reported by other researchers [84, 85, 86]. In addition, it is noteworthy that the obtained results of the *EDX* analysis of the fouled *IEMs* are in accordance with our previous findings [97]. It should be noted that using a pointed tweezer to attach the fouled *FKB* on a brass plate (before placing it under the microscope) caused a hole on the surface of the *FKB* membrane.

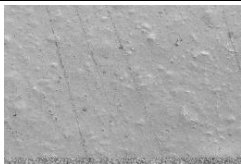
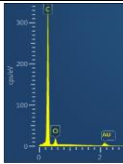

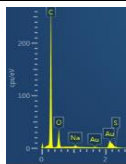
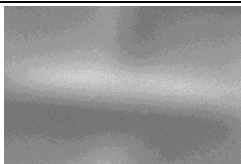
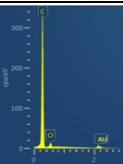
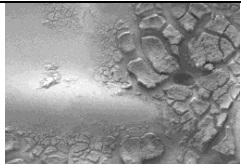
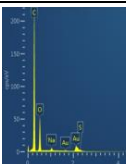

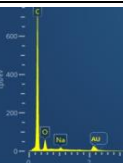
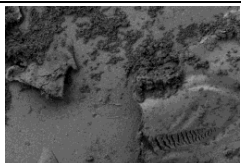
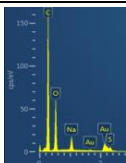
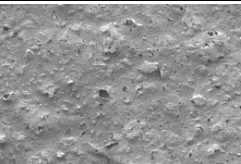
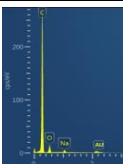
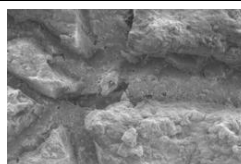
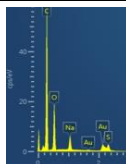

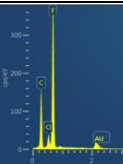
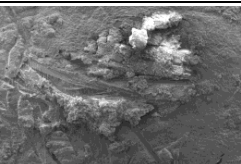
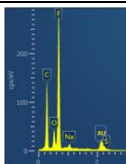
Membranes	(a) Fresh		(b) Fouled																									
	SEM (250 X)	EDX	SEM (250 X)	EDX																								
FBM		 <table><thead><tr><th>Element</th><th>Wt%</th></tr></thead><tbody><tr><td>C K</td><td>92.7</td></tr><tr><td>O K</td><td>7.3</td></tr><tr><td>S K</td><td>0</td></tr><tr><td>Na K</td><td>0</td></tr></tbody></table>	Element	Wt%	C K	92.7	O K	7.3	S K	0	Na K	0		 <table><thead><tr><th>Element</th><th>Wt%</th></tr></thead><tbody><tr><td>C K</td><td>71.3</td></tr><tr><td>O K</td><td>22.8</td></tr><tr><td>S K</td><td>4.8</td></tr><tr><td>Na K</td><td>1.1</td></tr></tbody></table>	Element	Wt%	C K	71.3	O K	22.8	S K	4.8	Na K	1.1				
Element	Wt%																											
C K	92.7																											
O K	7.3																											
S K	0																											
Na K	0																											
Element	Wt%																											
C K	71.3																											
O K	22.8																											
S K	4.8																											
Na K	1.1																											
FKB		 <table><thead><tr><th>Element</th><th>Wt%</th></tr></thead><tbody><tr><td>C K</td><td>95</td></tr><tr><td>O K</td><td>5</td></tr><tr><td>S K</td><td>0</td></tr><tr><td>Na K</td><td>0</td></tr></tbody></table>	Element	Wt%	C K	95	O K	5	S K	0	Na K	0		 <table><thead><tr><th>Element</th><th>Wt%</th></tr></thead><tbody><tr><td>C K</td><td>73.29</td></tr><tr><td>O K</td><td>21.8</td></tr><tr><td>S K</td><td>3.1</td></tr><tr><td>Na K</td><td>1.2</td></tr></tbody></table>	Element	Wt%	C K	73.29	O K	21.8	S K	3.1	Na K	1.2				
Element	Wt%																											
C K	95																											
O K	5																											
S K	0																											
Na K	0																											
Element	Wt%																											
C K	73.29																											
O K	21.8																											
S K	3.1																											
Na K	1.2																											
CMB		 <table><thead><tr><th>Element</th><th>Wt%</th></tr></thead><tbody><tr><td>C K</td><td>82.5</td></tr><tr><td>O K</td><td>15.8</td></tr><tr><td>S K</td><td>0</td></tr><tr><td>Na K</td><td>1.7</td></tr></tbody></table>	Element	Wt%	C K	82.5	O K	15.8	S K	0	Na K	1.7		 <table><thead><tr><th>Element</th><th>Wt%</th></tr></thead><tbody><tr><td>C K</td><td>69.2</td></tr><tr><td>O K</td><td>21.9</td></tr><tr><td>S K</td><td>5.1</td></tr><tr><td>Na K</td><td>3.8</td></tr></tbody></table>	Element	Wt%	C K	69.2	O K	21.9	S K	5.1	Na K	3.8				
Element	Wt%																											
C K	82.5																											
O K	15.8																											
S K	0																											
Na K	1.7																											
Element	Wt%																											
C K	69.2																											
O K	21.9																											
S K	5.1																											
Na K	3.8																											
CM (H)-PES		 <table><thead><tr><th>Element</th><th>Wt%</th></tr></thead><tbody><tr><td>C K</td><td>90</td></tr><tr><td>O K</td><td>8.1</td></tr><tr><td>S K</td><td>0</td></tr><tr><td>Na K</td><td>1.9</td></tr></tbody></table>	Element	Wt%	C K	90	O K	8.1	S K	0	Na K	1.9		 <table><thead><tr><th>Element</th><th>Wt%</th></tr></thead><tbody><tr><td>C K</td><td>64.3</td></tr><tr><td>O K</td><td>20.3</td></tr><tr><td>S K</td><td>10.7</td></tr><tr><td>Na K</td><td>4.7</td></tr></tbody></table>	Element	Wt%	C K	64.3	O K	20.3	S K	10.7	Na K	4.7				
Element	Wt%																											
C K	90																											
O K	8.1																											
S K	0																											
Na K	1.9																											
Element	Wt%																											
C K	64.3																											
O K	20.3																											
S K	10.7																											
Na K	4.7																											
Nafion 324		 <table><thead><tr><th>Element</th><th>Wt%</th></tr></thead><tbody><tr><td>C K</td><td>25.5</td></tr><tr><td>O K</td><td>5.5</td></tr><tr><td>FK</td><td>69</td></tr><tr><td>S K</td><td>0</td></tr><tr><td>Na K</td><td>0</td></tr></tbody></table>	Element	Wt%	C K	25.5	O K	5.5	FK	69	S K	0	Na K	0		 <table><thead><tr><th>Element</th><th>Wt%</th></tr></thead><tbody><tr><td>C K</td><td>26.9</td></tr><tr><td>O K</td><td>7.5</td></tr><tr><td>FK</td><td>60.2</td></tr><tr><td>S K</td><td>3.2</td></tr><tr><td>Na K</td><td>2.2</td></tr></tbody></table>	Element	Wt%	C K	26.9	O K	7.5	FK	60.2	S K	3.2	Na K	2.2
Element	Wt%																											
C K	25.5																											
O K	5.5																											
FK	69																											
S K	0																											
Na K	0																											
Element	Wt%																											
C K	26.9																											
O K	7.5																											
FK	60.2																											
S K	3.2																											
Na K	2.2																											

Figure 6.5 Scanning electron microscopy (*SEM*) and elemental analysis (*EDX*) of the (a) fresh and (b) fouled ion exchange membranes in contact with the *BL* solution

Cleaning the fouled *IEMs* with the caustic soda solution was successful and no contamination was detected on the *IEM* samples after the cleaning step (Figure 6.6 (a)). The cleaned membranes depicted the same appearance as the fresh ones (Figure 6.6 (a)-*SEM* images). Utilizing the fresh diluted *BL*, as the cleaning agent, was also practical and no obvious deposition was observed on the *IEMs*' surfaces during the *SEM* analysis (Figure 6.6 (b)). However, some holes were detected on the surface of the cleaned *CM(H) – PES*; also a part

of the cleaned Nafion 324 backbone was observed during the *SEM* analysis. Possibly, the cleaning agent (the fresh diluted *BL*) caused these alterations. In addition, the *EDX* results revealed the presence of a small percentage of sodium and sulfur on the surface of the cleaned *FKB* and *CM(H)–PES* membranes which may imply that a fraction of the foulants (lignin particles) remained on the surface or inside the holes of these cleaned membranes.

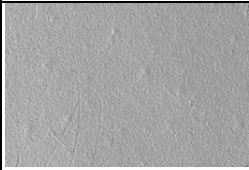
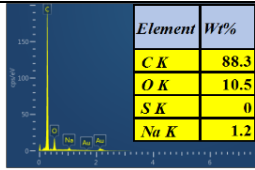
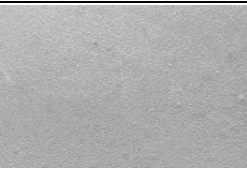
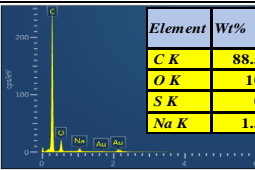

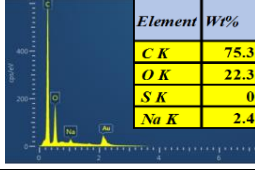
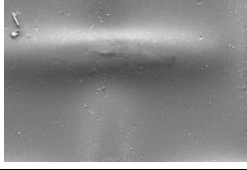
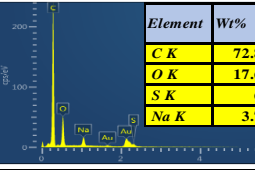

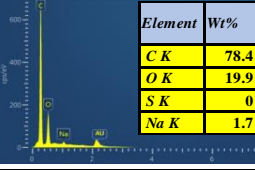

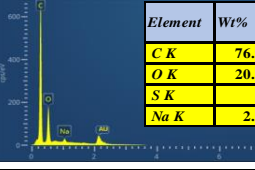

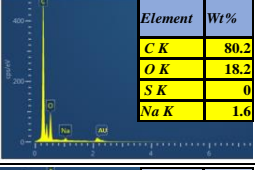

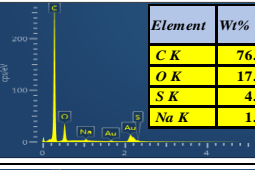

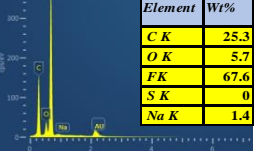
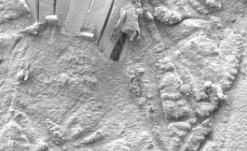
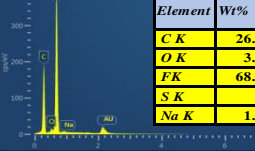
Membranes	(a) Cleaned with NaOH		(b) Cleaned with BL																									
	SEM (250 X)	EDX	SEM (250 X)	EDX																								
FBM		 <table><thead><tr><th>Element</th><th>Wt%</th></tr></thead><tbody><tr><td>C K</td><td>88.3</td></tr><tr><td>O K</td><td>10.5</td></tr><tr><td>S K</td><td>0</td></tr><tr><td>Na K</td><td>1.2</td></tr></tbody></table>	Element	Wt%	C K	88.3	O K	10.5	S K	0	Na K	1.2		 <table><thead><tr><th>Element</th><th>Wt%</th></tr></thead><tbody><tr><td>C K</td><td>88.5</td></tr><tr><td>O K</td><td>10</td></tr><tr><td>S K</td><td>0</td></tr><tr><td>Na K</td><td>1.5</td></tr></tbody></table>	Element	Wt%	C K	88.5	O K	10	S K	0	Na K	1.5				
Element	Wt%																											
C K	88.3																											
O K	10.5																											
S K	0																											
Na K	1.2																											
Element	Wt%																											
C K	88.5																											
O K	10																											
S K	0																											
Na K	1.5																											
FKB		 <table><thead><tr><th>Element</th><th>Wt%</th></tr></thead><tbody><tr><td>C K</td><td>75.3</td></tr><tr><td>O K</td><td>22.3</td></tr><tr><td>S K</td><td>0</td></tr><tr><td>Na K</td><td>2.4</td></tr></tbody></table>	Element	Wt%	C K	75.3	O K	22.3	S K	0	Na K	2.4		 <table><thead><tr><th>Element</th><th>Wt%</th></tr></thead><tbody><tr><td>C K</td><td>72.8</td></tr><tr><td>O K</td><td>17.6</td></tr><tr><td>S K</td><td>6</td></tr><tr><td>Na K</td><td>3.7</td></tr></tbody></table>	Element	Wt%	C K	72.8	O K	17.6	S K	6	Na K	3.7				
Element	Wt%																											
C K	75.3																											
O K	22.3																											
S K	0																											
Na K	2.4																											
Element	Wt%																											
C K	72.8																											
O K	17.6																											
S K	6																											
Na K	3.7																											
CMB		 <table><thead><tr><th>Element</th><th>Wt%</th></tr></thead><tbody><tr><td>C K</td><td>78.4</td></tr><tr><td>O K</td><td>19.9</td></tr><tr><td>S K</td><td>0</td></tr><tr><td>Na K</td><td>1.7</td></tr></tbody></table>	Element	Wt%	C K	78.4	O K	19.9	S K	0	Na K	1.7		 <table><thead><tr><th>Element</th><th>Wt%</th></tr></thead><tbody><tr><td>C K</td><td>76.9</td></tr><tr><td>O K</td><td>20.8</td></tr><tr><td>S K</td><td>0</td></tr><tr><td>Na K</td><td>2.3</td></tr></tbody></table>	Element	Wt%	C K	76.9	O K	20.8	S K	0	Na K	2.3				
Element	Wt%																											
C K	78.4																											
O K	19.9																											
S K	0																											
Na K	1.7																											
Element	Wt%																											
C K	76.9																											
O K	20.8																											
S K	0																											
Na K	2.3																											
CM (H)-PES		 <table><thead><tr><th>Element</th><th>Wt%</th></tr></thead><tbody><tr><td>C K</td><td>80.2</td></tr><tr><td>O K</td><td>18.2</td></tr><tr><td>S K</td><td>0</td></tr><tr><td>Na K</td><td>1.6</td></tr></tbody></table>	Element	Wt%	C K	80.2	O K	18.2	S K	0	Na K	1.6		 <table><thead><tr><th>Element</th><th>Wt%</th></tr></thead><tbody><tr><td>C K</td><td>76.3</td></tr><tr><td>O K</td><td>17.8</td></tr><tr><td>S K</td><td>4.8</td></tr><tr><td>Na K</td><td>1.1</td></tr></tbody></table>	Element	Wt%	C K	76.3	O K	17.8	S K	4.8	Na K	1.1				
Element	Wt%																											
C K	80.2																											
O K	18.2																											
S K	0																											
Na K	1.6																											
Element	Wt%																											
C K	76.3																											
O K	17.8																											
S K	4.8																											
Na K	1.1																											
Nafion 324		 <table><thead><tr><th>Element</th><th>Wt%</th></tr></thead><tbody><tr><td>C K</td><td>25.3</td></tr><tr><td>O K</td><td>5.7</td></tr><tr><td>FK</td><td>67.6</td></tr><tr><td>S K</td><td>0</td></tr><tr><td>Na K</td><td>1.4</td></tr></tbody></table>	Element	Wt%	C K	25.3	O K	5.7	FK	67.6	S K	0	Na K	1.4		 <table><thead><tr><th>Element</th><th>Wt%</th></tr></thead><tbody><tr><td>C K</td><td>26.9</td></tr><tr><td>O K</td><td>3.2</td></tr><tr><td>FK</td><td>68.5</td></tr><tr><td>S K</td><td>0</td></tr><tr><td>Na K</td><td>1.4</td></tr></tbody></table>	Element	Wt%	C K	26.9	O K	3.2	FK	68.5	S K	0	Na K	1.4
Element	Wt%																											
C K	25.3																											
O K	5.7																											
FK	67.6																											
S K	0																											
Na K	1.4																											
Element	Wt%																											
C K	26.9																											
O K	3.2																											
FK	68.5																											
S K	0																											
Na K	1.4																											

Figure 6.6 Scanning electron microscopy (*SEM*) and elemental analysis (*EDX*) of the cleaned ion exchange membranes with (a) caustic soda solution and (b) fresh diluted black liquor solution (*FBM* : bipolar membrane, FuMA-Tech, *FKB* : cation exchange membrane, FuMA-Tech, *CMB* : cation exchange membrane, Neosepta, *CM(H)–PES* : cation exchange membrane, Mega a.s., Nafion 324 : cation exchange membrane, DuPont)

Contact Angle

The CA data of the fresh, fouled and cleaned IEM s are listed in Table 6.4. Several factors influence the CA value such as membrane materials, membrane preparation techniques, roughness of the surface and the applied CA measurement method [106, 107]. In general, heterogeneous membranes have a higher CA value than homogeneous membranes because of its non-uniform distribution of ionic groups on its surface, which caused surface roughness [107]. In this study, the fresh heterogeneous $CM(H) - PES$ membrane had the highest CA . The fresh FBM and FKB also showed less hydrophilic surfaces than the fresh Nafion 324 and CMB .

Despite the fact that lignin was reported to be more hydrophobic than other wood components (cellulose and hemicellulose) [111], the precipitated Kraft lignin on the surface of the IEM s reduced the CA of the membranes. This can be due to the delignification process during the Kraft pulping. Throughout this process, which takes place in the cooking step (Figure 7.1), a large amount of polar functional (hydroxyl and carboxyl) form in the Kraft lignin macro-molecule structure and as a result, the polar groups contribution of the Kraft lignin increases [112, 113, 114]. Norgren *et al.*, also reported a notably low CA for a thin film of the Kraft lignin [115]. According to the thickness measurement data, the fouled FBM , $CM(H) - PES$ and FKB were more affected by the fouling phenomenon and had the thickest layers of the deposit lignin, respectively; presumably they should have the highest wettabilities (lowest CA s). The recorded CA values for the fouled FBM and FKB substantiated this hypothesis. However, the registered CA value for the fouled $CM(H) - PES$ was still high. Probably, formation of the non-uniform lignin on its surface can elucidate this discrepancy. By reviewing its SEM image (Figure 6.5 (b)), one can detect some deep grooves. These grooves induced the surface roughness and, consequently, elevated its CA . On the other hand, the thickness measurement results of the fouled CMB and Nafion 324 showed a thin layer of the precipitated lignin which means less polar contribution was presented on their surfaces and accordingly, their surfaces did not become completely hydrophilic.

After the $NaOH$ cleaning cycle, the registered CA values for all the IEM s were similar to their initial values. Nevertheless, it should be remarked that the CA data of the cleaned $CM(H) - PES$ and Nafion 324 had striking variations as a result of their rough and non-uniform surfaces. In other words, the roughness and the heterogeneity surface of these membranes would decrease the cleaning efficiency. Cleaning the IEM s with the fresh diluted BL could almost restore the original CA values of the FBM and CMB membranes, while the cleaned FKB and $CM(H) - PES$ recorded lower values than their initial ones. Presence of a minor fouling on the surface and inside these membranes (which was stated in

the previous part) caused the reduction in their CA values. Surprisingly, the cleaned Nafion 324 registered a high CA than its original CA . As observed on its SEM image (Figure 6.6 (b)), its surface was partially deteriorated which possibly amplified the surface roughness and subsequently the surface hydrophobicity.

Table 6.4 Contact Angle measurements ($^{\circ}$)

Membranes	Fresh	Fouled	Cleaned with $NaOH$	Cleaned with BL
FBM	$70 \pm 5^{a*}$	0 ± 0^b	70 ± 1^a	71 ± 3^a
FKB	64 ± 1^a	0 ± 0^b	63 ± 6^a	57 ± 4^a
CMB	47 ± 3^a	36 ± 1^b	46 ± 4^a	45 ± 3^a
$CM(H) - PES$	78 ± 3^a	65 ± 5^a	73 ± 10^a	68 ± 5^a
Nafion 324	53 ± 5^a	30 ± 9^c	56 ± 11^a	75 ± 5^b

Table 6.4 * The mean values (presented at each row) for fresh, fouled and cleaned membranes followed by different letters (a, b and c), are significantly different ($p < 0.05$)

Ion Exchange Capacity

Table 6.5 illustrates the experimentally determined IEC data of the fresh and cleaned $CEMs$. Both types of cleaning chemicals could restore the IEC of the CMB and Nafion 324 membranes, while none of the cleaning agent could reestablish the initial IEC values of the FKB and $CM(H) - PES$ membranes. Probably, the concentration of the active functional groups decreased as a result of the small contamination of the foulants on the surface or inside the cleaned membranes [116], or modification of the surface functional groups during the IEC measurement procedure may cause these differences. It should be mentioned that the $NaOH$ cleaning had less negative impact on the FKB and $CM(H) - PES$ membranes than the fresh diluted BL . In addition, the experimental findings corresponded to the fresh $CEMs$ are in a reasonable agreement with the data found in the literature and presented by the membrane suppliers [19, 117].

Table 6.5 Ion Exchange Capacity of Cation Exchange Membranes ($meq. g^{-1}$)

Membranes	Fresh	Cleaned with $NaOH$	Cleaned with BL
<i>FKB</i>	$1.13 \pm 0.02^{a*}$	0.82 ± 0.01^b	0.75 ± 0.02^c
<i>CMB</i>	3.11 ± 0.01^a	3.11 ± 0.01^a	3.12 ± 0.02^a
<i>CM(H) – PES</i>	2.33 ± 0.03^a	2.01 ± 0.02^b	1.94 ± 0.02^c
Nafion 324	0.92 ± 0.01^a	0.91 ± 0.01^a	0.91 ± 0.03^a

Table 6.5 * The mean values (presented at each row) for fresh and cleaned membranes followed by different letters (a, b and c), are significantly different ($p < 0.05$)

Membrane Electrical Resistance

The results of the electrical resistance measurements of the fresh and cleaned *CEMs* are given in Table 6.6. The fresh heterogeneous *CM(H) – PES* recorded the highest electrical resistance than the other examined *CEMs*. Generally, the heterogeneous *IEMs* possess a higher electrical resistance than the homogeneous ones, as the mobile ions have to go through a longer pathway in the *IEM* structure [30]. As can be noted, the lignin precipitation and the chemical cleaning process did not change the electrical resistance of the cleaned *CMB* and Nafion 324. However, the electrical resistance of the cleaned *FKB* and *CM(H) – PES* membranes were increased by 10%. This change was independent of the type of the applied cleaning solution and can be contributed to the presence of small amount of foulants (lignin particles) on the surface or inside these membranes [75, 104], or some minor damages of the membrane surface during the *EDBM* and/or the cleaning step(s). Generally, the depletion of the IEC leads to a rise in the membrane electrical resistance [116] and the results of the membrane electrical resistance for the cleaned *FKB* and *CM(H) – PES* membranes are in accordance with the IEC data. The electrical resistance values of the fresh *CEMs* are consistent with the data presented in other studies and the information provided by the membrane suppliers [19, 118].

Taking into account the membrane analysis findings, it can be deduced that the *CMB* and Nafion 324 were the most stable *CEMs* under the high alkaline conditions. From the economical point of view, *CMB* membrane is recommended to be utilized during the electrochemical acidification of the Kraft *BL* via *EDBM* process as it has a lower cost than Nafion 324. Also, the applied *BPM* showed a reasonable chemical and mechanical stability and can be used for this application.

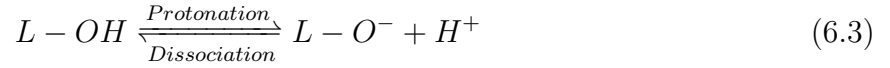
Table 6.6 Membrane Electrical Resistance (Ωcm^2)

Membranes	Fresh	Cleaned with $NaOH$	Cleaned with BL
<i>FKB</i>	$6.5 \pm 0.4^{a*}$	7.1 ± 0.6^a	7.2 ± 0.3^a
<i>CMB</i>	4.7 ± 0.3^a	4.7 ± 0.4^a	4.7 ± 0.5^a
<i>CM(H) - PES</i>	9.1 ± 0.5^a	9.9 ± 0.6^a	10.1 ± 0.5^a
Nafion 324	4.9 ± 0.3^a	4.9 ± 0.4^a	4.9 ± 0.4^a

Table 6.6 * The mean values (presented at each row) for fresh and cleaned membranes followed by a letters (a), are not significantly different ($p > 0.05$)

6.3.3 Chemical Cleaning Mechanisms

The macro-molecule Kraft lignin contains weakly ionic (mainly phenolic) groups and acts as a polyelectrolyte in an aqueous solution [5, 62, 63, 64]. These phenolic groups are presumed to be evenly distributed on the surface of the macro-molecule and therefore they can easily be in direct contact with an alkaline solution, become ionized and subsequently dissolve the lignin [5, 62]. The simplified dissociation (ionization) reaction of the phenolic groups can be written as :



Here, L represents the lignin macro-molecule and $-OH$ shows the lignin phenolic group. The dissociation constant can be defined as the ratio of the activities of $a_{(L-O^-)}$, $a_{(H^+)}$ and $a_{(L-OH)}$:

$$K_a = \frac{a_{(L-O^-)} a_{(H^+)}}{a_{(L-OH)}} \quad (6.4)$$

The logarithmic constant, pK_a , is mainly used to describe the lignin dissociation and protonation reaction and varies from 6.2 to 11.3 depending on the substantial pattern of the phenolic groups [5, 91].

Based on the well-known *DLVO* theory, the solubility of a polyelectrolyte (like Kraft lignin) is strongly dependent on the balance of the attractive and repulsive forces [92]. As stated in several studies [5, 62, 63, 64, 90], during the lignin association, the attractive forces become dominant due to the protonation of the phenolic groups and formation of hydrogen bonds by phenolic-phenolic linkages or phenolic- ether linkages. As a result, lignin starts to self-aggregate and, consequently, precipitate [97]. Therefore, it can be assumed that by inducing

the repulsive forces the precipitated lignin would become re-solubilized inside the aqueous solution. These forces are mainly influenced by the structure of the deposit layer (its cohesion and porosity) and the solution conditions such as pH, temperature and the ionic strength [63, 98, 99, 101]. Figure 6.7 (a and b), shows high magnification *SEM* images of the fouled layer on the surface of the *BPM*. The porous or loose structure of the precipitated layer favors an easier access for the cleaning agents to penetrate through it and accordingly, enhances the mass transfer and the cleaning efficiency [98, 99, 101].

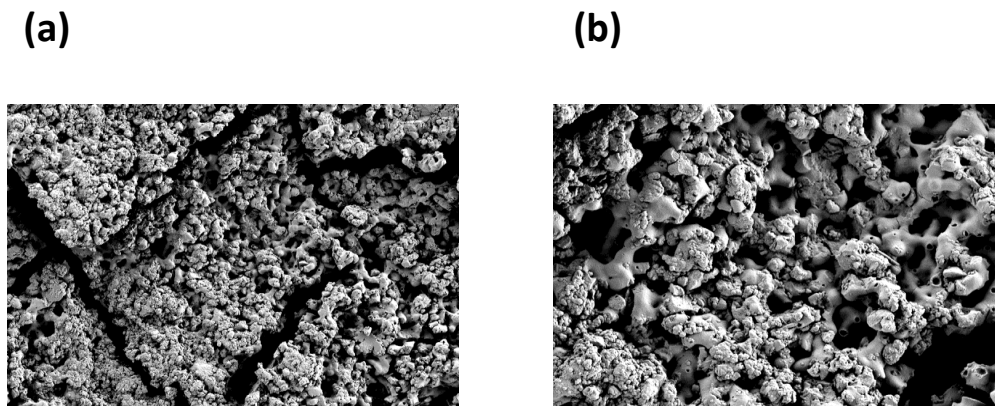


Figure 6.7 *SEM* images of the deposit lignin on the surface of the fouled *BPM* at (a) 2000 *X* and (b) 5000 *X*

Throughout the chemical cleaning cycle, the precipitated lignin was in direct contact with the cleaning solution (*NaOH* or *BL*). The cleaning chemical affected the balance between the repulsive and attractive forces (Figure 6.8 (a)) and penetrated through the deposit layer, broke the hydrogen bonds and split the lignin layer into smaller fragments. These fragments possess a larger surface area in contact with the alkaline medium (Figure 6.8 (b)). Hence, the existing phenolic groups on the surface of the macro-molecule collided with the hydroxide ions (from the alkaline solution) and became ionized (Figure 6.8 (c)). Finally, these negatively charged groups repelled each other and lignin became soluble inside the alkaline solution (Figure 6.8 (d)) [5].

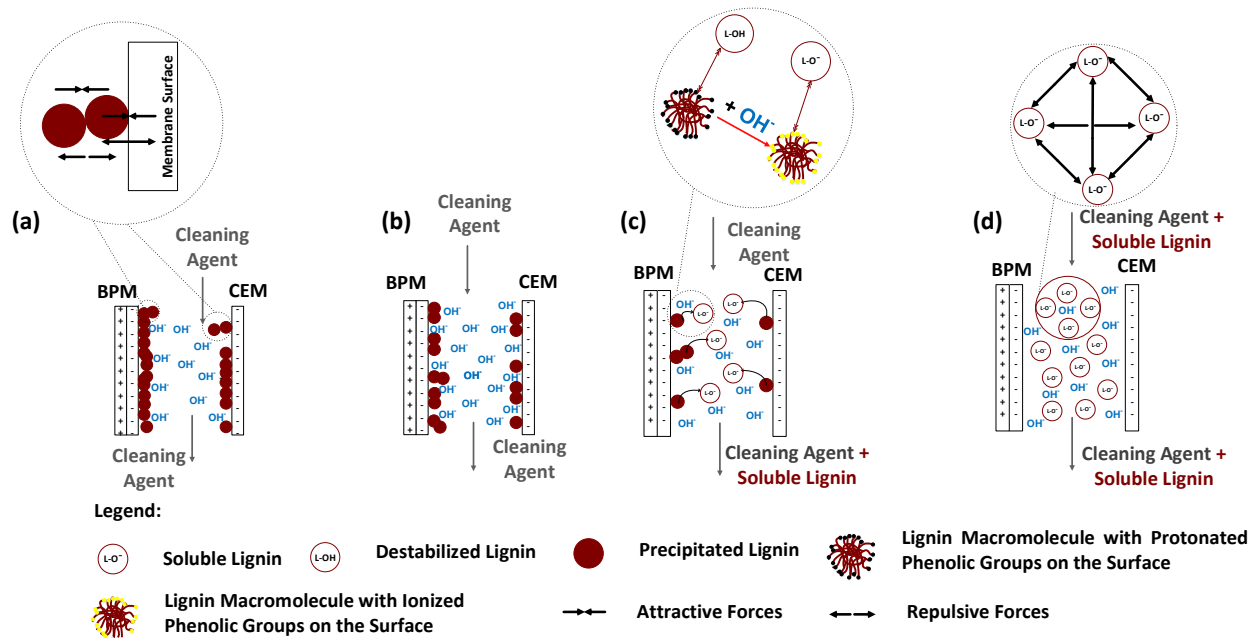


Figure 6.8 Chemical cleaning mechanisms : (a) the alkaline cleaning solution interacts with the attractive and repulsive forces, (b) cleavage of the lignin layer into smaller fragments with a larger surface area, (c) ionization of the lignin phenolic groups inside the alkaline medium, (d) repulsion of the charged phenolic groups and lignin solubility

Various parameters may affect the mass transfer and the dissociation reaction of the phenolic groups and consequently the lignin solubility such as the composition of the cleaning solution and the length of the cleaning step [99]. By drawing a comparison between the membrane analysis results of the cleaned membranes with the caustic soda and the fresh diluted *BL* solutions, one can perceive that the caustic soda solution had a better performance in the given cleaning period (30 minutes). This can be attributed to the difference in the ionic strength and hydroxide ion concentration of the caustic soda and the fresh diluted *BL* solutions. Perhaps, increasing the length of the cleaning period would improve the cleaning efficiency when the *BL* is used as the cleaning agent. Another potential option to control the fouling of the *IEMs* would be switching the *EDBM* mode from batch to feed and bleed with regular disconnection of the electrical field. This possibility was practiced for the electrolysis of the Kraft *BL* by Cloutier *et al.* [44]. If this preposition works for the *EDBM* application, the electrochemical acidification process can be carried out without any interruption for the chemical cleaning cycle and the *BL* would be available in situ and free of charge. However, further investigation is required to validate this supposition.

6.4 Conclusion

This investigation evaluated the impacts of the membrane fouling and the chemical cleaning cycle on the *IEMs*' integrity during the electrochemical acidification of Kraft *BL* via *EDBM* method. The fouled particles were removed successfully from the surface of the *IEMs* when an alkaline solution (caustic soda or fresh diluted *BL*) was utilized. Comparison of the analysis results of the fresh, fouled and cleaned membranes revealed that two *CEMs* i.e. *CMB* and Nafion 324 were the most chemically stable membranes under the alkaline conditions. Also, most of the initial properties of the *BPM* were reestablished after the chemical cleaning step. It should be highlighted that despite the fact that application of the caustic soda as the cleaning agent presented better results and cleaner membrane surface, from the sustainability point of view, utilization of in situ and free of charge *BL* instead of *NaOH* would be more eco-efficient and the produced *NaOH* (during the *EDBM* step) can be used in the Kraft or other processes.

In conclusion, it is evident that the fouling phenomenon and its footprints can be mitigated by selecting appropriate *IEMs*, periodic cleaning cycles and proper operating conditions. Throughout this study, the first two aspects were explored and the latter one will be addressed in future paper.

Acknowledgments

The financial support of NSERC and BioFuelNet Canada is acknowledged. In addition, the authors gratefully thank Hydro Quebec Energy Technology Laboratory (*LTEE*) for providing the experimental setup, Mega a.s. for kindly supplying the *CM(H) – PES* membranes and Mrs. Ir. E. Shahrabi for taking the *SEM* images.

CHAPTER 7 ARTICLE 4 : EFFECT OF PROCESS VARIABLES ON THE PERFORMANCE OF ELECTROCHEMICAL ACIDIFICATION OF KRAFT BLACK LIQUOR BY ELECTRODIALYSIS WITH BIPOLAR MEMBRANE

Maryam Haddad^a, Raynald Labrecque^b, Laurent Bazinet^c, Oumarou Savadogo^a, Jean Paris^a

a : Research Unit on Energy Efficiency and Sustainable Implementation of the Forest Biorefinery (*E²D²BF*), Department of Chemical Engineering, Polytechnique de Montréal, Canada

b : Laboratoire des technologies de l'énergie d'Hydro-Québec (*LTE*), Shawinigan, Canada

c : Institute of Nutrition and Functional Foods (*INAF*), Laboratory of food processing and electromembrane processes (*LTAPEM*), Department of Food Sciences, Université Laval, Canada

Abstract

Lignin which is dissolved in the residual black liquor stream of Kraft pulping mills can be extracted and converted into a wide range of value-added bio-based products. To this end, design and development of an eco-efficient lignin extraction method is crucial. Electro-membrane based technologies and particularly, electrodialysis with bipolar membrane (*EDBM*) is a promising and green avenue to acidify the black liquor and extract the lignin. Therefore, the intention of this study is to evaluate the performance of the *EDBM* acidification process in terms of current efficiency and energy consumption. The effect of main process variables such as operational temperature and black liquor chemical composition on the efficiency of the *EDBM* process have been evaluated. The experimental results demonstrated the substantial influence of these parameters on the *EDBM* current efficiency, energy consumption and fouling of the ion exchange membranes. Furthermore, it was indicated that promoting the hydrodynamics of the system could delay and mitigate the lignin self-aggregation and precipitation inside the *EDBM* stack. The highest current efficiency and, subsequently, the lowest energy consumption were achieved when the *EDBM* process was carried out at 55 °C with the *BL* solution containing 20 % (wt.) total dissolved solids.

Keywords : Bipolar membrane, electrodialysis, operational conditions, black liquor chemical composition, lignin extraction

7.1 Introduction

Kraft process is a predominant pulp and paper production method, worldwide. In most of the conventional Kraft pulping mills, around 50 % of the wood components (mainly hemicellulose and lignin) are dissolved in a residual stream called black liquor (*BL*) and combusted in the recovery boiler to produce steam, electricity and re-generate the cooking chemicals (Figure 7.1) [4, 5]. By contrast, in an integrated forest biorefinery (*IFBR*) concept, wood constituents are separated from the pulp stream and transformed into value-added bio-based products [3]. In particular, extracted lignin can be used as biofuels or as a precursor to a vast phenolic platform of chemical pathways [6]. Furthermore, lignin extraction can increase the capacity of the Kraft mill by decreasing the load of its recovery boiler [4, 5].

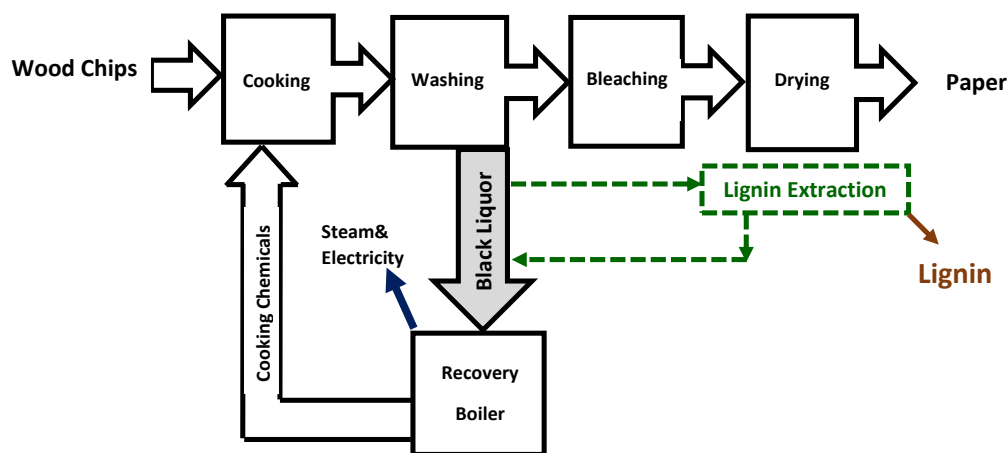


Figure 7.1 A simplified illustration of Kraft process

Different techniques have been examined to extract lignin from the *BL* [11, 39, 119]. Indeed, lowering the pH of the *BL* by CO_2 sparging is the most common process to acidify the *BL* and extract the lignin [4, 5]. However, in recent years, the increasing interests in green products and sustainable technologies encouraged researchers to look for eco-efficient pathways to extract the lignin. One of the most sustainable methods for this purpose is employing a membrane separation process such as ultrafiltration (*UF*) or electrochemical acidification methods using ion exchange membranes (*IEM*). An extensive study on lignin separation via the *UF* system was performed in Sweden [14, 120]. Application of the *UF* process resulted in lignin removal with a specific molecular weight; however, to enhance the lignin extraction yield, another acidification step such as *BL* carbonation was required [5, 119].

The *BL* is an electrolyte alkaline solution containing inorganic salts such as Na_2SO_4 , Na_2S , Na_2CO_3 and $NaOH$ as well as organic constituents; therefore, electrodialysis with bipolar

membrane (*EDBM*) is a green and promising electrochemical method to acidify the *BL* and, subsequently, extract the lignin. Earlier, we demonstrated that the acidification of the Kraft *BL* by means of the *EDBM* process resulted in a less chemical consumption than the conventional chemical acidification technique [66]. Furthermore, a valuable side-product i.e. *NaOH* solution was simultaneously produced which can be used in the Kraft mill or other chemical industries [66]. When the driving force (electric field) is applied in the *EDBM* system, water dissociation reaction occurs inside the bipolar membrane (*BPM*) and releases proton and hydroxide ions [17] :



The positively charged sodium ions present in the *BL* pass through the cation exchange membrane (*CEM*) and enter the basic compartment where they react with the hydroxide ions from the water splitting reaction and produce caustic soda [66]. The proton ions (produced from the water dissociation reaction) inside the *BL* compartment gradually, drop the pH of the *BL* [66]. As a result, the acidified *BL* and concentrated caustic soda solutions are the outlet streams from the *EDBM* stack. The lignin present in the acidified *BL* can be separated by means of a coagulation process followed by a simple filtration step [4, 66]. However, in the practical *EDBM* trials, membrane fouling was observed [66, 97, 121]. It was found that the protonation of the lignin phenolic groups resulted in formation of destabilized colloidal lignin which eventually formed a layer of lignin on the surface of the *IEMs* (bipolar and cation exchange membranes) and increased the global system resistance [66, 97].

In general, process conditions play an important role in controlling the fouling of the membranes and performance of the membrane-based technologies [18, 33]. The productivity of an *EDBM* process is governed by various parameters. The nature of the feed solutions and desired quality of the products determine a number of these parameters, while some process variables such as applied current density, electrical conductivity, viscosity and operational temperature of the feed solutions can be varied in specific ranges based on the stack and *IEMs*' properties and limitations [18]. However, except for the impact of the applied current density on the performance of the *EDBM* process (the applied current density equals to 75 % of the measured limiting current density value [22]), the influence and interdependencies of the other process variables have never been fully evaluated especially when a complex solution containing polyelectrolyte components like Kraft *BL* is acidified by means of the *EDBM* method.

In principle, the conductivity of a solution is defined as its ability to transmit an electric field by the motion of its charged ions. A high electrical conductivity decreases the global system

resistance and as a result enhances the current efficiency and minimizes the energy consumption of an electro-membrane process. Temperature, ionic strength (mineral concentration) and viscosity of a solution can affect its electrical conductivity [58]. In addition, the viscosity of the solution controls the agitation in the *EDBM* stack and subsequently, the fouling of the *IEMs* [19]. A number of parameters can influence the viscosity of a solution containing polyelectrolyte particles (in current study lignin) such as the concentration and molecular weight of the polyelectrolyte, ionic strength (mineral concentration) of the solution, temperature, shear rate and degree of ionization. However, there is no general theory explaining the correlations of these factors [122]. For that reason, it is essential to determine the evolution of the *BL* viscosity as a function of the temperature and *BL* chemical composition in order to maintain a high agitation in the system and minimize the *IEMs*' fouling [19]. Most of the *BL* properties have a direct or indirect correlation with its chemical composition. The chemical composition of the Kraft *BL* is strongly affected by type of the wood chips (softwood vs. hardwood) and the operational conditions of the Kraft mill. To evaluate the trends of the *BL* properties under different operational conditions its total dissolved solids (*TDS*) content is considered to be the key influencing factor. Roughly, lignin accounts for 30 - 45 % of the *TDS* content of a softwood Kraft *BL* and inorganic matters such as sodium salts comprise of about 30 - 35 % of the *BL TDS* content [4, 5]. Even though it is well-known that increasing the temperature would improve the dissociation of a large number of salts, there seems to be no common agreement on the impact of the temperature on lignin solubility in the literature : Norgren and co-workers claimed that elevating the *BL* temperature induced the protonation reaction of the lignin phenolic groups which decreased the lignin solubility and promoted its precipitation [6, 63, 64]. On the other hand, other researchers reported that the lignin solubility was improved in an alkaline solution with increasing the temperature [5, 123]. In addition, the *IEMs* and the components of the *EDBM* stack are mainly made of cost-effective polymers such as polyethylene (*PE*), poly polypropylene (*PP*), high density polyethylene (*HDPE*) and polyvinyl chloride (*PVC*) which do not possess a very high level of thermal stability [17]. Thus, screening the most appropriate temperature for the electrochemical acidification of the *BL* via the *EDBM* method is crucial.

To this end, the objectives of this study are (1) to investigate the effect of the *BL* chemical composition and temperature on its electrical conductivity and viscosity and (2) to determine the influence of the operational temperature and *BL* chemical composition on the performance of the *EDBM* process and ultimately the efficiency of the electrochemical acidification method. The outcome of this investigation would give a clear and general insight into the effect of the main process variables on the performance of the *EDBM* process, which

has gained less attention in previous studies dealing with the *EDBM* system. Moreover, the end results of this work would enable us to enhance the process efficiency and mitigate the *IEMs*' fouling in order to make this green electrochemical acidification method one step closer towards its practical implementation in a Kraft mill.

7.2 Experimental

7.2.1 Membranes and Materials

The membranes used in this study were Fumasep *FBM* bipolar membrane (FuMA-Tech Co., Germany) and *CMB* cation exchange membrane (Neosepta, Japan). Their main properties are given in Table 7.1.

Table 7.1 Ion exchange membranes specifications provided by their suppliers

Membrane	Type	Thickness (mm)	IEC ($meq.g^{-1}$)	Specific Area Resistance ($\Omega.cm^2$)	Stability (pH)	Temperature °C
<i>CMB</i>	Cation	0.18- 0.21	3.11	4.5	1 – 14	≤ 60
<i>FBM</i>	Bipolar	0.18- 0.20	-	-	1 – 14	≤ 60

A Canadian Kraft pulping mill provided the softwood black liquor with a *TDS* content of about 50 ± 2 (wt. %). This liquor was pre-filtered to remove any suspended solid particles larger than $0.010 \mu m$ utilizing a simple vacuum filtration apparatus and a filter paper (Whatman Grade 111105, UK). Analytical grade chemicals were purchased from Sigma-Aldrich, Canada and standard solutions were supplied by Fisher Scientific, Canada. Demineralized water was used to prepare all the aqueous solutions.

7.2.2 Electrochemical Acidification Apparatus and Protocol

As shown in Figure 7.2, a two-compartment cell was used. The *BPMs* and *CEMs* were placed in an alternating pattern and the *EDBM* stack was surrounded on one end by the anode compartment and on the other end by the cathode compartment (Figure 7.3). The main specifications of the *EDBM* stack are summarized in Table 7.2. The stack was hydraulically connected to three holding reservoirs via three pumps (Model : IWAKI Magnetic Drive Pump *MD.30 R*, Iwaki America Inc., USA). These reservoirs were filled with 2 L of *BL*, *NaOH* and electrode rinse solution (Na_2SO_4), respectively. In order to increase the turbulence inside the stack and minimize the membrane fouling [19], all the experiments were conducted at the maximum flowrate corresponding to the pumps and stack configuration. A jacket coil heat

exchanger was installed in each reservoir to maintain a constant temperature. The driving force of the system was provided by a *DC* power supply (Model : Xantrex *XKW* 40 – 25, USA) connected to the electrode pair. The main operational conditions are presented in Table 7.3. These conditions remained unchanged for all the experiments performed during the course of this study.

Table 7.2 Main specifications of the *EDBM* stack

Specifications	Data
Number of Operating Units	4
Effective Membrane Surface Area	0.0180 m^2
Thickness of each Compartment	0.0007 m
Hydraulic Diameter (D_H)	0.00111 m

Before starting each experiment, the set-up was rinsed for 30 minutes with demineralized water to wash any particle that could remain in the apparatus. All the experiments were carried out in batch mode and preliminary measurement of limiting current density was performed based on the Cowan and Brown method [55]. The *EDBM* stack was operated in a galvanostatic mode in which a constant current was applied and the voltage was allowed to vary during the *EDBM* process. The applied current, voltage drop as well as conductivity and temperature of each reservoir were monitored and recorded by means of a data acquisition system (Model : Agilent 34970 A, USA) connected to a data logger software. Each five minutes, a sample of *BL* was taken for pH measurement using a pH meter (Model : 916 Ti-Touch, Metrohm, Switzerland) equipped with an automatic temperature compensation probe. Three replicate were performed for each operational condition and the *EDBM* was stopped once either the maximum limit of the power supply was reached, or no notable evolution was observed in the electrodynamic parameters.

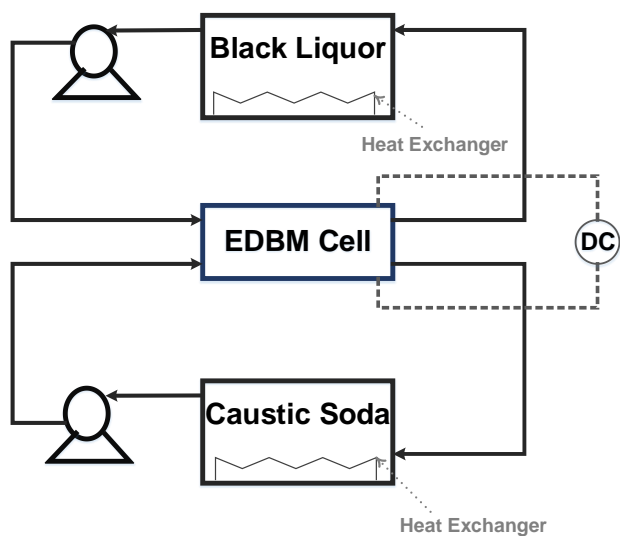


Figure 7.2 A simplified diagram of the electrochemical acidification set-up

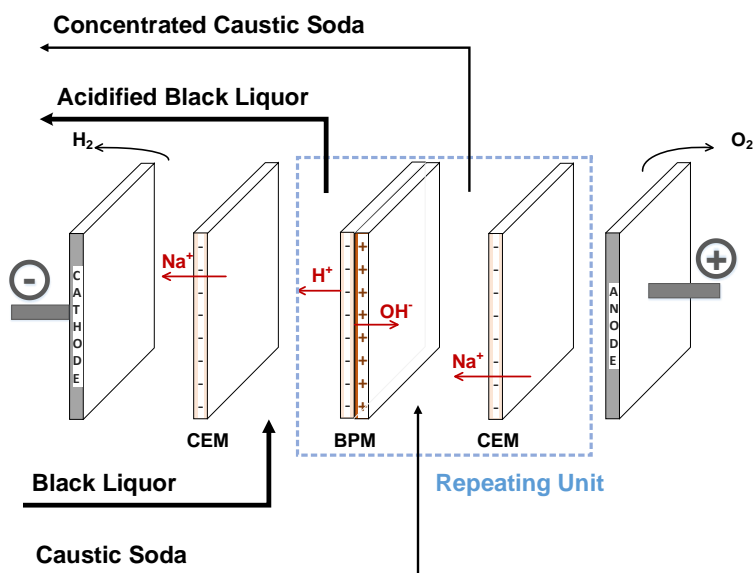


Figure 7.3 A schematic illustration of *EDBM* stack (*CEM* : cation exchange membrane and *BPM* : bipolar membrane)

Table 7.3 Applied Operational Conditions during Electrochemical Acidification of the Kraft *BL*

Operational Conditions	Data
Re-circulation Flow Rate	1 l. min^{-1}
Pressure Drop	34.5 kPa
Applied Current Density	330 A. m^{-2}
Initial NaOH concentration	0.5 M
Initial Na_2SO_4 concentration	0.5 M

7.2.3 Design of Experiments

Two sequential experimental phases were designed. The first experimental phase involved in the evaluation of the effect of temperature and *TDS* content of the *BL* on its electrical conductivity and dynamic viscosity. The main purpose of this experimental series was to specify a *TDS* concentration range where the electrical conductivity of the *BL* recorded the highest values and its dynamic viscosity was low enough to facilitate the fluid motion and induce the agitation inside the system. In order to identify this range, the electrical conductivity and dynamic viscosity of the *BL* solutions with different *TDS* contents (5 - 50 (wt. %)) were measured at two distinct and arbitrary temperatures (35 and 55 °C) using a conductivity meter equipped with an automatic temperature compensation probe (Model : 712 Conductometer, Metrohm, Switzerland) and a viscometer (Model : Visco88 8V Bohlin Reologi, AB, Sweden), respectively. It should be noted that the maximum temperature (55 °C) was chosen by considering the thermal stability of the *IEMs* and occurrence of heat generation at the *BPMs* [19]. Based on the finding of the first phase of the experimental plan, the focus of the second phase was to screen of an appropriate operational temperature and the *TDS* content of the *BL* with the intention of complementing the performance of the *EDBM* process and minimizing the *IEMs*' fouling.

7.2.4 Analysis and Process Evaluation

Feed Characterizations

The *TDS* content of the *BL* was measured by an overnight drying of the pre-weighted *BL* samples at 105 °C and measuring the weight of the residues [124]. Then, these residues were combusted at 950 °C for 16 hours to determine their ash content [120]. The ash content is defined as the weight ratio of the residue before and after its combustion. Lignin concentration of the *BL* solution was obtained by diluting of 2 g of *BL* in 100 mL of 0.1 M NaOH and

again diluting it with demineralized water to an absorbance of $0.3 - 0.8$ using a *UV* spectrophotometer (Model : Biochrom UltraSpec 60*PC* Double beam *UV/Vis* Spectrophotometer, Biochrom, UK) at wavelength of 280 nm with an absorption coefficient of $23.7\text{ dm}^3.\text{g}^{-1}.\text{cm}^{-1}$ [4]. Scan *N* 37 : 98 test method was utilized to determine the sodium content of the *BL* [56]. Residual effective alkali was calculated based on the Radiotis *et al.* procedure [57]. The *BL* density was measured using a pycnometer. In addition, the initial and final concentration of the caustic soda solution was obtained by titration of 20 ml of *NaOH* sample with 1.00 N *HCl* acid using a potentiometric titrator (Model : 916 -TiTouch, Metrohm, Switzerland) [66].

Global System Resistance

Ohm's law was applied to calculate the global system resistance :

$$R = \frac{U}{I} \quad (7.2)$$

Where R represents the global system resistance (Ω), I stands for the applied current (A) and U is the voltage drop across the *EDBM* stack (V) [71].

Reynolds Number

Dimensionless Reynolds number (Re) is an indicator used to evaluate the flow motion in a system. The higher the Re number, the greater the turbulence. This number is expressed as the ratio of the inertial or accretion forces to the viscose forces [125]. Therefore, Reynolds number can be described as a dimensionless correlation between density and dynamic viscosity of the fluid as well as the flow velocity and geometry of the flow channel [19] :

$$Re = \frac{2\rho \nu h}{\mu} \quad (7.3)$$

Where ρ is the density of the fluid ($\text{Kg}.\text{m}^{-3}$), ν denotes the average flow velocity ($\text{m}.\text{s}^{-1}$) in the *BL* and *NaOH* channel, h is the inter-membrane distance (m) and μ indicates the dynamic viscosity of the fluid ($\text{Pa}.\text{s}$) [126]. The average flow velocity in each channel can be determined as :

$$\nu = \frac{W}{gh} \quad (7.4)$$

Here, w stands for the flow rate through the channel and g is the porosity of the space between the *IEMs* [126].

Current Efficiency and Relative Energy Consumption

The performance of an electro-membrane process can be evaluated by determining its current efficiency and relative energy consumption levels [18]. The current efficiency of the *EDBM* process was calculated as [127] :

$$\text{Current Efficiency} = \frac{(V_f C_f - V_i C_i) F}{N I t} \quad (7.5)$$

Here, $V_f C_f$ and $V_i C_i$, respectively are the final and initial moles of *NaOH* solution, F is the Faraday constant ($96485 \text{ C.equivalent}^{-1}$), N represents the number of cell units, I stands for the applied current (A) and t shows the time of the *EDBM* operation (sec).

The relative energy consumption of each *EDBM* experiment was determined as [128] :

$$E_R = \frac{I \int_{t_f}^{t_i} U dt}{3600 M (V_f C_f - V_i C_i)} \quad (7.6)$$

Where, E_R is the total energy consumption ($Wh.g^{-1} NaOH$), U is the voltage drop (V) and M is the molar mass of *NaOH* ($39.997 \text{ g.mole}^{-1}$).

Statistical Analysis

The experimental data were reported as means \pm standard deviation and subjected to one-way and multiple-way statistical analysis using SigmaPlot software (version 13.0, SYSTAT software Inc., San Jose, CA, USA). The probability level was 5%.

7.3 Results and Discussion

7.3.1 Black Liquor Dynamic Viscosity

The dynamic viscosity of the examined Kraft *BL* elevated in an exponential fashion with increasing its *TDS* content, regardless of the temperature ($R^2 = 0.9932$) (Figure 7.4). The statistical analysis results indicated that the *TDS* content of the *BL* significantly controlled its dynamic viscosity ($P = 0.012$). Whereas, increasing the temperature of the *BL* solution had minor effect on its dynamic viscosity ($P = 0.97$).

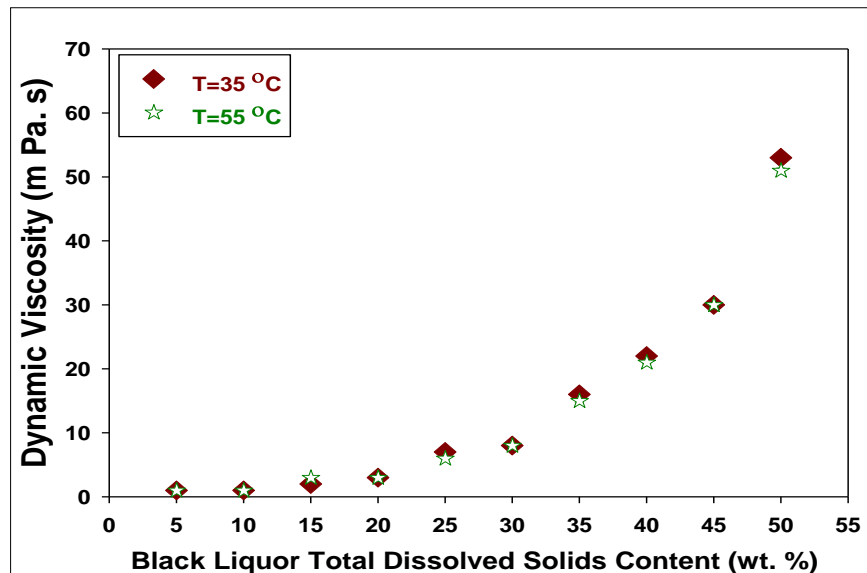


Figure 7.4 Evolution of the Kraft *BL* dynamic viscosity as a function of temperature and *TDS* content of the *BL* ($BL_{Dynamic\ Viscosity} = \exp(0.078 * BL_{TDS})$)

The viscosity of the *BL* is mostly affected by the concentration and weight of its high molecular weight components such as the lignin macro-molecules and carbohydrate chains [129, 130]. Thus, enhancing its *TDS* content resulted in the concentration of these high compounds and higher viscosity values. It should be pointed out that the exponential behavior of the *BL* viscosity curve as a function of its *TDS* content was also observed in previous studies [61, 129].

7.3.2 Black Liquor Electrical Conductivity

Figure 7.5 presents the electrical conductivity profiles of the examined Kraft *BL* for a given *TDS* concentration range (5 - 50 wt. %) and two arbitrary temperatures (35 and 55 °C). As can be seen, the variation of the *BL* electrical conductivity with its *TDS* content possessed a parabolic behavior, regardless of the temperature (R^2 between 0.9866 and 0.9896). This trend can be partitioned into two zones. In zone (1) the conductivity of the *BL* increases monotonously with the *TDS* content to reach a peak at about 30 (wt. %). Nonetheless, increasing the *BL* *TDS* content further caused its conductivity profiles to decline (zone (2)). The statistical analysis results indicate that *TDS* content and particularly the mineral or ash content of the *BL* significantly influence its electrical conductivity ($P < 0.001$). In addition, for all the examined *TDS* contents, elevating the temperature caused a notable increase in electrical conductivity of the *BL* solution ($P < 0.001$).

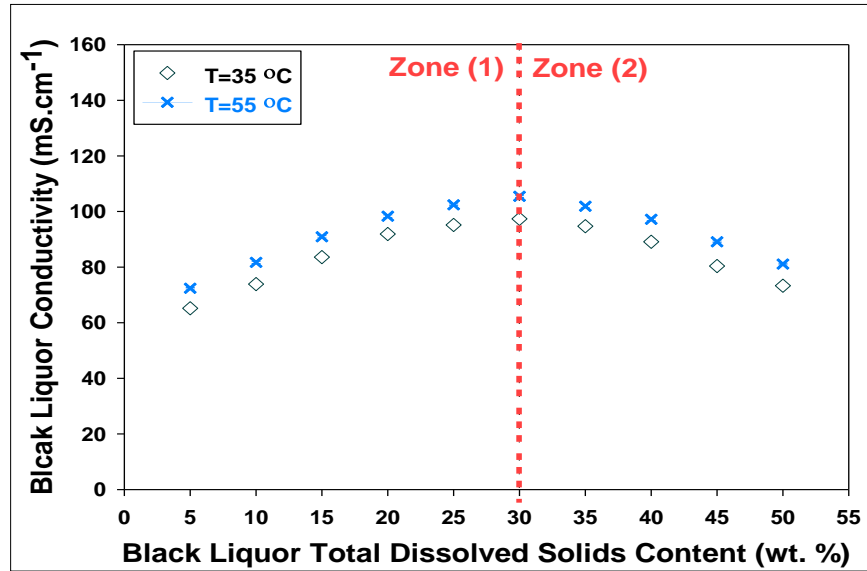


Figure 7.5 Evolution of the Kraft *BL* electrical conductivity as a function of temperature and *TDS* content of the *BL* ($BL_{Electrical\ Conductivity} = -a * (BL_{TDS})^2 + b * (BL_{TDS}) + c$ & $0.055 \leq a \leq 0.055$, $3.19 \leq b \leq 3.21$ and $49.0 \leq c \leq 56.4$)

The monotonic increase in the electrical conductivity of the *BL* can be attributed to the fact that at a higher *TDS* content more charged ions are present in the *BL* solution to carry the current [58]. On the other hand, in zone (2), the high viscosity of the concentrated *BL* (see Figure 7.4), negatively, impacted the ion mobility inside the solution. Furthermore, when the concentration of the electrolyte solution (*BL*) rises, the ion-ion interactions become more pronounced and accordingly, the conductivity of the solution decreases [58]. Clearly, the mobility of the ions in the *BL* solution was enhanced with increasing the temperature and improved the electrical conductivity of the *BL* solution up to a maximum [131].

7.3.3 Influence of Process Variables on Electrodialytic Parameters

Based on the *BL* electrical conductivity and dynamic viscosity measurement findings, the *TDS* content selected for the second phase of the experiments were 20, 25 and 30 (wt. %). The main specifications of these *BL* solutions are listed in Table 7.4. As can be noted, the chemical composition or the *TDS* content of the *BL* substantially affected the main properties of the solution.

Table 7.4 Characteristics of Kraft *BL* solutions

Measured Properties	Predefined <i>TDS</i>		
	30	25	20
<i>TDS</i> (wt. %)	30.1	24.9	20.1
UV Lignin (% <i>TDS</i>)	40.4	40.1	40.6
Ash Content (% <i>TDS</i>)	28.5	28.1	27.9
Sodium Concentration (% <i>TDS</i>)	18.1	17.8	17.9
Residual Alkali ($g. L^{-1}$)	7.2	6.0	5.5
Density ($Kg. m^{-3}$)	1160	1130	1110

Conductivity of Black Liquor and Caustic Soda solution

Figure 7.6 exhibits that the electrical conductivity profile of the *BL* decreased in a non-linear rate as the electrochemical acidification progressed, independently of the operational temperature and *BL* composition (R^2 between 0.9827 and 0.9946). At the same time, the electrical conductivity of the caustic soda solution elevation showed a non-linear trend regardless of the operational temperature and *TDS* content of the *BL* solution (R^2 between 0.9868 and 0.9988). As can be seen, for both of these solutions, the evolution rates of the electrical conductivity profiles are more pronounced at the beginning of the *EDBM* process and no significant change was observed in their progress, towards the end of the process. As expected, elevating the operational temperature had a significant improvement on both of the *BL* and *NaOH* conductivity trends ($P < 0.001$). In addition, enhancing the mineral concentration of the *BL* solution by means of increasing its *TDS* contents substantially upturned its electrical conductivity ($P = 0.007$).

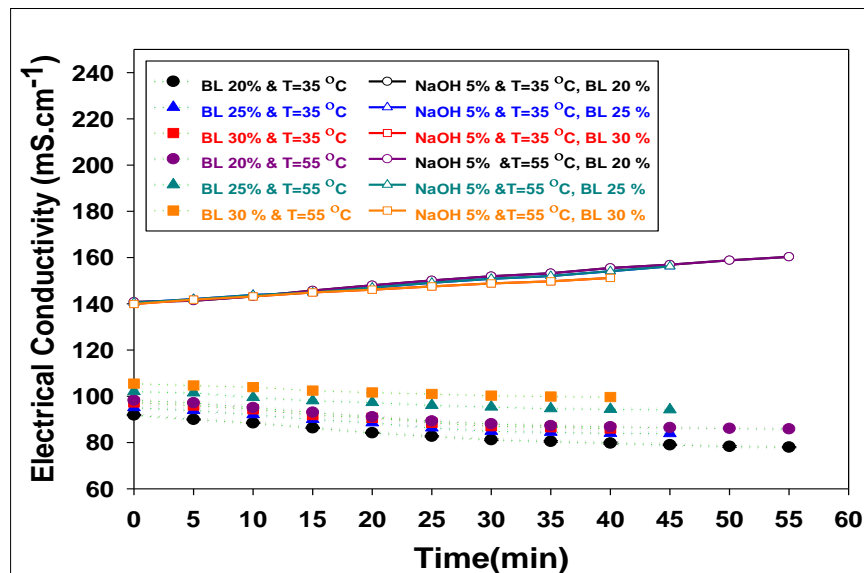


Figure 7.6 Electrical conductivity trends of the *BL* and *NaOH* solutions during the electrochemical acidification of Kraft *BL* via *EDBM* process (fitting equations can be found in Appendix A)

Throughout the *EDBM* experiments, the conductivity of the *BL* lessened and, subsequently, the conductivity of the caustic soda increased due to the migration of sodium ions from the *BL* compartment to the *NaOH* compartment. Also, the production of the hydroxide ions from the water splitting reaction affected the electrical conductivity of the caustic soda. Nonetheless, the occurrence of the *IEMs*' fouling impaired the ions transfer and no significant change was noticed on their conductivity profiles towards the end of the electrochemical acidification process. It should be remarked that these experimental results are in good agreement with our previous findings [66, 97].

Global System Resistance

Figure 7.7 illustrates the evolution of the global system resistance during the *EDBM* process as a function of the operational temperature and *TDS* content of the *BL*. As can be seen, the global system resistance of all the cases followed a cubic trend throughout the electrochemical acidification process (R^2 between 0.9519 and 0.9812). The general trend of the global system resistance can be described as : a linear increase at the beginning of the *EDBM* process which was accompanied by a drastic rise, towards the end of the process. It should be highlighted that the operational temperature and *TDS* content of the *BL* considerably influenced the duration of the linear and drastic incenses of the global system resistance profiles.. The length

of the slight increase was longer when the *TDS* content of the *BL* solution was 20 (wt. %) for both of the operational temperatures ($T = 35$ and 55 ° C). On the contrary, the sharp increase in the overall system resistance profile occurred faster when the *BL* solutions with 30 (wt. %) *TDS* was acidified independently of the operational temperature. The statistical analysis results reported that there were significant differences in the overall system resistance progress during the acidification process when the *TDS* content of the *BL* solution was changed (at $T = 35$ ° C : $P = 0.002$ and at $T = 55$ ° C : $P = 0.007$).

A close observation of Figure 7.7 reveals that increasing the operational temperature led to a significant decrease in the overall system resistance for all the examined *TDS* contents ($P = 0.002$). This difference can be explained by the fact that elevating the temperature enhanced the ion mobility and lowered the global system resistance [131]. Nevertheless, the protonation of the lignin phenolic groups and eventually the precipitation of the lignin on the surface and in the space between the *IEMs* led to the rapid rise of the global system resistance towards the end of the *EDBM* process [66, 121]. However, an increase in the operational temperature delayed this phenomenon.

Even though it was expected that at a higher *TDS* content more ions would be available to carry the current and the resistance inside the system would be decreased, we observed that by increasing the *TDS* content of the *BL* the global system resistance started to rise faster. Most probably the *BL* solution with 30 % *TDS* content possessed a greater abundance of high molecular weight lignin and these large macro-molecules acted as nuclei and provided more sites for attraction of the smaller lignin molecules. As a results, the lignin self-aggregation and precipitation was induced [64].

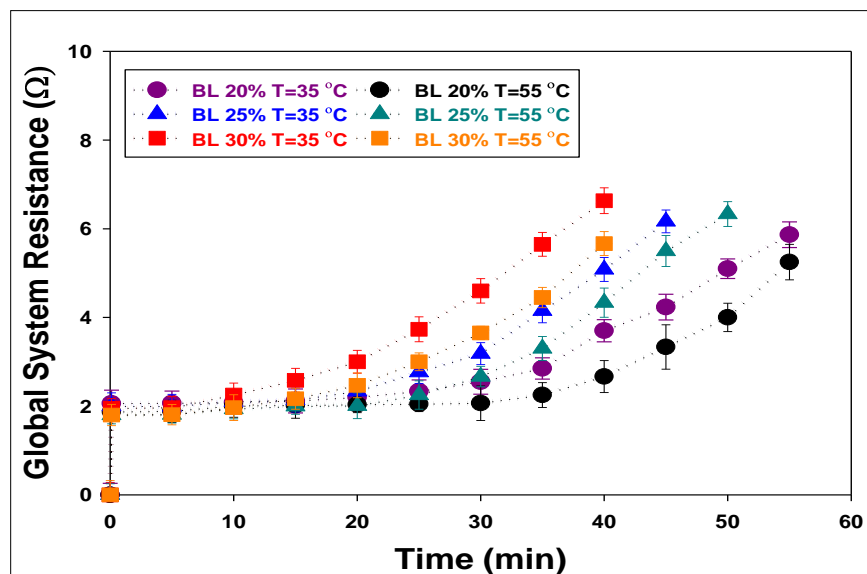


Figure 7.7 Global system resistance progress during the electrochemical acidification of Kraft *BL* via *EDBM* process (fitting equations can be found in Appendix A)

Furthermore, increasing the mineral concentration of the *BL* via increasing its *TDS* content may trigger a partial salting-out effect and phase separation phenomenon which subsequently, led to flocculation of particles inside the *BL* solution. Norgren *et al.* [6, 132] reported that lignin tends to flocculate when the ionic strength or in other words the mineral concentration of the solution increases. Hence, it can be presumed that, particularly at 30 (wt. %) *TDS* content, the lignin solubility decreased due to one or a combination of both mentioned possibilities (a larger amount of high molecular weight lignin molecules and partial salting-out effect). As a consequence, these flocculated particles might precipitate on the surface or in the space between the *IEMs* and cause the pronounced rise in the global system resistance curve.

pH of the Black Liquor

The progress of the pH of the *BL* throughout the electrochemical acidification process is depicted in Figure 7.8. Non-linear regressions of the pH trend as a function of time were calculated and provided coefficients of determination between 0.9790 and 0.9984. In most of the cases, the pH profile reached a plateau towards the end of the *EDBM* experiment. Increasing the operational temperature and the *TDS* content resulted in significant difference in the pH progress of the *BL* ($P < 0.001$). The initial and final pH values of the *BL* were lower at 55 °C regardless of the *TDS* content. Increasing the *TDS* content of the *BL* solution

resulted in higher initial and final pH values at both operational temperatures. As can be noted from Figure 7.8, the *BL* with 20 (wt. %) *TDS* content at 55 °C registered the lowest final pH value (10.45). It is noteworthy that when the *BL* with 30 (wt. %) *TDS* content was acidified the quick and drastic increase in its global system resistance forced to terminate the *EDBM* process after 40 minutes and as a result the final pH of the acidified *BL* was higher than the other acidified *BL* with the lower *TDS* contents.

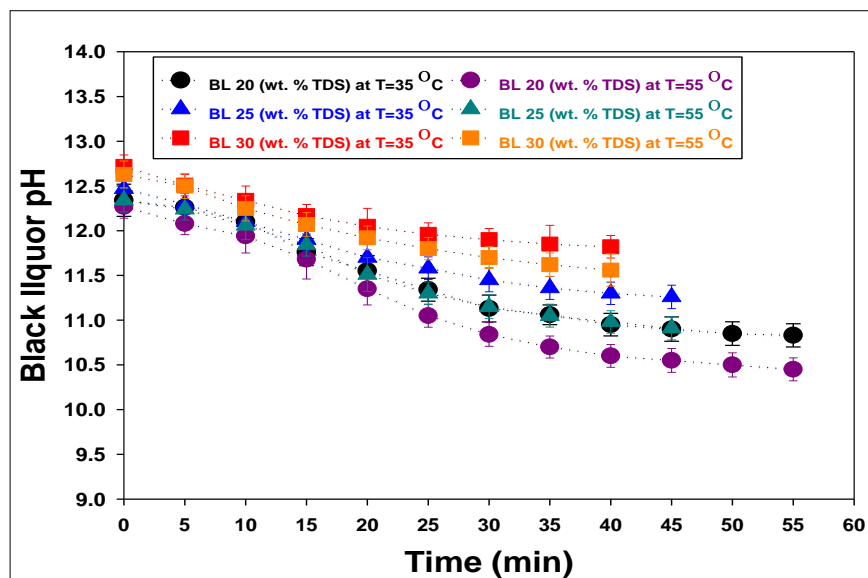


Figure 7.8 Evolution of the pH of the *BL* during the electrochemical acidification of Kraft *BL* via *EDBM* process (fitting equations can be found in Appendix A)

Based on Wallmo *et al.* and Zhu [5, 133] findings, the pH profile of the *BL*, during its acidification step, consisted of different regions : at the beginning, the alkaline neutralization of the *BL* solution occurs, then the protonation of the lignin phenolic groups takes place and if the acidification process was continued further, some buffering reactions of hydrogen sulfide and carbonate systems would happen [5, 134]. However, throughout the acidification process of the Kraft *BL* via the *EDBM* method, the lignin self-aggregation and precipitation elevated the overall system resistance drastically and forced the termination of the *EDBM* process [66, 97, 121]. Hence, the protonation of the lignin phenolic groups (second step of acidification progress) was not completed when the *BL* with high *TDS* content was acidified. According to the information found in the literature, for an effective lignin extraction, the best pH range of the acidified *BL* should be in the range of 8 – 10 [4, 5]; while the lowest obtained pH of the acidified *BL* was 10.45. Moreover, with regard to the *BL* properties presented in Table 7.4, by increasing the *TDS* content of the *BL* its residual alkali concentration was increased and elevated the initial pH value of the *BL* [134]. On the contrary, increasing the operational

temperature lowered the initial pH of the *BL* solution due to the water autoprotolysis [63]. By considering the global system resistance, pH trend of the *BL* and the progress of the solutions' conductivity profiles, one can perceive that once the global system resistance started to rise drastically, the acidification process and particularly the pH progress became slower. In addition, the ion mobility and the rate of ion transfer decreased. The non-linear regression curves obtained from the pH and conductivity experimental data substantiate that the lignin precipitation inside the *EDBM* stack adversely affected the electrodynamic parameters.

As stated in the literature, the lignin macro-molecules act as polyelectrolytes inside the *BL* solution [6, 63]. Hence, according to the well-known *DLVO* theory the solubility of a polyelectrolyte is greatly controlled by the balance between the attractive and repulsive forces [92]. A number of parameters can disturb this balance and eventually the lignin solubility such as the pH of the solution, ionic strength (or mineral concentration), temperature and the initial lignin concentration [63, 64, 90]. Our experimental findings are in accordance with Zhu and Evstigneev results. These researchers indicated that the lignin solubility increases by elevating the temperature and the pH of the solution [5, 123]. Throughout the electrochemical acidification of the Kraft *BL*, the gradual decrease in the pH of the *BL*, reduced the lignin solubility. However, the rate of this solubility decrease was different for each case. The higher *TDS* contents yielded faster and more pronounced rise in the overall system resistance which was a sign of severe *IEMs*' fouling.

7.3.4 Influence of Process Variables on System Hydrodynamics (Reynolds Number)

The *Re* numbers obtained for the three *TDS* contents at both of the operational temperatures ($T = 35$ and $55\text{ }^{\circ}\text{C}$) are outlined in Figure 7.9. As can be noted, at both of the operational temperatures the *Re* numbers follow the same evolution pattern and the difference in the *TDS* content of the *BL* significantly influenced the agitation inside the *EDBM* system ($P = 0.02$). The lowest *Re* number was obtained when the *BL* solution with 30 (wt. %) *TDS* content was acidified at $35\text{ }^{\circ}\text{C}$; while, the highest *Re* number was assigned to the *BL* solution with 20 (wt. %) *TDS* content at $55\text{ }^{\circ}\text{C}$. Based on the statistical analysis findings, changing the operational temperature had no significant impact on the *Re* numbers regardless of the *TDS* content ($P = 0.7$). The range of the obtained *Re* numbers are in good agreement with the information found in the literature from the previous studies [19].

As quoted earlier, the stack geometry, flow velocity and solution properties (dynamic viscosity and density) directly influence the dimensionless *Re* number. Throughout the course of this study, the stack geometry and flow velocity were constant; therefore, the *BL* properties

accounted for the deviations of Re number at the applied operational conditions. Based on the BL density data reported in Table 7.4, we can assume that the variations of the BL density was negligible. Accordingly, it can be deduced that the viscosity of the BL controlled the agitation inside the $EDBM$ stack and the significant difference in the Re numbers is because of the exponential progress of the BL viscosity with increasing its TDS content. As a result, the BL solution with 30 (wt. %) TDS content at $35^{\circ}C$ recorded the lowest Re number. An earlier study reported that performing an electrodialysis system with a $Re > 180$ would improve the agitation inside the stack [135]. Hence, we can conclude that the higher agitation inside the $EDBM$ system when the BL with 20 (wt. %) TDS content at $55^{\circ}C$ was acidified resulted in superior performance of the electrochemical acidification process and less membrane fouling. The minor impact of the operational temperature on the hydrodynamics of the system can be attributed to the insignificant alteration of the BL dynamic viscosity with increasing the temperature from 35 to $55^{\circ}C$.

By drawing a correlation between the evolution of the electrodialytic parameters and the trend of the hydrodynamics of the $EDBM$ system during the electrochemical acidification of the Kraft BL via the $EDBM$ method, it is evident that improving the agitation in the system delayed and mitigated the lignin self-aggregation and precipitation on the surface and in the space between the $IEMs$, to some extent. Such a result was also observed by Bazinet *et al.* on protein fouling during the electrochemical acidification of milk [54]. Perhaps by further promotion of the agitation of the BL solution it would be possible to fully disperse the destabilized colloidal lignin inside the solution and facilitate the progression of the electrochemical acidification process.

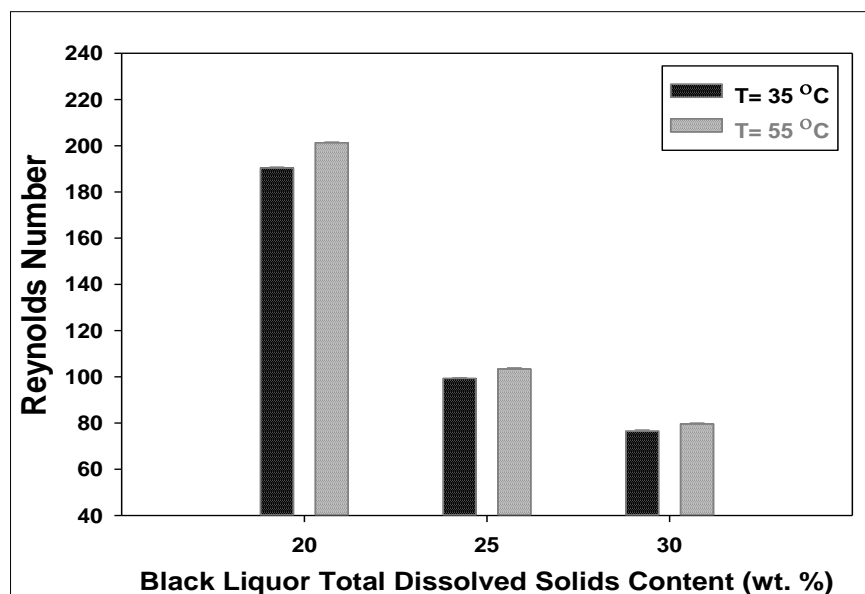


Figure 7.9 Evolution of the Reynolds number as a function of the operational temperature of the *EDBM* process and *TDS* content of the *BL*

7.3.5 Evolution of System Performance

Current Efficiency

Figure 7.10 shows that the slope of a linear regression curve ($y = ax + b$) can represent the progress of the current efficiency of the Kraft *BL* electrochemical acidification via the *EDBM* method at each operational temperature. Here, y is the current efficiency of the system and x indicates the *TDS* content of the *BL* solution. The statistical analysis results indicated that there is a significant variance between the current efficiency values at different *TDS* contents ($P = 0.007$). In addition, the effectiveness of the Kraft *BL* electrochemical acidification process was enhanced by increasing its operational temperature independently of the *TDS* content ($P = 0.038$).

This improvement can be explained by the fact that elevation of the operational temperature increased the effectiveness of the ion migration and eventually led to a higher current efficiency. The highest current efficiency was assigned to the *BL* solution with the *TDS* content of about 20 (wt. %) at $55\text{ }^{\circ}\text{C}$. Nevertheless, it should be noted that when the *BL* solution with 30 (wt. %) *TDS* content was acidified, the rapid increase in its global system resistance impaired the ion transfer phenomenon, forced the quick termination of the electrochemical acidification process and consequently, diminished the system productivity and efficiency.

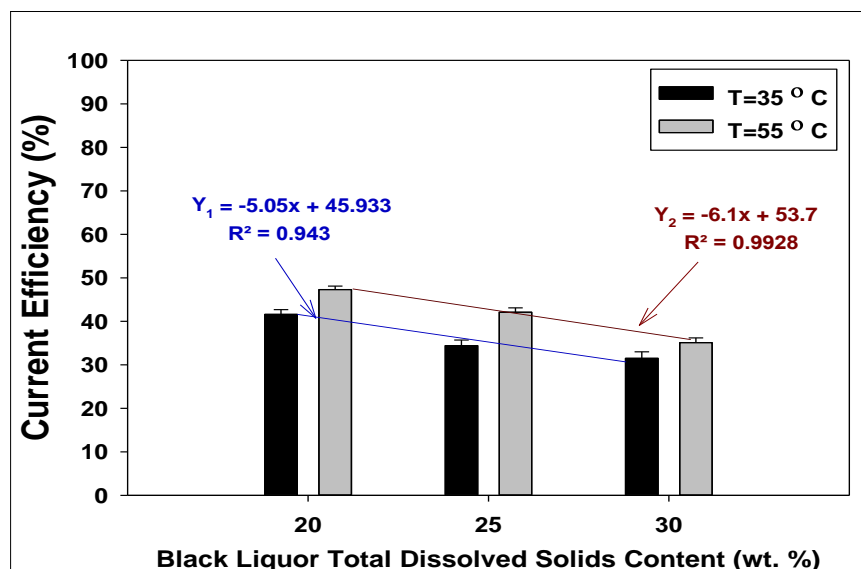


Figure 7.10 Influence of the operational temperature and *TDS* content of the *BL* on the current efficiency of the *EDBM* acidification process

Relative Energy Consumption

Similar to the current efficiency trend, the rate of the relative energy consumption of the electrochemical acidification process can be explained by the slope of a linear regression curve ($y = ax + b$) at a given operational temperature (Figure 7.11); where, y shows the current efficiency of the system and x is the *TDS* content of the *BL* solution.

It was not surprising that the acidification of the *BL* with the *TDS* content of about 20 (wt. %) at 55 °C consumed less energy because of its lower and delayed global system resistance increase. On the other hand, when the *BL* solution with the *TDS* content of about 30 wt. % was acidified more energy was required to overcome the high global system resistance and the electrochemical acidification process became too energy intensive.

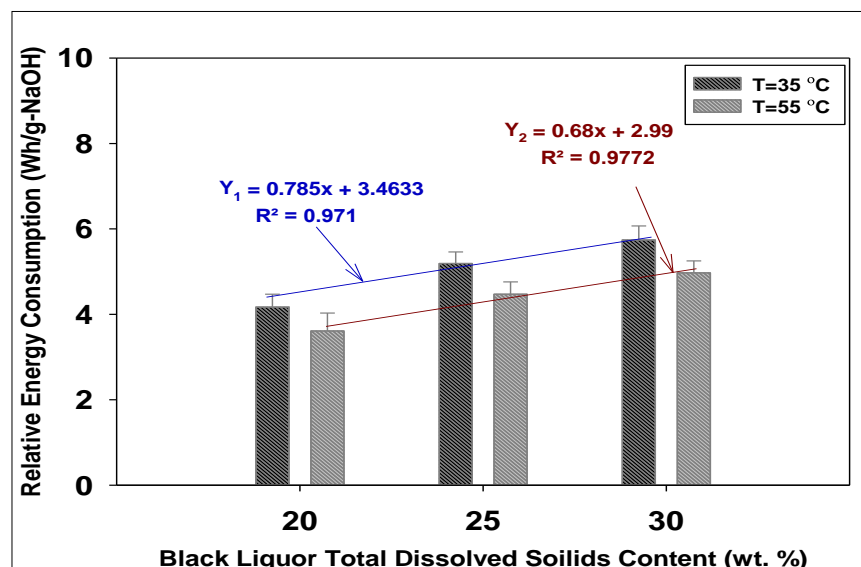


Figure 7.11 Effect of the operational temperature and *TDS* content of the *BL* on the energy consumption of the *EDBM* acidification process

7.4 Conclusion

An experimental study was performed to determine the performance of electrochemical acidification of the Kraft *BL* via *EDBM* method, in terms of current efficiency and energy consumption. The influence of the main operational parameters i.e. the operational temperature and chemical composition of the *BL* were assessed. From the outcome of our investigation, it can be concluded that these process variables had substantial impacts on the *EDBM* performance and the *IEMs*' fouling.

According to the experimental findings, among the examined operational conditions, the highest current efficiency (47.3 %) and greatest *Re* number (201) as well as the lowest energy consumption ($3.61 \text{ Wh} \cdot \text{g}^{-1} \text{ NaOH}$) were achieved when the *BL* with the *TDS* of about 20 (wt. %) was acidified at 55°C . Therefore, it can be concluded that improving the operational conditions of the *EDBM* process increased the performance of the system and reduced the fouling of the *IEMs*. However, as we discussed in our previous work, a chemical cleaning step is inevitable in order to maintain the integrity of the *IEMs* [121]. Furthermore, to facilitate the lignin filterability and enhance the lignin extraction yield the final pH of the acidified *BL* should be in a range of 8 - 10 [4]. Throughout the course of this study, the lowest obtained pH value of the acidified *BL* was 10.45. For that reason, it would be preferable to terminate the *EDBM* step just before the fast rise in the overall system resistance would take place and continue the acidification process via a chemical acidification method to prevent an energy

intensive process [66].

Another possible solution to this problem would be utilization of an in-line cleaning step such as implementation of pulsed electric field (*PEF*). Ruiz *et al.* [80] showed that application of the *PEF* during the electrodialysis of a casein solution could minimize the fouling of *IEMs*. Thus, further investigation is required to demonstrate the impact of the *PEF* on eliminating the precipitation of the lignin macro-molecules on the surface of the *IEMs* during the electrochemical acidification of the Kraft *BL* via the *EDBM* method.

Acknowledgments

The financial support of NSERC and BioFuelNet Canada is acknowledged. In addition, the authors gratefully thank Hydro-Québec Energy Technology Laboratory (*LTE*) for providing the experimental set-up.

Appendix A

Fitting equation of electrical conductivity trend of the *BL* solution :

$$BL_{Electrical\ Conductivity} = d \exp(-ft) + g$$

Table 7.5 Parameters of the *BL* electrical conductivity fitting equations

<i>TDS</i> (%)	<i>T</i> (° C)	<i>d</i>	<i>f</i>	<i>g</i>	<i>R</i> ²
20	35	18.63	0.03	73.73	0.9946
25	35	17.57	0.03	78.21	0.9827
30	35	21.93	0.02	75.89	0.9878
20	55	16.16	0.03	82.99	0.9863
25	55	11.37	0.03	91.15	0.9889
30	55	9.67	0.03	96.02	0.9888

Fitting equations of electrical conductivity trend of the *NaOH* solution :

$$NaOH_{Electrical\ Conductivity} = h(1 - \exp(-it)) + j$$

Table 7.6 Parameters of the *NaOH* electrical conductivity fitting equations

T (° C)	h	i	t	R^2
35	28.88	0.01	139.99	0.9988
55	50.67	0.02	141.62	0.9868

Fitting equations of global system resistance trend during *EDBM* process :

$$R = kt^3 - lt^2 + mt + n$$

Table 7.6 Table C.3 : Parameters of the global system resistance fitting equations

TDS (%)	T (° C)	k	l	m	n	R^2
20	35	0.0001	0.006	0.186	0.546	0.9519
25	35	0.0002	0.001	0.243	0.378	0.9644
30	35	0.0002	0.001	0.275	0.284	0.9620
20	55	0.0001	0.009	0.225	0.400	0.9628
25	55	0.0001	0.007	0.188	0.438	0.9676
30	55	0.0002	0.012	0.273	0.238	0.9812

Fitting equations of the *BL* pH trend during *EDBM* process :

$$BL_{pH} = p \exp(-qt) + z$$

Table 7.7 Parameters of the *BL* pH fitting equations

TDS (%)	T (° C)	p	q	z	R^2
20	35	2.22	0.03	10.25	0.9795
25	35	1.74	0.03	10.77	0.9952
30	35	1.08	0.05	11.65	0.9984
20	55	2.71	0.03	9.67	0.9790
25	55	2.74	0.02	9.70	0.9794
30	55	1.5	0.03	11.09	0.9950

CHAPTER 8 ARTICLE 5 : ELECTROCHEMICAL ACIDIFICATION OF KRAFT BLACK LIQUOR : IMPACTS OF PULSED ELECTRIC FIELD APPLICATION ON BIPOLAR MEMBRANE COLLOIDAL FOULING AND PROCESS INTENSIFICATION

Maryam Haddad ^a, Laurent Bazinet ^b, Oumarou Savadogo ^a, Jean Paris ^a

a : Research Unit on Energy Efficiency and Sustainable Implementation of the Forest Biorefinery (*E²D²BF*), Department of Chemical Engineering, Polytechnique de Montréal, Canada

b : Institute of Nutrition and Functional Foods (*INAF*), Laboratory of food processing and electromembrane processes (*LTAPEM*), Department of Food Sciences, Université Laval, Canada

Abstract

Lately, interest has emerged in biorefineries that use non-food biomass residues. Lignin is a lignocellulosic biomass which can be extracted from a residual stream, called black liquor, in the Kraft pulping process and converted to a variety of value-added products. A recent study was carried out to acidify the black liquor and extract the lignin by means of electrodialysis with bipolar membrane (*EDBM*) method. Despite the fact that this green pathway enjoyed an in-situ production of caustic soda as a valuable byproduct and significantly reduced the chemical consumption than the chemical acidification approach, the occurrence of severe colloidal fouling on the cation exchange layer of the bipolar membrane impaired its productivity. To resolve this obstacle, this investigation was performed to determine, for the first time, the impact of the non-stationary pulsed electric field on mitigation of bipolar membrane colloidal fouling and improvement of the process performance in terms of current efficiency, energy consumption and membrane integrity.

A comparison between the experimental results obtained from four pause lapses (6, 12, 18 and 24 seconds) with a pulse lapse of 6 seconds and a *DC* current indicated that application of a rigorous selected pulse/pause ratio can limit the growth of the colloidal particle, suppress the fouling on the bipolar membrane and intensify the *EDBM* process. The pulse/pause ratio of 6 (s)/24 (s) was found to be the most appropriate ratio which yielded a high current efficiency ($\simeq 80\%$), a low global system resistance and relative energy consumption ($2.6 \text{ Wh/g} - \text{NaOH}$) and a final pH value of 9.7 which would facilitate an efficient lignin extraction process.

Keywords : Bipolar membrane fouling, Electrodialysis, Pulsed electric field, Colloidal fouling, Kraft black liquor, Lignin extraction

8.1 Introduction

In light of the integrated wood-based biorefinery concept, a fraction of wood components (cellulose, hemicellulose and lignin) can be separated and transformed into precursors of novel and non-paper commodities [3]. In particular, the lignin constituent which is entrained in the residual stream, black liquor (*BL*), of Kraft pulping mills can be removed and converted into a wide array of bio-based products such as biofuels or carbon fibers [6]. Moreover, the lignin extraction can increase the capacity of the mill by decreasing the load of its recovery boiler. In addition, the conversion of the lignin to new products would create new alternatives for the receptor mill to diversify its portfolio and grow its revenue [4].

In general, lowering the pH of the *BL* is considered the most efficient technique to extract the lignin. Chemical acidification and especially *BL* carbonation process has been studied and practiced extensively for several years [4, 5, 11]. However, the practical implementation of this method raised some serious concerns for a receptor Kraft pulping mill such as interfering with its sodium-sulfur balance as well as the cost-intensive installation of CO_2 recapturing equipment and its environmental footprints [4].

To resolve these issues and based on the electrolytic nature of the *BL* medium, an electrochemical acidification process by means of electrodialysis with bipolar membrane (*EDBM*) method was recently proposed as a novel and more sustainable pathway to acidify the *BL* and extract the lignin [66]. In this framework, a two-compartment *EDBM* cell comprising of bipolar (*BPM*) and cation exchange membranes (*CEM*) was used. In addition, a value-added side product i.e. caustic soda solution was simultaneously produced, which can be utilized in the Kraft mill or in other chemical industries [66]. Nevertheless, similar to most of the electrodialysis (*ED*) and *EDBM* applications, the fouling of its ion exchange membranes (*IEM*) impaired the process performance and adversely affected the *IEMs'* integrity [121].

Even though the fouling and scaling mechanisms of the *CEMs* and anion exchange membranes (*AEM*) have been expensively studied [37, 74, 75, 136], the fouling of the *BPM* has never been addressed in the literature. For the first time, in our earlier work, we observed a deposit of colloidal lignin on the surface of cation exchange layer (*CEL*) of the *BPM* during the *EDBM* process. This deposit occurred as a result of protonation of lignin phenolic groups and lignin self-aggregation which eventually led to the lignin precipitation inside the *EDBM* stack. It was found that the abundance of the proton ions on the *CEL* surface of

the *BPM* facilitated the formation of lignin clusters [97]; these clusters grew and expanded along the *EDBM* process and covered the surface and space between the *IEMs* [97, 121].

Among all the suggested techniques to minimize the fouling and scaling mechanisms of the *CEMs* and *AEM*, several researchers showed that application of a non-stationary electric current regime such as pulsed electric field (*PEF*) can significantly enhance the charge transfer across the *CEMs* and *AEMs*, disrupt the concentration polarization phenomenon [137, 138] and mitigate the scaling and fouling during the electro-membrane processes [34, 37, 77, 80, 139, 102]. Additionally, the simplicity and cost-effective implementation of the *PEF* mode makes it an attractive and feasible in-line cleaning option for industrial and large scale applications [37].

To the best of our knowledge, it is the first time that (1) *PEF* regime is proposed to mitigate the *BPM* colloidal fouling during *EDBM* process of the Kraft *BL* and (2) the screening of the most appropriate *PEF* ratio ($r = t_{pulse}/t_{pause}$) was investigated in order to complement the *BL* electrochemical acidification performance in terms of improving its current efficiency and lowering the relative energy consumption of the system. The generated results of this study can be employed to design and improve an *EDBM* process under the *PEF* regime when the *BPM* fouling is the main process obstacle. Furthermore, by suppressing the *IEMs*' fouling, the green electro-membrane acidification of the Kraft *BL* process would be one step closer to its scale-up implementation in a Kraft mill.

8.2 Experimental

8.2.1 Membranes and Materials

The commercially available *IEMs* used in this investigation were Fumasep *FBM* bipolar membrane (FuMA-Tech Co., Germany) and *CMB* cation exchange membrane (Neosepta, Japan). Their main characterizations are given in Table 8.1.

Table 8.1 Ion exchange membranes specifications provided by their suppliers

Membrane	Type	Thickness (mm)	IEC ($meq.g^{-1}$)	Specific Area Resistance ($\Omega.cm^2$)	Stability (pH)	Temperature °C
<i>CMB</i>	Cation	0.18- 0.21	3.11	4.5	1 – 14	≤ 60
<i>FBM</i>	Bipolar	0.18- 0.20	-	-	1 – 14	≤ 60

The softwood *BL* was provided by a Canadian Kraft pulping mill with a total dissolved solids (*TDS*) content around 50 ± 2 (wt. %). This liquor was diluted to 20 (wt. %) and pre-filtered to

remove any suspended solid particles larger than $0.010\ \mu m$ utilizing a simple vacuum filtration apparatus and a filter paper (Whatman Grade 111105, UK). Information about the *BL* chemical composition is presented in Table 8.2 and the details of its analysis procedures can be found in our earlier work [66]. Analytical grade chemicals were purchased from Sigma-Aldrich, Canada and standard solutions were supplied by Fisher Scientific, Canada. Demineralized water was used to prepare all the aqueous solutions.

Table 8.2 Characteristics of Kraft Black Liquor

Characteristics	Data
Total Dissolved Solids (<i>TDS</i>) (%)	20.1
UV Lignin (% <i>TDS</i>)	40.6
Ash Content (% <i>TDS</i>)	27.9
Sodium Concentration (% <i>TDS</i>)	17.9
Residual Alkali ($g. L^{-1}$)	5.5

8.2.2 Electrochemical Acidification Set-up

As mentioned in the introduction, a two- compartment *EDBM* cell was used in the batch mode for all the performed experiments. Inside the *EDBM* stack the *BPMs* and *CEMs* were positioned in an alternative pattern between two electrodes and the electrode pair was connected to the electric field (Figure 8.1). A schematic drawing of the experimental set-up is illustrated in Figure 8.2. This apparatus consisted of the *EDBM* stack which was hydraulically connected to the *BL*, *NaOH* and electrolyte rinse solution (Na_2SO_4) reservoirs via three pumps (Model : IWAKI Magnetic Drive Pump *MD. 30 R*, Iwaki America Inc., USA). Each reservoir was filled with 2 *L* of solution and its temperature was maintained constant by a coil jacket heat exchanger connected to a hot water bath.

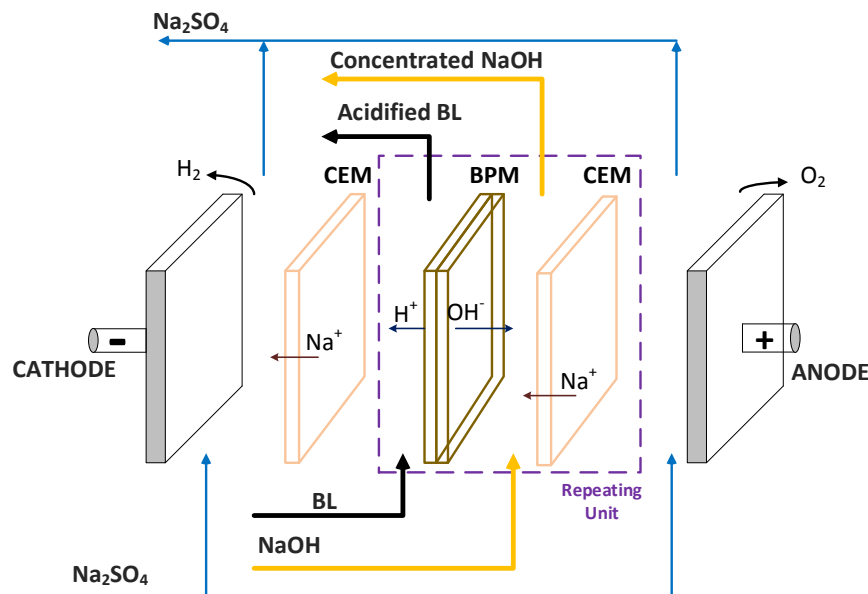


Figure 8.1 Electrodialysis with bipolar membrane (*EDBM*) stack (*BPM* : bipolar membrane and *CEM* : cation- exchange membrane)

8.2.3 Protocol

To conduct an accurate evaluation of the *PEF* influence on the performance of the *EDBM* process, two electric current regimes were applied in a galvanostatic mode : a steady state direct current (*DC*) and a non-stationary pulsed electric current or *PEF*. Both regimes were conducted at sub-limiting current density conditions and the applied current density value was equaled to 75% of the limiting current density measured, based on the Cowan and Brown procedure [55]. The *DC* regime was considered as the control case. In the *PEF* condition, the predefined pulse and pause periods were established by means of a specially designed pulse generator, made at our laboratory. This device was connected from one end to a computer to program and adjust the pulse and pause lapses and on the other end to a power supply (Model : Xantrex *XKW* 40 – 25, USA). The applied current, voltage variation, conductivity and temperature of each reservoir were monitored and recorded by means of a data acquisition system (Model : Agilent 34970 *A*, USA) connected to a data logger software. Every five minutes, a sample of *BL* was taken for pH measurement using a pH meter (Mode : 916 *Ti-Touch*, Metrohm, Switzerland) equipped with an automatic temperature compensation probe. In addition, the sodium concentration and lignin content of these samples were determined based on the procedure described in [66]. The *EDBM* experiment for each condition was carried out with a fresh set of *IEMs* and three replicates of the same conditions were done. Before starting the *EDBM* run, the set-up was rinsed

for 30 minutes with demineralized water to wash any particle that might have remained in the apparatus. The electrochemical acidification process was stopped once (1) : the limiting voltage of the power supply was reached, or (2) no notable progress was observed in the evolution of the electrodialysis parameters, or (3) when the pH of the *BL* solution reached the value of about 9.7. Table 8.3 gives the *EDBM* process conditions.

The original membrane properties were measured on fresh membranes cut from the sheet and after each set of the conditions, the *EDBM* stack was dismantled and the *IEMs* were taken for analysis.

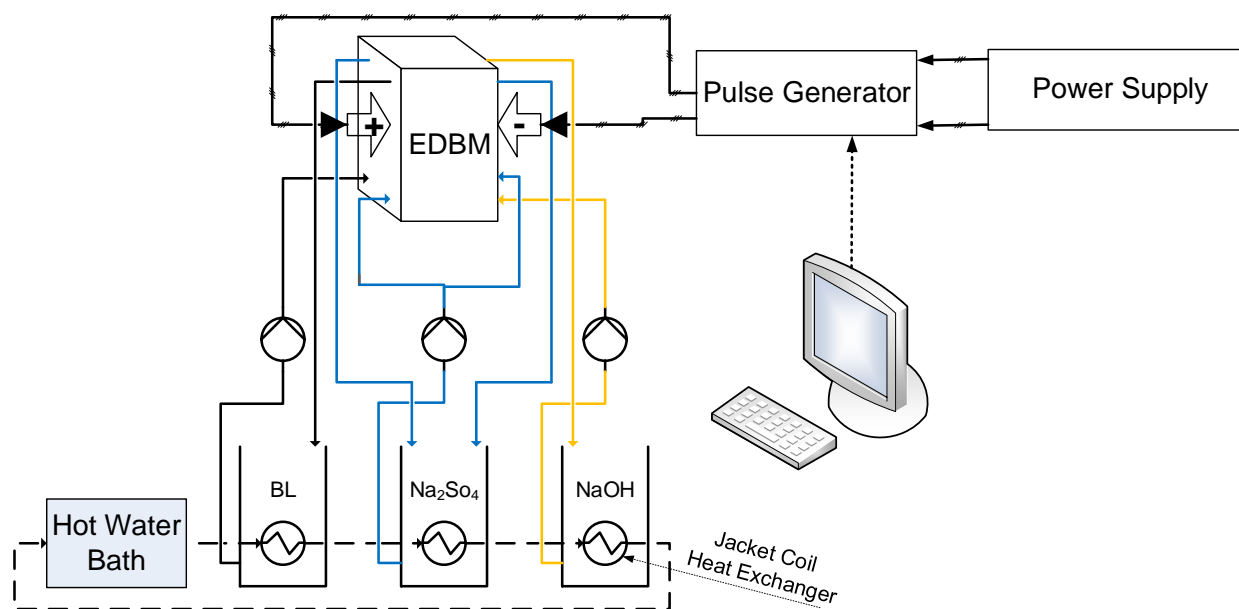


Figure 8.2 Schematic diagram of the electrochemical acidification set-up

According to the information found in the literature, the application of short pulse and pause periods would increase the liquid motion, better electrophoretic movements and result in a higher productivity rate [102, 140]. Screening the most appropriate the t_{pulse}/t_{pause} ratio can highly upturn the process performance by mitigating the *IEMs*' fouling [34, 77, 80, 102, 139]. Thus, the electrochemical acidification of the Kraft *BL* via the *EDBM* technique was carried out under four different *PEF* conditions with pulse/pause ratios of : $r = 1$, $r = 0.5$, $r = 0.33$ and $r = 0.25$. The selection of 6 second as the shortest pulse and/or pause lapse was based on the adaptability of the utilized experimental set-up and the accuracy of the data acquisition system.

Table 8.3 Applied Operating Conditions during Electrochemical Acidification of the Kraft Black Liquor

Operating Conditions	Data
Number of Operating Units	4
Re-circulation Flow Rate	$1 \text{ L} \cdot \text{min}^{-1}$
Pressure Drop	34.5 KPa
Applied Current Density	$330 \text{ A} \cdot \text{m}^{-2}$
Effective Membrane Surface Area	0.0180 m^2
Operating Temperature	$55 \text{ }^{\circ}\text{C}$

8.2.4 Membrane Analyses

Based on the findings of our previous work [121], two fundamental membrane analyses were selected as the key analysis indicators to visualize and detect the presence of a fouling layer on the surface of the *BPMs* and *CEMs* : membrane thickness measurement and scanning electron microscopy with energy dispersive X-ray analysis (to take images from the membrane surface and perform elemental analysis). Furthermore, the outcome of these analyses would give an insight on *PEF* effect on the membrane properties and integrity.

Membrane Thickness

The thickness of each membrane was measured on ten different locations using a plastic film measurement device (Model : Mitutoyo ID : *C112 EB*, Japan), with $1 \mu\text{m}$ accuracy and a range of 12.7 mm . The average value was reported as the *IEM* thickness.

Scanning Electron Microscopy and Elemental Analysis

Scanning electron microscopy (*SEM*) images were taken at $250 \times$ magnification from the fresh and used *IEMs*' surfaces in direct contact with the *BL* solution during *EDBM* process by means of a field emission gun electron microscope (Model : *JMS-7600 FEG-SEM*, Jelo, USA). Then, an energy dispersive spectrometer (Model : Oxford X-Max silicon drift detector, Oxford Instrument, UK) was connected to the microscope to perform the elemental analysis of the membrane surface (*EDX*). The *EDX* analysis was carried out at the same magnification as the *SEM* analysis ($250 \times$), at 5 kV accelerating voltage and a 15 mm working distance. All the samples were vacuum dried and coated with a thin layer of gold to improve the image quality [77].

8.2.5 Process Evaluation

Global System Resistance

The global system resistance was obtained by recording the applied current and voltage variation along the *EDBM* run employing the Ohm's law :

$$R = \frac{U}{I} \quad (8.1)$$

Where R is the global system resistance (Ω), I is the applied current (A) and U represents the voltage drop across the *EDBM* stack (V) [71].

Number of Charges Transported

For the purpose of simplicity and consistency in comparison between different applied electric field modes, the electrodialysis parameters were plotted as a function of number of charges transported, since the application of different pause lapses in the *PEF* regime influenced the time elapsed [139]. This number can be determined as :

$$Q = I * t \quad (8.2)$$

Here, Q represents the number of transported charges (C) and t shows the duration of the *EDBM* operation (*sec*).

Current Efficiency and Relative Energy Consumption

The performance of an electro-membrane process can be evaluated by determining the current efficiency and energy consumption of the system [18].

The current efficiency is defined as the percentage ratio of the ions transferred through the *IEMs* and the number of Faradays passing through the stack during the electro-membrane process [18] :

$$Current\ Efficiency = \frac{(V_f C_f - V_i C_i) F}{N I t} \quad (8.3)$$

Where $V_f C_f$ and $V_i C_i$, respectively are the initial and final and moles of $NaOH$, F is the Faraday constant ($96485\ C.equivalent^{-1}$) and N represents the number of cell units.

The relative energy consumed in each *EDBM* condition was determined as [128] :

$$E_R = \frac{I \int_{t_f}^{t_i} U dt}{3600 M (V_f C_f - V_i C_i)} \quad (8.4)$$

Here, E_R is the relative energy consumption ($Wh.g^{-1} NaOH$) and M shows the molar mass of $NaOH$ ($39.997 g.mole^{-1}$). Note that the consumed energy of the pumps and hot water bath were not included in the E_R calculation.

Statistical Analysis

The experimental data were presented as means \pm standard deviation and subjected to one-way and multiple-way statistical analyses using SigmaPlot software (version 13.0, SYSTAT software Inc., San Jose, CA, USA) with the probability level of 5%.

8.3 Results and Discussion

8.3.1 Membrane Analysis

Membrane Thickness

The thickness data of the *IEMs* are given in Table 8.4. The first point to consider is that the *CEM* was less affected by the fouling phenomenon, as observed earlier [97, 121], except at $r = 0.25$ ($t_{pulse}/t_{pause} = 6(s)/24(s)$) in which none of the *IEM* was covered by foulants. The highest value was assigned to the used *BPM* in the *DC* mode (control case). The second highest thickness value was allocated to the *BPM* used for the *PEF* mode with $r = 1$ ($t_{pulse}/t_{pause} = 6(s)/6(s)$); increasing the pause lapse decreased the difference between the thickness of the fresh and used *BPMs* and at $r = 0.25$ ($t_{pulse}/t_{pause} = 6(s)/24(s)$) the thickness of the used *BPM* showed no detectable increase. Even though the thickness elevation of the used *CEMs* was less pronounced than the used *BPMs*, one can note that its thickness value increased around 13 % in the control case. In the *PEF* regime, by prolonging the pause period, less deposit was formed on the surface of the *CEMs* and, as a result, its thickness increment was not significant. These measured thickness values are in accordance with our previous findings [97, 121]. It should be remarked that, based on membrane water content measurements (data not shown), swelling phenomenon had a negligible influence on the thickness measurement results.

Table 8.4 Membrane Thickness (mm)

	Fresh	Control (DC)	$r = 1$	$r = 0.5$	$r = 0.33$	$r = 0.25$
BPM	$0.181 \pm 0.001^{d*}$	0.794 ± 0.038^a	0.752 ± 0.017^b	0.736 ± 0.014^b	0.231 ± 0.011^c	0.183 ± 0.002^d
CEM	0.180 ± 0.001^c	0.203 ± 0.006^a	0.201 ± 0.003^a	0.191 ± 0.004^b	0.184 ± 0.002^c	0.182 ± 0.003^c

Table 8.4 * The mean values (presented at each row) for fresh, used membranes followed by different letters (a , b , c and d), are significantly different ($p < 0.05$)

The significant difference between the extent of the deposit layer on the CEL of the BPM s and the CEM s can be attributed to the fact that the generation and presence of proton ions on the CEL of the BPM , as a result of the water splitting reaction inside the BPM , could trigger the protonation of the lignin phenolic groups and, ultimately, the lignin cluster precipitation. These clusters would grow and expand over time and fill out the space in between the IEM s and eventually attach to the surface of the CEM . In addition, hydroxide ion leakage through the CEM might disturb the formation of lignin clusters on its surface, to some extent [97].

Scanning Electron Microscopy and Elemental Analysis

The SEM images showed that a deposit layer was formed on the surface of the IEM s during the $EDBM$ experiment under the DC mode. In addition, the EDX analysis results reported that oxygen and carbon constituted this fouling layer with a small quantity of sodium and sulfur (Figure 8.3 (a) and (b)).

Applying a 6-second pause period after a 6-second pulse lapse did not substantially prevent the occurrence of the IEM s fouling and similar to the control case (DC) the precipitated layer on the membrane surface was composed of oxygen, carbon and a small amount of sodium and sulfur. However, by expanding the pause period from 6 seconds to 12, 18 and finally to 24, seconds the accumulation of the foulant matters on the surface of the IEM s was reduced significantly. As it is shown in Figure 8.3 (a) and (b), when the PEF mode with $r = 0.25$ ($t_{pulse}/t_{pause} = 6(s)/24(s)$) was applied no detectable foulant particle was observed on the surface of the used IEM s and these used membranes presented almost the same appearance and the EDX analysis results as the fresh ones. It should be pointed out that the used CEM at $r = 0.33$ also presented a clean surface during the SEM analysis, but traces of sulfur and sodium were recorded in its EDX analysis outcome. Thereby, it can be presumed that this membrane was slightly affected by the fouling phenomenon ; however,

the foulant particles were not detected at the 250 X magnification. Note that the *SEM* and *EDX* analysis results of the *IEM* sides in direct contact with the *NaOH* solution were not shown here as these sides presented a clean surface with no fouling or alteration in the membrane properties [97, 121].

The *O/C* ratio of the deposit layer fell in the range of 0.25 - 0.4 which is in good agreement with the *O/C* ratio of the Kraft lignin obtained in our previous investigations and reported by other researchers [84, 85, 86]. In addition, the presence of a small amount of sodium and sulfur in the lignin deposit can be considered as lignin impurity. According to Uloth *et al.* [15], the Kraft lignin separated from the *BL* solution contains some impurities such as sodium and sulfur.

Based on the membrane analysis findings, it can be concluded that the *BPM* was severely affected by the fouling of colloidal lignin and the deposit layer on the surface of the *CEM* seemed to be less compact and loosely attached to its surface. Moreover, performing the electrochemical acidification of the Kraft *BL* via the *EDBM* method under the *PEF* regime with $r = 0.25$ ($t_{pulse}/t_{pause} = 6(s)/24(s)$) could suppress the lignin precipitation on the surface of the *IEMs*.

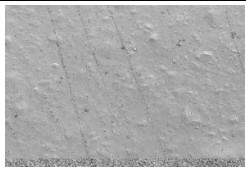
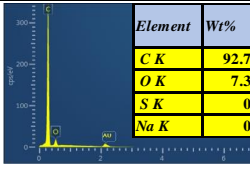
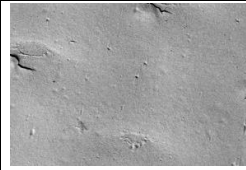
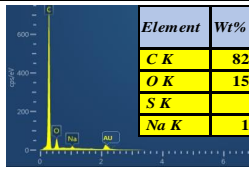

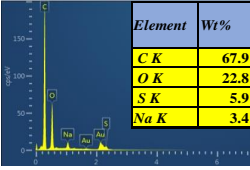
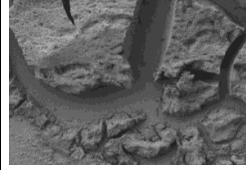
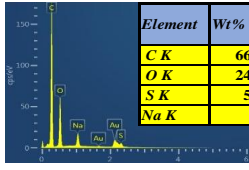
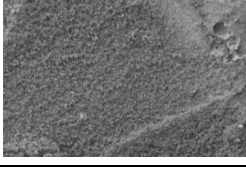
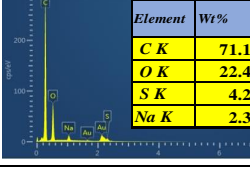
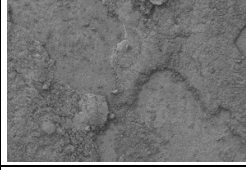
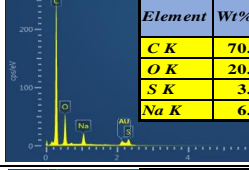
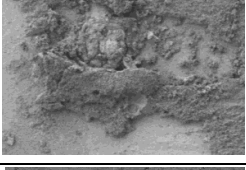
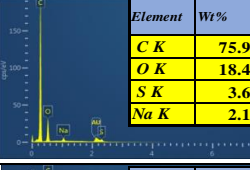

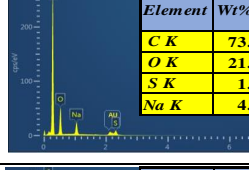

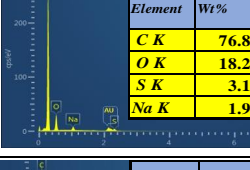
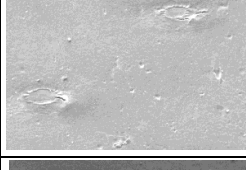
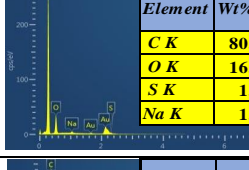

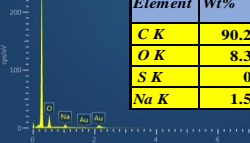
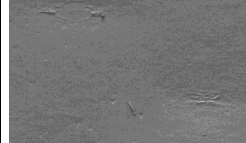
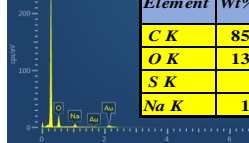
Membranes	(a) BPM		(b) CEM																					
	SEM (250 X)	EDX	SEM (250 X)	EDX																				
Fresh		 <table><thead><tr><th>Element</th><th>Wt%</th></tr></thead><tbody><tr><td>C K</td><td>92.7</td></tr><tr><td>O K</td><td>7.3</td></tr><tr><td>S K</td><td>0</td></tr><tr><td>Na K</td><td>0</td></tr></tbody></table>	Element	Wt%	C K	92.7	O K	7.3	S K	0	Na K	0		 <table><thead><tr><th>Element</th><th>Wt%</th></tr></thead><tbody><tr><td>C K</td><td>82.5</td></tr><tr><td>O K</td><td>15.8</td></tr><tr><td>S K</td><td>0</td></tr><tr><td>Na K</td><td>1.7</td></tr></tbody></table>	Element	Wt%	C K	82.5	O K	15.8	S K	0	Na K	1.7
Element	Wt%																							
C K	92.7																							
O K	7.3																							
S K	0																							
Na K	0																							
Element	Wt%																							
C K	82.5																							
O K	15.8																							
S K	0																							
Na K	1.7																							
Control (DC)		 <table><thead><tr><th>Element</th><th>Wt%</th></tr></thead><tbody><tr><td>C K</td><td>67.9</td></tr><tr><td>O K</td><td>22.8</td></tr><tr><td>S K</td><td>5.9</td></tr><tr><td>Na K</td><td>3.4</td></tr></tbody></table>	Element	Wt%	C K	67.9	O K	22.8	S K	5.9	Na K	3.4		 <table><thead><tr><th>Element</th><th>Wt%</th></tr></thead><tbody><tr><td>C K</td><td>66.3</td></tr><tr><td>O K</td><td>24.1</td></tr><tr><td>S K</td><td>5.6</td></tr><tr><td>Na K</td><td>4</td></tr></tbody></table>	Element	Wt%	C K	66.3	O K	24.1	S K	5.6	Na K	4
Element	Wt%																							
C K	67.9																							
O K	22.8																							
S K	5.9																							
Na K	3.4																							
Element	Wt%																							
C K	66.3																							
O K	24.1																							
S K	5.6																							
Na K	4																							
PEF: r=1		 <table><thead><tr><th>Element</th><th>Wt%</th></tr></thead><tbody><tr><td>C K</td><td>71.1</td></tr><tr><td>O K</td><td>22.4</td></tr><tr><td>S K</td><td>4.2</td></tr><tr><td>Na K</td><td>2.3</td></tr></tbody></table>	Element	Wt%	C K	71.1	O K	22.4	S K	4.2	Na K	2.3		 <table><thead><tr><th>Element</th><th>Wt%</th></tr></thead><tbody><tr><td>C K</td><td>70.8</td></tr><tr><td>O K</td><td>20.6</td></tr><tr><td>S K</td><td>3.2</td></tr><tr><td>Na K</td><td>6.5</td></tr></tbody></table>	Element	Wt%	C K	70.8	O K	20.6	S K	3.2	Na K	6.5
Element	Wt%																							
C K	71.1																							
O K	22.4																							
S K	4.2																							
Na K	2.3																							
Element	Wt%																							
C K	70.8																							
O K	20.6																							
S K	3.2																							
Na K	6.5																							
PEF: r=0.5		 <table><thead><tr><th>Element</th><th>Wt%</th></tr></thead><tbody><tr><td>C K</td><td>75.9</td></tr><tr><td>O K</td><td>18.4</td></tr><tr><td>S K</td><td>3.6</td></tr><tr><td>Na K</td><td>2.1</td></tr></tbody></table>	Element	Wt%	C K	75.9	O K	18.4	S K	3.6	Na K	2.1		 <table><thead><tr><th>Element</th><th>Wt%</th></tr></thead><tbody><tr><td>C K</td><td>73.6</td></tr><tr><td>O K</td><td>21.7</td></tr><tr><td>S K</td><td>1.9</td></tr><tr><td>Na K</td><td>4.8</td></tr></tbody></table>	Element	Wt%	C K	73.6	O K	21.7	S K	1.9	Na K	4.8
Element	Wt%																							
C K	75.9																							
O K	18.4																							
S K	3.6																							
Na K	2.1																							
Element	Wt%																							
C K	73.6																							
O K	21.7																							
S K	1.9																							
Na K	4.8																							
PEF: r=0.33		 <table><thead><tr><th>Element</th><th>Wt%</th></tr></thead><tbody><tr><td>C K</td><td>76.8</td></tr><tr><td>O K</td><td>18.2</td></tr><tr><td>S K</td><td>3.1</td></tr><tr><td>Na K</td><td>1.9</td></tr></tbody></table>	Element	Wt%	C K	76.8	O K	18.2	S K	3.1	Na K	1.9		 <table><thead><tr><th>Element</th><th>Wt%</th></tr></thead><tbody><tr><td>C K</td><td>80.4</td></tr><tr><td>O K</td><td>16.3</td></tr><tr><td>S K</td><td>1.8</td></tr><tr><td>Na K</td><td>1.5</td></tr></tbody></table>	Element	Wt%	C K	80.4	O K	16.3	S K	1.8	Na K	1.5
Element	Wt%																							
C K	76.8																							
O K	18.2																							
S K	3.1																							
Na K	1.9																							
Element	Wt%																							
C K	80.4																							
O K	16.3																							
S K	1.8																							
Na K	1.5																							
PEF: r=0.25		 <table><thead><tr><th>Element</th><th>Wt%</th></tr></thead><tbody><tr><td>C K</td><td>90.2</td></tr><tr><td>O K</td><td>8.3</td></tr><tr><td>S K</td><td>0</td></tr><tr><td>Na K</td><td>1.5</td></tr></tbody></table>	Element	Wt%	C K	90.2	O K	8.3	S K	0	Na K	1.5		 <table><thead><tr><th>Element</th><th>Wt%</th></tr></thead><tbody><tr><td>C K</td><td>85.2</td></tr><tr><td>O K</td><td>13.7</td></tr><tr><td>S K</td><td>0</td></tr><tr><td>Na K</td><td>1.1</td></tr></tbody></table>	Element	Wt%	C K	85.2	O K	13.7	S K	0	Na K	1.1
Element	Wt%																							
C K	90.2																							
O K	8.3																							
S K	0																							
Na K	1.5																							
Element	Wt%																							
C K	85.2																							
O K	13.7																							
S K	0																							
Na K	1.1																							

Figure 8.3 Scanning electron microscopy (*SEM*) and elemental analysis (*EDX*) of the *BL* sides of (a) *BPM* and (b) the *CEM* used at *DC* and *PEF* regimes

8.3.2 Evolution of Electrodialytic Parameters

Conductivity of Black Liquor and Caustic Soda solution

The electrical conductivity plots of the *BL* and *NaOH* solutions are shown in Figure 8.4. The statistical analysis results revealed that the implementation of different applied electric current modes substantially affected the evolution of the electrical conductivity of the *BL*

and caustic soda solutions ($P < 0.001$). Aside from the *PEF* mode with $r = 0.25$, the electrical conductivity profiles of the *BL* and *NaOH* solutions depicted a non-linear behavior (R^2 between 0.9355 and 0.9946). As can be seen, their progress rates are more obvious at the beginning of the *EDBM* process and no pronounced variation was detected in their trends towards the end of the experiment. Although, it is noteworthy to mention that, implementing the *PEF* mode postponed the smooth progression of the electrical conductivity profiles. Moreover, performing the *EDBM* process under the *PEF* regime with $r = 0.25$ ($t_{pulse}/t_{pause} = 6(s)/24(s)$) resulted in a linear evolution of the *BL* and *NaOH* electrical conductivities (R^2 between 0.9727 and 0.9958).

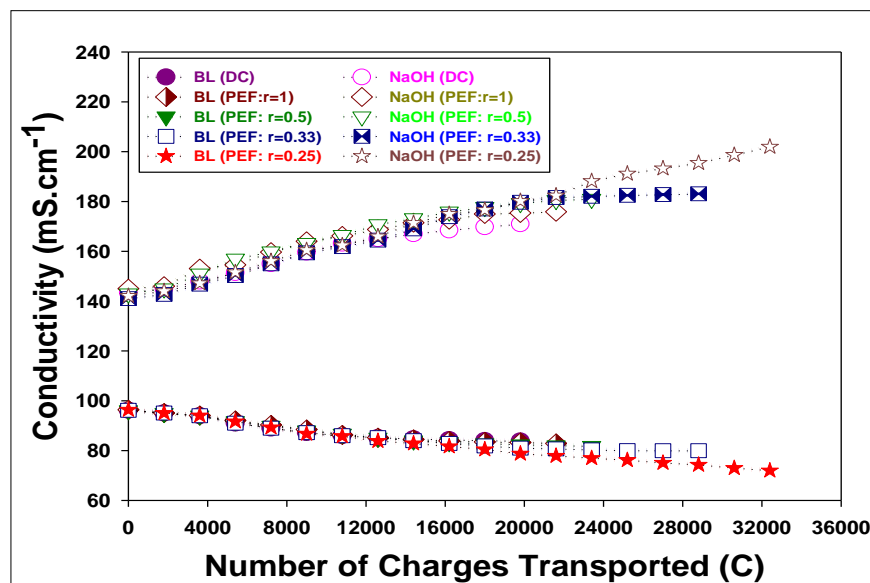


Figure 8.4 Conductivity trends of the *BL* and *NaOH* solutions during electrochemical acidification of Kraft *BL* via *EDBM* process under *DC* and *PEF* regimes (fitting equations can be found in Appendix A)

Indeed, the migration of the sodium ions from the *BL* compartment to the caustic soda compartment and the desalination phenomenon simultaneously lowered the electrical conductivity of the *BL* and enhanced the electrical conductivity of the *NaOH* solution. The more efficient the ion transfer, the more pronounced the electrical conductivity progress. Based on the experimental results, application of the *PEF* mode substantially improved the ion transfer and subsequently enhanced the desalination process. Similar results were reported by other researchers when the *PEF* regime was utilized in *ED* and *EDBM* treatments [80, 141].

Global System Resistance

Figure 8.5 shows the progress of the global system resistance throughout the *EDBM* process at different applied current regimes. According to the statistical analysis results, there is a significant difference between the global system resistance trends of the examined conditions ($P < 0.001$). In the control case, after 35 minutes (equals to 12600 *C*) of the acidification process a drastic rise in the global system resistance profile was observed. Application of the *PEF* mode with $r = 1$ ($t_{pulse}/t_{pause} = 6(s)/6(s)$) slightly delayed the sharp increase in the global system resistance for about 10 minutes (equals to 16200 *C*). By twofold and threefold increments of the relaxation period, the global system resistance profiles started to elevate with time lags of about 10 and 20 minutes, respectively. In addition, the global system resistance for the *PEF* cases with $r = 0.5$ and $r = 0.33$ elevated with less sharper slopes. Once the *PEF* mode with $r = 0.25$ ($t_{pulse}/t_{pause} = 6(s)/24(s)$) was applied, no considerable change or drastic increase was observed in the global system resistance progress. Thus, it can be summarized that the evolution of the global system resistance of all cases except for *PEF* mode with $r = 0.25$, presented a cubic trend (R^2 between 0.8307 and 0.9628). For the *PEF* mode with $r = 0.25$, the gradual increase in the global system resistance rate can be described by a linear regression curve ($R^2 = 0.9198$).

As stated in the literature, the initial value of the global system resistance corresponds to the intrinsic resistance of the *IEMs* and solution as well as the other compartments of the *EDBM* stack such as spacers [18]; whereas, the acidification and demineralization rates as well as the fouling of the *IEMs* highly control the final value of the global system resistance [78, 79]. Thus, by coupling the membrane analysis results with the global system resistance trends, it can be presumed that the fouling of the *IEMs* adversely caused the sharp increase of the global system resistance profiles when the *EDBM* experiments were carried out under the *DC* regime, or under *PEF* mode with $r = 1$, $r = 0.5$ and $r = 0.33$ ratios. On the contrary, in the absence of the fouling in the *EDBM* process under the *PEF* mode with $r = 0.25$, the linear increase of the global system resistance was due to the *BL* mineral depletion and reduction of its electrical conductivity along the acidification process (See Figure 8.4). It is worth mentioning that other researchers also reported a considerable reduction in the global system resistance when they applied the *PEF* regime in *ED* and *EDBM* treatments of different solutions [77, 80, 102].

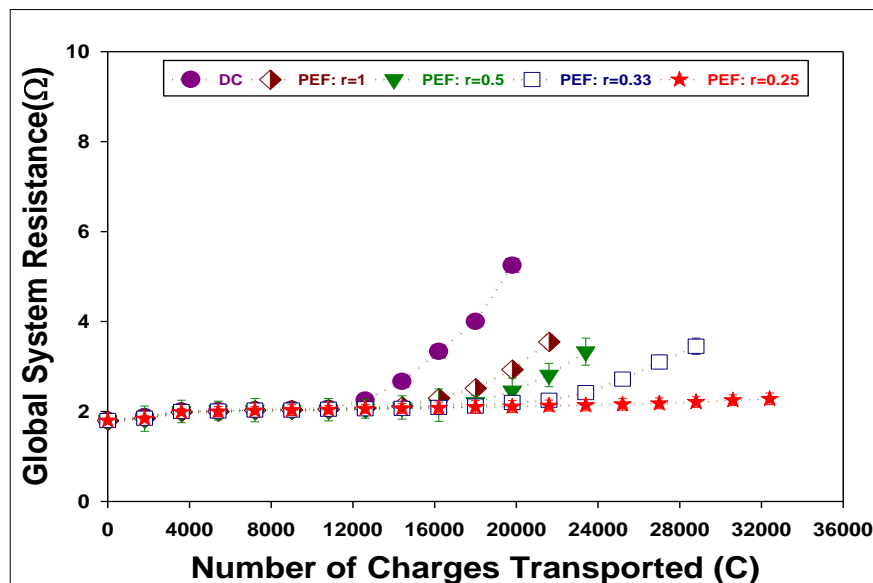


Figure 8.5 Global system resistance progress during electrochemical acidification of Kraft *BL* via *EDBM* process under *DC* and *PEF* regimes (fitting equations can be found in Appendix A)

pH of the Black Liquor

By tracking the pH trends of the *BL* under the *DC* and *PEF* regimes, one can note that changing the mode of applied current affected the pH progress of the *BL* and the statistical findings indicated that this influence was significant ($P < 0.001$). Excluding the *PEF* mode with $r = 0.25$, all the pH profiles exhibited a non-linear reduction rate which reached a plateau towards the end of the *EDBM* run (R^2 between 0.9790 and 0.9899); although, by increasing the pause lapse, this plateau shape appeared at a lower pH value. When the electrochemical acidification of the Kraft *BL* was carried out under *PEF* mode with the pulse/pause ratio of $r = 0.25$, its pH profile displayed a linear decrease ($R^2 = 0.9947$). By further expansion of the pause period (24 seconds), the acidification process was intensified and the desired final pH value was obtained as a consequence of the suppression of the *BPM* fouling. Such a process intensification was also addressed by Cifuentes-Araya *et al.* and Mikhaylin *et al.* when they applied the *PEF* regime with a long pause period in the *ED* treatments of model solutions containing mineral salts [77, 142].

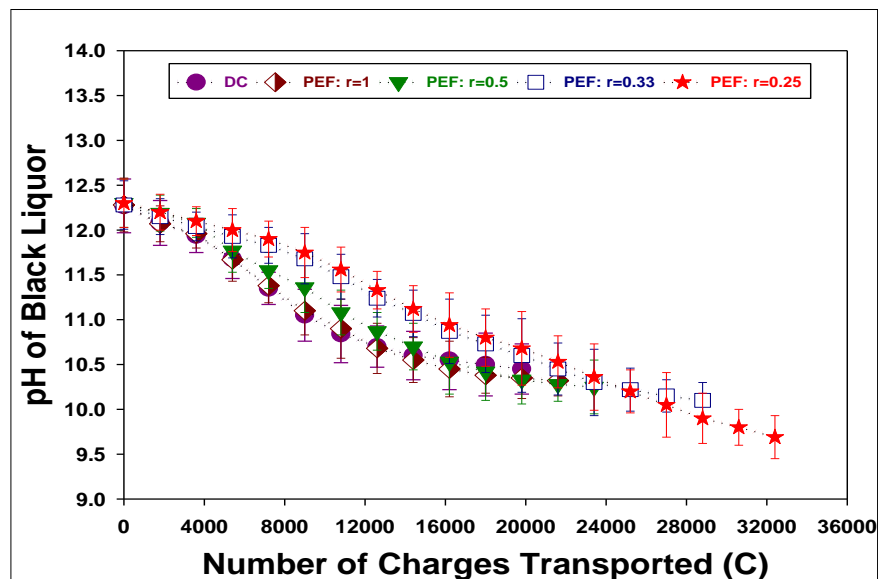


Figure 8.6 Evolution of the pH of the *BL* during the electrochemical acidification of Kraft *BL* via *EDBM* process under *DC* and *PEF* regimes (fitting equations can be found in Appendix A)

As Wallmo *et al.* [133] reported, the acidification of the *BL* takes place in sequential steps : at the beginning, the *BL* alkaline neutralization happens ; the second step is the protonation of the lignin phenolic groups and, finally, further advancement of the *BL* acidification process yields some buffering reactions of the hydrogen sulfide and carbonate systems ; however, this last step of the *BL* acidification is less desirable due to the production of unwanted H_2S acid [4]. Except for the *PEF* mode with $r = 0.25$ condition, the experimental results of the global system resistance, electrical conductivity and pH of the *BL* indicated that occurrence of the lignin precipitation inside the *EDBM* stack impaired the ion transfer through the *IEMs* and subsequently, disrupted the acidification progress of the *BL*. Therefore, for these aforementioned conditions, the *EDBM* experiments were stopped before reaching the final pH of about 9.7. When $r = 0.25$, the *EDBM* process was stopped when the pH value of the *BL* reached 9.7 similar to the final pH value when the chemical acidification of the *BL* was carried out by other researches [4, 12]. These researchers claimed that performing the lignin extraction at this pH value would facilitate the lignin filterability and enhance the lignin extraction yield [4].

Evolution of Sodium Concentration and Lignin Content of the Black Liquor

The evolution pattern of sodium concentration in the *BL* solution is presented in Figure 8.7. Based on the statistical analysis report, altering the applied electric field regime had a great influence on the progress of the *BL* sodium concentration ($P < 0.001$). In the control case, at the beginning of the *EDBM* experiment, the alternation of the sodium concentration in the *BL* solution was distinguishable; although, towards the end of the experiment, no major change was detected in the sodium content of the *BL*. Similar behaviors in the *BL* sodium content evolutions were observed when the *EDBM* experiment was carried out under the *PEF* mode of $r = 1$, $r = 0.5$ and $r = 0.33$ ratios. The only difference between the above-mentioned *PEF* cases and the control case was that expansion of the pause period postponed the inception of the monotonous sodium content level in the *BL* solution. It was not surprising that, when the *EDBM* process was run at the *PEF* condition with $r = 0.25$, the sodium ion concentration in the *BL* solution decreased linearly. This can be attributed to the efficient ion transfer through the *CEM* in the absence of the membrane fouling; while, in the other examined conditions, the severe fouling of the *IEMs* slowed down the migration of the sodium ions from the *BL* compartment to the caustic soda compartment. As stated earlier, the great impact of the *PEF* on efficient ion transfer across the *IEM* in model solutions was reported in the literature [79, 80, 141].

Performing the electrochemical acidification of the Kraft *BL* via the *EDBM* process under different applied electric field regimes greatly influenced the *BL* lignin content ($P < 0.001$). When the process was carried out by applying the *DC* regime, the lignin content of the *BL* started to decrease half way through the end of the acidification process. Application of *PEF* regime during the *EDBM* process could significantly diminish the decrement of the *BL* lignin content. As can be seen in Figure 8.8, by increasing the duration of pause lapse to 12 and 18 seconds, the non-linear *BL* lignin content reduction pattern was delayed and finally when the relaxation period was prolonged to 24 seconds, no significant change was observed in the evolution of the *BL* lignin content along the *EDBM* experiment.

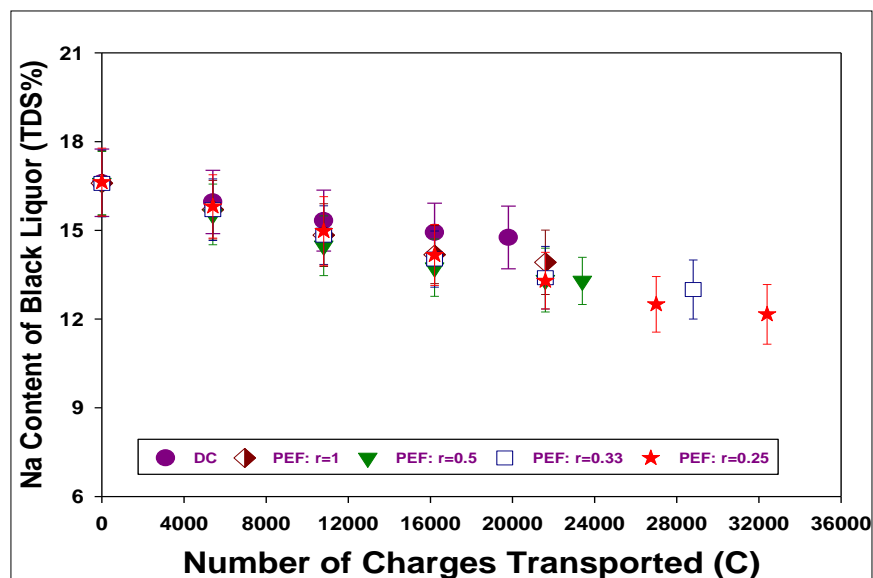


Figure 8.7 Evolution of sodium concentration in the *BL* solution during electrochemical acidification of Kraft *BL* via *EDBM* process under *DC* and *PEF* regimes (fitting equations can be found in Appendix A)

The measurement of the *BL* lignin content is a key indicator in detecting the occurrence of lignin precipitation inside the *EDBM* stack. The significant difference between the initial and final *BL* lignin content amounts corroborated the *EDX* analysis results and indicated that the fouling layer formed on the surface of the *IEMs* was mainly composed of lignin. Clearly, by exerting sequential relaxation periods, less lignin was accumulated inside the *EDBM* stack and the variance between the initial and final *BL* lignin content values diminished. Obviously, at the *PEF* regime with $r = 0.25$, no lignin was precipitated and the lignin content of the *BL* remained constant. It is noteworthy that Ruiz *et al.* also showed that by applying a longer pulse lapse, during the *ED* treatment of a casein solution, the accumulation of the protein on the surface of the *AEM* decreased and at a pulse/ pause ratio of 10 (s)/40 (s), the fouling of the membrane was completely suppressed [80].

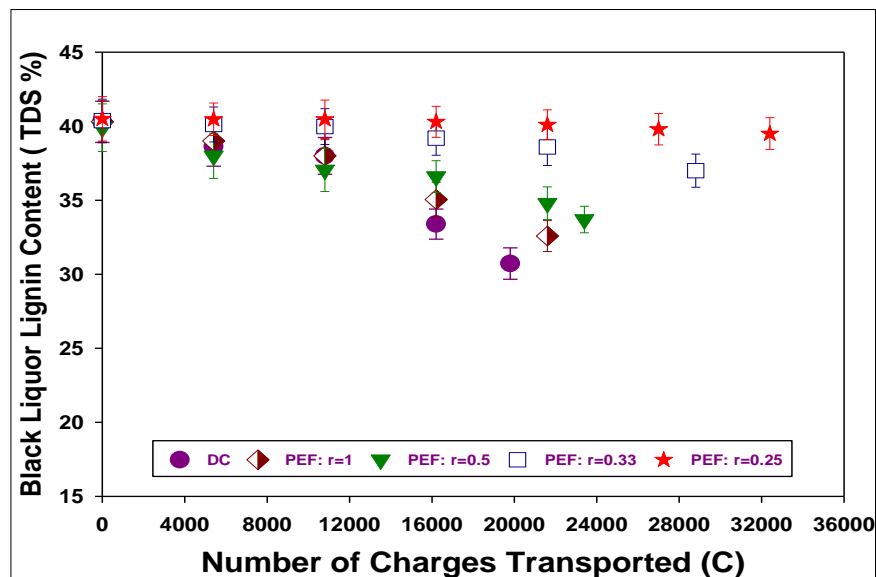


Figure 8.8 Evolution of *BL* lignin content during electrochemical acidification of Kraft *BL* via *EDBM* process under *DC* and *PEF* regimes (fitting equations can be found in Appendix A)

8.3.3 Evolution of System Performance

Current Efficiency

The computed current efficiency values of the *EDBM* trials under different applied electric field modes are outlined in Figure 8.9 (a). Statistical analysis findings reported a significant difference in the current efficiency rates when the applied electric field mode has been changed ($P < 0.001$). As illustrated in Figure 8.9 (a), the lowest current efficiency value i.e. 47.3% was obtained when the *EDBM* experiment was performed under the *DC* regime (control case) and in contrarily, conducting the *EDBM* experiments under the *PEF* mode with the pulse/pause ratio of 0.25 registered the highest current efficiency value around 80%. Figure 8.9 (b) exhibits the non-linear behavior of the current efficiency as a function of the pause lapse under the *PEF* regime ($R^2 = 0.9899$). Prolonging the pause time, at a fixed pulse period, exponentially improved the current efficiency of the system. Thus, the pulse/pause ratio is a key determining factor that substantially influences the efficiency of the *EDBM* system under *PEF* regime.

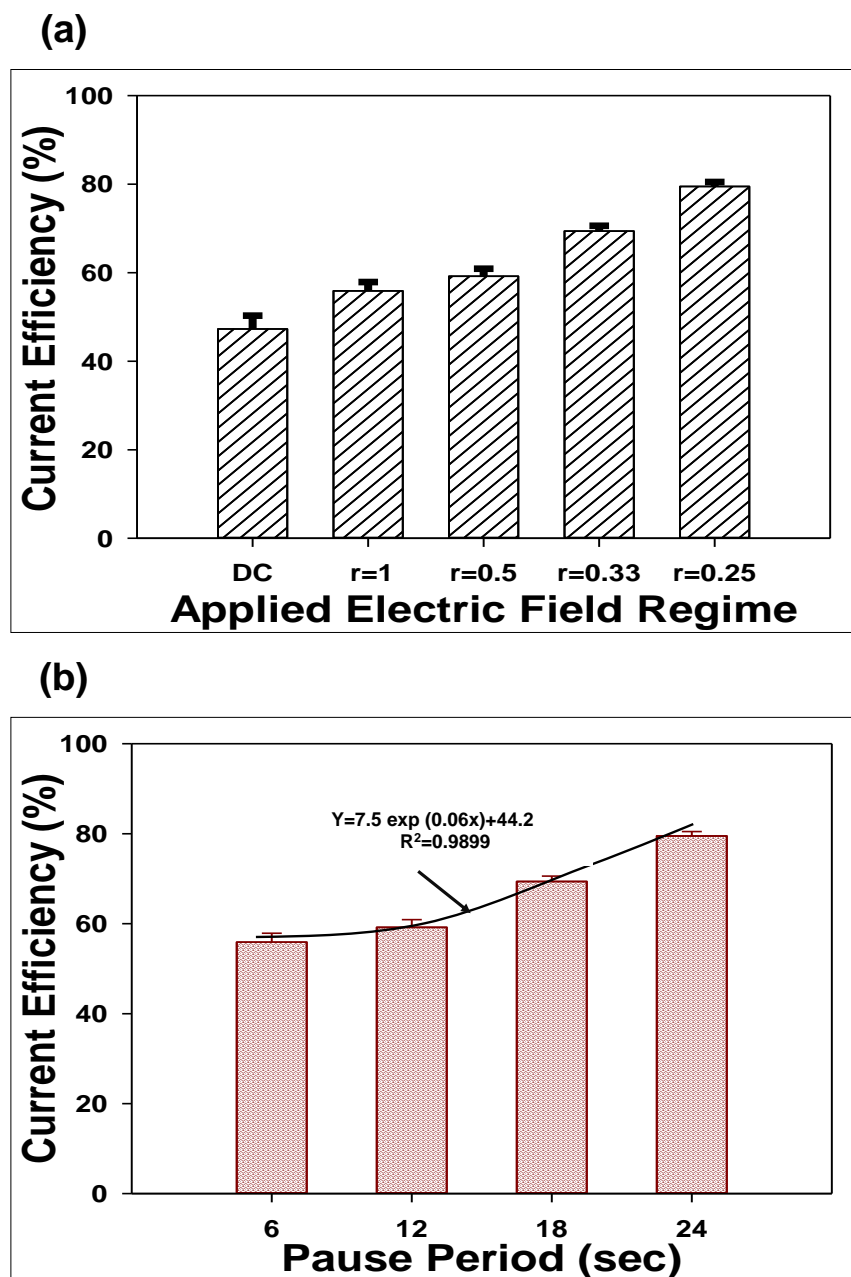


Figure 8.9 (a) Current efficiency of the *EDBM* acidification process under *DC* and *PEF* regimes with different pulse/pause ratios (b) current efficiency trend as a function of the pause lapse at *PEF* regime

In fact, the effectiveness of the ion transfer across the *IEMs* can influence the current efficiency of an electro-membrane system. Based on the electrical conductivity trends of the *BL* and caustic soda solutions at different examined conditions, one can deduce that fouling of the *IEMs* impaired the passage of the ions during the *EDBM* process and, as a result, the current efficiency of the system decreased. At the *PEF* regime, on the other hand, the

extension of the relaxation period led to the membrane fouling mitigation and ion passage improvement. Based on the current efficiency formula (Equation 8.3), the efficiency of the *EDBM* process enhances by increasing the ion transfer rate. At $r = 0.25$, the sodium ions pass through the *CEMs* effectively and hence, the current efficiency of the system increased. It is worth mentioning that the productiveness impact of the *PEF* application on the system efficiency was also addressed by other researchers [77, 78].

Relative Energy Consumption

Figure 8.10 (a) presents the relative energy consumption of the *EDBM* system under the two different applied electric field regimes. Clearly, the relative energy consumption of the control case (*DC* regime) presented the highest value ($3.6 \text{ Wh} / g - \text{NaOH}$). However, when the *PEF* regime was implemented the relative energy consumption of the system decreased significantly ($P < 0.001$). The lowest relative energy consumption value was achieved when the *EDBM* process was carried out at the *PEF* regime with the pulse/pause ratio of $r = 0.25$. In addition, a close observation of the relative energy consumption trend as a function of the pause lapse reveals that increasing the relaxation period resulted in a non-linear reduction in relative energy consumption (Figure 8.10 (b)).

The global system resistance and ion transfer rate highly control the energy demand of an electro-membrane system [18]. According to the relative energy consumption formula (Equation 8.4), the global system resistance and ion transfer rate have opposing effects on relative energy consumption of the system : increasing the global system resistance leads to increment of the relative energy consumption ; while, decreasing the ion transfer rate makes the *EDBM* process energy intensive. Therefore, when the membrane fouling takes place, the global system resistance increases and the ion passage become disrupted, consequently, more energy is required to overcome the high resistance inside the *EDBM* stack. Conversely, at the *PEF* regime with $r = 0.25$, no fouling occurred and the ions transferred through the *IEMs* effectively and, as a result, the system became energy efficient [139, 79].

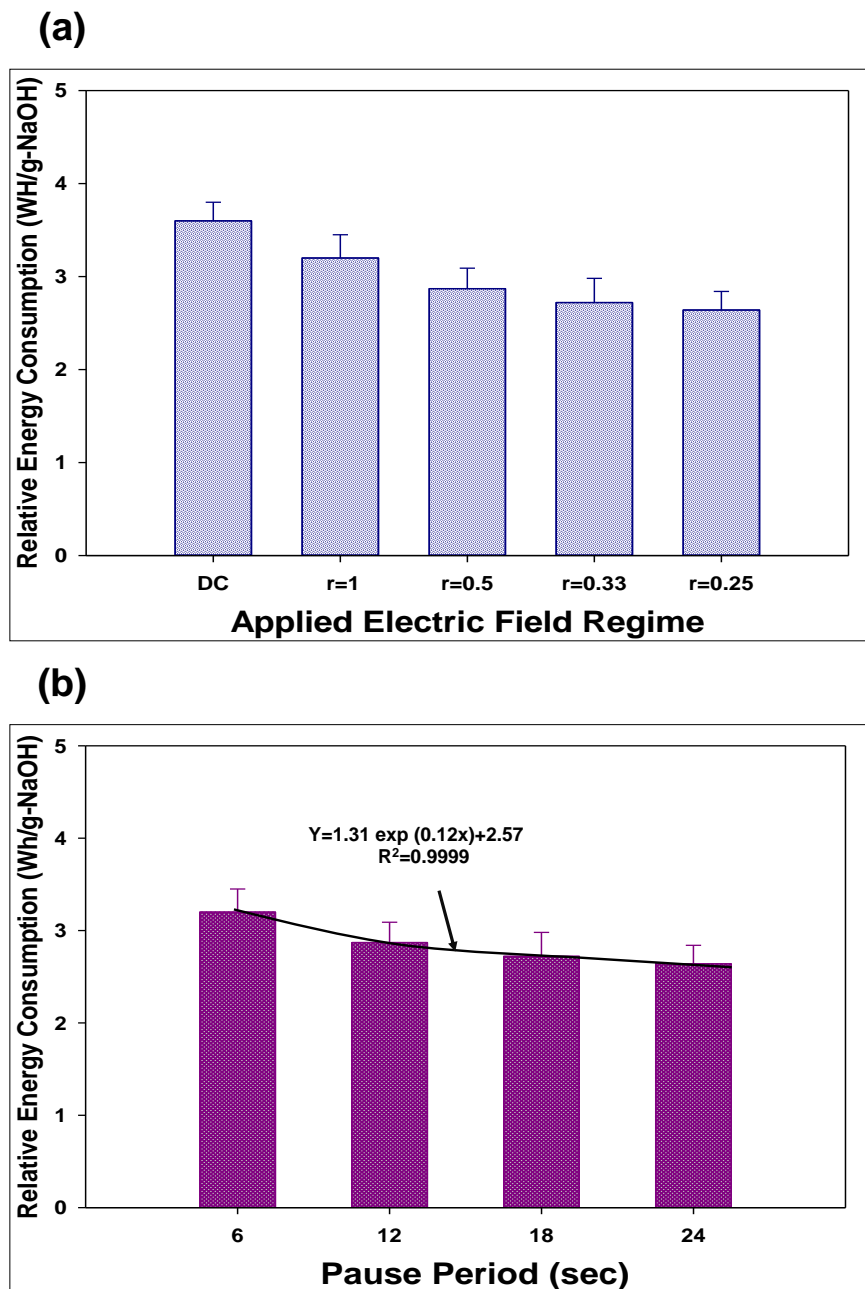


Figure 8.10 (a) Relative energy consumption of the *EDBM* acidification process under *DC* and *PEF* regimes with different pulse/pause ratios (b) relative energy consumption trend as a function of the pause lapse at *PEF* regime

8.3.4 Proposed Pulsed Electric Field Mechanisms

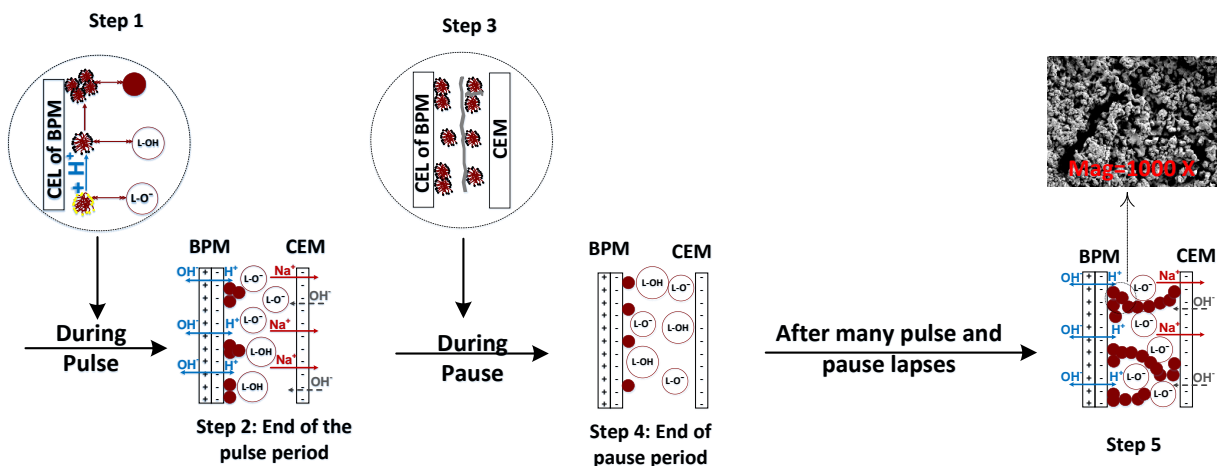
The Kraft Lignin macro-molecule acts as a polyelectrolyte in the alkaline *BL* solution and its colloidal stability can be described by the well-known *DLVO* theory [6]. Based on this theory,

an interplay between the attractive and repulsive forces dictates the colloidal stability in a solution [92]. Thereby, if attraction forces like van der Waals forces become predominant, the lignin self-aggregation and precipitation occurs; conversely, when the repulsive forces such as electrical double layer repulsive forces overcome the attractive forces, the lignin remains stable in the BL solution [6, 5]. The extent and rate of these repulsive forces is highly governed by the structure of the aggregated lignin cluster (its cohesion and porosity) as well as the temperature, pH and ionic strength of the solution [6, 90, 98].

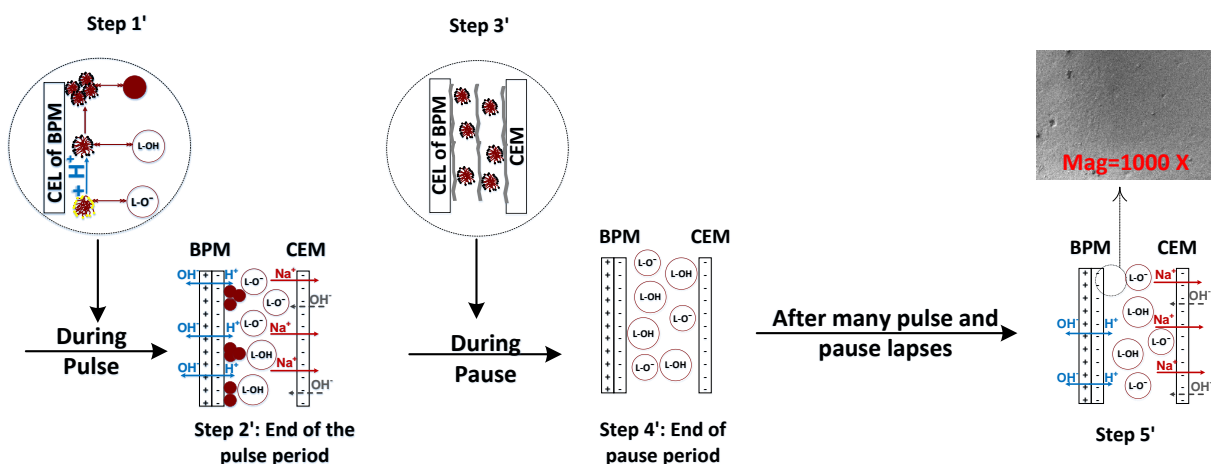
As quoted earlier, the decrement in the *BL* pH during the *EDBM* experiment triggers the protonation of the lignin acidic groups, induces the lignin self-aggregation and forms lignin nuclei. These nuclei can attach to the *CEL* of the *BPM* via hydrogen bonds, grow in size and number and ultimately form lignin clusters on the membrane surface. It should be taken into account that even though the lignin precipitation inside the *EDBM* stack is not desirable, the protonation of the lignin acidic groups is considered as one of the main steps of the *BL* acidification process for an efficient lignin extraction [133]. Thus, these protonation reactions cannot be prevented during the electrochemical acidification method. Hence, in the *DC* mode, due to the continuous generation of the proton ions, the lignin clusters formed on the surface of the *CEL* of the *BPM* can expand throughout the *EDBM* process, cover the entire surface of the membrane, fill out the space between the *IEMs* and, finally, attach to the *CEM* surface [97]. On the contrary, the discontinuous generation of the proton ions in the *PEF* regime can disrupt the lignin precipitation progress by increasing the electrophoretic movements of the colloidal lignin particles and retain them far from one another and the *IEM* surface [34].

Figure 8.11 presents a schematic illustration of the *BL* medium at different exerted pulse/pause ratios. During the pulse period, when the electrical field is established across the stack, the lignin nucleus, created due to the protonation of the lignin acidic groups, goes towards the *CEL* of the *BPM* and attaches to its surface. This nucleus can provide available sites for attraction of the other lignin molecules [64]. The growth rate and significance of the lignin cluster on the surface of the *CEL* of the *BPM* depends on the length of the pulse lapse (Figure 8.11 : steps 1 and 2).

(a)



(b)



Legend:

Soluble Lignin

Destabilized Lignin

Precipitated Lignin Cluster

Cleavage Sign

Ion transport through the IEM

Ion leakage through the IEM

Figure 8.11 Schematic illustration of the *BL* medium under the *PEF* regime when a (a) short and (b) long pause lapse was applied (steps 1 and 2 illustrate the pulse lapse, steps 3 and 4 show the pause period and step 5 represents the *BL* medium after several pulse-pause lapses)

During the pause period and in the absence of the electrical field and proton ions generation, the formed lignin clusters get attacked by the flux of the *BL* solution, circulating inside the

stack, detach from the membrane surface, split into smaller fragments and become suspended in the *BL* medium. Depending on the duration of the pause lapse, these fragments can be broken into even smaller parts and dispersed in the solution or remain as is and tend to sediment in the stack or stick to the surface of the *IEMs*. In parallel, the *BL* flux removes the remaining lignin particles from the membrane surface (Figure 8.11 : steps 3 and 4).

Figure 8.11 (a) shows the case when the length of the pause period was shorter than the time that the *BL* flux required to completely detach the lignin clusters from the membrane surface and split them into smaller particles. Accordingly, by exerting the next pulse lapse, the suspended lignin particles reattach to the lignin cluster remaining on the *CEL* surface of the *BPM* and the expansion of this cluster would continue. These clusters may also undergo the aging phase [143] and form a denser lignin layer on the membrane surface which cannot be easily split into smaller parts (Figure 8.11 (a) : step 5). Hence, it can be deduced that, in this case, the applied *PEF* ratio was not robust enough to suppress the formation and growth of the colloidal lignin cluster. Based on the experimental findings and the *IEMs* analyses results, one can note that the aforementioned case can simulate the performed *EDBM* experiments under the *PEF* mode with $r = 1$ ($t_{pulse}/t_{pause} = 6(s)/6(s)$), or $r = 0.5$ ($t_{pulse}/t_{pause} = 6(s)/12(s)$), or $r = 0.33$ ($t_{pulse}/t_{pause} = 6(s)/18(s)$) ratios.

On the other hand, when the most appropriate *PEF* ratio is applied i.e. $r = 0.25$ ($t_{pulse}/t_{pause} = 6(s)/24(s)$), the *BL* flux could completely remove all the colloidal lignin attached to the *BPM* surface and thoroughly disperse them in the *BL* solution. In such a condition, the *BL* medium became a stabilized suspension medium and the chance of the lignin-lignin aggregation decreases (Figure 8.11 (b) : step 5).

8.4 Conclusion

For the first time, in the course of this study, the impact of the *PEF* regime on suppression of the *BPM* colloidal fouling was demonstrated. The membrane analysis data and the *EDBM* experimental results revealed that application of the *PEF* mode with pulse/pause ratio of $6(s)/24(s)$ could efficiently prevent the precipitation of colloidal lignin inside the *EDBM* stack and maintain the integrity of the *IEMs*. Moreover, carrying out the *EDBM* process under the aforementioned condition yielded a high current efficiency of about 80% as well as a low relative energy consumption ($2.6 Wh/g - NaOH$) and a smooth global system resistance evolution. In addition, the final pH of the acidified *BL* solution reached a value of about 9.7 from which the lignin can be easily and effectively extracted.

The last part of this investigation covered the elucidation of the *PEF* mechanisms ruling

the mitigation of the *BPM* colloidal fouling. Based on the proposed *PEF* mechanisms and the experimental findings, it was concluded that a careful selection of the pulse/pause ratio was critical in preventing the colloidal growth of the lignin macro-molecules and eventually eliminating the fouling of the *BPM*. Also, it was found that the application of the *PEF* regime can enhance the electrophoretic movements of the colloidal lignin, disperse them in the *BL* solution and as a result, sustain the colloidal stability of the *BL* medium.

On the basis of the promising results presented in this paper, one can conclude that the green electrochemical acidification of the Kraft *BL* via the *EDBM* method by applying the *PEF* regime is an eco-efficient approach. Yet, to propose this method as an alternative to the chemical acidification technique, a systematic comparison between these two pathways is still necessary. Thus, work on this remaining topic is continuing and will be presented in a future publication.

Acknowledgments

This work was financially supported by the NSERC and BioFuelNet Canada. The authors are grateful to Hydro-Québec Energy Technology Laboratory (*LTE*) for providing the experimental set-up and the Kraft pulping mill for supplying the black liquor samples. In addition, we also thank Mrs. Ir. E. Shahrabi for taking the *SEM* images and Mr. D. Pilon for building and programming the pulse generator device.

Appendix A

Fitting equation of electrical conductivity trend of the *BL* solution :

$$BL_{Electrical\ Conductivity} = a \exp(-bq) + c$$

Table 8.5 Parameters of the *BL* electrical conductivity fitting equations

Regime	ratio	<i>a</i>	<i>b</i>	<i>c</i>	<i>R</i> ²
<i>DC</i>	-	16.7	9.2×10^{-5}	80.5	0.9775
<i>PEF</i>	1	19.7	6.2×10^{-5}	77.6	0.9812
<i>PEF</i>	0.50	20.6	6.4×10^{-5}	76.5	0.9856
<i>PEF</i>	0.33	21.5	6.6×10^{-5}	75.75	0.9913

For *PEF* regime with *r* = 0.25 : $BL_{Electrical\ Conductivity} = -7 \times 10^{-4}q + 94.9$ & $R^2 = 0.9727$

Fitting equations of electrical conductivity trend of the *NaOH* solution :

$$NaOH_{Electrical\ Conductivity} = d(1 - \exp(-eq)) + f$$

Table 8.6 Parameters of the $NaOH$ electrical conductivity fitting equations

Regime	ratio	d	e	f	R^2
DC	-	50.7	4.6×10^{-5}	141.6	0.9868
PEF	1	44.9	4.6×10^{-5}	77.6	0.9812
PEF	0.50	54.5	5.9×10^{-5}	141.3	0.9946
PEF	0.33	75.9	3.6×10^{-5}	138.7	0.9528

For PEF regime with $r = 0.25$: $NaOH_{Electrical\ Conductivity} = -2 \times 10^{-4}q + 142.2$ & $R^2 = 0.9958$

Fitting equations of global system resistance trend during $EDBM$ process :

$$R = gq^3 - hq^2 + iq + j$$

Table 8.6 Table C.3 : Parameters of the global system resistance fitting equations

Regime	ratio	g	h	i	j	R^2
DC	-	2.6×10^{-12}	7.1×10^{-8}	6×10^{-4}	0.40	0.9628
PEF	1	1.6×10^{-12}	5.4×10^{-8}	5.4×10^{-4}	0.44	0.8817
PEF	0.50	1.25×10^{-12}	4.5×10^{-8}	5.0×10^{-4}	0.83	0.9620
PEF	0.33	7.3×10^{-13}	3.1×10^{-8}	4.1×10^{-4}	0.60	0.8307

For PEF regime with $r = 0.25$: $R = 1.1 \times 10^{-5}q + 1.92$ & $R^2 = 0.9198$

Fitting equations of the BL pH trend during $EDBM$ process :

$$BL_{pH} = k \exp(-lq) + m$$

Table 8.7 Parameters of the BL pH fitting equations

Regime	ratio	k	l	m	R^2
DC	-	2.71	6.9×10^{-5}	9.67	0.9790
PEF	1	2.95	6.3×10^{-5}	9.44	0.9838
PEF	0.5	3.82	4.0×10^{-5}	8.63	0.9867
PEF	0.33	2.39	1.0×10^{-5}	9.99	0.9899

For PEF regime with $r = 0.25$: $BL_{pH} = -8.3 \times 10^{-5}q + 1.40$ & $R^2 = 0.9947$

Fitting equations of the BL sodium concentration trend during $EDBM$ process :

$$BL_{Na} = n \exp(-pq)) + w$$

Table 8.8 Parameters of the BL sodium concentration fitting equations

Regime	ratio	n	p	w	R^2
DC	-	2.98	5.1×10^{-5}	13.64	0.9978
PEF	1	4.1	5.3×10^{-5}	12.6	0.9952
PEF	0.5	4.8	5.7×10^{-5}	11.9	0.9925
PEF	0.33	9.0	2.1×10^{-5}	7.58	0.9996

For PEF regime with $r = 0.25$: $BL_{Na \text{ concentration}} = -1.0 \times 10^{-4}q + 16.54$ & $R^2 = 0.9922$

Fitting equations of the BL lignin content trend during $EDBM$ process :

$$BL_{lignin} = r \exp(-sq)) - t$$

Table 8.9 Parameters of the BL lignin content fitting equations

Regime	ratio	r	s	t	R^2
DC	-	6.6×10^3	7.2×10^{-8}	6.6×10^3	0.9579
PEF	1	4.2×10^3	8.6×10^{-8}	4.1×10^3	0.9838
PEF	0.5	3.4×10^2	6.4×10^{-8}	299×10^3	0.9633
PEF	0.33	1.14×10^3	6.8×10^{-8}	1100	0.9653

For PEF regime with $r = 0.25$: $BL_{lignin \text{ content}} = 40.5 \pm 1.0$

CHAPTER 9 BLACK LIQUOR ACIDIFICATION FOR LIGNIN EXTRACTION : A PRELIMINARY COMPARISON BETWEEN CHEMICAL AND ELECTROCHEMICAL ACIDIFICATION PATHWAYS

9.1 Introduction

For the last decade, the pulp and paper (*P & P*) industry in mature countries including Canada has been experiencing tough economic conditions as a result of declining demand for traditional *P & P* commodities and international competitions [1]. Transformation of the *P & P* industry and particularly Kraft pulping mills into integrated forest biorefinery (*IFBR*) is as an effective alternative to increase the revenues of the mills and substantially diversify their product portfolio [2, 4].

Within the Kraft *IFBR* context, a fraction of lignin can be extracted from a residual stream, called black liquor (*BL*), and transformed into a broad spectrum of bio-products and biochemical [4]. In chapter 8, it was shown that application of electrodialysis with bipolar membrane (*EDBM*) under pulsed electric field (*PEF*) regime provided simultaneous advantages of *BL* electrochemical acidification and caustic soda production without any chemical consumption.

The objective of this study was to draw a preliminary comparison between the performance of the electrochemical and chemical acidification processes used for the *BL* acidification and subsequently the lignin extraction in terms of lignin filtration rate and efficiency. In addition, we aim to demonstrate the influences of the acidification methods on lignin impurity (ash content) as well as the amount of chemicals consumed during the washing step of the extracted lignin. This comparison allows us to emphasize the assets of the green and sustainable electrochemical acidification pathway and elaborate some suggestions for further process improvement.

9.2 Experimental

9.2.1 Membranes and Materials

The commercially available *IEMs* used in this work were Fumasep *FBM* bipolar membrane (FuMA-Tech Co., Germany) and *CMB* cation exchange membrane (Neosepta, Japan). Their main specifications are given in Table 9.1.

Table 9.1 Ion exchange membranes specifications provided by their suppliers

Membrane	Type	Thickness (mm)	IEC ($meq.g^{-1}$)	Specific Area Resistance ($\Omega.cm^2$)	Stability (pH)	Temperature °C
<i>CMB</i>	Cation	0.18- 0.21	3.11	4.5	1 – 14	≤ 60
<i>FBM</i>	Bipolar	0.18- 0.20	-	-	1 – 14	≤ 60

The softwood *BL* was provided by a Canadian Kraft pulping mill with a total dissolved solids (*TDS*) content was 50 ± 2 (wt. %). This liquor was diluted to 20 (wt. %) and pre-filtered to remove any suspended solid particles larger than $0.010 \mu m$ utilizing a simple vacuum filtration apparatus and a filter paper (Whatman Grade 111105, UK). Analytical grade chemicals were purchased from Sigma-Aldrich, Canada and standard solutions were supplied by Fisher Scientific, Canada. Demineralized water was used to prepare all the aqueous solutions and perform the washing step.

9.2.2 Chemical Acidification Apparatus and Protocol

The chemical acidification process was carried out in a laboratory scale set-up consisting of a 2L open jacket reactor connected to a hot water bath (to maintain the operating temperature), a burette and a pitched blade turbine (*PBT*) impeller attached to a mixer (Model : Caframo *BDC 2002*, Caframo Limited, Canada) with a 1 *RPM* accuracy (Figure 9.1).

The pH of 2 L BL was brought to 9.7 by manually adding 10.00 N sulfuric acid. The solution was vigorously mixed. Once the desired pH was obtained the operational temperature was adjusted to $75^\circ C$ and the mixing was carried out for one hour with 150 *RPM* speed as recommended by Kannangara [4]. This phase is referred to as the aging step. The slurry of the aging phase was cooled down to room temperature and then filtered using a simple vacuum filtration setup (buchner funnel connected to a 2 L filtration flux) at 75 *kPa*. A lignin cake was formed on top of the filter paper (Whatman Grade 113, UK). In the washing step, 0.80 N sulfuric acid and water were poured on top of the lignin cake, respectively. The amounts of utilized acid and water were noted. The wet lignin was weighted, then it was dried (24 hours air dried and an overnight oven drying at $105^\circ C$). Finally, the weight of the dried lignin was recorded. It should be mentioned that pre-weighed lignin samples were taken before and after the washing step for the ash content measurement.

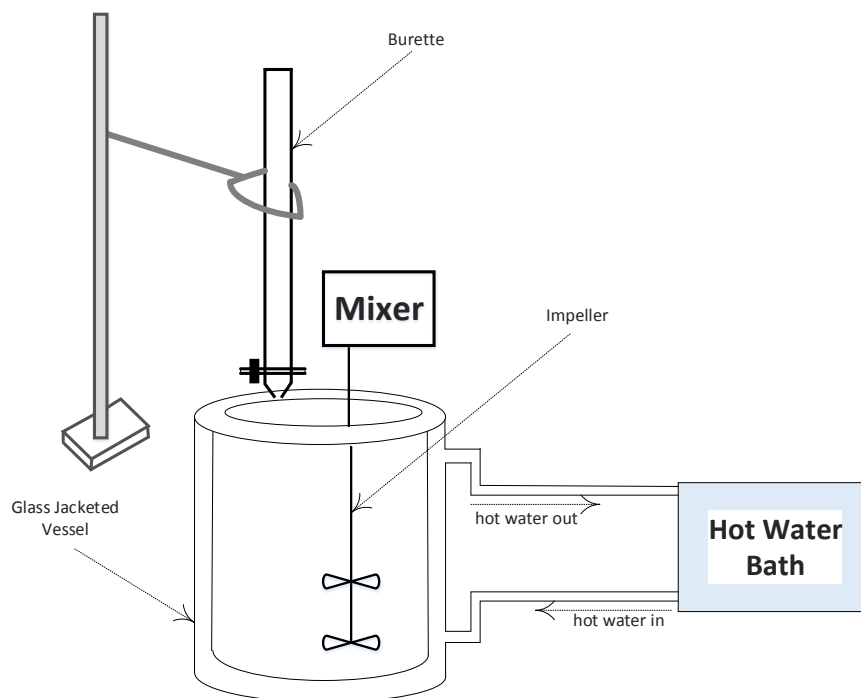


Figure 9.1 A schematic drawing of the chemical acidification apparatus

9.2.3 Electrochemical Acidification Apparatus and Protocol

Electrochemical acidification process was performed using the same cell configuration and experimental set-up described in chapter 8. The *PEF* regime with pulse/pause ratio of $6(sec)/24(sec)$ was applied and the *EDBM* process was terminated when the final pH of the *BL* reached 9.7. Then, the acidified *BL* was transferred to the chemical acidification set-up to perform the aging step. Both chemical and electrochemical acidification processes were carried out at $55^{\circ}C$. The aging and filtration conditions were the same for both of the cases and each experiment repeated three times under the same operational conditions.

9.2.4 Analyses

Black liquor and Lignin Analysis

Total dissolved solid (*TDS*) content, ash content, lignin and sodium concentrations as well as residual effective alkali (*RA*) of the *BL* solution were measured employing the same procedures described in chapter 4. The raw *BL* chemical composition is presented in Table 9.2

Table 9.2 Characteristics of Kraft Black Liquor

Characteristics	Data
Total Dissolved Solids (<i>TDS</i>) (%)	20.1
UV Lignin (% <i>TDS</i>)	40.6
Ash Content (% <i>TDS</i>)	27.9
Sodium Concentration (% <i>TDS</i>)	17.9
Residual Alkali ($g. L^{-1}$)	5.5

Lignin ash content was determined first by drying overnight the samples at $105^{\circ} C$; then, weighing the dried sample and a 16-hours combustion at $950^{\circ} C$. The ash content is the weight ratio of the residue before and after the combustion step.

Lignin Precipitation Yield

Yield of lignin precipitation was computed as follow :

$$Lignin\ Precipitation\ Yield = \frac{L_{BL} - L_f}{L_{BL}} \times 100 \quad (9.1)$$

Where, L_{BL} and L_f are the lignin content of the fresh and the filtrated *BL* ($g\ Kg^{-1}\ TDS$), respectively.

Filtration Rate

The filtration rate was determined as the ratio of the extracted lignin (kg) per surface area per hour ($m^{-2}\ h^{-1}$) [12].

Statistical Analysis

The experimental data were presented as means \pm standard deviation and subjected to one-way and multiple-way statistical analysis using SigmaPlot software (version 13.0, SYSTAT software Inc., San Jose, CA, USA) with the probability level of 5%.

9.3 Results and Discussion

9.3.1 Comparison of Electrochemical Acidification and Chemical Acidification Methods

The filtration rate and lignin precipitation yield of the electrochemical and chemical acidification methods are given in Table 9.3. Based on the statistical analysis results, no significant differences in the filtration rate and lignin precipitation yield were detected employing these two acidification techniques ($P_{filtration\ rate} = 0.626$ and $P_{lignin\ yield} = 0.848$). Hence, the acidification method had insignificant impact on the filtration rate and the final lignin precipitation yield.

Table 9.3 Acidification parameters obtained from electrochemical and chemical acidification steps

Parameters	Electrochemical Acidification	Chemical Acidification
Filtration Rate ($kg\ m^{-2}\ h^{-1}$)	125.9 ± 1.3	126.4 ± 0.9
lignin Precipitation Yield (%)	55.1 ± 2.2	54.7 ± 2.5
Consumed Sulfuric Acid (10.00 <i>N</i>) during the Acidification Step (<i>ml</i>)	-	38 ± 1
Relative Energy Consumption (<i>Wh</i>)	126.7 ± 0.2	-
Total Caustic Soda Production (<i>g</i>)	47.2 ± 1.1	-

In addition to the lignin precipitation yield and filtration rate information, Table 9.3 also presents the amount of energy and acid consumed to acidify the *BL* as well as the total amount of produced caustic soda during the *EDBM* process. Note that the consumed energy to run the pumps, mixer and maintain a constant operational temperature were not included in relative energy consumption calculation. However, the consumed energy for mixing and maintaining a constant temperature were the same for both cases. As can be seen, the electrochemical acidification method was successfully performed with no added acid and the final pH of the *BL* was 9.7. By contrast, around 40 *ml* sulfuric acid with 10.00 *N* concentration was utilized to drop the pH of 2 *L BL* to 9.7. Thereby, it can be concluded that the electrochemical acidification approach was more eco-friendly.

By comparing the filtration rate results presented in chapter 4 with the current data one can note that the *TDS* content of the *BL* highly affects the lignin filtration rate and lignin precipitation yield. The higher filtration rate of the *BL* with 20 wt. % *TDS* content can be related to the viscosity of the solution. In chapter 7, it was shown that the dynamic

viscosity of the *BL* increases exponentially with increasing its *TDS* content. Thus, the less viscous *BL* was filtered faster. The difference in the lignin precipitation yield results can be explained by the difference in the lignin content of the *BL* solutions with 30 and 20 wt. % *TDS* contents. Obviously, the *BL* solution with 20 wt. % *TDS* content has less lignin. The lower lignin content decreases the probability of particle-particle collisions and aggregation [4, 64]. However, the aggregation rate and subsequently the lignin precipitation yield of the *BL* solution with 20 wt. % *TDS* content can be improved by modifying the operational conditions of the agitation and filtration steps i.e. reducing the agitation rate and temperature [5] along with prolonging the aging residence time [4] and/or increasing the ionic strength of the acidified *BL* at the aging step [5, 144]. It should be highlighted that decreasing the lignin precipitation yield by reducing the *TDS* content of the *BL* have been observed in earlier studies [4, 10, 11].

9.3.2 Lignin Impurities

Table 9.4 outlines the lignin ash content before and after the washing step together with the amount of water and acid utilized in this step. According to the statistical analysis findings, the type of the acidification process greatly affects the lignin ash content and amount of acid consumption ($P < 0.001$).

The ash content of the extracted lignin after the *EDBM* acidification step was around 50 % lower than the ash content of the extracted lignin after the chemical acidification step. Hence, considerably less 0.80 *N* sulfuric acid was consumed to purify the lignin with 6.24 % impurity than the lignin with 12.12 % ash content. The same volume of demineralized water (1200 *ml*) was utilized to perform the final washing step in both cases.

Table 9.4 Lignin ash content and consumed acid during the washing steps

Parameters	Electrochemical Acidification	Chemical Acidification
Unwashed Lignin Ash content (%)	6.24 ± 0.51	12.12 ± 0.46
Washed Lignin Ash content (%)	0.32 ± 0.03	0.31 ± 0.03
Consumed Sulfuric Acid (0.80 <i>N</i>) during the Washing Step (<i>ml</i>)	1000	2600
Consumed water during the Washing Step (<i>ml</i>)	1200	1200

The significant difference between the ash content data of unwashed lignin is attributed to

the sodium content of the acidified *BL*. According to the information found in the literature, the unwashed precipitated Kraft lignin contains a considerable amount of chemically bonded sodium (up to 16 wt. %) and sulfur (around 2 wt. %) [11]. The presence of these component in the Kraft lignin causes the lignin impurity. Throughout the electrochemical acidification of the *BL* via the *EDBM* process, the sodium ions migrates from the *BL* compartment to the *NaOH* compartment and as a result the final sodium concentration of the acidified *BL* decreases [66]. Thus, less sodium ions would be available in the acidified *BL* medium to bond to the lignin and increase its ash content. Clearly, the less the impurity, the less chemical (sulfuric acid) consumption and the less effluent production. Perhaps, conducting a two- stage acid washing, as recommended by Kouisni *et al.* [145], can minimize the ash content of the *BL* to less than 0.1%. It should be remarked that Bazinet *et al.* [146] also observed a significant decrease in the ash content of proteins when they used electrochemical acidification method.

9.4 Conclusion and Perspectives

To perform the electrochemical acidification process, an electrical field was used as the driving force in the *EDBM* system. Two products were obtained by the electrochemical approach i.e. acidified *BL* and concentrated caustic soda ; while by the chemical acidification, acidified *BL* was the only product. The chemical acidification of 2 *L* Kraft *BL* consumed about 40 *ml* sulfuric acids (10.00 *N*), while no acid was consumed during the electrochemical acidification step.

The experimental results and chemical consumption values show that application of the electrochemical acidification process via the *EDBM* method substantially reduced the chemical consumption and effluent generation. Furthermore, the in situ production of the valuable side product i.e. caustic soda can make the *EDBM* process an eco-efficient and profitable operational unit inside the *IFBR* plant. The produced *NaOH* can be utilized in the cooking and bleaching stages inside the mill or in other chemical industries.

The findings of this preliminary comparison substantiated the practical feasibility and substantial advantages of the green electrochemical acidification method ; however, further investigations are recommended in order to determine the optimum aging and washing operational conditions. Further more, it is recommended to perform a life analysis cycle assessment in order to confirm the eco-efficiency of the process.

CHAPTER 10 GENERAL DISCUSSION

In the essence of the wood-based biorefinery, it is imperative to identify, design and develop eco-efficient extraction processes to separate wood components and convert them into a vast spectrum of value-added bio-products. The objective of this research project was to demonstrate the feasibility of a green and sustainable black liquor (*BL*) acidification technique for an effective lignin extraction. The focus of this PhD thesis was on proofing the concept of electrochemical acidification approach as an alternative to the conventional chemical acidification process, controlling the colloidal fouling of the ion exchange membranes (*IEM*) and ultimately improving the efficiency of the process. In the following sections the key results and challenges of the electrochemical acidification method will be discussed.

As the first step for conducting this pioneering research, a technical feasibility study was carried out to address the advantages and limitations of the electrochemical acidification of the Kraft *BL* via *EDBM* method. In this regard, two parallel acidification methods (electrochemical and chemical) were applied to lower the pH of the *BL* with 30 (wt. %) total dissolved solids (*TDS*) content. The obtained results of this work corroborated the technical feasibility of the electrochemical acidification method. Nevertheless, it was found that formation of a brownish deposit layer inside the *EDBM* stack and subsequently, fouling of the *IEMs* was the only disadvantage of the *EDBM* method which forced the termination of the *EDBM* process before reaching the desirable pH. A comparison between these two techniques in terms of lignin precipitation yield, chemical consumption and filtration rate revealed that application of the *EDBM* method resulting in less chemical consumption than the conventional chemical acidification process (Chapter 4, Article 1). However, to achieve a high filtration rate and lignin precipitation yield and consume less energy, it was recommended to terminate the *EDBM* process just before the occurrence of membrane fouling and perform further acidification of the *BL* via a chemical acidification technique. Another possible solution was to analyze the deposit layer in order to explore the cause of the membrane fouling and take appropriate efforts to diminish this process drawback.

In chapter 5 (Article 2), the fouling layer was analyzed in order to identify its composition and its formation mechanisms. A series of fundamental membrane analyses were conducted. The obtained data from membrane thickness and ash content measurements, together with scanning electron microscopy (*SEM*), elemental analysis (*EDX*) and X-ray photoelectron spectrometry (*XPS*) indicated that cation exchange membranes (*CEM*) were less prone to the membrane fouling than the bipolar membranes (*BPM*). Furthermore, it was found that

organic matters mainly formed the fouling layer with a small fraction of sodium and sulfur. The O/C ratio of the deposit layer fell in the range of 0.25 – 0.44. The main functional groups of the fouling layer were $C1$ and $C2$ with relative percentages of about 50 and 40, respectively. By coupling the membrane analyses findings with evolution of the BL chemical composition before and after the $EDBM$ process, it was discovered that the deposit layer was mainly composed of lignin. The proposed fouling mechanisms were based on the parameters that highly affect the Kraft lignin solubility inside an aqueous solution such as pH, operational temperature, lignin content and ionic strength of the solution [5, 62, 63, 64, 90]. It was found that during the electrochemical acidification process, the pH of the BL gradually decreases and as a result more proton ions would be available inside the BL medium. These proton ions could facilitate the protonation reaction of the lignin phenolic groups and decrease the lignin solubility. As a result, destabilized lignin macro-molecules started to self-aggregate and formed nuclei [5, 62]. Due to the abundance of the proton ions on the surface of the cation exchange layers (CEL) of the $BPMs$, these nuclei could attach to their surfaces via hydrogen bounds and form lignin clusters. Over the time, these lignin clusters covered the entire surface of the CEL and the spaces between the $IEMs$ and finally, attached to the surface of the CEM . Formation of thinner deposit layer on the surface of the $CEMs$ can be related to the hydroxide ion leakage through these membranes. These hydroxide ions re-dissolved some of the lignin molecules and disturbed the lignin accumulation on the surface of the $CEMs$.

Based on the final results and conclusions of the first phase, the focus of the second phase was on process configuration in order to improve the performance of the system and minimize the membrane fouling. Thus, two protocols were conducted to (1) screen the most durable and commercially available $IEMs$ which were less prone to the fouling phenomenon and also (2) select the most appropriate cleaning procedure to remove the fouling layer from the surface of the $IEMs$.

In the first protocol, four commercially available $CEMs$ were tested. It should be noted that that due to the limited number of commercially available $BPMs$ and restrictions against the BPM analysis from some of the membrane suppliers, only one type of these membranes was examined. Evaluation of the global system resistance trend during the $EDBM$ process showed that changing the type of the CEM could not diminish the membrane fouling and a chemical cleaning cycle was required. The cleaning procedure was selected based on the nature of the fouling layer, the chemical compatibility of the stack components and potential availability of the cleaning agent inside a Kraft pulping mill [98, 99, 100]. As mentioned earlier, lignin was the main component of the fouling layer and according to the information found in the literature Kraft lignin is soluble in alkaline solution [5, 62, 63, 64, 90]. Thereby, caustic soda and fresh diluted BL solutions were selected as the chemical cleaning agents. An

arbitrary period of 30 minutes was chosen for the chemical cleaning cycle. Membrane analyses findings indicated that the fouled particles were removed successfully from the surface of the *IEMs* after the chemical cleaning step. Comparison of the analysis results of the fresh, fouled and cleaned membranes revealed that two *CEMs* i.e. *CMB* and Nafion 324 were the most chemically stable membranes under the alkaline conditions. Also, most of the initial properties of the *BPM* were reestablished after the chemical cleaning step. Although, application of the caustic soda as the cleaning agent presented better results and cleaner membrane surface, it was recommended to utilize in situ and free of charge fresh diluted *BL* as the chemical cleaning agent and increase the duration of the chemical cleaning cycle in order to make the chemical cleaning step more eco-efficient.

In the second protocol of the process configuration phase, the effects of process variables on the performance of the electrochemical acidification of the Kraft *BL* were demonstrated. Article 4 described the effect of the *BL* temperature and chemical composition on its electrical conductivity and viscosity evolution and also the influences of the operational temperature and *BL* chemical composition on the performance of the electrochemical acidification process.

The experimental results showed that elevating the operational temperature could highly improve the electrical conductivity of the *BL*, lignin solubility and current efficiency of the *EDBM* process and, consequently, decrease the energy consumption of the *EDBM* system due to the lower global system resistance. Although, the influence of the applied operational temperatures on the hydrodynamics of the process was less pronounced. Additionally, the chemical composition or the *TDS* content of the *BL* considerably affected its dynamic viscosity, mineral concentration and lignin content. It was demonstrated that the dynamic viscosity of the *BL* increased exponentially with increasing its *TDS* content and yielded in an exponential reduction of Reynolds number by decreasing the agitation inside the *EDBM* system which ultimately prompted the fouling of the *IEMs*. Furthermore, by increasing the *TDS* content of the *BL* solution its mineral concentration and lignin content elevated and led to a quick precipitation inside the *EDBM* stack which, in turn, caused a drastic rise in the global system resistance profile, a higher energy consumption level and a lower current efficiency, regardless of the operational temperature. It was presumed that the *BL* solution with a high *TDS* content had a greater abundance of high molecular weight lignin and these large macro-molecules acted as potential nucleus and provided more sites for attraction of the smaller lignin molecules. As a consequence, the lignin self-aggregation and precipitation was triggered. Electrochemical acidification of the *BL* solution containing 20 wt. % *TDS* at 55 °C provided the highest current efficiency and, subsequently, the lowest energy consumption. In this case, the more pronounced agitation inside the stack could delay and diminish the lignin self-aggregation phenomenon and the formation of the lignin clusters on the sur-

face and in the space between the *IEMs*, to some degree. However, towards the end of the electrochemical acidification process, the lignin started to deposit inside the *EDBM* stack, leading to the membrane fouling and eventually, resulted in a sharp rise in the global system resistance profile. In regards to the experimental findings of this step, it was concluded that the most appropriate range of the process variables could improve the *EDBM* process performance and lessen the fouling of the *IEM*, to some extent; but, a chemical cleaning cycle was inevitable to remove the fouling layer and clean the apparatus, completely.

Application of an in-line cleaning step was considered as a possible option to eliminate the membrane fouling, intensify the acidification process and minimize the amount of effluent produced from the chemical cleaning step [34, 37, 77, 80, 139, 102]. Accordingly, the goal of the final phase of this research project was set on the evaluating the influence of a promising and cost effective in-line cleaning method, i.e. application of pulsed electric field (*PEF*) during *EDBM* process in order to prevent the formation of lignin colloidal clusters on the surface of the *IEMs* and intensify the electrochemical acidification process.

In the course of this study, the pulse lapse was kept constant while four different pause periods were applied. It was found that when the *EDBM* process was carried out under the *PEF* regime with the pulse/pause ratio of 6(s)/24(s), no deposit layer was formed on the surface or in the space between the *IEMs*. The suppression of the fouling layer improved the ion transfer through the *IEMs* and also led to further progression of the *BL* acidification. Furthermore, the integrity of the *IEMs* was restored. It should be pointed out that, under the aforementioned conditions, the current efficiency of the *EDBM* system was close to 80%, which was almost twofold higher than the current efficiency of the *EDBM* system when no relaxation period was exerted during the process. The relative energy consumption of the *EDBM* process under the *PEF* regime with the pulse/pause ratio of 6(s)/24(s) was 2.6 *Wh* for one gram *NaOH* production which was round 30% lower than the *DC* regime. Obtaining such a low value of relative energy production can be explained by the fact that in the absence of fouling layer, the global system resistance exhibited a smooth increase along the *EDBM* process due to desalination of the *BL*. Hence, no extra energy was required to overcome the excessive resistance of the *EDBM* stack. The end results of this investigation revealed that a rigorous selection of the pulse/pause ratio yields in prevention of the colloidal growth of the lignin macro-molecules and subsequently elimination of the fouling of the *IEMs*. Also, in accordance with previous studies [102, 140], it was assumed that the application of the *PEF* regime can enhance the electrophoretic movements of the colloidal lignin, disperse them in the *BL* solution and as a result, preserve the colloidal stability of the *BL* medium.

Furthermore, as stated earlier, the fouling of the *BPM* has never been elaborated in the

literature. Therefore, the originality of this research lies in the fact that, throughout the course of this study, we detected a fouling layer on the surface of the *BPM*, identified the fouling composition and mechanisms and, finally, exerted adequate efforts to suppress it. Thereby, the generated results of this study can be employed to design and improve an *EDBM* system when the *BPM* fouling is the main process drawback.

Even though the main objective of this research was to design and develop the green electrochemical acidification of the Kraft *BL* via the *EDBM* process, it ends with an additional study presenting a preliminary comparison between the electrochemical and chemical acidification techniques. In this study, the lignin precipitation yield, purity and filtration rate as well as the amount of chemical and energy consumption were considered as the comparison criteria. It should be mentioned that the main differences between the findings of this work with the results of the feasibility study presented in chapter 4 are :

- The *TDS* content of the utilized *BL* was 20 wt. % instead of 30 wt. %.
- Due to the absence of the fouling of the *IEMs*, the electrochemical acidification was not interrupted and the pH of its outlet acidified *BL* stream was 9.7 without any acid addition.

It was found that the type of the acidification method had no significant impact on the lignin precipitation yield and filtration values. However, the lignin extracted from the *BL* which was electrochemically acidified contained less ash. Therefore, less acid was consumed during the washing step to purify this lignin and lower its ash content to less than 1%. Less acid consumption means in less effluent production and more eco-efficient system. In addition, pure caustic soda was produced as a valuable side products. It should be mentioned that the aging and filtration conditions were similar to the conditions that Kannangara [4] applied for carbonation of the oxidized Kraft *BL*. However, he showed that aging and filtration conditions highly affect the filtration rate as well as the lignin precipitation yield and impurity. Accordingly, it was recommended to improve and eventually optimize the aging and filtration conditions in order to substantially decrease the filtration resistance and lignin ash content and enhance the sustainability of the electrochemical acidification method for an efficient lignin extraction.

CHAPTER 11 CONCLUSIONS, ORIGINAL CONTRIBUTIONS AND RECOMMENDATIONS

11.1 Conclusions

The main objective of this PhD project was to identify, design and develop a novel method to acidify Kraft black liquor (*BL*) for lignin extraction. The proposed method must be an attractive alternative to the conventional chemical acidification technique and accomplish the requirements in terms of a high efficiency, a low chemical and energy consumption along with environmental constraints. To this end, electrochemical acidification process by means of electrodialysis with bipolar membrane (*EDBM*) technique was proposed as a innovative and more sustainable pathway to acidify the *BL* and extract the lignin. A two-compartment *EDBM* cell comprising of bipolar (*BPM*) and cation exchange membranes (*CEM*) was used. In addition, a value-added side product i.e. caustic soda solution was simultaneously produced, which can be utilized in the Kraft mill or in other chemical industries. The main findings of this research study are summarized as follow :

- The results of a technical feasibility study on the *EDBM* method indicated that electrochemical acidification of the *BL* via *EDBM* process resulted in less chemical consumption than conventional chemical acidification approach; however, membrane fouling impaired its performance.
- Based on our proposed mechanisms protonation of lignin phenolic groups led to formation of destabilized colloidal lignin and subsequently lignin precipitation on the surface of the *IEMs* which increased the global system resistance.
- Application of a post chemical cleaning cycle using an alkaline cleaning agent such as caustic soda or fresh diluted *BL* could successfully remove the lignin deposit from the surface of the *IEMs* and reestablish their integrity.
- Chemical composition of the *BL* and operational temperature significantly influenced the *EDBM* current efficiency, energy consumption and fouling of *IEMs*.
- Lignin self-aggregation and precipitation inside the *EDBM* stack was diminished by improving the hydrodynamics of the system.
- Implementation of an in-line cleaning step i.e. pulsed electric field (*PEF*) regime with a rigorous pulse/pause ratio substantially suppressed the growth of the colloidal lignin due to effective reduction of the *BL* mineral content and tackling the lignin-lignin aggregation. As

a result, the *BPM* fouling was impeded; the *BL* acidification process was intensified and reached a desirable pH from which the lignin was separated efficiently. Furthermore, application of *PEF* regime considerably improved the current efficiency of the *EDBM* process and decreased its relative energy consumption.

- Extracted lignin from the acidified *BL* after the *EDBM* process possessed less impurity and accordingly consumed less acid in the washing step. In consequence, less effluent was generated and the eco-efficiency of the process was enhanced.

11.2 Original Contributions

To the best of our knowledge, this is the first study performed to investigate the viability of the electrochemical acidification of the Kraft *BL* via the *EDBM* method. The generated results substantiated the practical feasibility of the electrochemical acidification process and demonstrated its major advantages over the conventional chemical acidification approach :

- Production of caustic soda as a valuable side-product which can be utilized in the cooking or bleaching steps inside the Kraft mill or in other chemical industries.
- Lowering the lignin ash content by decreasing the mineral concentration of the acidified *BL*.
- No chemical consumption during the acidification step and
- Less chemical consumption and effluent generation during the lignin washing step.

Additionally, for the first time and throughout the course of this study, the fouling of the *BPMs* was systematically investigated and substantial efforts were exerted to suppress this process drawback. Thereby, the end results of this study can be employed to design and improve an *EDBM* system when the fouling of the *BPM* is the main process drawback.

11.3 Recommendations

- It was demonstrated that the chemical composition of the *BL* highly affect the process performance. Therefore, it is recommended to evaluate the influence of the *BL* type (oxidized vs non-oxidized) and origin (softwood vs. hardwood) on the electrochemical acidification efficiency.
- It was observed that hydrodynamic conditions of the system can highly impact the lignin colloidal fouling. Thus, it is proposed to improve the *EDBM* stack design and especially the design of the spacers in order to increase agitation inside the stack and impede the formation

of lignin clusters.

- It would be interesting to apply different pulse lapses and also shorter pulse and pause periods in order to increase the liquid motion inside the *EDBM* stack and ultimately optimize the *PEF* regime for the *BL* electrochemical acidification.
- With the intention of increasing the filtration rate and lignin precipitation yield, optimization of aging and filtration steps during the lignin extraction process is highly recommended.
- Performing a life cycle assessment is suggested to confirm the eco-efficiency of the electrochemical acidification pathway.
- A systematic study for integration of the *EDBM* process to the lignin-based biorefinery is essential.
- Further characterization of the extracted lignin and identification of its potential applications are recommended.

REFERENCES

- [1] M. Kannangara, M. Marinova, M. Perrier, and J. Paris, "Forest Biomass and Paper Industry, a Pathway to Green Biofuels ," in *ENV2015-1800*, (Athens, Greece), 2015.
- [2] W. E. Mabey, D. J. Gregg, and J. N. Saddler, "Assessing the Emerging Biorefinery Sector in Canada," *Applied Biochemistry and Biotechnology*, vol. 123, no. 1-3, pp. 765–778, 2005.
- [3] A. Van-Heiningen, "Converting a Kraft Pulp Mill into an Integrated Forest Biorefinery," *Pulp and Paper Canada*, vol. 107, no. 6, pp. 38–43, 2006.
- [4] M. Kannangara, *Development and Integration of Acid Precipitation Based Lignin Biorefineries in Kraft Pulping Mills*. PhD thesis, Polytechnique de Montreal, Montreal, Canada, 2015.
- [5] W. Zhu, *Precipitation of Kraft Lignin*. PhD thesis, Chalmers University of Technology, Gothenburg, Sweden, 2015.
- [6] M. Norgren, H. Edlund, and L. Wågberg, "Lignin : Recent Advances and Emerging Applications," *Current Opinion in Colloid & Interface Science*, vol. 19, no. 5, pp. 409–416, 2014.
- [7] L. Da-Re and L. Papinutti, "Black liquor Decolorization by Selected White-Rot Fungi," *Applied Biochemistry and Biotechnology*, vol. 165, no. 2, pp. 406–415, 2011.
- [8] D. Dimmel and J. Bozell, "Pulping Catalysts from Lignin," *TAPPI Journal*, vol. 74, no. 5, p. 239, 1991.
- [9] A. S. Jonsson and O. Wallberg, "Cost Estimates of Kraft Lignin Recovery by Ultrafiltration," *Desalination*, vol. 237, pp. 254–267, 2009.
- [10] R. Alen, P. Patja, and E. Sjostrom, "Carbon Dioxide Precipitation of Lignin from Pine Kraft Black Liquor," *Tappi Journal*, vol. 62, pp. 108–110, 1979.
- [11] H. Loutfi, B. Blackwell, and V. Uloth, "Lignin Recovery from Kraft Black Liquor : Preliminary Process Design," *Tappi Journal*, vol. 74, no. 1, pp. 203–210, 1991.
- [12] L. Kouisni, P. Holt-Hindle, K. Maki, and M. Paleologou, "The Lignoforce System : A New Process for the Production of High-Quality Lignin from Black Liquor," *J-FOR : The Journal of Science and Technology for Forest Products and Processes*, vol. 2, pp. 6–10, 2012.
- [13] J. N. Cloutier, M. K. Azarniouch, and D. Callender, "Electrolysis of Weak Black Liquor Part II : Effect of Process Parameters on the Energy Efficiency of the Electrolytic Cell," *Journal of Applied Electrochemistry*, vol. 25, no. 5, pp. 244–248, 1994.

- [14] A. Toledano, L. Serrano, A. Garcia, I. Mondragon, and J. Labidi, "Comparative Study of Lignin Fractionation by Ultrafiltration and Selective Precipitation," *Chemical Engineering Journal*, vol. 157, no. 1, pp. 93–99, 2010.
- [15] V. C. Uloth and J. T. Wearing, "Kraft Lignin Recovery : Acid Precipitation versus Ultrafiltration Part II : Technology and Economics," *Pulp & Paper Canada*, vol. 90, no. 10, pp. 34–37, 1989.
- [16] C. Negro, A. Blanco, J. Tijero, S. Villarin, J. V. Erkel, and M. C. P. D. Jong, "Electrochemical Treatment of Straw Weak Black Liquor from a Kraft Pulping Plant," *Cellulose Chemistry and Technology*, vol. 39, no. 1-2, pp. 129–136, 2005.
- [17] A. J. B. Kemperman, *Handbook on Bipolar Membrane Technology*. University of Twente, Enschede, The Netherlands, 2000.
- [18] H. Strathmann, *Ion-Exchange Membrane Separation Processes*. Elsevier, 2004.
- [19] Y. Tanaka, *Ion Exchange Membranes : Fundamentals and Applications*. Elsevier Science, 2007.
- [20] J. Mulder, *Basic Principles of Membrane Technology*. Springer, 1996.
- [21] R. W. Baker, *Membrane Technology and Applications*. Wiley, England, 2nd ed., 2004.
- [22] G. Pourcelly and L. Bazinet, *Developments of Bipolar Membrane Technology in Food and Bio-Industries*. CRC Press, 2009.
- [23] A. A. Zagorodni, *Ion Exchange Materials : Properties and Applications*. Elsevier, 2007.
- [24] E. Drioli and L. Giorno, *Membrane Operations : Innovative Separations and Transformations*. Wiley-VCH, 2009.
- [25] J. Balster, D. F. Stamatialis, and M. Wessling, "Electro-Catalytic Membrane Reactors and the Development of Bipolar Membrane Technology," *Chemical Engineering and Processing : Process Intensification*, vol. 43, no. 9, pp. 1115–1127, 2004.
- [26] F. Posar, "Method for making a bipolar membrane," *U.S. Patent*, no. 5849167, 1998.
- [27] G. J. Dege, F. P. Chlanda, L. T. C. Lee, and K. J. Liu, "Method of making novel two component bipolar ion exchange membranes," *U.S. Patent*, no. 4253900, 1981.
- [28] H. Mueller and H. Puetter, "Process for the preparation of bipolar membranes," *European Application Publication Patent*, no. 0193959, 1986.
- [29] J. H. Hao, C. Chen, L. Li, L. Yu, and W. Jiang, "Preparation of Bipolar Membranes (I)," *Journal of Applied Polymer Science*, vol. 80, no. 10, pp. 1658–1663, 2001.
- [30] H. Strathmann, "Electrodialysis, a Mature Technology with a Multitude of New Applications," *Desalination*, vol. 264, no. 3, pp. 268–288, 2010.

- [31] T. A. Davis, V. Grebenyuk, and O. Grebenyuk, *Electromembrane Processes*. Wiley, 2001.
- [32] K. Scott, *Handbook of Industrial Membranes*. Elsevier Science, 1996.
- [33] R. Field, *Fundamentals of Fouling*. Wiley-VCH Verlag GmbH & Co. KGaA, 2010.
- [34] H. J. Lee, S. H. Moon, and S. P. Tsai, “Effects of Pulsed Electric Fields on Membrane Fouling in Electrodialysis of *NaCl* solution Containing Humate,” *Separation and Purification Technology*, vol. 27, no. 2, pp. 89–95, 2002.
- [35] J. W. Post, *Blue Energy : Electricity Production from Salinity Gradients by Reverse Electrodialysis*. PhD thesis, Wageningen University, Wageningen, The Netherlands, November 2009.
- [36] T. Xu, “A Review : Ion Exchange Membranes : State of their Development and Perspective,” *Journal of Membrane Science*, vol. 263, no. 1-2, pp. 1–29, 2005.
- [37] S. Mikhaylin and L. Bazinet, “Fouling on Ion-Exchange Membranes : Classification, Characterization and Strategies of Prevention and Control,” *Advances in Colloid and Interface Science*, vol. 229, pp. 34–56, 2016.
- [38] G. Pourcelly, “Electrodialysis with Bipolar Membranes : Principles, Optimization, and Applications,” *Russian Journal of Electrochemistry*, vol. 38, no. 8, pp. 919–926, 2002.
- [39] J. N. Cloutier, M. K. Azarniouch, and D. Callender, “Electrolysis of Weak Black Liquor Part I : Laboratory Study,” *Journal of Pulp and Paper Science*, vol. 19, no. 6, pp. 244–248, 1993.
- [40] J. N. Cloutier, M. K. Azarniouch, and D. Callender, “Electrolysis of Weak Black Liquor Part III : Continuous Operation Test and System Desion Considerations,” *Pulp & Paper Canada*, vol. 95, no. 5, pp. 210–241, 1994.
- [41] A. Blanco, C. Negro, J. Tijero, M. C. P. D. Jong, and D. Schmal, “Electrochemical Treatment of Black Liquor from a Straw Pulping,” *Separation Science and Technology*, vol. 31, no. 19, pp. 2705–2712, 1996.
- [42] A. K. Mishra and P. K. Bhattacharya, “Alkaline Black Liquor Treatment by Batch Electrodialysis,” *The Canadian Journal of Chemical Engineering*, vol. 62, no. 5, pp. 723–727, 1984.
- [43] A. K. Mishra and P. K. Bhattacharya, “Alkaline Black Liquor Treatment by Continuous Electrodialysis,” *Journal of Membrane Science*, vol. 33, no. 1, pp. 83–95, 1987.
- [44] J. N. Cloutier, P. Champagne, and R. Labrecque, “Electrolytic Treatment of Black Liquor with Caustic Recovery,” in *2013 PEERS Conference*, (USA), 2013.

- [45] J. A. Koumoundouros, S. Oshen, and S. F. Sobczynski, "Recaustization of kraft black liquor via bipolar electrodialysis : Final report," Technical Report DOE/CE/40865-1, United States. Dept. of Energy. Office of Conservation and Renewable Energy. Office of Industrial Programs, 1990.
- [46] M. Manttari, J. Lahti, H. Hatakka, M. Louhi-Kultanen, and M. Kallioinen, "Separation Phenomena in UF and NF in the Recovery of Organic Acids from Kraft Black Liquor," *Journal of Membrane Science*, vol. 490, pp. 84–91, 2015.
- [47] O. Wallberg, A. Holmqvist, and A. S. Jonsson, "Ultrafiltration of Kraft Cooking Liquors from a Continuous Cooking Process," *Desalination*, vol. 180, pp. 109–118, 2005.
- [48] A. Keyoumu, R. Sjodahl, G. Henriksson, M. Ek, G. Gellerstedt, and M. E. Lindstrom, "Continuous Nano- and Ultra-Filtration of Kraft Pulping Black Liquor with Ceramic Filters : A Method for Lowering the Load on the Recovery Boiler While Generating Valuable Side-Products," *Industrial Crops and Products*, vol. 20, no. 2, pp. 143–150, 2004.
- [49] O. Wallberg and A. S. Jonsson, "Influence of the Membrane Cut-off During Ultrafiltration of Kraft Black Liquor with Ceramic Membranes," *Chemical Engineering Research and Design*, vol. 81, no. 10, pp. 1379–1384, 2003.
- [50] E. A. M. R. Olsson and T. Berntsson, "Exporting Lignin or Power from Heat-integrated Kraft Pulp Mills : A Techno-economic Comparison using Model Mills," *Nordic Pulp and Paper Research Journal*, vol. 21, pp. 476–484, April 2006.
- [51] W. Jin, R. Tolba, J. Wen, K. Li, and A. Chen, "Efficient Eextraction of Lignin from Black Liquor via a Novel Membrane-assisted Electrochemical Approach," *Electrochimica Acta*, vol. 107, pp. 611 – 618, 2013.
- [52] L. Bazinet, F. Lamarche, and D. Ippersiel, "Bipolar-Membrane Electrodialysis : Applications of Electrodialysis in the Food Industry," *Trends in Food Science & Technology*, vol. 9, no. 3, pp. 107–113, 1998.
- [53] S. P. Nunes and K. Peinemann, *Membrane Technology : in the Chemical Industry*. Wiley, 2006.
- [54] L. Bazinet, F. Lamarche, D. Ippersiel, and J. Amiot, "Bipolar-Membrane Electroacidification to Produce Bovine Milk Casein Isolate," *Journal of Agricultural and Food Chemistry*, vol. 47, no. 2, pp. 5291–5296, 1999.
- [55] D. A. Cowan and J. H. Brown, "Effect of Turbulence on Limiting Current in Electrodialysis Cells," *Industrial & Engineering Chemistry*, vol. 51, no. 12, pp. 1445–1448, 1959.

- [56] P. Scandinavian Pulp and B. T. Committee, "SCAN-N 37 :98 : Sodium and potassium contents," Test Methods , July 1998.
- [57] T. Radiotis, J. Sullivan, M. MacLeod, and S. Syed, "Improved Methods for Measuring Residual Effective Alkali in Kraft Black Liquors, Part 2 : comparison of Titration Methods," in *TAPPI Engineering, Pulping and Environmental Conference Proceedings*, (Jacksonville, Finland), pp. 21–24, 2007.
- [58] C. G. Zoski, *Handbook of Electrochemistry*. Elsevier, 2007.
- [59] M. Cardoso, E. D. de Oliveira, and M. Passos, "Chemical Composition and Physical Properties of Black Liquors and their Effects on Liquor Recovery Operation in Brazilian Pulp Mills," *Fuel*, vol. 88, pp. 756–763, 2009.
- [60] F. L. T. Shee, P. Angers, and L. Bazinet, "Microscopic Approach for Identification of Cationic Membrane Fouling during Cheddar Cheese Whey Electro Acidification," *Journal of Colloid and Interface Science*, vol. 322, pp. 551–557, 2008.
- [61] W. J. Frederick, *Kraft Recovery Boiler*. Tappi Pr, 1997.
- [62] M. Norgren and B. Lindström, "Dissociation of Phenolic Groups in Kraft Lignin at Elevated Temperatures," *Holzforschung*, vol. 54, no. 5, pp. 519–527, 2000.
- [63] M. Norgren, H. Edlund, L. Wågberg, B. Lindström, and G. Annergren, "Aggregation of Kraft Lignin Derivatives under Conditions Relevant to the Process, Part I : Phase Behaviour," *Colloids and Surface*, vol. 194, pp. 85–96, 2001.
- [64] M. Norgren, H. Edlund, and L. Wågberg, "Aggregation of Kraft Lignin Derivatives under Alkaline Conditions. Kinetics and Aggregate Structure," *Langmuir*, vol. 18, pp. 2859–2865, 2002.
- [65] E. Ayala-Bribiesca, G. Pourcelly, and L. Bazinet, "Nature Identification and Morphology Characterization of Cation-Exchange Membrane Fouling during Conventional Electrodialysis," *Journal of Colloid and Interface Science*, vol. 300, pp. 663–672, 2006.
- [66] M. Haddad, L. Bazinet, O. Savadogo, and J. Paris, "A Feasibility Study of a Novel Electro-Membrane Based Process to Acidify Kraft Black Liquor and Extract Lignin," *Submitted*, 2016.
- [67] L. Bazinet, D. Ippersiel, D. Montpetit, B. Mahdavi, J. Amiot, and F. Lamarche, "Neutralization of Hydroxide Generated during Skim Milk Electroacidification and its Effect on Bipolar and Cationic Membrane Integrity," *Journal of Membrane Science*, vol. 216, no. 1-2, pp. 229–239, 2003.
- [68] E. Korngold, F. de Korosy, R. Rahav, and M. Taboch, "Fouling of Anion selective Membranes in Electrodialysis," *Desalination*, vol. 8, no. 2, pp. 195–220, 1970.

- [69] V. Lindstrand, G. Sundströma, and A. Jönsson, "Fouling of Electrodialysis Membranes by Organic Substances," *Desalination*, vol. 128, no. 1, pp. 91–102, 2000.
- [70] G. Amy, "Fundamental Understanding of Organic Matter Fouling of Membrane," *Desalination*, vol. 231, no. 1-3, pp. 44–51, 2008.
- [71] L. Bazinet, D. Ippersiel, D. Montpetit, B. Mahdavi, J. Amiot, and F. Lamarche, "Effect of Membrane Permselectivity on the Fouling of Cationic Membranes during Skim Milk Electroacidification," *Journal of Membrane Science*, vol. 174, no. 1, pp. 97–110, 2000.
- [72] H. J. Lee, J. H. Choi, J. Cho, and S. H. Moon, "Characterization of Anion Exchange Membranes Fouled with Humate during Electrodialysis," *Journal of Membrane Science*, vol. 203, no. 1-2, pp. 115–126, 2002.
- [73] H. J. Lee, M. K. Hong, S. D. Han, J. Shim, and S. H. Moon, "Analysis of Fouling Potential in the Electrodialysis Process in the Presence of an Anionic Surfactant Foulant," *Journal of Membrane Science*, vol. 325, no. 2, pp. 719–726, 2008.
- [74] H. J. Lee, M. K. Hong, S. D. Han, S. H. Cho, and S. H. Moon, "Fouling of an Anion Exchange Membrane in the Electrodialysis Desalination Process in the Presence of Organic Foulants," *Desalination*, vol. 238, no. 1-3, pp. 60–69, 2009.
- [75] Q. wang, P. Yang, and W. Cong, "Cation-Exchange Membrane Fouling and Cleaning in Bipolar Membrane Electrodialysis of Industrial Glutamate Production Wastewater," *Separation and Purification Technology*, vol. 79, no. 1, pp. 103–113, 2011.
- [76] L. Bazinet, D. Montpetit, D. Ippersiel, J. Amiot, and F. Lamarche, "Identification of Skim Milk Electroacidification Fouling : A Microscopic Approach," *Journal of Colloid and Interface Science*, vol. 237, pp. 62–69, 2001.
- [77] N. Cifuentes-Araya, G. Pourcelly, and L. Bazinet, "Impact of Pulsed Electric Field on Electrodialysis Process Performance and Membrane Fouling during Consecutive Demineralization of a Model Salt Solution Containing a High Magnesium/Calcium Ratio," *Journal of Colloid and Interface Science*, vol. 361, no. 1, pp. 79–89, 2011.
- [78] C. Casademont, M. Araya-Farias, G. Pourcelly, and L. Bazinet, "Impact of Electro-dialytic Parameters on Cation Migration Kinetics and Fouling Nature of Ion-Exchange Membranes during Treatment of Solutions with Different Magnesium/Calcium Ratios," *Journal of Membrane Science*, vol. 325, no. 1, pp. 570–579, 2008.
- [79] C. Casademont, P. Sistat, B. Ruiz, G. Pourcelly, and L. Bazinet, "Electrodialysis of Model Salt Solution Containing Whey Proteins : Enhancement by Pulsed Electric Field and Modified Cell Configuration," *Journal of Membrane Science*, vol. 328, no. 1-2, pp. 238–245, 2009.

- [80] B. Ruiz, P. Sístat, P. Huguet, G. Pourcelly, M. Araya-Farias, and L. Bazinet, “Application of Relaxation Periods during Electrodialysis of a Casein Solution : Impact on Anion-Exchange Membrane Fouling,” *Journal of Membrane Science*, vol. 287, no. 1, pp. 41–50, 2007.
- [81] M. J. Walzak, R. Davidson, and M. Biesinger, “The Use of XPS, FTIR, SEM/EDX, Contact Angle, and AFM in the Characterization of Coatings,” *Journal of Materials Engineering and Performance*, vol. 7, no. 3, pp. 317–323, 1998.
- [82] E. Sjöström and R. Alén, *Analytical Methods in Wood Chemistry, Pulping, and Paper-making*. Springer, 1999.
- [83] P. Mjöberg, “Chemical Surface Analysis of Wood Fibers by means of ESCAPE,” *Cellulose Chemistry and Tehnology*, vol. 15, pp. 481–486, 1981.
- [84] M. Ek, G. Gellerstedt, and G. Henriksson, *Pulping Chemistry and Technology*. Walter de Gruyter, 2009.
- [85] M. Crocker, *Thermochemical Conversion of Biomass to Liquid Fuels and Chemicals*. Royal Society of Chemistry, 2010.
- [86] A. P. Dodd, J. F. Kadla, and S. K. Straus, “Characterization of Fractions Obtained from Two Industrial Softwood Kraft Lignins,” *ACS Sustainable Chemistry & Engineering*, vol. 3, no. 1, pp. 103–110, 2014.
- [87] M. A. Hubbed, D. J. Gardner, and W. Shen, “Contact Angles and Wettability of Cellulosic Surfaces : A Review of Proposed Mechanisms and Test Strategies,” *BioResources*, vol. 10, no. 4, pp. 1–93, 2015.
- [88] N. El-Mansouri and J. Salvadó, “Structural Characterization of Technical Lignins for the Production of Adhesives : Application to Lignosulfonate, Kraft, Soda-Anthraquinone, Organosolv and Ethanol Process Lignins,” *Industrial Crops and Products*, vol. 24, no. 1, pp. 8–1, 2006.
- [89] A. G. Vishtal and A. Kraslawski, “Challenges in Industrial Applications of Technical Lignins,” *BioResources*, vol. 6, no. 3, pp. 3547–3568, 2011.
- [90] S. Rudatin, L. S. Yasar, and L. W. Douglas, *Association of kraft lignin in aqueous solution*. American Chemical Society, 1989.
- [91] M. Ragnara, C. T. Lindgrenb, and N. O. Nilvebrantc, “pKa-Values of Guaiacyl and Syringyl Phenols Related to Lignin,” *Journal of Wood Chemistry and Technology*, vol. 20, no. 3, pp. 277–305, 2000.
- [92] N. I. Lebovka, *Aggregation of Charged Colloidal Particles*. Springer, 2012.

- [93] D. F. Evans and H. Wennerströ, *The Colloidal Domain : Where Physics, Chemistry, Biology, and Technology Meet*. Wiley-VCH, 1994.
- [94] I. H. Leubner, “Particle Nucleation and Growth Models,” *Current Opinion in Colloid & Interface Science*, vol. 5, no. 1-2, pp. 151–159, 2000.
- [95] C. Gavach, J. L. Bribes, A. Chapotot, J. Maillols, G. Pourcelly, J. Sandeaux, R. Sandeaux, and I. Tugas, “Improvements of the Selectivity of Ionic Transport through Electrodialysis Membranes in Relation with the Performances of Separation Electromembrane Processes,” *Journal De Physique IV*, vol. 4, no. C1, pp. 233–243, 1994.
- [96] J. S. Jaime-Ferrer, E. Couallier, G. Durand, and M. Rakib, “Three Compartment Bipolar Membrane Electrodialysis for Splitting of Sodium Formate into Formic Acid and Sodium Hydroxide : Role of Diffusion of Molecular Acid,” *Journal of Membrane Science*, vol. 325, no. 2, pp. 528–536, 2008.
- [97] M. Haddad, S. Mikhaylin, L. Bazinet, O. Savadogo, and J. Paris, “Fouling Identification of Ion-Exchange Membranes during Acidification of Kraft Black Liquor by Electrodialysis with Bipolar Membrane,” *Submitted*, 2016.
- [98] Z. Yan-jun, W. Kai-fen, W. Zheng-jun, Z. Liang, and L. Shu-shen, “Fouling and Cleaning of Membrane : A review,” *Journal of Environmental Sciences*, vol. 12, no. 2, pp. 241–251, 2000.
- [99] C. Liu, S. Caothien, J. Hayes, and T. Caothuy, “Membrane Chemical Cleaning : from Art to Science,” in *AWWA 2000 Water Quality Technology Conference*, (Denver, USA), pp. 1–25, 2001.
- [100] N. Porcelli and S. Judd, “Chemical cleaning of potable water membranes : A review,” *Separation and Purification Technology*, vol. 71, no. 2, pp. 137–143, 2010.
- [101] A. M. Pritchard and P. Freyer, *Fouling Science and Technology*. Kluwer Academic Publishers, 1988.
- [102] S. Mikhaylin, V. Nikonenko, N. Pismenskaya, G. Pourcelly, S. Choi, H. J. Kwon, J. Han, and L. Bazinet, “How Physico-Chemical and Surface Properties of Cation-Exchange Membrane Affect Membrane Scaling and Electroconvective Vortices : Influence on Performance of Electrodialysis with Pulsed Electric Field,” *Desalination*, vol. In Press, 2015.
- [103] P. E. Dlugolecki, *Mass Transport in Reverse Electrodialysis for Sustainable Energy Generation*. PhD thesis, University of Twente, Enschede, The Netherlands, 2009.
- [104] S. Mikhaylin, *Impact des Champs Électriques Pulsés à Courte Durée d’Impulsion/Pause sur le Colmatage des Membranes en Cours de Procédés*

- Électromembranaires : Mécanismes d' Action et Influence sur les Performances des Procédés*. PhD thesis, Université Laval, Quebec City, Canada, 2015.
- [105] R. Lteif, L. Dammak, C. Larchet, and B. Auclair, "Conductivité Électrique membranaire : Étude de l'effet de la concentration, de la nature de l'électrolyte et de la structure membranaire," *European Polymer Journal*, vol. 37, no. 7, pp. 1187–1195, 1999.
 - [106] A. E. Childress, J. A. Brant, P. Rempala, W. P. D, and P. Kwan, "Evaluation of membrane characterization methods," Web Report 4102, Water Research Foundation, 2012.
 - [107] Y. Yuan and T. R. Lee, *Contact Angle and Wetting Properties*. Springer, 2013.
 - [108] E. J. Roche and M. P. an R. Duplessix, "Phase Separation in Perfluorosulfonate Ionomer Membranes," *Journal of Polymer Science Part B : Polymer Physics*, vol. 20, no. 1, pp. 107–116, 1982.
 - [109] S. Banerjee and D. E. Curtin, "Nafion perfluorinated membranes in fuel cells," *Journal of Fluorine Chemistry*, vol. 125, no. 8, pp. 1211–1216, 2004.
 - [110] K. A. Mauritz and R. B. Moore, "State of Understanding of Nafion," *Chemical Reviews*, vol. 104, no. 10, pp. 4535–4585, 2004.
 - [111] A. Ferrer, E. Quintana, I. Filpponen, I. Solala, T. Vidal, A. Rodriguez, J. Laine, and O. J. Rojas, "Effect of Residual Lignin and Heteropolysaccharides in Nanofibrillar Cellulose and Nanopaper from Wood Fibers," *Cellulose*, vol. 19, no. 6, pp. 2179–2193, 2012.
 - [112] F. S. Chakar and A. J. Ragauskas, "Review of Current and Future Softwood Kraft Lignin Process Chemistry," *Industrial Crops and Products*, vol. 20, no. 2, pp. 131–140, 2004.
 - [113] J. Wang, K. Yao, A. L. Korich, S. Li, S. Ma, H. J. Ploehn, P. M. Iovine, C. Wang, F. Chu, and C. Tang, "Combining Renewable Gum Rosin and Lignin : Towards Hydrophobic Polymer Composites by Controlled Polymerization," *Journal of Polymer Science Part A : Polymer Chemistry*, vol. 49, no. 17, pp. 3728–3738, 2011.
 - [114] M. Alekhina, O. Ershova, A. Ebert, S. Heikkinen, and H. Sixta, "Softwood Kraft Lignin for Value-Added Applications : Fractionation and Structural Characterization," *Industrial Crops and Products*, vol. 66, pp. 220–228, 2015.
 - [115] S. M. Notley and M. Norgren, *Lignin : Functional Biomaterial with Potential in Surface Chemistry and Nanoscience*. Wiley, 2009.
 - [116] R. Ghalloussi, W. Garcia-Vasquez, L. Chaabane, L. Dammak, C. Larchet, S. Deabate, E. Nevakshenova, V. Nikonenko, and D. Grande, "Ageing of Ion-Exchange Membranes

- in Electrodialysis : A Structural and Physicochemical Investigation,” *Journal of Membrane Science*, vol. 436, no. 1, pp. 68–78, 2013.
- [117] M. Kang, Y. J. Choi, I. Choi, T. H. Yoon, and S. H. Moon, “Electrochemical Characterization of Sulfonated Poly(arylene ether sulfone) (S-PES) Cation-Exchange Membranes,” *Journal of Membrane Science*, vol. 216, no. 1-2, pp. 39–53, 2003.
- [118] N. Berezina, N. Kononenko, O. Dyomina, and N. Gnusin, “Characterization of Ion-Exchange Membrane Materials : Properties vs Structure,” *Advances in Colloid and Interface Science*, vol. 139, no. 1-2, pp. 3–28, 2008.
- [119] V. C. Uloth and J. T. Wearing, “Kraft Lignin Recovery : Acid Precipitation versus Ultrafiltration Part I : Laboratory Test Results,” *Pulp & Paper Canada*, vol. 90, no. 9, pp. 67–71, 1986.
- [120] O. Wallberg and A. S. Jonsson, “Separation of Lignin in Kraft Cooking Liquor from a Continuous Digester by Ultrafiltration at Temperatures above 100 °C,” *Desalination*, vol. 195, no. 1-3, pp. 187–200, 2006.
- [121] M. Haddad, S. Mikhaylin, L. Bazinet, O. Savadogo, and J. Paris, “Electrochemical Acidification of Kraft Black Liquor by Electrodialysis with Bipolar Membrane : Effect of Fouling and Chemical Cleaning on Ion-Exchange Membranes Integrity,” *Submitted*, 2016.
- [122] J. Lyklema, *Fundamentals of Interface and Colloid Science*. Elsevier Science, 2005.
- [123] E. Evstigneev, “Factors affecting lignin solubility,” *Russian Journal of Applied Chemistry*, vol. 84, no. 6, pp. 1040–10456, 2011.
- [124] T. T. Divisions, “Solids content of black liquor TAPPI/ANSI Test Method T 650 om-15,” Test Methods, 2009.
- [125] F. A. Morrison, *An Introduction to Fluid Mechanics*. Cambridge University Press, 2013.
- [126] C. Larchet, V. I. Zabolotsky, N. Pismenskaya, V. Nikonenko, A. Tskhay, K. Tastanov, and G. Pourcelly, “Comparison of Different ED Stack Conceptions When Applied for Drinking Water Production from Brackish Waters,” *Desalination*, vol. 222, no. 1-3, pp. 489–496, 2008.
- [127] M. P. Mier, R. Ibañez, and I. Ortiz, “Influence of Ion Concentration on the Kinetics of Electrodialysis with Bipolar Membranes,” *Separation and Purification Technology*, vol. 59, no. 2, pp. 197–205, 2008.
- [128] Y. Wei, C. Li, Y. Wang, X. Zhang, Q. Li, and T. Xu, “Regenerating Sodium Hydroxide from the Spent Caustic by Bipolar Membrane Electrodialysis (BMED),” *Separation and Purification Technology*, vol. 86, pp. 49–54, 2012.

- [129] F. Öhman, *Precipitation and Separation of Lignin from Kraft Black Liquor*. PhD thesis, Chalmers University of Technology, Gothenburg, Sweden, 2006.
- [130] J. E. Roberts, S. A. Khan, and J. S. R, “Controlled Black Liquor Viscosity Reduction through Salting-in,” *AIChE Journal*, vol. 42, no. 8, pp. 2319–2326, 1996.
- [131] J. J. Barron and A. C, “The Effect of Temperature on Conductivity Measurement,” *TSP*, vol. 7, no. 73, pp. 1–5, 2005.
- [132] M. Norgren and H. Edlund, “Ion Specific Differences in Salt Induced Precipitation of Kraft Lignin,” *Nordic Pulp & Paper Research Journal*, vol. 18, no. 4, pp. 400–403, 2003.
- [133] H. Wallmo, H. Theliander, A. S. Jönsson, O. Wallberg, and K. Lindgren, “The Influence of Hemicelluloses during the Precipitation of Lignin in Kraft Black Liquor,” *Nordic Pulp & Paper Research Journal*, vol. 24, no. 2, pp. 165–171, 2009.
- [134] H. Wallmo, T. Richards, and H. Theliander, “Lignin Precipitation from Kraft Black Liquors : Kinetics and Carbon Dioxide Absorption,” *Paperi ja Puu : Paper and Timber*, vol. 7, no. 8, pp. 436–442, 2007.
- [135] G. Belfort and G. A. Guter, “An experimental Study of Electrodialysis Hydrodynamics,” *Desalination*, vol. 10, no. 3, pp. 221–262, 1972.
- [136] P. Saremirad, H. Gomaa, and J. Zhu, “Effect of Flow Oscillations on Mass Transfer in Electrodialysis with Bipolar Membrane,” *Journal of Membrane Science*, vol. 405–406, pp. 158–166, 2012.
- [137] N. A. Mishchuk, L. K. Koopal, and F. Gonzalez-Caballero, “Intensification of Electrodialysis by Applying a Non-stationary Electric Field,” *Colloids and Surfaces A : Physicochemical and Engineering Aspects*, vol. 176, no. 2–3, pp. 195–212, 2001.
- [138] N. A. Mishchuk, L. K. Koopal, and F. Gonzalez-Caballero, “Concentration Polarization and Specific Selectivity of Membranes in Pulse Mode,” *Colloid Journal*, vol. 63, no. 5, pp. 586–595, 2001.
- [139] N. Cifuentes-Araya, G. Pourcelly, and L. Bazinet, “Water Splitting Proton-Barriers for Mineral Membrane Fouling Control and their Optimization by Accurate Pulsed Modes of Electrodialysis,” *Journal of Membrane Science*, vol. 477, no. 15, pp. 433–441, 2011.
- [140] N. Cifuentes-Araya, G. Pourcelly, and L. Bazinet, “How Pulse Modes Affect Proton-Barriers and Anion-Exchange Membrane Mineral Fouling during Consecutive Electrodialysis Treatments,” *Journal of Colloid and Interface Science*, vol. 392, no. 15, 2012.
- [141] S. Mikhaylin, V. Nikonenko, G. Pourcelly, and L. Bazinet, “Hybrid Bipolar Membrane Electrodialysis/Ultrafiltration Technology Assisted by a Pulsed Electric Field for Casein Production,” *Green Chemistry*, vol. 18, no. 1, pp. 307–314, 2016.

- [142] S. Mikhaylin, V. Nikonenko, G. Pourcelly, and L. Bazinet, “Intensification of Demineralization Process and Decrease in Scaling by Application of Pulsed Electric Field with Short Pulse/Pause Conditions,” *Journal of Membrane Science*, vol. 468, pp. 389–399, 2014.
- [143] D. Shaw, *Introduction to Colloid and Surface Chemistry (Fourth Edition)*. Elsevier, 1992.
- [144] H. Theliander, “The lignoboost process : Solubility of lignin,” in *International Chemical Recovery Conference*, (Williamsburg, VA, USA), pp. 33–42, 2010.
- [145] L. Kouisni, Y. Fang, M. Paleologou, B. Ahvazi, J. Hawari, Y. Zhang, and X. M. Wang, “Kraft Lignin Recovery and its Use in the Preparation of Lignin-Based Phenol Formaldehyde Resins for Plywood,” *Cellulose Chemistry and Technology*, vol. 45, no. 7-8, pp. 515–520, 2011.
- [146] L. Bazinet, F. Lamarche, and D. Ippersiel, “Comparison of Chemical and Bipolar-Membrane Electrochemical Acidification for Precipitation of Soybean Proteins,” *Journal of Agricultural and Food Chemistry*, vol. 46, no. 5, pp. 2013–2019, 1998.